

UNCLASSIFIED

AD NUMBER	
AD501370	
CLASSIFICATION CHANGES	
TO:	UNCLASSIFIED
FROM:	CONFIDENTIAL
LIMITATION CHANGES	
TO: Approved for public release; distribution is unlimited.	
FROM: Distribution authorized to U.S. Gov't. agencies and their contractors; Administrative/Operational Use; APR 1969. Other requests shall be referred to Air Force Rocket Propulsion Lab., Edwards AFB, CA.	
AUTHORITY	
30 Apr 1981, DoDD 5200.10 ; AFRPL ltr 5 Feb 1096	

THIS PAGE IS UNCLASSIFIED

SECURITY

MARKING

The classified or limited status of this report applies to each page, unless otherwise marked.

Separate page printouts MUST be marked accordingly.

THIS DOCUMENT CONTAINS INFORMATION AFFECTING THE NATIONAL DEFENSE OF THE UNITED STATES WITHIN THE MEANING OF THE ESPIONAGE LAWS, TITLE 18, U.S.C., SECTIONS 793 AND 794. THE TRANSMISSION OR THE REVELATION OF ITS CONTENTS IN ANY MANNER TO AN UNAUTHORIZED PERSON IS PROHIBITED BY LAW.

NOTICE: When government or other drawings, specifications or other data are used for any purpose other than in connection with a definitely related government procurement operation, the U.S. Government thereby incurs no responsibility, nor any obligation whatsoever; and the fact that the Government may have formulated, furnished, or in any way supplied the said drawings, specifications, or other data is not to be regarded by implication or otherwise as in any manner licensing the holder or any other person or corporation, or conveying any rights or permission to manufacture, use or sell any patented invention that may in any way be related thereto.

CONFIDENTIAL

AFRPL-TR-69-88

April 1969

AD 501370

(Title Unclassified)

**PBPS ENGINE DEVELOPMENT PROGRAM
AND
SYSTEM DESIGN**

Final Report

Roy E. Jones

**Liquid Rocket Operations
Propulsion Division
Aerojet-General Corporation**

MAY 8 1969

Technical Report AFRPL-TR-69-88

**Air Force Rocket Propulsion Laboratory
Air Force Systems Command
Edwards, California**

"In addition to security requirements, which must be met, this document is subject to special export controls and each transmittal to foreign governments or foreign nationals may be made only with prior approval of AFRPL (RPOR/STINFO), Edwards CA 93523."

GROUP 4

DOWNGRADED AT 3 YEAR INTERVALS DECLASSIFIED AFTER 12 YEARS

**THIS MATERIAL CONTAINS INFORMATION AFFECTING THE NATIONAL DEFENSE OF
THE UNITED STATES WITHIN THE MEANING OF THE ESPIONAGE LAWS, TITLE 18,
U.S.C. SECTION 793 OR 794. THE TRANSMISSION OR REVELATION OF WHICH IN
ANY MANNER TO AN UNAUTHORIZED PERSON IS PROHIBITED BY LAW.**

1128

CONFIDENTIAL

**DOWNGRADED AT 3 YEAR INTERVALS;
DECLASSIFIED AFTER 12 YEARS
DOD DIR 5200.10**

CONFIDENTIAL

"When U.S. Government drawings, specifications, or other data are used for any purpose other than a definitely related Government procurement operation, the Government thereby incurs no responsibility nor any obligation whatsoever, and the fact that the Government may have formulated, furnished, or in any way supplied the said drawings, specifications, or other data, is not to be regarded by implication or otherwise, or in any manner licensing the holder or any other person or corporation, or conveying any rights or permission to manufacture, use, or sell any patented invention that may in any way be related thereto."

CONFIDENTIAL

(This page is Unclassified)

CONFIDENTIAL

(TITLE UNCLASSIFIED)

**PBPS ENGINE DEVELOPMENT PROGRAM
AND
SYSTEM DESIGN**

FINAL REPORT

Roy E. Jones

"In addition to security requirements, which must be met, this document is subject to special export controls and each transmittal to foreign governments or foreign nationals may be made only with prior approval of AFRPL (RPOR/STINFO), Edwards CA 93523."

GROUP 4

DOWNGRADED AT 3 YEAR INTERVALS DECLASSIFIED AFTER 12 YEARS

THIS MATERIAL CONTAINS INFORMATION AFFECTING THE NATIONAL DEFENSE OF THE UNITED STATES WITHIN THE MEANING OF THE ESPIONAGE LAWS, TITLE 18, U.S.C. SECTION 793 OR 794. THE TRANSMISSION OR REVELATION OF WHICH IN ANY MANNER TO AN UNAUTHORIZED PERSON IS PROHIBITED BY LAW.

1128

AEROJET-GENERAL CORPORATION
A SUBSIDIARY OF THE GENERAL TIRE & RUBBER COMPANY

CONFIDENTIAL

CONFIDENTIAL

Report AFRPL-TR-69-88

FOREWORD

This is the Final Technical Report for Contract F04611-67-C-0095, PBPS Engine Development Program and System Design, which was under the cognizance of Mr. M. Rogers, RPRPM, Project Engineer, AFFTC (FTMKR-2), Edwards Air Force Base, California 93523. It is submitted by the Aerojet-General Corporation (Liquid Rocket Operations, Sacramento, California 95813) in accordance with the requirements of Item B006, DD1423, Exhibit B and in fulfillment of said contract. It covers the complete period of 1 April 1967 through 31 January 1969.

This technical report has been reviewed and is approved.

Melvin Rogers
Re-entry Propulsion Section
Air Force Rocket Propulsion Laboratory

CONFIDENTIAL

(This page is Unclassified)

UNCLASSIFIED

Report AFRPL-TR-69-88

ABSTRACT

The increased size and extended mission duty cycles of planned Post-Boost Propulsion Systems (PBPS) for Advanced ICBM applications identified the need for improvements in liquid propellant propulsion technology. Although liquid propellant propulsion systems have demonstrated an operational flexibility and performance capability, improvements in the inherent storability, maintainability, and reliability were desired for an optimum strategic weapon system.

The PBPS Engine Development Program was initiated to develop a bipropellant N_2O_4 and MMH attitude control system (ACS) wherein integral fluidic controls are used to perform ACS propellant flow control, thereby controlling vehicle attitude with a minimum of moving parts. Developmental problems with the fluidic control elements resulted in the termination of the integral fluidic ACS development and the associated minimum ACS engine studies.

The program was redirected to provide the development of a conventionally-controlled 75 lb thrust attitude control engine as well as the demonstration testing of PBPS pressurization and positive expulsion propellant tank subsystems. An Aerojet-General proprietary injector concept in conjunction with a bimetallic, conductively-cooled combustion chamber was used in the ACS engine developed. This engine was demonstrated in altitude performance and pulse testing. The monopropellant hot gas pressurization subsystem was used to demonstrate propellant expulsion (both monomethylhydrazine and N_2O_4) from the full-size, ring-stabilized expulsion propellant tanks.

UNCLASSIFIED

Report AFRPL-TR-69-88

TABLE OF CONTENTS

	<u>Page</u>
I. <u>INTRODUCTION</u>	1
II. <u>SUMMARY</u>	2
A. ACS WITH INTEGRAL FLUIDIC CONTROLS	2
B. MINIMUM ACS ENGINE STUDY	2
C. BIPROPELLANT ACS ENGINE DEVELOPMENT	3
D. POSITIVE EXPULSION PROPELLANT TANK DEMONSTRATION	5
E. MAJOR CONCLUSIONS AND RECOMMENDATIONS	5
III. <u>ACS WITH INTEGRATED FLUIDIC CONTROLS</u>	7
A. OBJECTIVES AND APPROACH	7
B. INTEGRATED ACS ENGINE DESIGN	9
1. <u>Preliminary Design</u>	9
a. Doublet Injector	11
b. Swirl-Cup Injector	11
c. Impinging Sheet Injector	14
d. Direct Vortex Injection Pentad	14
2. <u>Analyses</u>	14
a. Performance Analyses	14
b. Thermal Analyses	18
c. Thermal Analyses of Vortex Valve	19
3. <u>Plastic Flow Models</u>	20
a. Criteria	21
b. Design	21
c. Flow Model Evaluation	26
C. ACS ENGINE FLUIDIC CONTROLS EVALUATION	26
1. <u>Controls Configuration Definition</u>	26
a. Vortex Throttle Design	26
b. Fabrication of Controls Flow Models	29
c. Flow Model Testing	29
2. <u>Vortex Throttle Analysis and Evaluation</u>	39
a. Design and Analysis	39

TABLE OF CONTENTS (cont.)

	<u>Page</u>
(1) On-Off Stability	39
(2) Flow Stability	40
(3) Throttling Ability	41
(4) Response Time	44
b. Fabrication of Evaluation Model	44
c. Test Evaluation	44
(1) Test Description	44
(2) Test Results	46
3. <u>Conclusions</u>	54
4. <u>Recommendations</u>	55
IV. <u>MINIMUM ACS ENGINE STUDY</u>	58
A. OBJECTIVE	58
B. ACS STUDY	58
C. CONCLUSIONS AND RECOMMENDATIONS	66
V. <u>BIPROPELLANT ACS ENGINE DEVELOPMENT</u>	67
A. OBJECTIVES AND APPROACH	67
B. ENGINE PRELIMINARY DESIGN AND ANALYSIS	70
1. <u>Bimetallic Combustion Chamber</u>	70
a. Altitude Expansion Chamber	72
b. Sea-Level Expansion Chamber	72
2. Injector Design	72
a. Conventional Orificed Doublet Injector	74
b. Baffled Injector	77
c. Flat-Faced Injector	80
3. <u>Torque Motor Bipropellant Valve</u>	80
4. <u>Pre-Test Analyses</u>	80
a. Performance	80
b. Stability	83
c. Thermal	83

TABLE OF CONTENTS (cont.)

	<u>Page</u>
C. ENGINE SEA-LEVEL TEST EVALUATION	93
1. <u>Fabrication</u>	93
2. <u>Doublet Injector Evaluation</u>	93
a. Sea-Level Testing	93
b. Doublet Injector Test Conclusions	109
3. <u>Baffled Injector</u>	109
4. <u>Injector Evaluation</u>	112
a. Sea-Level Testing	112
b. Test Results and Evaluation	115
(1) 700°F Maximum Chamber Temperature, 15 sec Minimum Coast	115
(2) 400°F Maximum Injector Temperature	120
D. ALTITUDE TEST EVALUATION	120
1. <u>Altitude Chamber Redesign and Fabrication</u>	120
2. <u>Altitude Testing</u>	125
a. Fuel Film Coolant and Chamber Variations	125
b. Altitude Demonstration	136
c. Test Results	165
(1) Thermal	165
(2) Performance	176
(3) Stability	180
E. CONCLUSIONS AND RECOMMENDATIONS	182
VI. <u>POSITIVE EXPULSION PROPELLANT TANK DEMONSTRATION</u>	185
A. OBJECTIVE	185
B. EXPULSION BLADDER DEVELOPMENT	191
1. <u>Contract AF 04(611)-11614 Bladder Development</u>	191
2. <u>Expulsion Bladder Fabrication</u>	192
a. Increased Diameter Control Wire Evaluation	192
b. Flame Spray Metal Coating of Shell	195
(1) Braze Problems	195
(2) Flame Spraying Problems	195

TABLE OF CONTENTS (cont.)

	<u>Page</u>
3. <u>Bladder Collapse Mode Evaluation</u>	200
a. Acrylic Tank Evaluation of S/N 67 Bladder	200
b. S/N 65 Flame-Spray-Coated Bladder Evaluation	204
c. S/N 83 Bladder Evaluation of Large Wires	206
C. <u>BLADDER EXPULSION EVALUATION</u>	206
1. <u>Rated Pressure Expulsion</u>	206
2. <u>Hot Gas Expulsion</u>	210
a. Monopropellant N_2H_4 Gas Pressurization Checkout	210
b. Initial Hot Gas Expulsion - S/N 75 Bladder	210
c. Bladder Rework Verification Expulsion Tests	219
D. <u>FLIGHTWEIGHT TANK EVALUATION</u>	231
1. <u>Flightweight Tank Fabrication</u>	231
a. Verification Tank Assembly - S/N 1	231
b. Demonstration Tank Assemblies	231
2. <u>Flightweight Tank Propellant Expulsion</u>	232
a. Propellant Expulsion Test Set-Up	232
b. Hot Gas Expulsion of MMH	235
c. Hot Gas Expulsion of N_2O_4	235
E. <u>CONCLUSIONS AND RECOMMENDATIONS</u>	241
1. <u>Ring-Stabilized Expulsion Propellant Tank</u>	241
2. <u>Monopropellant Gas Pressurization</u>	247
REFERENCES AND BIBLIOGRAPHY	248
DD FORM 1473	

UNCLASSIFIED

Report AFRPL-TR-69-88

LIST OF TABLES

<u>No.</u>	<u>Title</u>	<u>Page</u>
I.	Integral Fluidic ACS Engine Design Criteria	8
II.	Design Data for Vortex Throttle	28
III.	Vortex Throttle Types for Selected Injection Concepts	28
IV.	Study Configurations	60
V.	Preliminary Results - Typical Performance and Weight Values	65
VI.	Bipropellant ACS Engine Design Goals	69
VII.	Combustion Chamber Geometric Parameters	71
VIII.	PBPS Doublet Injector Parameter Summary	76
IX.	Predicted Performance Summary	82
X.	Sea-Level ACS Test Summary (3 Sheets)	97
XI.	Identification of Sea-Level Chamber Thermocouple Location	108
XII.	Propellant Expulsion Tank Design Criteria	187
XIII.	Expulsion Bladder Summary	197

UNCLASSIFIED

UNCLASSIFIED

Report AFRPL-TR-69-88

LIST OF FIGURES

<u>No.</u>	<u>Title</u>	<u>Page</u>
1.	Bipropellant ACS Engine	4
2.	PBPS Propellant Tank for Hot Gas Expulsion	6
3.	Doublet Injector Side-By-Side Vortex Valves	12
4.	Swirl-Cup Injector - Coaxial Vortex Valve	13
5.	Impinging Sheet Injector, Axially-Mounted Vortex Valves	15
6.	Direct Injection Pentad Multiple Vortex Valves	16
7.	Flow Model Doublet Injector, Oxidizer Orifice	22
8.	Flow Model Doublet Injector, Fuel Circuit	23
9.	Flow Model Swirl Cup Injector, Oxidizer Circuit	24
10.	Flow Model Swirl Cup Injector, Fuel Circuit	25
11.	ACS Oxidizer Vortex Valve	27
12.	Simple Vortex Throttle	30
13.	Coaxial Vortex Throttle	31
14.	Vortex Throttle Test Assembly	32
15.	Vortex Throttle Test Hardware	33
16.	Fluid Chambers and Outlet Fittings	34
17.	Test Schematic	35
18.	Views of Vortex Throttle Test Set-Up	36
19.	Pressure Drop Comparison	38
20.	Theoretical Two-Phase Flow Curve for Homogeneously-Mixed Fluid Through an Orifice	42
21.	Comparison of Laminar and Turbulent Control Gas Inlet Orifice Characteristics	43
22.	Modified Vortex Throttle Assembly	45
23.	Metal vs. Plastic Throttle Performance	47
24.	Typical Flow Oscillations	48
25.	Effect of Inlet Pressure	49
26.	Effect of Backpressure Level	50
27.	Effect of Fixed vs. Variable Backpressure	51
28.	Throttling Operation Hysteresis	52
29.	Vortex Throttle Flow Transient	56

x

UNCLASSIFIED

UNCLASSIFIED

Report AFRPL-TR-69-88

LIST OF FIGURES (cont.)

<u>No.</u>	<u>Title</u>	<u>Page</u>
30.	ACS Study Plan	59
31.	ACS Study Guidance and Control Loop Schematic	61
32.	ACS Study Control Logic	63
33.	Five-Engine Computer Control Evaluation	64
34.	Bipropellant ACS Engine	68
35.	Preliminary Design of ACS Engine	73
36.	75 lb Thrust ACS Engine	75
37.	Baffled Alternative Injector	78
38.	Injector Assembly Sequence	79
39.	Sensitive Time-Lag Injector Evaluation	84
40.	Empirical Stability Study Results	85
41.	Principle of Operation of Bimetallic Heat Pump Nozzle	86
42.	Gas-Side Heat Transfer Coefficient vs. Axial Distance	87
43.	Predicted Nozzle Temperature Transients	89
44.	Predicted Nozzle Temperature Transients	90
45.	Predicted Nozzle Isotherms at 700 sec of Firing	91
46.	Predicted Nozzle Temperature Transients - Sea-Level	92
47.	Prototype Engine Components	94
48.	Doublet Injector Flow Characteristics	95
49.	Baffled Alternative Injector Flow Characteristics	96
50.	Prototype Engine Test Data (5 Sheets)	102
51.	Sea-Level Chamber Thermocouple Location (Cross-Section)	107
52.	Eroded Alternative Injector	111
53.	Injector Flow Characteristics	113
54.	Typical Wall Temperature Data	116
55.	Steady-State Wall Temperatures at 35% Film Cooling	117
56.	Steady-State Wall Temperatures at 40% Film Cooling	118
57.	Steady-State Wall Temperatures for Cold and Hot Starts	119
58.	Thermal Data Comparison with Model Predictions	121
59.	Steady-State Temperature Prediction for 40:1 Thrustor Design	122

UNCLASSIFIED

UNCLASSIFIED

Report AFRPL-TR-69-88

LIST OF FIGURES (cont.)

<u>No.</u>	<u>Title</u>	<u>Page</u>
60.	Altitude Chamber Cross-Section	123
61.	Bipropellant ACS Engine - Initial Design	124
62.	Altitude Engine Test No. OC-5-146 (5 Plots) (5 Sheets)	126
63.	Altitude Engine Test No. OC-5-151 (5 Plots) (5 Sheets)	131
64.	Chamber Modifications and Thermocouple Location	137
65.	ACS Engine in Altitude Facility	138
66.	Thermal Soak Duty Cycle Test No. OC-5-169 (3 Plots) (3 Sheets)	140
67.	Pulsing Characteristics (2 Oscillograph Traces) (2 Sheets)	143
68.	Pulsing Performance - Bit Impulse	145
69.	Pulse Data - Test No. OC-5-171 (6 Plots) (6 Sheets)	146
70.	Pulse Data - Test No. OC-5-172 (6 Plots) (6 Sheets)	152
71.	Pulse Data - Test No. OC-5-173 (6 Plots) (6 Sheets)	158
72.	Oscillographs from Varying Electrical Coast Width	164
73.	Pulse Data - Test No. OC-5-174 (3 Plots) (3 Sheets)	166
74.	Pulse Data - Test No. OC-5-175 (3 Plots) (3 Sheets)	169
75.	Pulse Data - Test No. OC-5-176 (3 Plots) (3 Sheets)	172
76.	Measured and Predicted Wall Temperatures	175
77.	Effect of Percentage of Coolant Flow Upon Percentage of Specific Impulse	178
78.	Effect of Percentage of Coolant Flow Upon Characteristic Velocity	179
79.	Effects of Mixture Ratio Upon Corrected Specific Impulse	181
80.	Tankage/Expulsion Subsystem Interface Drawing	186
81.	Flightweight Propellant Expulsion Tank	188
82.	Full-Scale Welded Tank Fabrication and Test	189
83.	Conospheroid Diaphragm Reversal Test, S/N 61 Bladder	190
84.	Conospheroid Diaphragm Reversal Test, S/N 71 Bladder	193
85.	Arde Ring-Stabilized Expulsion Bladder Configurations	194
86.	Flame-Spray-Metal on Bladder Shell	196
87.	Bladder S/N 62 Braze Voids in Hemispherical Region	198
88.	Expulsion Bladder Shell Indentations	199

UNCLASSIFIED

UNCLASSIFIED

Report AFRPL-TR-69-88

LIST OF FIGURES (cont.)

<u>No.</u>	<u>Title</u>	<u>Page</u>
89.	Arde Ring-Stabilized Diaphragm Reversal	201
90.	Arde Ring-Stabilized Diaphragm Reversal	202
91.	Diaphragm S/N 67 After Expulsion	203
92.	Ring-Stabilized Bladder S/N 65 Water Expulsion	205
93.	Bladder S/N 83 After Reversal Attempt	207
94.	Bladder S/N 83 After Reversal Attempt	208
95.	Bladder S/N 69 Prior to Expulsion Demonstration	209
96.	Bladder S/N 69 After Rated Pressure Expulsion	211
97.	Integrated Test Set-Up	212
98.	PBPS Integration Test Schematic	213
99.	Hot Gas Water Expulsion Test No. SP-23-101 (4 Plots) (4 Sheets)	215
100.	Bladder S/N 66 After Hot Gas Water Expulsion	220
101.	Bladder S/N 66 After Hot Gas Water Expulsion	221
102.	Bladder S/N 66 After Hot Gas Water Expulsion	222
103.	Bladder S/N 66 Hot Gas Water Expulsion Data (3 Plots) (3 Sheets)	223
104.	Bladder S/N 62 After Hot Gas Water Expulsion	226
105.	Bladder S/N 62 After Hot Gas Water Expulsion	227
106.	Bladder S/N 62 Hot Gas Water Expulsion Data (3 Plots) (3 Sheets)	228
107.	Flightweight Tank X-Ray Inspection	233
108.	Flight-Type Tank During Propellant Expulsion	234
109.	Propellant Tank Hot Gas Expulsion Test Set-Up	236
110.	Tank S/N 2 Hot Gas Expulsion of MMH - Recorded Data (3 Plots) (3 Sheets)	237
111.	Propellant Tank S/N 2 After Hot Gas Expulsion of MMH	240
112.	Tank S/N 5 Hot Gas Expulsion of N_2O_4 - Recorded Data (3 Plots) (3 Sheets)	242
113.	Propellant Tank S/N 5 After Hot Gas Expulsion of N_2O_4	245

UNCLASSIFIED

UNCLASSIFIED

Report AFRPL-TR-69-88

SECTION 1

INTRODUCTION

The objective of the PBPS Engine Development Program and System Design (Contract FO4611-67-C-0095) was to demonstrate the acceptability of a bipropellant ($\text{N}_2\text{O}_4/\text{MMH}$) altitude control engine with integrated fluidic engine controls for post-boost propulsion mission applications. The original contract contained the additional objective of providing the detailed design of a complete Post-Boost Propulsion Subsystem utilizing conventional controls only. This was a progressive extension of the subsystem technology generated by the Air Force Rocket Propulsion Laboratory through Contract AF 04(611)-11614 (Demonstration of Advanced Post-Boost Propulsion Subsystems). Improved propulsion subsystem technology in the areas of maintenance-free storability, reliability, and low production costs were needed to provide an optimum liquid propulsion system for the next generation of strategic weapon systems. Engine fluidic controls were evaluated as a possible means for achieving these goals.

The evaluation of an integral beryllium heat-sink engine and fluidic controls was terminated and the contract effort redirected when it was determined that additional basic fluidic component technology was required prior to engine propellant system integration. This contractual redirection eliminated the PBPS design requirement and terminated the minimum ACS engine study which was in process. The program was redirected by the Air Force to provide the continuation of a propellant expulsion tank subsystem demonstration initiated under Contract AF 04(611)-11614 and to develop a conventionally-controlled bipropellant ACS engine.

The propellant expulsion tank concept is the ring-stabilized expulsion bladder tank^(*) developed by a subcontractor (Arde, Inc.). The feasibility of the expulsion bladder concept was demonstrated during the prior contract in the size identified for the anticipated Advanced ICBM post-boost vehicle. Further demonstration of the propellant tank under this contract included propellant expulsion at operational pressure levels using the monopropellant N_2H_4 gas generator subsystem as a pressurizing source.

The conventionally-controlled 75 lb thrust ACS engine development was conducted to provide a fast-response, bipropellant engine with an unlimited operational life. The engine propellants are $\text{N}_2\text{O}_4/\text{MMH}$. The conductively-cooled combustion chamber provides the required operational flexibility.

The redirected program was successfully completed to provide a demonstration of the major subsystem technology for a liquid bipropellant ($\text{N}_2\text{O}_4/\text{MMH}$) Post-Boost Propulsion System. The axial thrust engine assembly remains the only subsystem to be developed for a complete bipropellant PBPS.

(*) Arde, Inc., proprietary concept covered by patents 3,197,851 and 3,339,803.

UNCLASSIFIED

UNCLASSIFIED

Report AFRPL-TR-69-88

SECTION II

SUMMARY

The contractual effort for the development of a PBPS attitude control engine with integral fluidic controls was initiated on 1 April 1967. A design and fluidic component evaluation program was conducted and it identified the need for additional advancements in fluidic component technology before the controls and injector could be satisfactorily integrated.

The program was redirected in October of 1967 to provide for the development of a heat-sink bipropellant engine with conventional controls and to continue the demonstration of the previously contracted (AF 04(611)-11614) PBPS propellant positive expulsion tank. This technical report identifies the results of each of these efforts.

A. ACS WITH INTEGRAL FLUIDIC CONTROLS

The initial development of an integrated ACS engine with fluidic controls was to be a three-phase effort which included a plastic flow model test phase followed by workhorse and prototype engine test evaluations of the selected concepts. However, no engine hardware was fabricated because fluidic component operational difficulties were encountered during component and flow model flow tests.

Engine conceptual designs with integrated fluidic controls were developed in conjunction with the fluidic controls subcontractor (Bowles Engineering Company of Silver Spring, Maryland). Plastic flow models of the components for these designs were fabricated and evaluated.

The water flow tests of the plastic flow models of the vortex valves identified a basic flow stability problem. The flow characteristics were extremely erratic at low liquid flow conditions. These data were verified by concurrent flow problems experienced with workhorse controls under Contract AF 04(611)-11614. In addition, the response times for these components exceeded the specified engine requirements.

B. MINIMUM ACS ENGINE STUDY

A minimum ACS engine study was included in the System Design phase of the original contract scope of work. This study was intended to provide an evaluation of the effects that a reduced number of ACS engines would have upon the PBV control capability and performance. However, the original contract was terminated and a new scope of work issued prior to completion of the study effort.

UNCLASSIFIED

CONFIDENTIAL

Report AFRPL-TR-69-88

II, Summary (cont.)

C. BIPROPELLANT ACS ENGINE DEVELOPMENT

(C) The ACS engine development activity was a two-phase program to demonstrate a bimetallic combustion chamber suitable for PBPS ACS applications. The first phase consisted of a sea-level test series during which 26 tests (not including checkout and performance verification testing) were conducted to provide thermal and performance data for use in the design of a 40:1 expansion area ratio chamber. Three injector designs were tested during this phase; an 8-element unlike doublet injector was the primary injector concept and a baffled HIPERTHIN (**) was an alternative. An unbaffled HIPERTHIN design also was tested after the fuel coolant ring of the baffled design eroded during an attempted hot restart. Stable thermal conditions could not be achieved with the doublet injector in tests over a range of coolant flow rates and mixture ratios.

(C) The unbaffled HIPERTHIN injector was selected for the altitude test series with the 40:1 expansion area ratio bimetallic chamber. Twenty-two tests (not including system balance tests) were conducted during this phase. The testing included pulse mode, multiple restart worst thermal conditions and extended duration tests within the limit of the facility vacuum tank. Tests were conducted at high and low values of mixture ratio and chamber pressure to demonstrate flexibility at off design conditions.

(U) The thrust chamber assembly shown on Figure No. 1 demonstrated excellent transient characteristics and durability. Demonstrated altitude performance was approximately 2% below the design goal partially as a result of injector compromises made to allow the use of a common chamber with both injector concepts. The following is a summary of achievements:

Transient Response

Start, Fire-Switch-One (FS ₁) to 90%F	0.014 sec
Shutdown, Fire-Switch-Two (FS ₂) to 5%F	0.008 sec

Test Firing duration, FS₁ to FS₂

Minimum	0.010 sec
Maximum	1000 sec

<u>Hardware Firing Exposure:</u>	<u>Unbaffled Injector</u>	<u>Chamber</u>
Total duration, sec	4990	4610 (Sea-Level) 970 (Altitude)
Starts	159	102 (Altitude)
Tests	55	41 (Sea-Level)

(**) An Aerojet-General proprietary concept covered by Patent No. 3,413,704 as well as other pending patents.

CONFIDENTIAL

CONFIDENTIAL

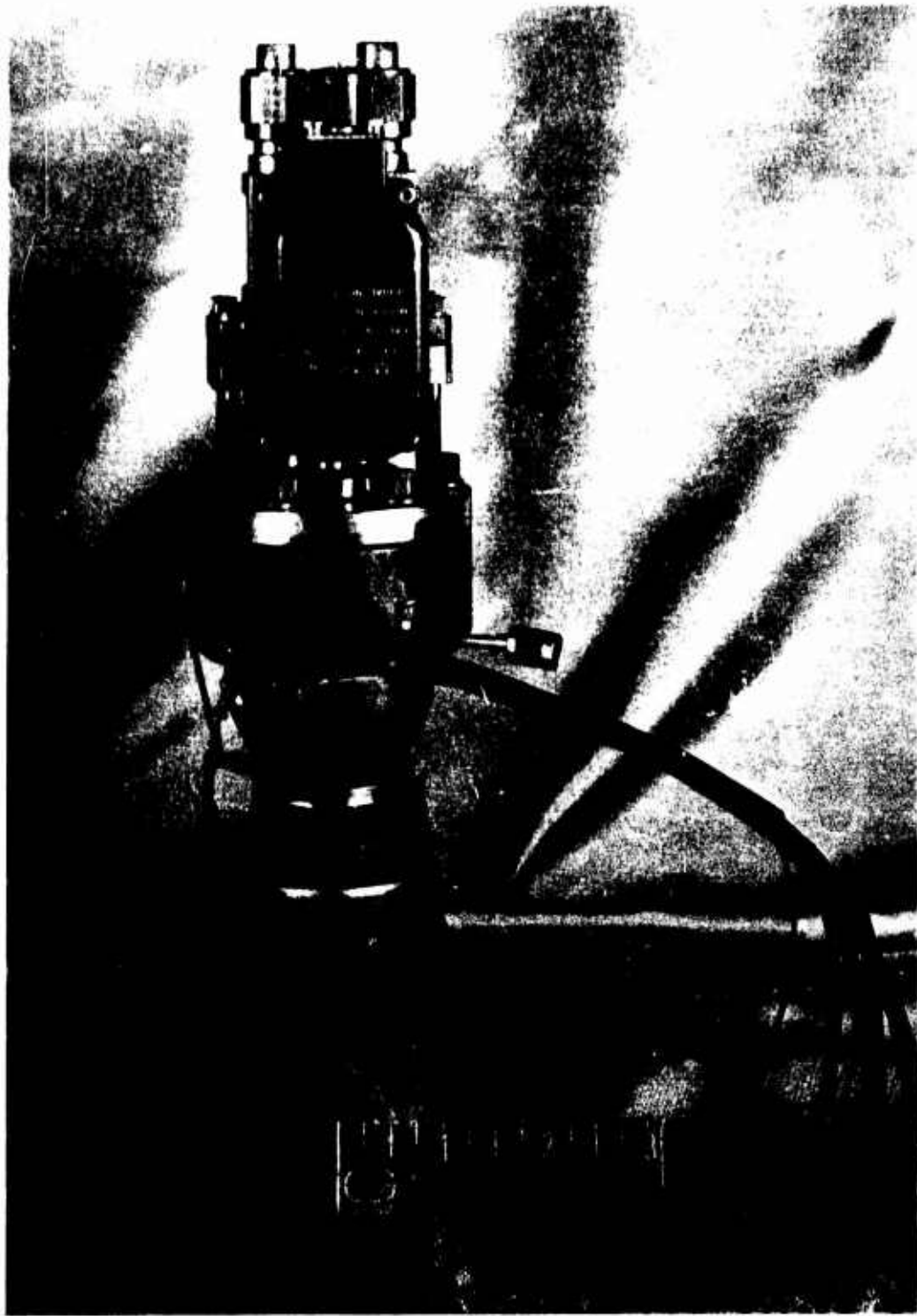


Figure 1. Bipropellant ACS Engine

Page 4

CONFIDENTIAL

(This page is Unclassified)

CONFIDENTIAL

Report AFRPL-TR-69-88

II, Summary (cont.)

D. POSITIVE EXPULSION PROPELLANT TANK DEMONSTRATION

(U) The original feasibility demonstration of a ring-stabilized propellant expulsion tank was by subcontract to Arde, Inc. of Mahwah, New Jersey under the prime Aerojet-General Contract AF 04(611)-11614. These initial expulsion bladder tests demonstrated the feasibility of the concept in a propellant tank size which was equivalent to the expected Advanced ICBM PBPS. Additional development and demonstration of the ring-stabilized expulsion bladders were accomplished as part of the redirection of Contract FO4611-67-C-0095. This led to the fabrication of flightweight propellant tanks and satisfactory demonstration of propellant expulsion using monopropellant N_2H_4 hot gas pressurization (see Figure No. 2).

(U) Bladder shell fabrication difficulties were encountered during the program and resulted in non-uniform shell thicknesses. Developmental fabrication and test iterations were conducted to identify a means for providing bladder shell control during expulsion with the non-uniform thickness shells. A procedure for metal-flame-spraying a portion of the bladder shell to provide additional structural margin was adopted, but only was partially successful.

(U) The final demonstration of the flightweight propellant tanks was conducted with the expulsion of N_2O_4 and MMH, using the hot gas pressurization subsystem.

E. MAJOR CONCLUSIONS AND RECOMMENDATIONS

(U) The fluidic controls technological level has not advanced sufficiently to provide integral fluidic controls within the bipropellant ACS engine. Further fluidic component development with high pressure and temperature fluids is needed to provide the basic design parameters for the units before they can be incorporated into a system.

(C) The bipropellant PBPS ACS engine demonstrated excellent transient response and reproducibility with the HIPERTHIN injector concept as a result of small injector propellant manifold volumes and the low characteristic length (L^*) of the combustion chamber. The conductively-cooled, bimetallic chamber provided a thruster which is as rugged and durable as a workhorse steel unit while demonstrating an unlimited duration capability.

(U) The ring-stabilized expulsion tank concept provides a unique capability for containment and positive expulsion of a large mass of propellant with a very lightweight tank assembly. This concept offers many advantages over other positive expulsion tanks because of its lightweight welded steel method of constructions. However, it would be desirable to conduct another fabrication development iteration to produce the necessary bladder shell thickness before a tank assembly of this configuration is utilized for an Advanced ICBM.

CONFIDENTIAL

CONFIDENTIAL

REPORT NUMBER 100-100-100

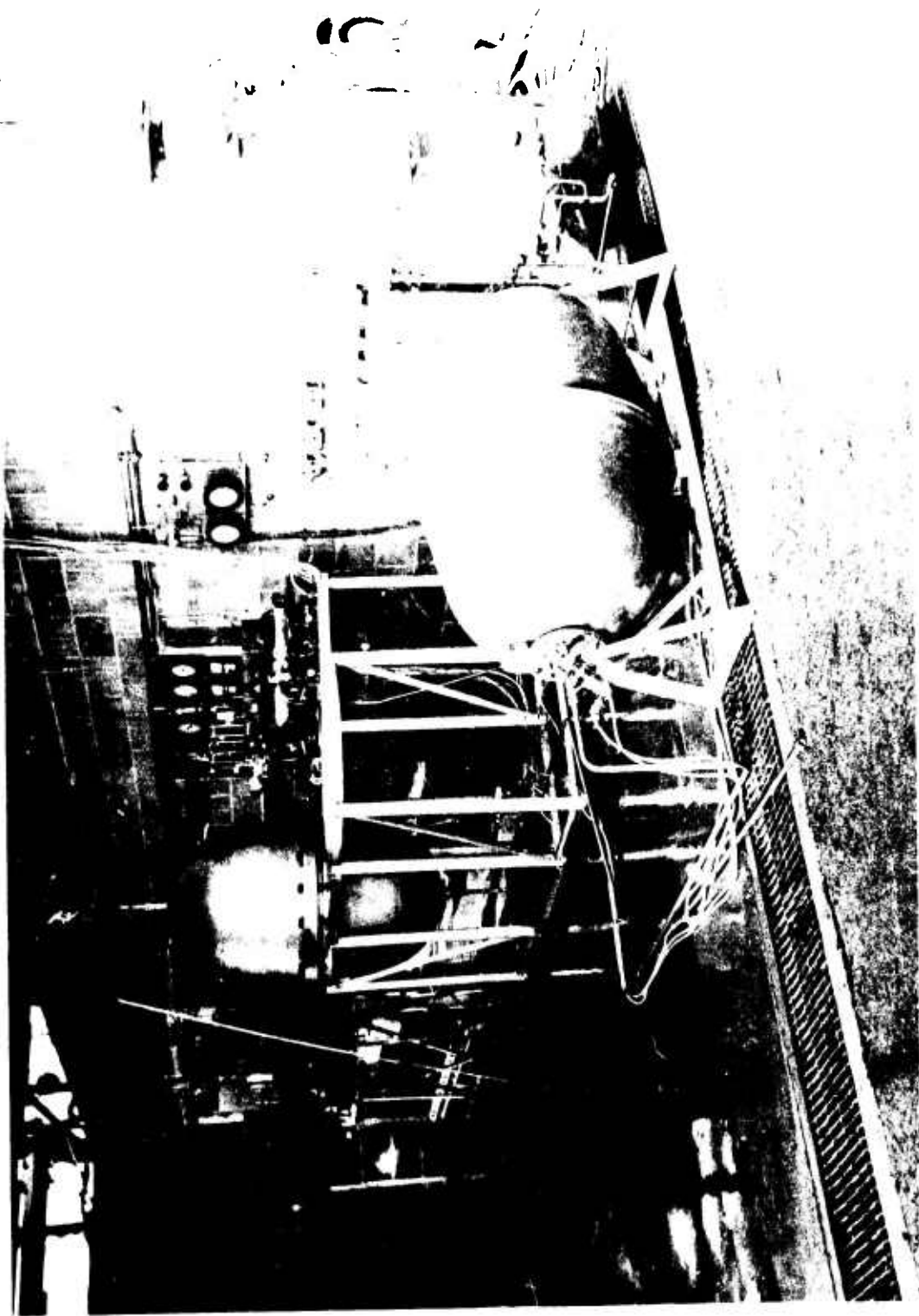


Figure 2. PBPS Propellant Tank for Hot Gas Expulsion

Page 6

CONFIDENTIAL

(This page is Unclassified)

CONFIDENTIAL

Report AFRPL-TR-69-88

SECTION III

ACS WITH INTEGRATED FLUIDIC CONTROLS

A. OBJECTIVES AND APPROACH

An initial program objective was the design and demonstration of an attitude control engine equipped with fluidic controls that were integral with the engine injector. These controls would serve to regulate the bipropellants (N_2O_4/MMH) as they pass through the injector and enter into the combustion chamber at either throttled operation of the thruster or when it is in the pulsing mode. Hot gas, provided by the monopropellant decomposition of hydrazine, would be utilized as the control fluid. This control fluid displaces the propellants in the control components thereby throttling and terminating the flow of propellant into the combustion cavity of the engine.

The program also specified that a heat-sink beryllium combustion chamber would be utilized with the integrated injector and controls to demonstrate the initial feasibility, performance capability, and operational life of a complete PBPS mission. The engine design criteria are shown on Table I.

This aspect of the program represented an application of the fluidic control component technology developed in the Advanced PBPS System Demonstration (Contract AF 04(611)-11614). This previous program was conducted for the purpose of developing the basic fluidic control component technology to provide control of propellants by utilizing the decomposition products of a monopropellant N_2H_4 gas generator and was to culminate in a demonstration of such propellant control in a workhorse bipropellant engine. The fluidic control development was subcontracted to the Bowles Engineering Company of Silver Springs, Maryland. Thus, the application of fluidic controls as a basic component of the injector in the program being reported herein was contingent upon the attainment of the necessary fluidic component technology in the previous program. The integration of fluidic control called for the following primary technological achievements:

- Development of vortex throttle technology to the point that throttles of slightly different configuration and orientation could be designed successfully.
- Development of the control modules for the vortex throttle valves to a level that only repackaging of an existing design would be necessary for control integration.

The development of an integrated injector/fluidic valve for use with a beryllium combustion chamber was programmed as a three-phase effort. It consisted of plastic flow model testing followed by workhorse and prototype engine tests. An initial selection process was needed to ascertain which injector/valve designs should be considered for flow model testing. However,

Page 7

CONFIDENTIAL

(This page is Unclassified)

CONFIDENTIAL

Report AFRPL-TR-69-88

TABLE I

INTEGRAL FLUIDIC ACS ENGINE DESIGN CRITERIA (U)

Design Goals

Thrust, lbf	75±10% (3 sigma)
Specific Impulse, sec	270 ± 5 sec (3 sigma)
Cut-Off Impulse (Signal to 10%) lbf-sec	2.25 ± 10% (3 sigma)
Mixture Ratio	1.6 ± 3% (3 sigma)
Total Mission Duration, sec	Worst case thermal duty cycle for a typical 900 sec PBPS mission

Established Design Criteria

Chamber Pressure, psia	150
Injector Orifice Pressure Drop, psi	100
Injector Manifold Pressure Drop, psi (max)	5
Control Gas Temperature, °F	1400
Control Turn Down Ratio	50:1 target
External Thermal Environment	Space
Allowable External Temperature Profile	400°F max backside temperature
Propellants	N ₂ O ₄ /MMH

CONFIDENTIAL

UNCLASSIFIED

Report AFRPL-TR-69-88

III, A, Objectives and Approach (cont.)

the concept selected had to be compatible with the flight hardware design requirements. Therefore, the first program activity was the preliminary design and analysis of prototype engine concepts. Layouts and preliminary analyses of flight hardware designs were completed and served as the basis for selecting the concepts for flow model testing.

Aerojet-General was to construct and evaluate at least three plastic flow models during the ACS injector design phase. Different approaches for achieving integration were to be utilized for each model. In one approach, the vortex valve also would serve as the propellant injector orifice. Following cold flow evaluations, an integrated injector control approach would be selected based upon turndown ratio, mixture ratio distribution, and the ease of quality control.

Development problems were encountered during the plastic model flow testing in this program. When these problems were evaluated in context with those experienced in the previous program (Contract AF 04(611)-11614) where the workhorse fluidic valves were subjected to propellant flow testing (Ref. 1), the deficiencies relating to the basic fluidic vortex throttle and hot gas control module were identified. It was found that the technology for the basic vortex throttle and the components of the hot gas control module was not sufficiently advanced to provide the operational control required for the ACS engine propellants. While these problems could be resolved through additional development effort, such work was not within the scope of the existing contractual funding.

The following sections identify the sequence of the integrated thruster design and component evaluation.

B. INTEGRATED ACS ENGINE DESIGN

1. Preliminary Design

The basic fluidic control component used for the engine propellant control is the vortex throttle concept designed and fabricated by the Bowles Engineering Company. The throttle consists of a cylindrical upper liquid chamber and a cylindrical lower gas chamber. Both the liquid and gas are injected tangentially into their respective chambers with both fluids expelled axially out of the bottom of the throttle. Vortex action is generated by the tangential injection and this swirling motion continues down the exit tube. Fluid inlet pressures establish the flow mode which can vary from all-liquid-flow-with-no-gas to all-gas-flow-with-no-liquid-flow.

The operation of the vortex valve uniquely influenced injector design. Certain assumptions were made and reviewed with the valve subcontractor. These assumptions were used to establish injector design criteria to

UNCLASSIFIED

UNCLASSIFIED

Report AFRPL-TR-69-88

III, B, Integrated ACS Engine Design (cont.)

ensure compatibility between the valve and the injector. These assumptions were:

- There will be some control gas entrained in the propellants even during full thrust operation. This gas-liquid mixture will not necessarily be homogenous.
- The propellants will be swirling at the exit from the vortex throttle.
- The centrifugal forces caused by the swirling will tend to stratify the gas-liquid mixture in the valve outlet tube resulting in a gaseous core-liquid annulus distribution pattern.
- Flow passage designs within the injector manifolds must include capability for nonpreferential distribution of the multi-phase gas-liquid mixture to the injector orifices to ensure that equal amounts of gas and liquid will flow through individual orifices during engine throttling.
- The influence of vehicle-induced acceleration forces resulting from asymmetry or angular orientation of the valves is not expected to influence the operation of the fluidic components.

The criteria used in the concept and design phase were the specified performance and system operational goals, a 10:1 throttling capability, and the requirement that the valve outlet orifice would be used in at least one concept as the injector inlet orifice to provide direct injection from the valve into the combustion chamber. Other considerations were that fuel film cooling would be required and that proven film coolant injection techniques would be used. A coolant flow rate of approximately 40% of the total fuel flow was assumed to be needed to operate for the worst thermal duty cycle based upon the data available from earlier programs.

Conceptual design studies were made to identify injector/valve configurations to meet the requirements of this program. Five basic injector types were considered. Design variations of some injector types were made to improve earlier concepts or to incorporate throttling capability. Layout drawings of the five flightweight injector concepts with various valve designs were made to define workable prototype hardware for further analysis and concept selection. Subsequent to design reviews and informal communication with AFRPL representatives, four concepts were selected for plastic flow model design.

UNCLASSIFIED

UNCLASSIFIED

Report AFRPL-TR-69-88

III, B, Integrated ACS Engine Design (cont.)

The injector/valve combinations selected for further analysis and plastic flow model design were:

- Doublet injector with side-by-side valves. It was expected that this would be the most easily developed design for nonthrottling application.
- Swirl-cup injector with coaxial valves to provide improved throttleability and shorter response time than could be achieved with the side-by-side valves.
- Impinging sheet injector with axially-mounted valves to provide chamber cooling without the use of complex coolant distribution manifolds.
- Direct injection pentad with multiple valves to provide short engine response and an injector simplified by the absence of manifolds between the valve and the combustion chamber.

The following are descriptions of each injector concept selected for flow model and analysis.

a. Doublet Injector

Figure No. 3 shows an eight-element, unlike doublet injector with side-by-side orientation of the propellant control valves. In this concept, a conventional injector pattern design and a manifold design suitable for liquid propellants only is used. This design incorporates provisions for uniform propellant distribution during throttling. The manifold design introduces the fuel into the annular distribution manifold tangent to the outer periphery to provide uniform distribution. An alternative manifold design is shown which has a deflector ring integral with the manifold to ensure circumferential motion prior to exposing the fuel to the outlet ports. The distribution of the fuel from the manifold to the injector elements and the film cooling orifices is accomplished by the use of 24 equally-spaced outlets in the manifold. The identical geometry of each orifice inlet and the use of separate passages results in nonpreferential distribution of the gas-liquid mixture to each combustion fuel and fuel coolant orifice.

b. Swirl-Cup Injector

Figure No. 4 presents a four-element, swirl-cup injector using manifolding to supply the elements from one fuel and one oxidizer propellant control valve. Although coaxial valves were used in this configuration, a side-by-side valve arrangement also is possible by utilizing the previously

UNCLASSIFIED

UNCLASSIFIED

Report AFRPL-TR-69-88

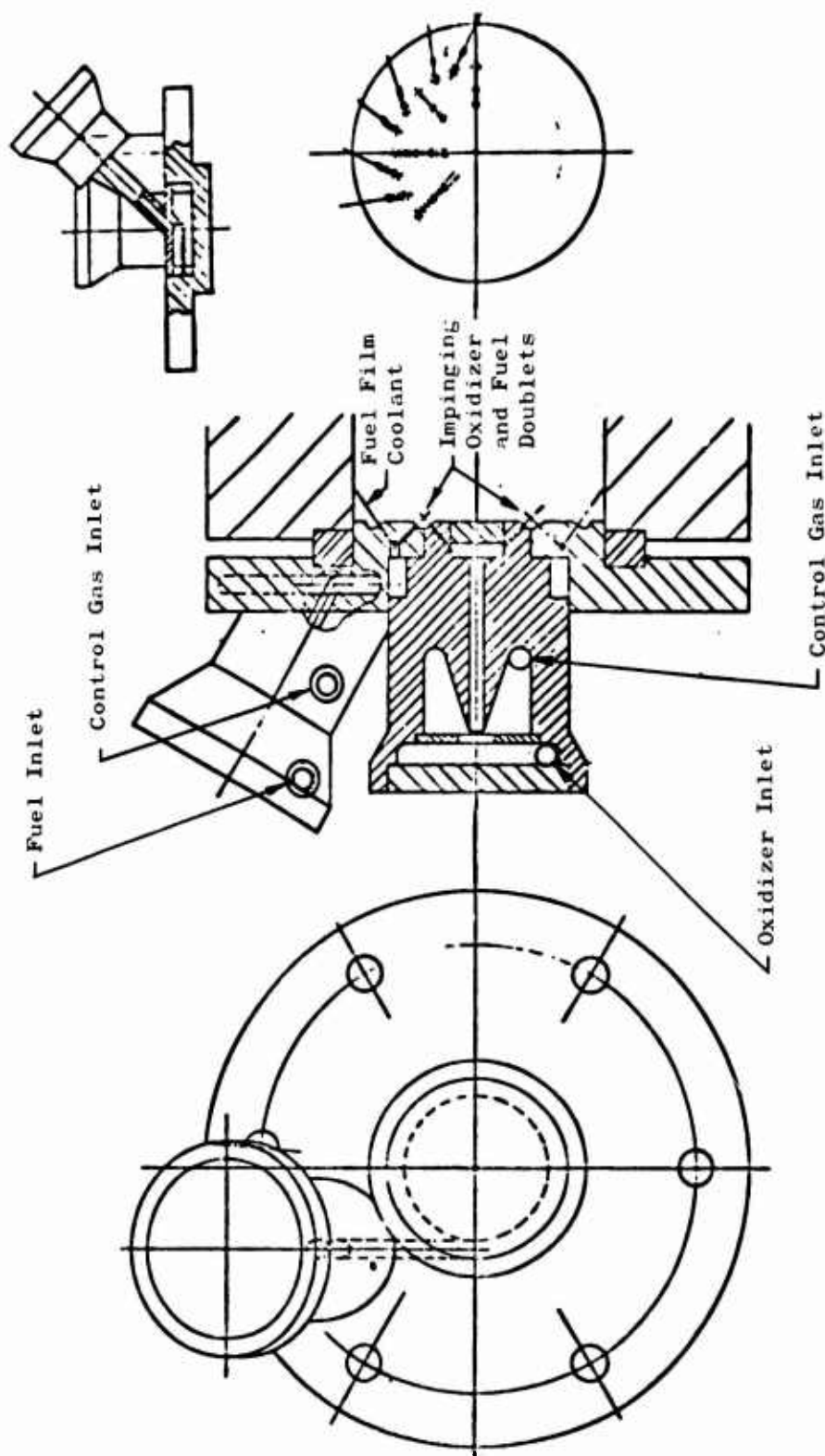


Figure 3. Doublet Injector Side-By-Side Vortex Valves

UNCLASSIFIED

UNCLASSIFIED

Report AFRPL-TR-69-88

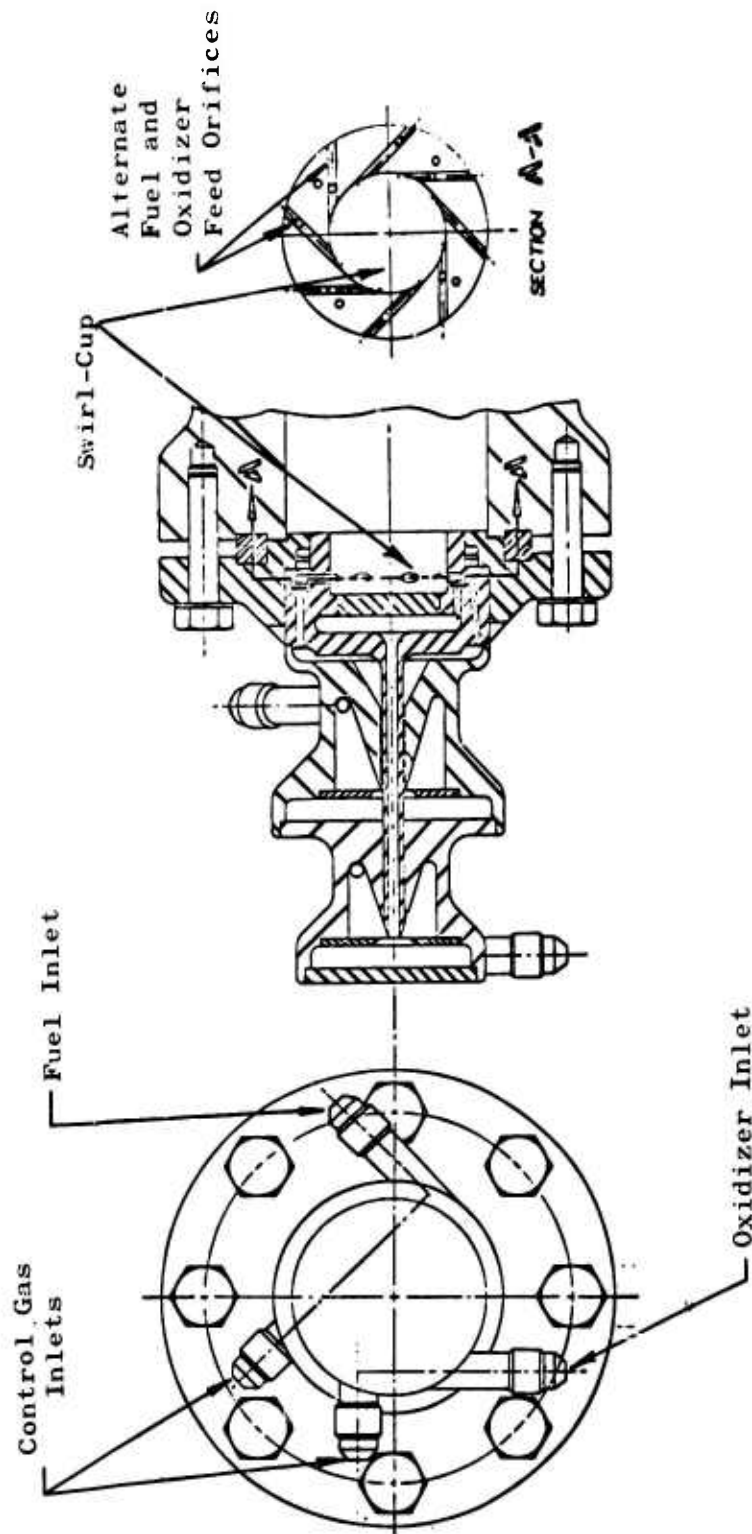


Figure 4. Swirl-Cup Injector - Coaxial Vortex Valve

UNCLASSIFIED

UNCLASSIFIED

Report AFRPL-TR-69-88

III, B, Integrated ACS Engine Design (cont.)

described manifold design. The use of four elements instead of two, such as was used in the multiple valve design, will provide improved performance. The manifolding will result in longer response times than are available with the direct injection design.

c. Impinging Sheet Injector

Figure No. 5 illustrates an impinging sheet injector concept with axially-mounted propellant control valves. In this design, the forward end of the beryllium combustion chamber is used as the deflector for the fuel. The presence of all of the fuel on the forward end of the combustion chamber is intended to serve as the heat-sink for conductively-cooling the chamber and eliminates the need for secondary boundary layer cooling. Manifolding and propellant distribution techniques are similar to those used for the previously described doublet injectors, except that they are simplified by the absence of the secondary coolant manifolds.

d. Direct Vortex Injection Pentad

Figure No. 6 shows a direct injection design which requires a single oxidizer valve and four fuel valves. This concept depends upon the swirling action of the vortex valves to develop hollow spray cones to give adequate mixing of the fuel and oxidizer. Also, a portion of the fuel from the outer four valves is impinged upon the combustion chamber wall for chamber cooling. Tests with a plastic valve model and various outlet configurations showed the angle of the resultant spray cone to be erratic over a range of throttling. No further effort was attempted with this concept.

2. Analyses

a. Performance Analyses

Performance, heat transfer, and design analyses were completed to aid in the evaluation of injector concepts under consideration. The depth of these analyses varied from the screening of potential concepts to the detailed performance analysis of a specific injector design. A cursory, qualitative type analysis was made to rank various injector concepts as a basis for selecting those for possible integration with the vortex valves.

Design analysis and performance predictions were made for an eight-element, unlike doublet injector for use with 40% fuel film coolant. The operating conditions of this design were:

$$\begin{aligned}\Gamma_v &= 75 \text{ lbf} \\ P_v &= 150 \text{ psia} \\ A_e/A_t &= 40:1\end{aligned}$$

UNCLASSIFIED

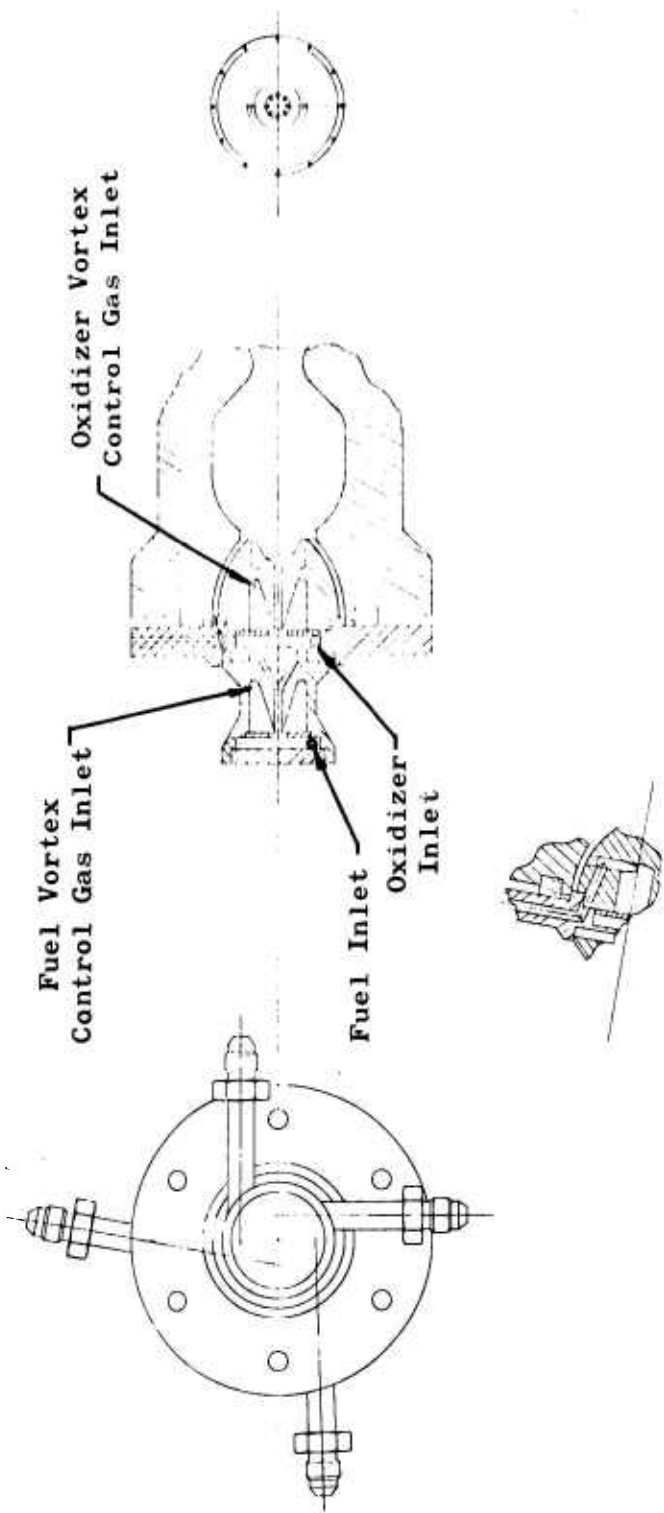


Figure 5. Impinging Sheet Injector, Axially-Mounted Vortex Valves

UNCLASSIFIED

Report AFRPL-TR-69-88

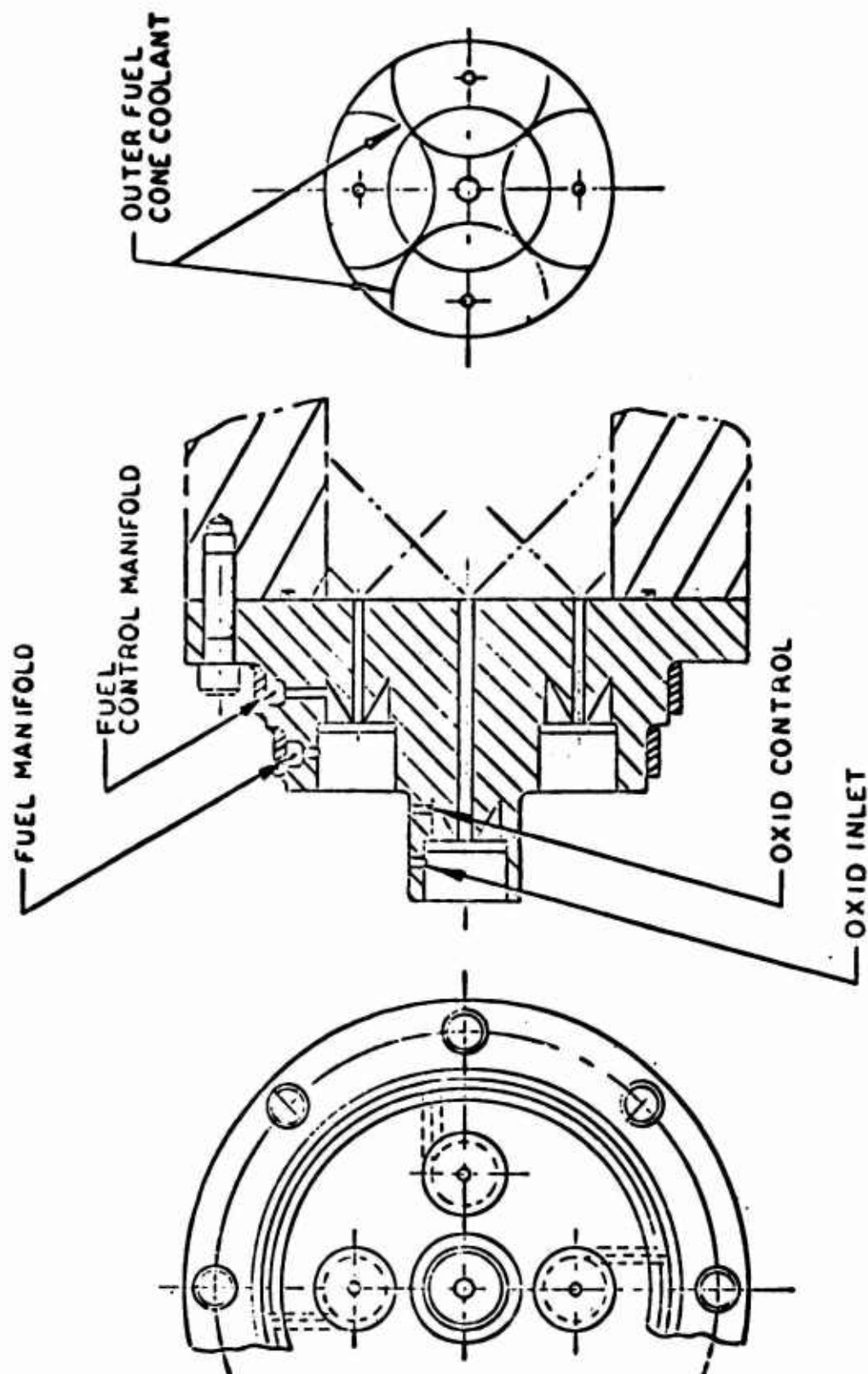


Figure 6. Direct Injection Pentad Multiple Vortex Valves

UNCLASSIFIED

CONFIDENTIAL

Report AFRPL-TR-69-88

III, B, Integrated ACS Engine Design (cont.)

N_2O_4 /Propellant
O/F = 1.6 with 40% of fuel film coolant
Contraction Ratio = 7.3
Chamber Length = 2.2-in. (injector face to throat)
Chamber Diameter = 1.750-in.

A summary of the recommended design parameters for the injector are:

N_2O_4 Orifice Diameter, $d_o = 0.024$; $L/d = 7$, $P_o = 100$ psi
MMH Orifice Diameter, $d_f = 0.020$; $L/D = 7$; $P_f = 48.5$ psi = 27-degree (defined on Figure No. 1)
Impingement Angle = 90-degrees

(C) The injector was predicted to obtain $97 \pm 2\%$ energy release, with 282 ± 10 sec of specific impulse predicted at the design conditions.

(C) The basic vaporization model (Ref. 2) was used to synthesize the injector parameters. The "splash plate" factor of 22% was applied to droplet sizes as discussed in Appendix A and the following results were obtained:

% N_2O_4 Vaporized = 99%
% Core Fuel Vaporized = 95%
% Fuel Film Coolant Vaporized = 100%
Core ER = 97%
Theoretical Core $I_s = 335.0$ sec
Energy Release Loss = 10.0 sec
Core I_{sp} without nozzle losses = 325.0 sec
Theoretical Coolant $I_{sp} = 242$ sec (monopropellant)
Max $I_{sp} = 311$ sec (core)
Friction Loss = 1.9%
Geometry Loss = 1.4%
Kinetic Loss = 5.4%
Nozzle Losses = 8.7%
Nozzle Losses = $8.7\% \times 330 = 28.7$ sec
Predicted $I_{sp} = 311 - 28.7 = 282.3$ sec

(C) A tolerance of ± 10 sec was applied to the predicted I_{sp} because of the following qualifications:

CONFIDENTIAL

CONFIDENTIAL

Report AFRPL-TR-69-88

III, B, Integrated ACS Engine Design (cont.)

With 40% fuel film coolant, sufficient mixing between core and coolant probably would occur to an extent that the assumption of stream tube flow would be somewhat in error. This affects the mixture ratio distribution loss as well as the nozzle kinetic loss because the latter is very mixture ratio sensitive (e.g., the kinetic loss varies from 2% at $O/F = 1.6$ to 6% at $O/F = 2.5$). Partial mixing of the coolant with the core would alter the core mixture ratio; therefore, the kinetic loss was estimated to be between the over-all mixture ratio and the core mixture ratio.

b. Thermal Analyses

The impinging sheet injector pioneered by the Jet Propulsion Laboratory was one of the injector concepts selected for use with the fluidic vortex valves. In this concept, a liquid propellant stream directed upon a flat surface is used to create a reflected sheet of liquid. The thin sheets of fuel and oxidizer provide excellent mixing when they are made to impinge. The purpose of this investigation was to evaluate the possibility of utilizing the injector in conjunction with a heat-sink chamber design to provide essentially steady-state operating capability without the use of secondary boundary layer cooling.

A two-dimensional heat transfer analysis was performed to investigate the feasibility of combining the impinging sheet injection concept with a regenerative heat-sink type of chamber design that uses no film cooling. The theory of operation in this design is that all of one or both propellants can be used to absorb heat from the chamber prior to mixing and combustion. This technique would reduce the combustion efficiency loss associated with film cooling and provide a less complex manifold design. The results showed that for the selected conditions, the propellant flow rate was more than sufficient to accommodate the heat input from bulk temperature rise aspect; however, the rate of heat input was too severe from a burnout consideration. It was apparent that the film cooling technique, as used in past regenerative heat-sink designs, provided two necessary functions. It absorbs heat from the heat-sink chamber and reduces the heat input to the chamber via boundary-layer mixture ratio control. It is the latter which was lacking in the impinging sheet injection concept. This heat input reduction function might be provided by a composite chamber design, wherein higher surface temperatures are maintained, or by adding film cooling to the existing design.

Heat flux levels to the fuel were found to be quite high across the wetted surface for the assumed conditions of this particular design. For example, a wetted surface area of 1.5 sq in. would produce a heat flux

CONFIDENTIAL

(This page is Unclassified)

UNCLASSIFIED

Report AFRPL-TR-69-88

III, B, Integrated ACS Engine Design (cont.)

level of 5.0 Btu/in.² sec. This heat flux was the maximum allowable for monomethyl-hydrazine flowing in a tube at a velocity of 100 ft/sec and a sub-cooling of 200°F. Indications were that the burnout heat flux for a liquid flowing adjacent to a wall and having a free boundary exposed to gas would be less than that for the liquid flowing in a tube at similar conditions (Ref. 3). One explanation for this is that vapor bubbles, formed at the liquid-wall interface by the nucleate boiling process, are forced to enter the main liquid stream in the case of a tube, whereas in the free boundary case, the vapor bubbles tend to push the liquid layer away from the wall and into the gas stream, forming liquid droplets. The wall cooling phenomena is reduced to a forced convection mechanism downstream of the point at which liquid droplets are formed as opposed to continued nucleate boiling in the case of a tube.

Injector design calculations showed that for the selected conditions, wetted surface areas above 0.5 sq in. would result in element designs that would produce non-uniform liquid sheets resulting in reduced combustion efficiency. Thus, it was apparent that the input heat flux had to be lowered to utilize this method because the throat surface temperatures associated with the smaller wetted areas were excessively high for beryllium application and would require a significant increase in wall thickness to become acceptable.

Successful operation of the impinging sheet injector might have been possible by using composite chamber designs (i.e., copper-inconel) to decrease input heat flux and/or the utilization of film cooling to decrease the over-all heat input to the chamber. In addition, it could have become necessary to generate the liquid sheets by flow-through tubes of rectangular cross-section rather than by impinging a liquid stream upon a flat surface. This technique would have eliminated the possibility of liquid droplet formation as well as allowed an increase in wetted surface areas for the regenerative cooling operation.

The heat transfer rates for this analysis were obtained analytically and appear to be somewhat conservative. Workhorse chamber testing is necessary to provide thermal data for a more detailed analysis. Burnout heat fluxes, for flow over the injector element, must be obtained by laboratory testing.

c. Thermal Analysis of Vortex Valve

Thermal analysis of the vortex valve assembly to provide criteria for hardware design was completed. The analysis of the vortex valve was performed to provide additional background information for use in selecting the design concept for the valve. This analysis represented a simplified approach to facilitate the investigation of the influence of geometry effects upon the suppression of two-phase (liquid-vapor) propellant flow through the valves. The influence of the injector was neglected because of the small manifold surface area in contact with the propellants in comparison with the valve.

UNCLASSIFIED

UNCLASSIFIED

Report AFRPL-TR-69-88

III, B, Integrated ACS Engine Design (cont.)

Two valve body designs were investigated in the analysis. The first one was designated as the nominal design and consisted of a relatively massive body design in comparison to the fluid cavity. The second one consisted of very thin walls surrounding the fluid cavity. In both cases, the body was assumed to be stainless steel and the controlled liquid was assumed to be nitrogen tetroxide. The internal heat transfer coefficients were estimated using conventional Nusselt number correlations for pipe flow. Surface velocities were predicted by free vortex flow equations and equivalent pipe radii were set equal to the radii from the valve axis to the surfaces in question. The thermal response of the bulk valve body was calculated for exposure to control gas (hydrazine combustion products) flow at 1300°F. It was determined that the valve body essentially reaches equilibrium with the control gas for durations approaching 10 minutes.

Upon initiation of subcooled liquid flow through the high temperature valve body, a condition of film boiling would be established and maintained until the internal wall temperature cooled sufficiently to establish the mechanism of localized nucleate boiling. As the valve walls would have cooled further, a condition of forced convection, without boiling, would occur. This preliminary thermal analysis was simplified to the point where only the forced convection mechanism was considered. This simplification was considered to be sufficient for establishing the advantages of thin wall over thick wall construction of the valve body. The influence of valve response delay provided by the mechanisms of film and nucleate boiling (which would provide two-phase flow) was present in each design; however, the duration of these boiling mechanisms would be less for a thin wall design because of the lower thermal capacitance of thin wall construction. The actual effect of these mechanisms would have to be established by laboratory experiment. The effect of the forced convection mechanism presented herein is added to that of the boiling mechanism.

This analysis indicated that a thin wall (low mass) valve could cause the N_2O_4 to film boil for 200 millisec while a heavier, higher heat capacity valve could cause film boiling for over 1 sec (based upon an initial valve temperature equal to the control gas temperature). In either case, the bulk temperature rise of the nitrogen tetroxide would be below the vaporization temperature of the N_2O_4 in approximately 30 millisec. The cooling rate of the low mass valve, upon introduction of the N_2O_4 , would be significantly faster than a heavier unit resulting in the shorter duration of film boiling.

3. Plastic Flow Models

The objective of the plastic flow model test program was to verify satisfactory valve operation with the downstream loads imparted by the injector; to determine the hydraulic characteristics of the injector caused

UNCLASSIFIED

UNCLASSIFIED

Report AFRPL-TR-69-88

III, B, Integrated ACS Engine Design (cont.)

by the swirling of the propellants and control gas; and to verify that the injector manifold designs would provide uniform propellant distribution over the range of throttling.

a. Criteria

The primary criteria used in the injector flow model design were that the fuel and oxidizer flow models could be made of separate hardware except in cases where the observance of the interaction between the fuel and oxidizer was necessary. Such a condition was possible with the impinging sheet injector where the control gas could have become entrapped and formed a barrier to prevent adequate mixing of the propellants. Provisions were made in these designs to duplicate, where possible, exact details of the manifolds to ensure that the data obtained was directly applicable to the prototype injectors.

b. Design

Designs of the doublet and swirl-cup injector flow models were completed. The oxidizer circuit of the doublet is shown on Figure No. 7. Multiple valve outlet orifices were designed to assist in evaluating the influence of the flow swirl component upon pressure drop. A short, cylindrical section of clear plastic, which simulated the chamber wall, was provided to permit close observation of the flow.

The doublet fuel circuit shown on Figure No. 8 provided three distribution manifold designs. Each was varied to determine the influence of configuration changes upon response time and distribution. Many components of this assembly were common with those made for the doublet oxidizer flow model.

Figure No. 9 shows the oxidizer circuit of the swirl-cup flow model. A simple, four-slot distribution manifold was used in this design. No orifice plugs were used in this hardware because momentum ratio variation was not required for swirl-cup injector design.

The swirl-cup fuel circuit is shown on Figure No. 10. The valve for this injector design is the annular valve of a coaxial valve assembly. Milled slots were used for the distribution of the fuel for combustion film cooling.

An adapter was designed to allow flow testing of the injectors without the valves to establish a baseline for comparing hydraulic data both with and without swirling flow.

UNCLASSIFIED

UNCLASSIFIED

Report AFRPL-TR-69-88

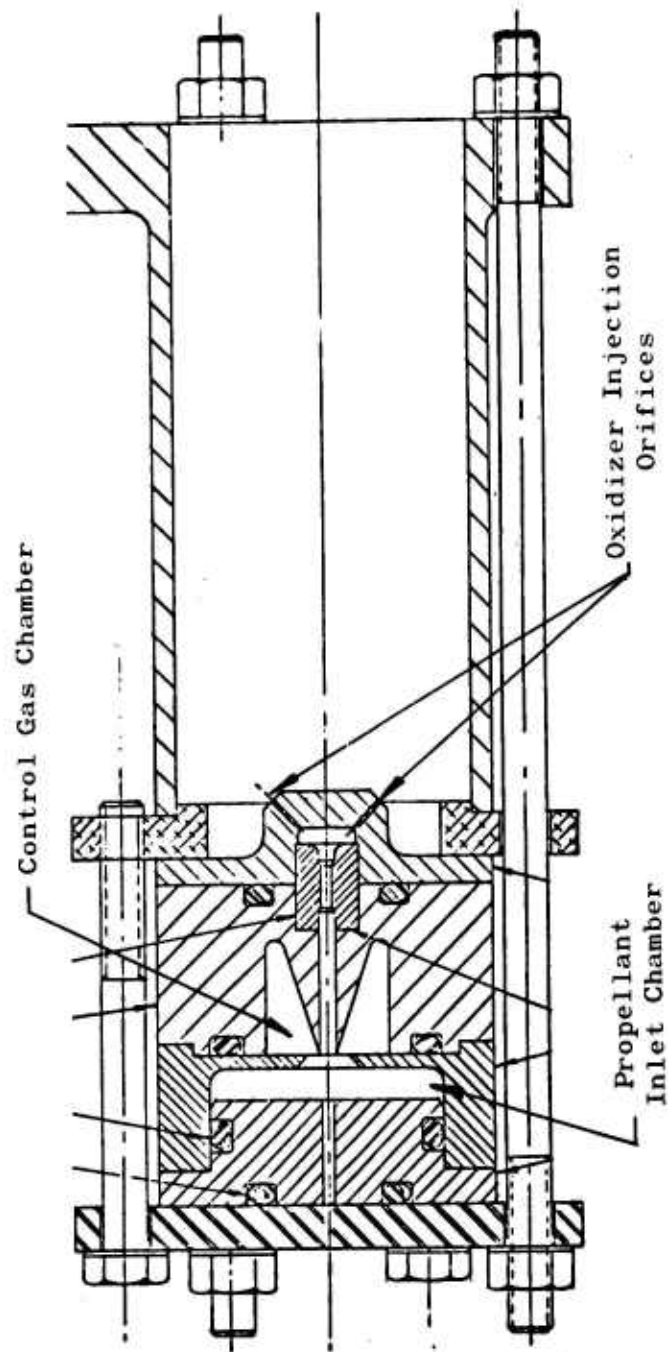


Figure 7. Flow Model Doublet Injector, Oxidizer Orifice

UNCLASSIFIED

UNCLASSIFIED

Report AFRPL-TR-69-88

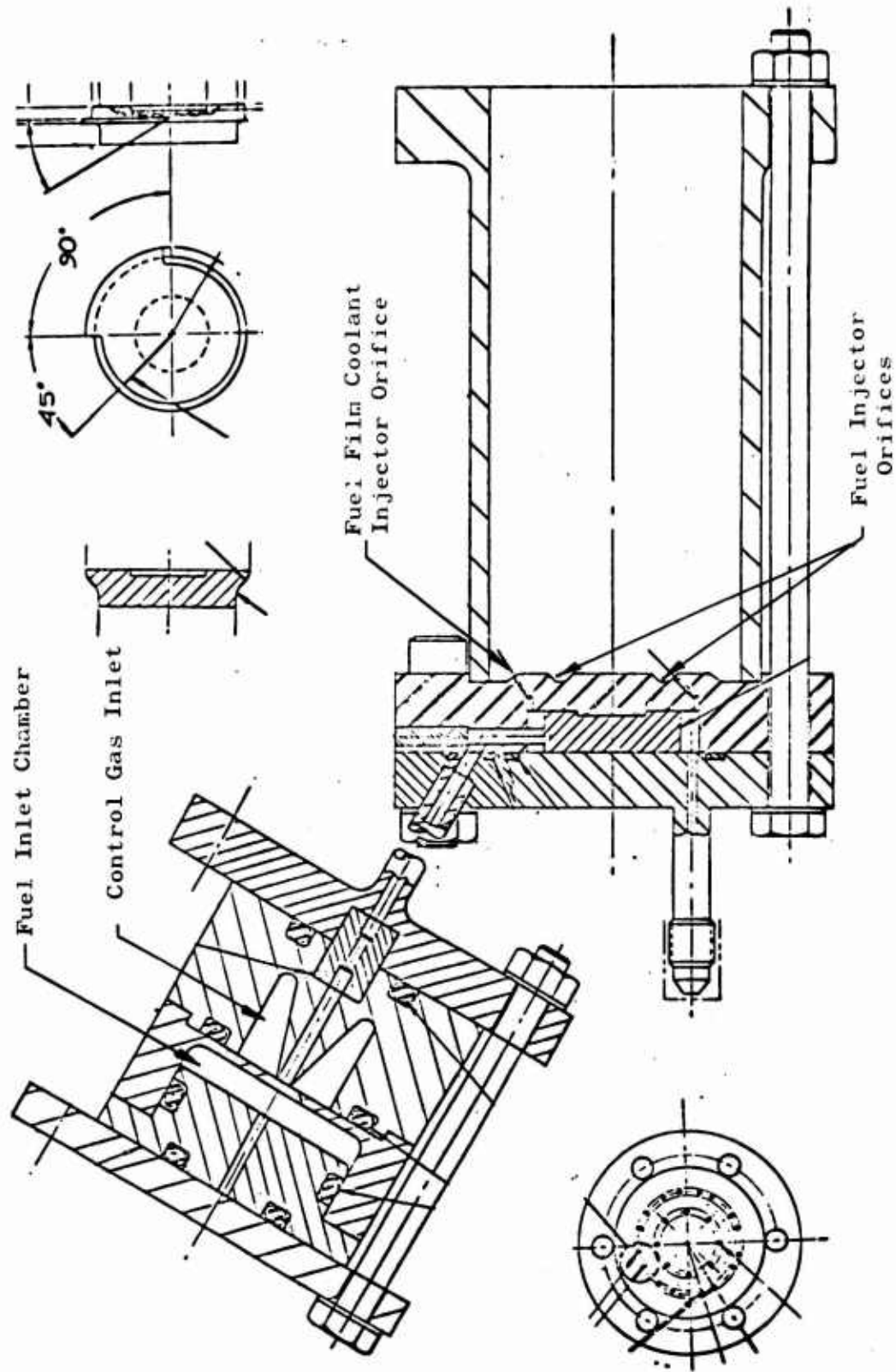


Figure 8. Flow Model Doublet Injector, Fuel Circuit

UNCLASSIFIED

UNCLASSIFIED

Report AFRPL-TR-69-88

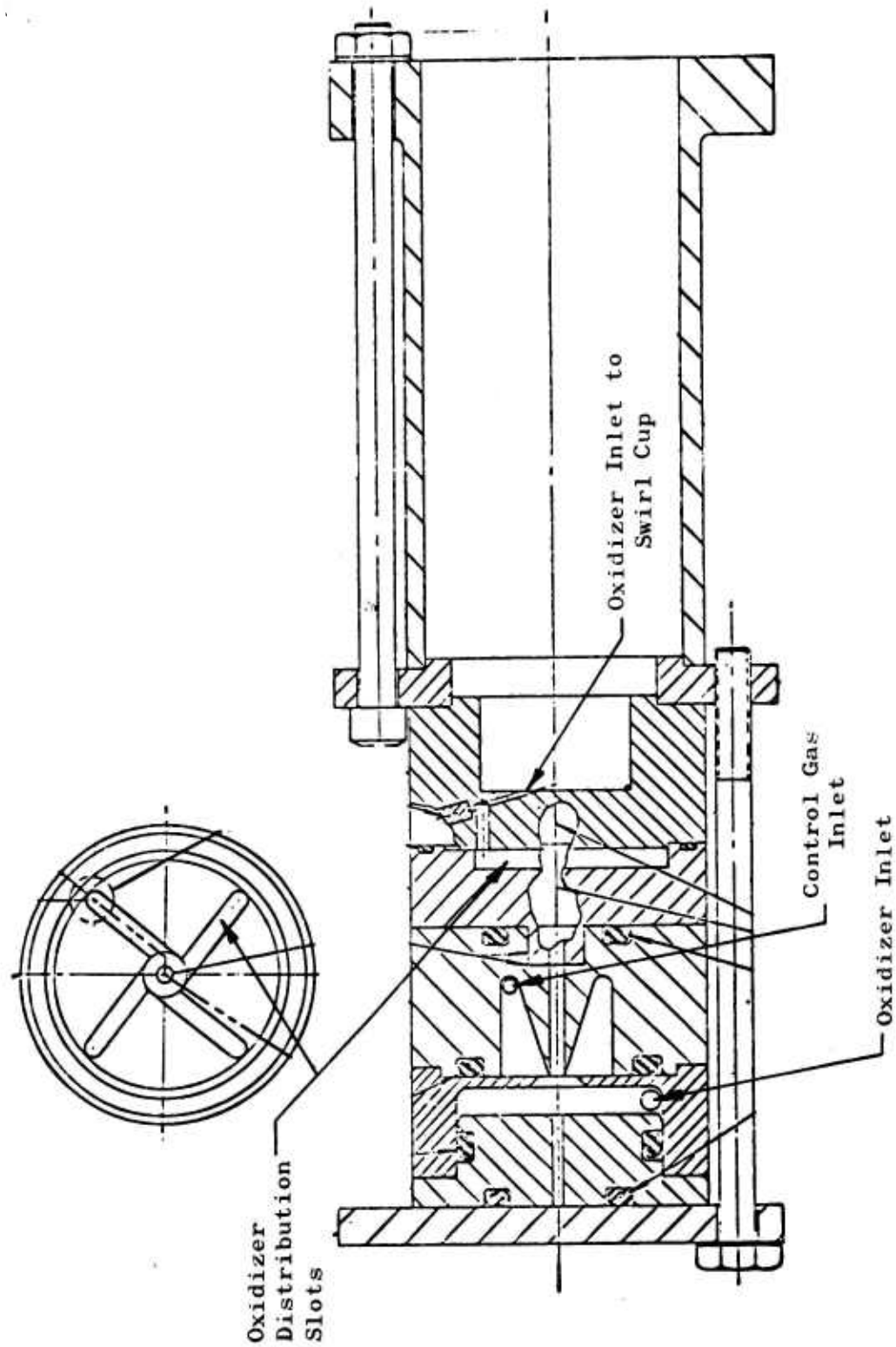


Figure 9. Flow Model Swirl Cup Injector, Oxidizer Circuit

UNCLASSIFIED

UNCLASSIFIED

Report AFRPL-TR-69-88

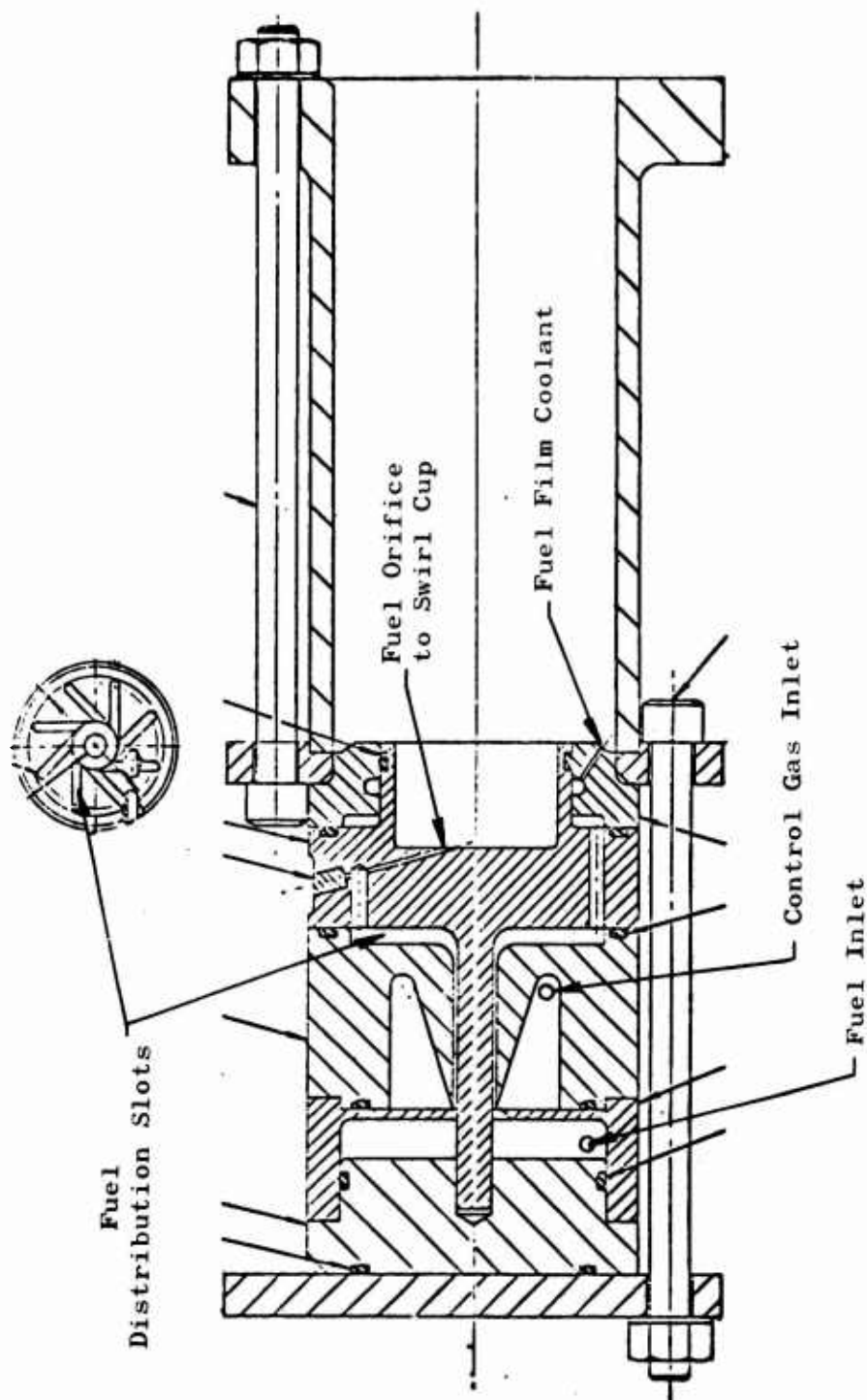


Figure 10. Flow Model Swirl Cup Injector, Fuel Circuit

UNCLASSIFIED

UNCLASSIFIED

Report AFRPL-TR-69-88

III, B, Integrated ACS Engine Design (cont.)

c. Flow Model Evaluation

The doublet oxidizer circuit was fabricated and flow-tested with the adapter only. No flow testing with the valves was accomplished. Fabrication of the other injectors was delayed pending the results of the propellant control valve development tests.

Flow tests of a plastic valve were made to evaluate the feasibility of the direct injection pentad concept. The results, described in Section III,A, indicated that the spray emanating from the valve outlet would not provide adequate mixing for efficient combustion and that the spray pattern varied over the throttling range.

C. ACS ENGINE FLUIDIC CONTROLS EVALUATION

1. Controls Configuration Definition

a. Vortex Throttle Design

The basic vortex throttle concept used in this program had been designed, fabricated, and tested in the previous effort under Contract AF 04(611)-11614. The workhorse oxidizer throttle and attached hot gas control module from that effort is shown on Figure No. 11. Both had been designed and fabricated by the Bowles Engineering Company under subcontract. Another subcontract was awarded to Bowles Engineering in this program for the purpose of designing vortex throttles that would permit integration of this throttle concept into an ACS engine. In addition, Bowles Engineering was required to participate at conceptual evaluation meetings held at Aerojet-General and to design as well as supply prints of vortex throttles that would satisfy the design objectives of an ACS throttle control. Aerojet-General was to perform the integration design effort and the model fabrication for plastic flow model testing.

Many integrated throttle/injector concepts were devised at the outset of the program, including direct injection concepts, integration with conventional injectors, integration with swirl-cup injectors, and impinging sheet injection approaches. Approaches using multiple vortex throttles, coaxial vortex throttles, and inverted vortex throttles were included in these concepts.

The number of candidate concepts was reduced as a result of the Aerojet-General/Bowles Engineering evaluation meetings and three basic throttles were defined to accommodate the remaining concepts. Table II is a listing of the basic criteria while Table III defines the configurations that were to be designed. It also was decided to eliminate the cone and turning vanes from the liquid chamber of the vortex throttle. This was done to assure

UNCLASSIFIED

UNCLASSIFIED

Report AFRPL-TR-69-88

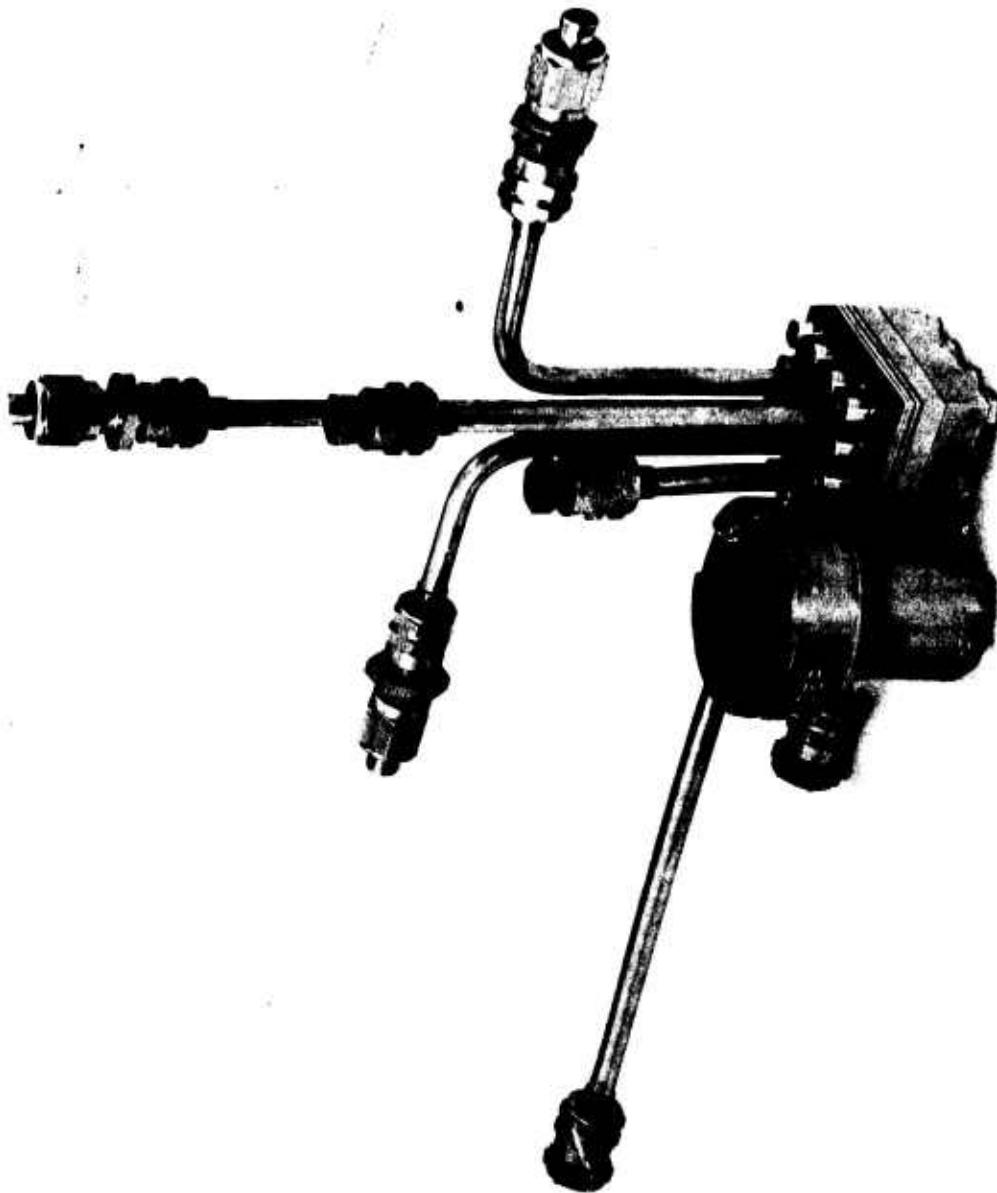


Figure 11. ACS Oxidizer Vortex Valve

UNCLASSIFIED

UNCLASSIFIED

Report AFRPL-TR-69-88

TABLE II
DESIGN DATA FOR VORTEX THROTTLE

Type of Control:	on-off
Propellants:	MMH and N_2O_4
Control Gas:	Decomposed hydrazine at 1300°F
Propellant Weight Flows:	Fuel 0.107 lb/sec Oxidizer 0.107 lb/sec
Pressure Drop:	Direct injection 100 psi Conventional injection 20 psi
Propellant Inlet Pressure:	304 psia
Environmental Conditions:	
Temperature	+40 - 140°F
Vibration	1.4 grams at 10-300 cps 3.0 grams at 300-2000 cps
Shock	14G parallel to vehicle axis 3G lateral axis

TABLE III
VORTEX THROTTLE TYPES FOR SELECTED INJECTION CONCEPTS

<u>Throttle Configuration</u>	<u>Flow Capacity</u>	<u>Pressure Drop, psi</u>
Conventional	rated	20
Conventional	rated	100
Conventional	1/4 rated	100
Coaxial	rated	20
Coaxial	rated	100

UNCLASSIFIED

UNCLASSIFIED

Report AFRPL-TR-69-88

III, C, ACS Engine Fluidic Controls Evaluation (cont.)

conical spreading of the throttle effluent (considered necessary for direct injection concepts) as well as to simplify fabrication and inspection (RFP-defined objective) although it represented a change from the configuration that was being fabricated for the demonstration contract effort. Another factor considered was the possibility of throttling the engine instead of operating it as strictly on-and-off. Propellant swirl would have been highly desirable for throttling operation because it would provide more homogenous mixing of the gas and liquid. Also, removal of the turning vanes permitted the vortex swirl action generated in the liquid chamber to be continued down the outlet tube and in the injector manifolds. This swirling would have tended to provide a more uniform mixing and more reproducible injection.

The basic throttle geometry shown on Figures No. 12 and No. 13 was designed by Bowles Engineering, based upon design requirements. Then, the full-size, single vortex geometry shown on Figure No. 14 was designed into a test throttle.

b. Fabrication of Controls Flow Models

Vortex throttle parts for the plastic flow model were machined from Plexiglas to the design shown on Figure No. 14. In addition to the basic throttle and retaining plates, special outlets were fabricated from Plexiglas to allow for evaluation of direct injection patterns. These parts are shown on Figures No. 15 and No. 16. Two gas chamber sections were fabricated with different outlet hole diameters to duplicate the sizes defined for use with an injector downstream of the throttle and for direct injection. A vortex suppressor was another part fabricated from Plexiglas. It was made after high pressure drop across the throttle was noted. This suppressor was centered in the liquid chamber of the vortex throttle and retained by the clamping force on the assembly.

c. Flow Model Testing

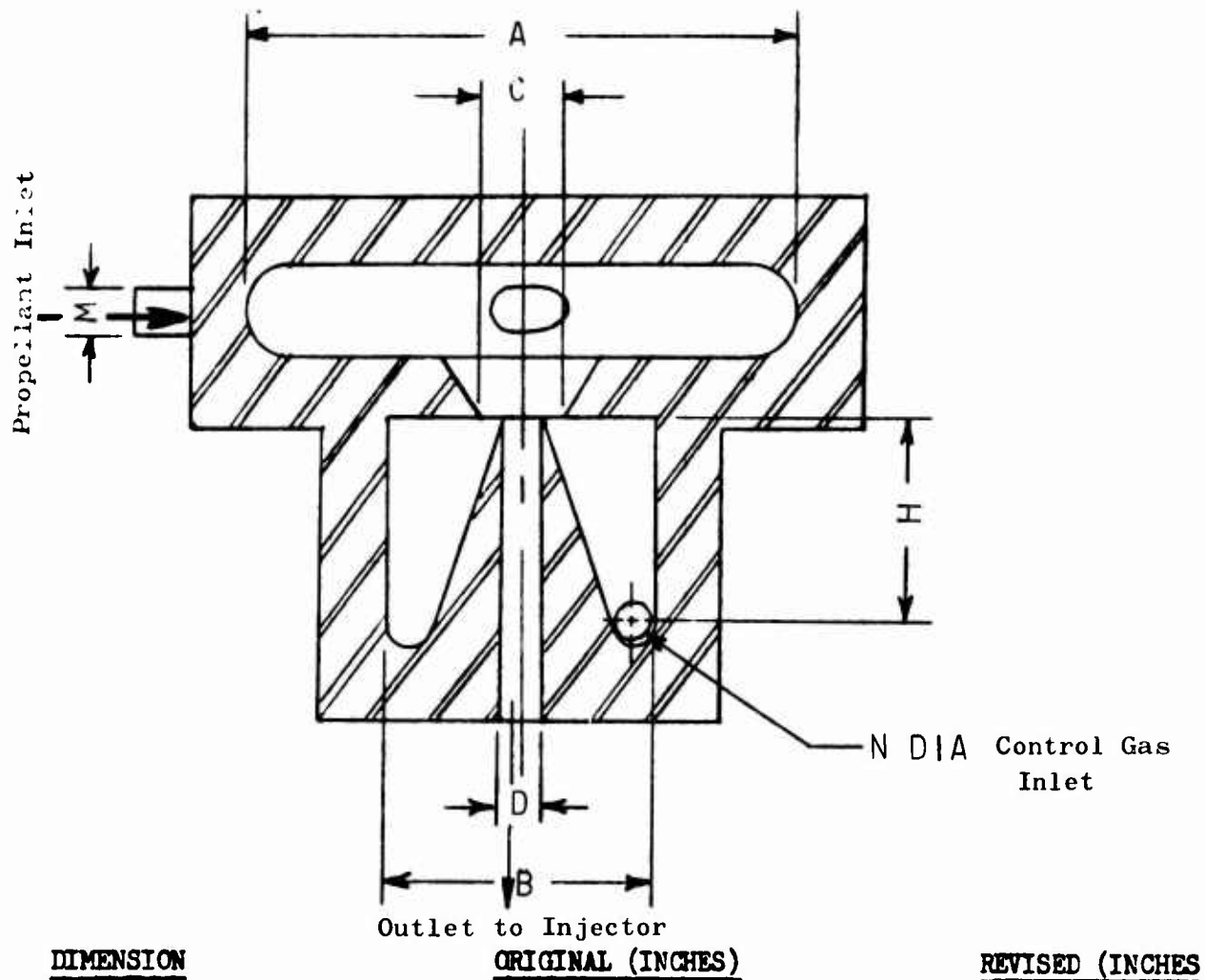
The plastic vortex throttle was tested using ambient GN₂ and water as the test fluids with the throttle discharging to atmospheric pressure. Figure No. 17 is a test schematic. The basic test set-up shown on Figure No. 18 include the modifications added for subsequent throttle testing. The major additions were the pressure transducers, snubber-isolation valves for pressure sensing lines, a backpressure valve, and a bladder accumulator in the water supply line.

Initial tests were run with the basic vortex throttle only. These tests revealed an excessive pressure drop for liquid flow. The design pressure drop values were 20 psi at rated flow for the throttle used with a conventional injector and 100 psi for the direct injection throttle.

UNCLASSIFIED

UNCLASSIFIED

Report AFRPL-TR-69-88



DIMENSION

ORIGINAL (INCHES)

REVISED (INCHES)

A	1.375	1.950
B	.750	.980
C	.250	.325
D	.100	.140
H	.594	.655
M	.125	.181
N	.125	.181

Figure 12. Simple Vortex Throttle

UNCLASSIFIED

UNCLASSIFIED

Report AFRPL-TR-69-88

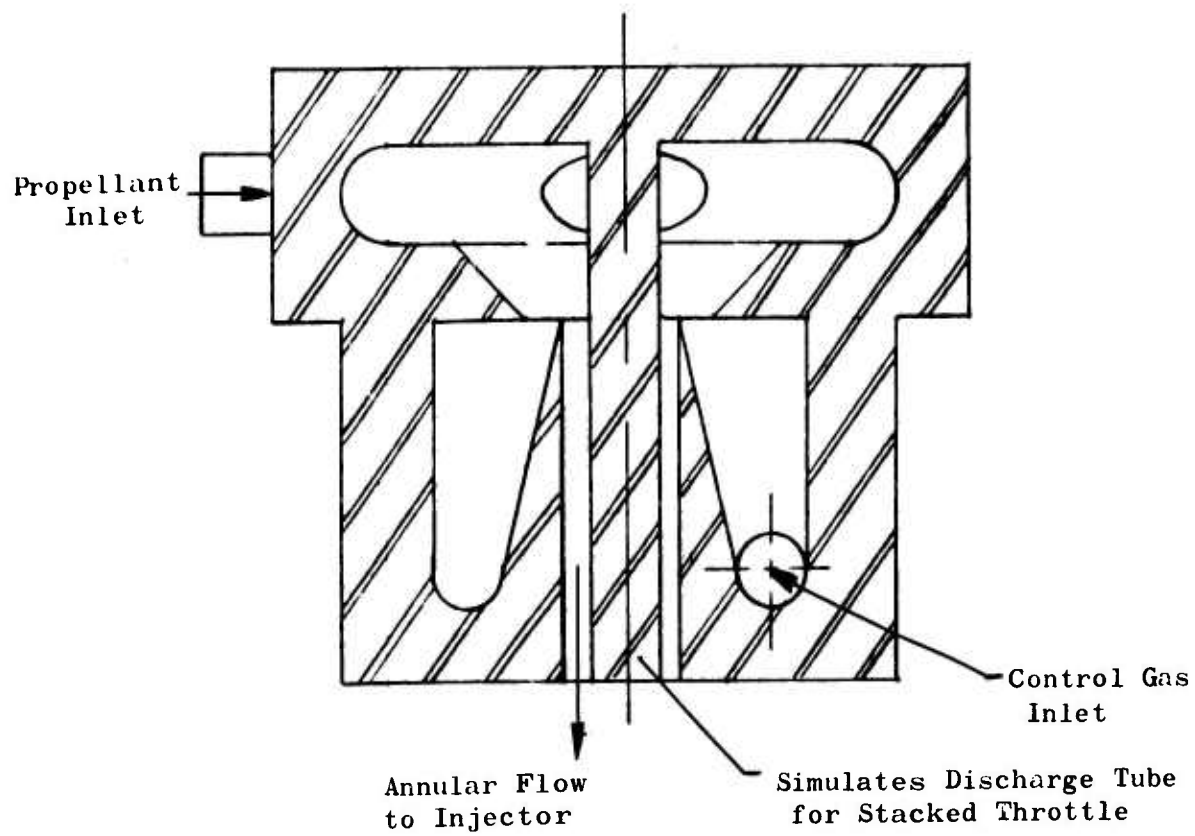


Figure 13. Coaxial Vortex Throttle

Page 31

UNCLASSIFIED

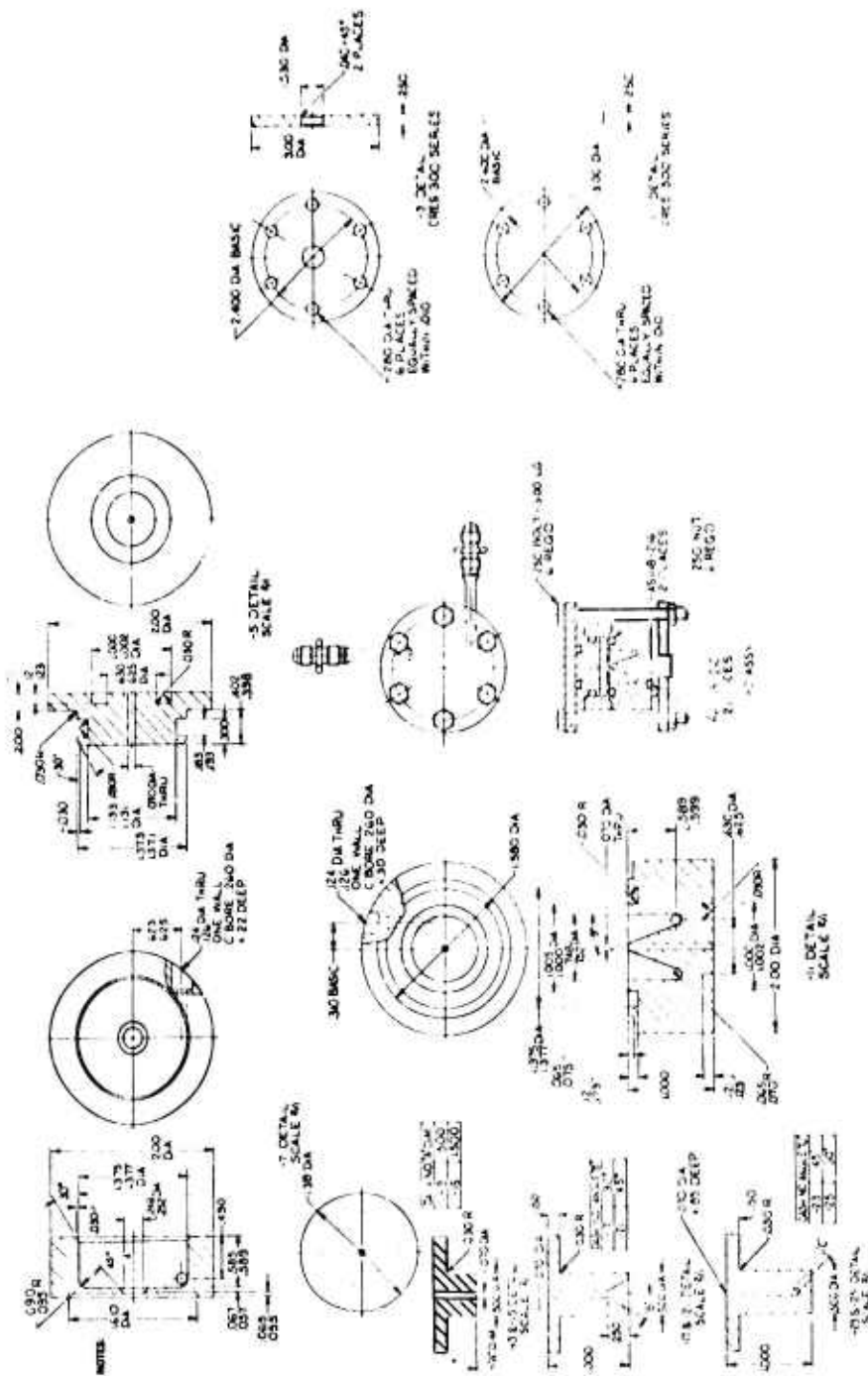


Figure 14. Vortex Throttle Test Assembly

UNCLASSIFIED

UNCLASSIFIED

Report ADP 11-60-5

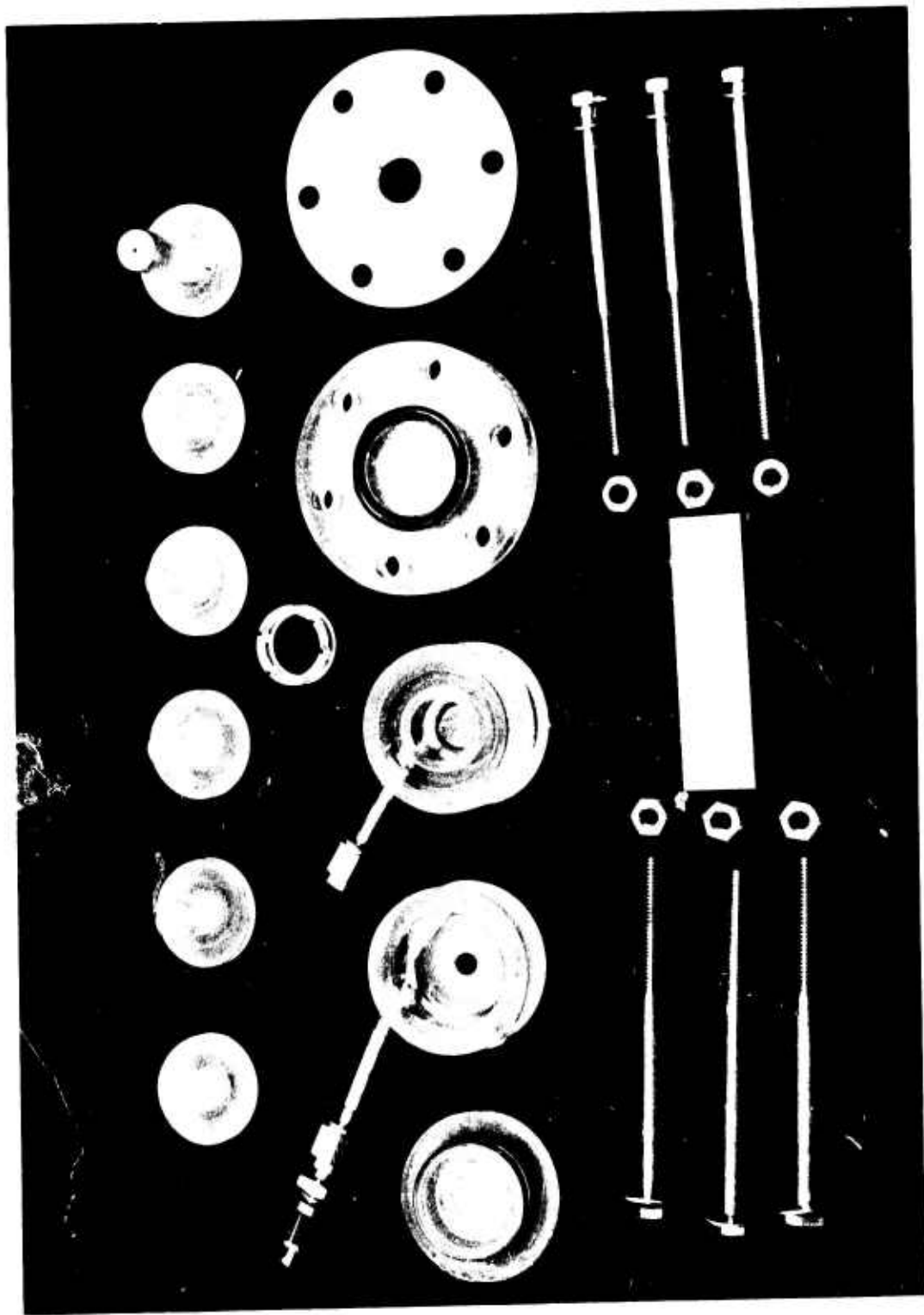


Figure 15. Vortex Throttle Test Hardware

UNCLASSIFIED

UNCLASSIFIED

REPORT NUMBER 11-60-41

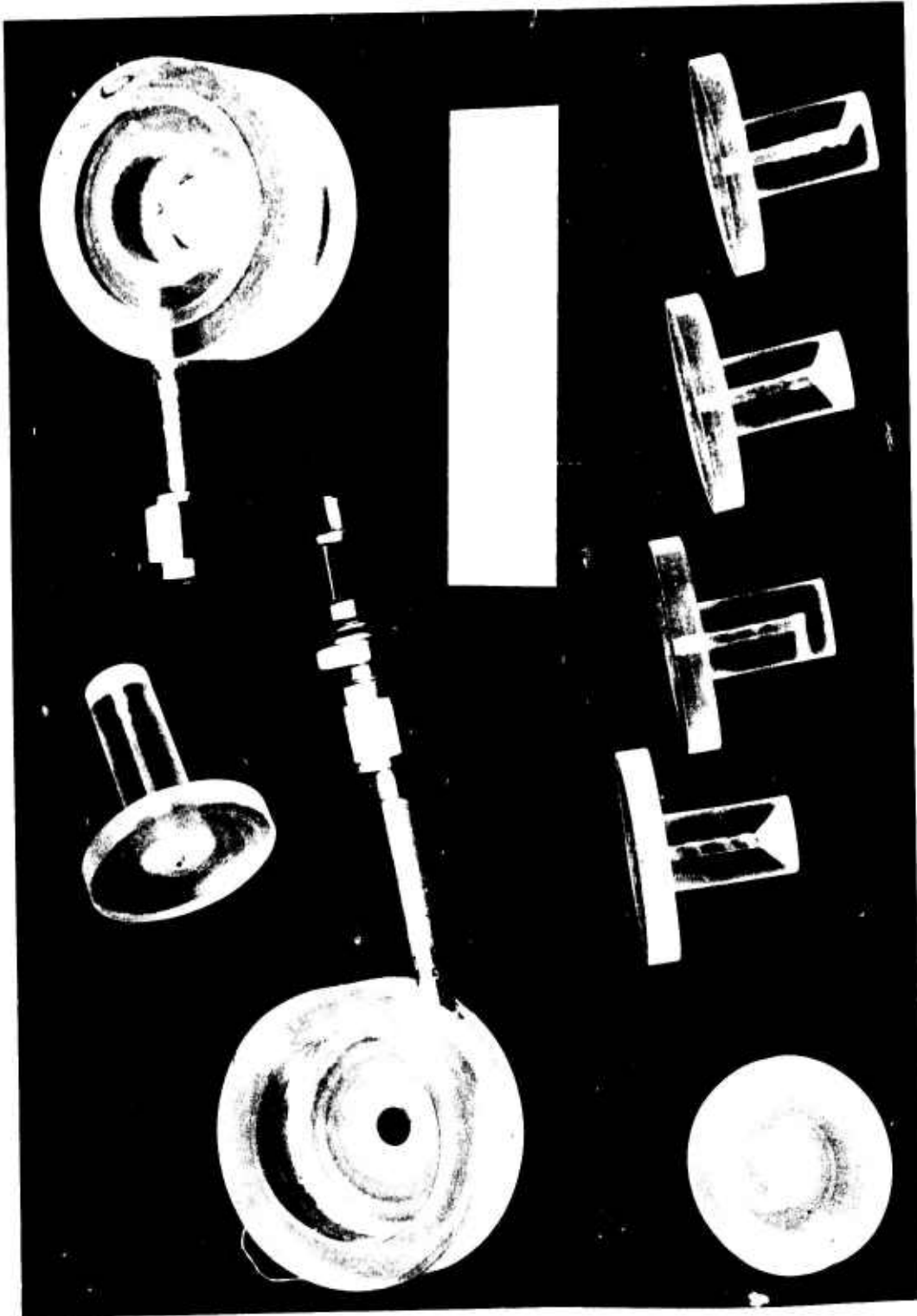


Figure 16. Fluid Chambers and Outlet Fittings

UNCLASSIFIED

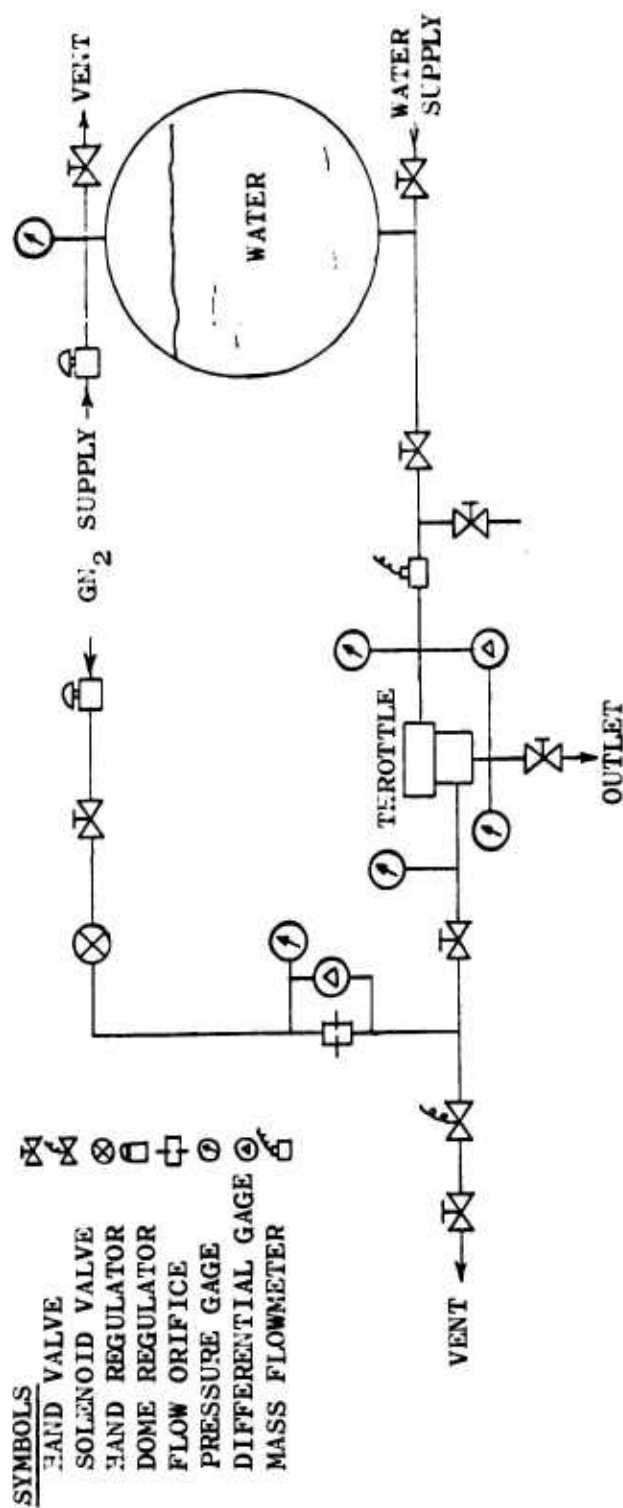


Figure 17. Test Schematic

UNCLASSIFIED

Report AFRPL-TR-69-88

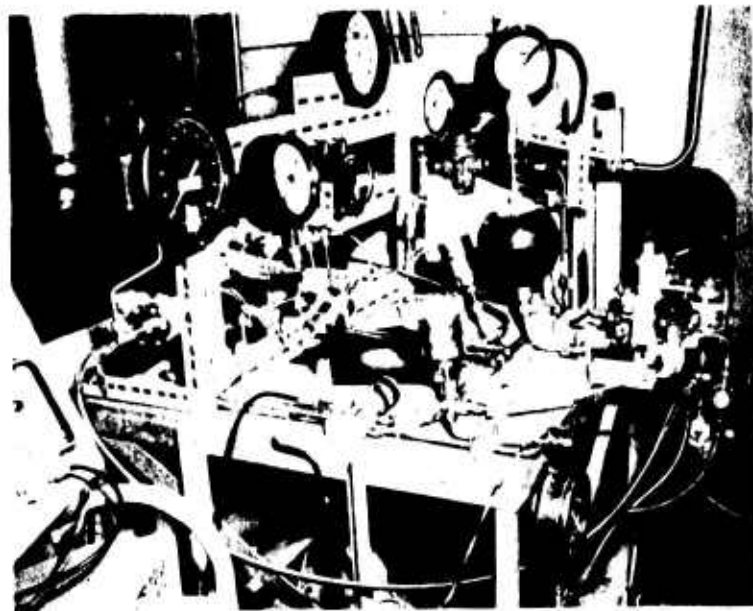
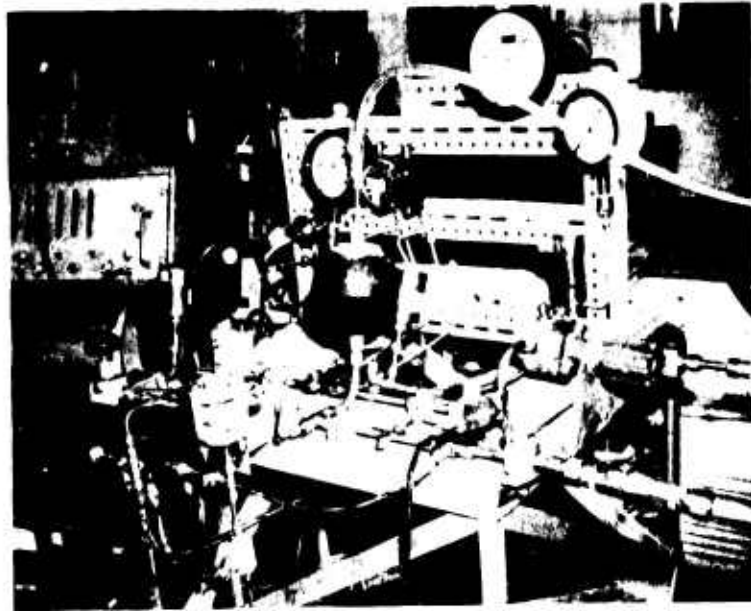


Figure 18. Views of Vortex Throttle Test Set-Up

Page 36

UNCLASSIFIED

UNCLASSIFIED

Report AFRPL-TR-69-88

III, C, ACS Engine Fluidic Controls Evaluation (cont.)

The water weight flow equivalent to rated fuel flow is 0.114 lb/sec. With the direct injection throttle, this flow rate was not achieved because of excessive pressure drop.

The pressure drop problem resulted in a series of tests to define the areas in which pressure drop was occurring and evolve means for reducing the pressure drop. These tests were conducted at reduced flows to maintain acceptable levels of inlet pressures for the plastic throttle. Figure No. 19 shows several comparisons resulting from these tests. The curves illustrate that the liquid chamber alone contributes an approximate 23.5 psi pressure drop at rated fuel flow. The curves also show the need for a considerably larger exit diameter. Exit length was indicated as a contributing factor but not as significant a one as exit diameter. These factors also were defined analytically and resulted in revised vortex throttle dimensions for subsequent models.

In conjunction with defining methods to reduce the pressure drop for the liquid chamber, several means for reducing vortex strength were considered. The simple addition of a 0.040-in. diameter wire placed across the bottom of the liquid chamber had a significant effect. The vortex suppressor was conceived as a dual purpose device. The thin ring with angled slots would reduce vortex strength and aid in establishing a gas-liquid interface within the liquid chamber during the off condition. The tests showed a reduction in vortex throttle pressure drop of approximately 18%, which was less than anticipated; however, with this device installed, a liquid-gas interface was established in the throttle-off condition.

These tests were suspended and information transmitted to Bowles Engineering for their recommendation as to the most desirable method for reducing the pressure drop to design values.

Additional tests with the original vortex throttle configuration were limited to determining the effects of different outlets upon the effluent pattern. This was needed for a valid evaluation of direct injection concepts. The outlet configurations tested included straight holes of different lengths, coned outlets, and angle-drilled outlets. The effluent characteristics of four, typical outlets flowing all-liquid and with approximately 50% throttling were ascertained.

General observations made from test data were that several trends could be noted. The amount of fluid spread did not appear to be affected by the flow rate except at very low flows. Once a full flow condition was established, the amount of spread was constant even though the flow rate was increased. The effluent for the all-liquid condition exited as a stream or sheet and as this broke up, the resulting drops of water were

UNCLASSIFIED

UNCLASSIFIED

Report AFRPL-TR-69-88

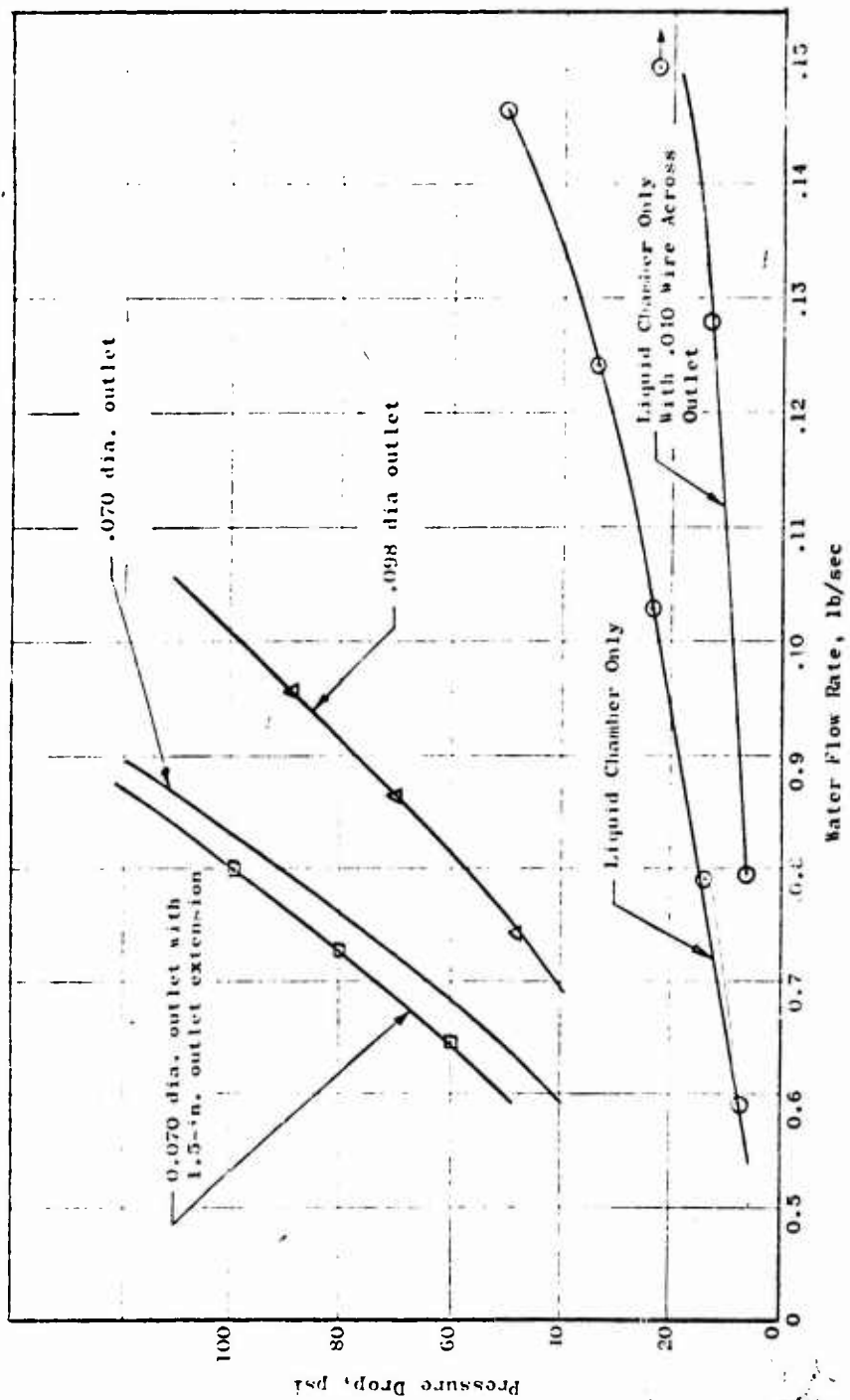


Figure 19. Pressure Drop Comparison

UNCLASSIFIED

UNCLASSIFIED

Report AFRPL-TR-69-88

III, C, ACS Engine Fluidic Controls Evaluation (cont.)

quite large. Outlet length had a noticeable effect upon the spreading action. Without any added outlet, a coning effect was obtained with the water forming the surface of the cone and a void existed in the center of the cone. As outlet length increased, the amount of conical spread was greatly reduced although there was still slight evidence of spreading even with the angle-drilled outlet. With the conical drilled outlet, spreading action was essentially the same as with the straight-through hole. The effect of throttling was to increase the effluent velocity. Throttling reduced the amount of spread with outlets that had a significant spread in the all-liquid condition. With outlets having little spread in the all-liquid condition, throttling operation did not cause much change in the amount of spread. The most significant effect of throttling was the change in effluent drop size and throughout the throttling range, the liquid exited as a fine mist.

As a result of these preliminary tests, the direct injection concepts under consideration were eliminated as candidates for advancement to the metal hardware stage. This decision was prompted by the findings that the droplet size was large, cone spread was less than that anticipated, and cone spread was significantly changed during throttling. Thus, in view of the above factors and the short combustion chamber, the direct injection concepts did not compare favorably with other concepts.

2. Vortex Throttle Analysis and Evaluation

Concurrent with the pressure drop testing of the vortex throttle, other problem areas were noted (i.e., on-off stability, chugging in the near off condition, and oscillations during throttled operation). Response tests conducted in the previous -11614 contract showed a relatively slow (150 millisecc) turn on response with ambient fluids. The modified Bowles Engineering throttle dimensions which were intended to decrease the pressure drop also would slow the response because of the larger chamber volumes. These factors prompted a change in the effort from a design definition of the throttle and injector to one of determining the probability of developing an engine control that would be functional and competitive with conventional controls. Whereas prior vortex throttle effort had been concentrated upon improving turndown ratio, the new effort was directed toward the evaluation of several factors and their relationships. The aspects to be evaluated included on-off stability with respect to pressure sensitivity, flow stability during throttling, throttling ability, response time, and turndown ratio.

a. Design and Analysis

(1) On-Off Stability

The primary concern with this aspect was whether a gas-liquid interface could be established within the vortex throttle during

UNCLASSIFIED

UNCLASSIFIED

Report AFRPL-TR-69-88

III, C, ACS Engine Fluidic Controls Evaluation (cont.)

the on and off conditions as well as the effect of fluid pressure variations upon this interface. An interface of this type was not established in the basic plastic vortex throttle tests conducted at Aerojet-General. In the full-on condition, liquid entered the control gas line and gas entered the liquid line in the off condition.

Analysis of this condition showed that any interface would be unstable. However, it was possible that a pulsating interface could have been established in the off condition. The viscous shear forces between the gas swirling in the liquid chamber and the liquid could have generated a weak vortex within the residual liquid. This vortex action would have produced a higher pressure at the chamber wall than the pressure at the gas interface. Thus, a small increase in gas pressure would have moved the interface toward the wall until the gas and liquid pressures again were balanced. A small decrease in gas pressure would have allowed the interface to move away from the chamber wall. The liquid entering the chamber as the interface contracted would have tended to maintain the slight vortex action in the liquid. Thus, theoretically, it might have been possible to establish this unstable gas-liquid interface and maintain it within the liquid chamber. No such theory was defined for establishment of an interface in the gas chamber for the full-on condition.

Although a rigorous analysis of this theory was not attempted, it is believed that the pressure variation that could have been accommodated within the confines of this size vortex throttle would have been extremely small, to a point that would have been impractical from a system aspect.

The major performance factor affected by a failure to establish and maintain an interface in the throttle was response time. Aside from thermal effects, volume was the major factor in determining response time. Dependent upon the rate of interface propagation and the time before a different command signal was received, the volume to be filled before full flow was initiated would have been variable.

(2) Flow Stability

The concern with flow stability was the ability to maintain a constant flow rate for any set condition throughout the range from on to off. This capability was not explored in depth because the effort was terminated before much work was completed. Flow instability is affected by many factors such as control pressure variations, liquid supply pressure variations, gas chamber volume, gas-liquid mixing, and outlet configuration. The main concern with unstable flow was that pressure perturbations could reflect both up and downstream of the vortex throttle thereby inducing or amplifying system and/or combustion instabilities.

UNCLASSIFIED

UNCLASSIFIED

Report AFRPL-TR-69-88

III, C, ACS Engine Fluidic Controls Evaluation (cont.)

(3) Throttling Ability

Flow stability is a factor in throttling ability; however, the primary concern in this section is with the shape of the liquid weight flow (\dot{W}_l) versus the gas weight flow (\dot{W}_g) curve through the throttling regime. This is a two-phase flow condition; therefore, the basic curve shape would be similar to that shown on Figure No. 20. This curve shows that liquid weight flow is greatly reduced by a small weight flow of gas; therefore, flow rate is quite sensitive to gas flow rate in the high liquid flow range. A second aspect of the problem is the relationship between gas weight flow and control gas pressure. The liquid weight flow would be significantly affected by fluid supply pressure changes. These interrelationships are discussed in some detail later in the report.

With the off stability problem (i.e., fluid back-up in supply lines), a throttling mode of operation was considered as an alternative. However, the usable throttling range would have to be reduced to avoid fluid back-up. In the full-on condition, there would still be some gas flowing and in the off condition, there would still be a small amount of liquid flowing. The shape of the two phase flow curve for the throttle and definition of expected pressure variations would define the usable operating range.

The two-phase flow phenomena was analyzed in an attempt to determine whether the basic curve shape could be altered in a manner that would permit a wider operating range without concern for fluid back-up in the supply lines. The portion of the \dot{W}_l versus \dot{W}_g curve for the vortex throttle is quite steep in the range of 100% to approximately 40% of liquid flow and this was the region of concern. The analysis offered little hope of significantly changing the curve shape in the manner required to extend the throttling range. Test results confirmed the analysis.

Effort then was directed toward methods for changing the control gas pressure (P_g) versus gas weight flow (\dot{W}_g) curve. The intent here was to obtain a wider spread in control pressure from the full-on to full-off condition. Decreasing the control gas inlet area increases pressure spread, but it provides very little gain in the low gas flow region while showing a wide increase at high flow. The use of a laminar flow restriction in the control gas inlet would have improved the situation by providing more gas pressure spread in the low gas flow region without a large pressure increase being needed to attain maximum gas flow. The comparison between a turbulent gas inlet restriction and a laminar restriction is shown on Figure No. 21.

The effect of laminar outlet flow also was examined briefly. With laminar outlet flow, the fluid flow out of the throttle would not be affected by gas inclusion nearly as much as with turbulent outlet flow.

UNCLASSIFIED

UNCLASSIFIED

Report AFRPL-TR-69-88

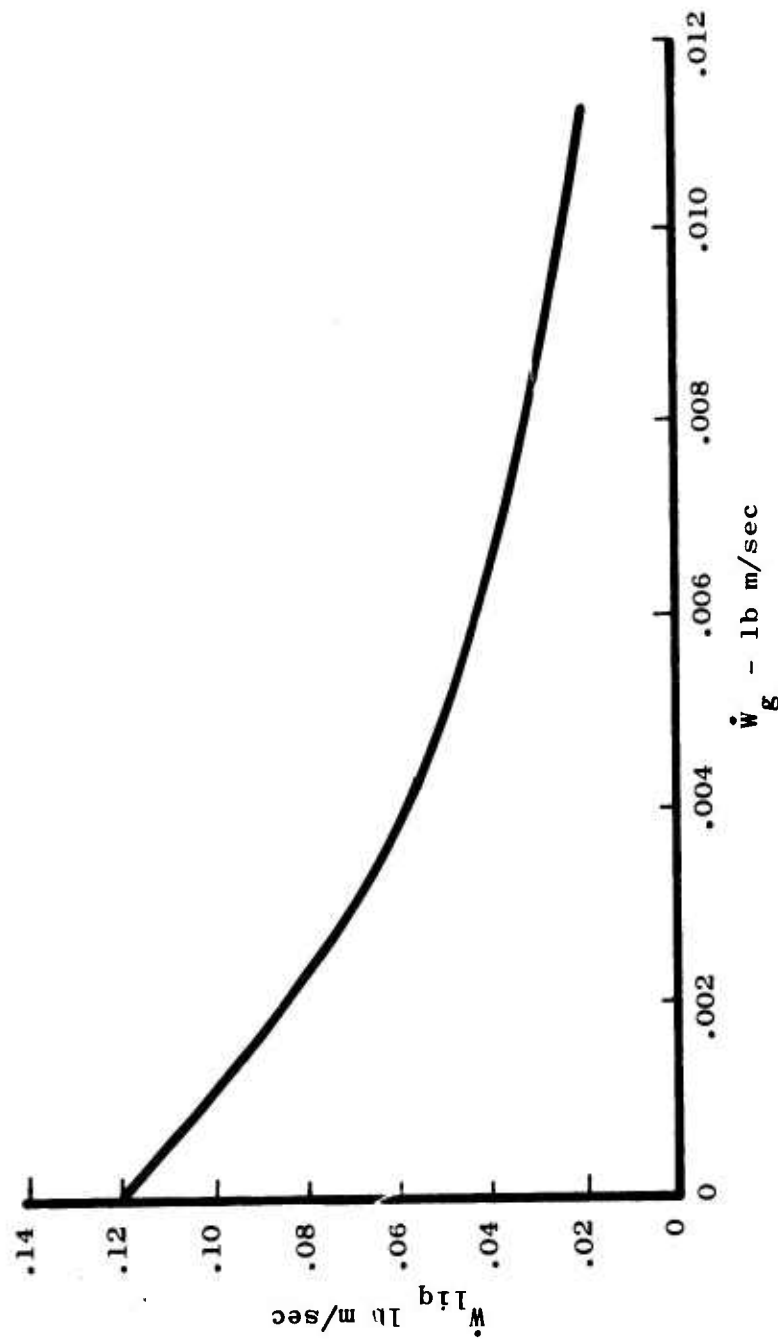


Figure 20. Theoretical Two-Phase Flow Curve for Homogeneously-Mixed Fluid Through an Orifice

UNCLASSIFIED

UNCLASSIFIED

Report AFRPL-TR-69-88

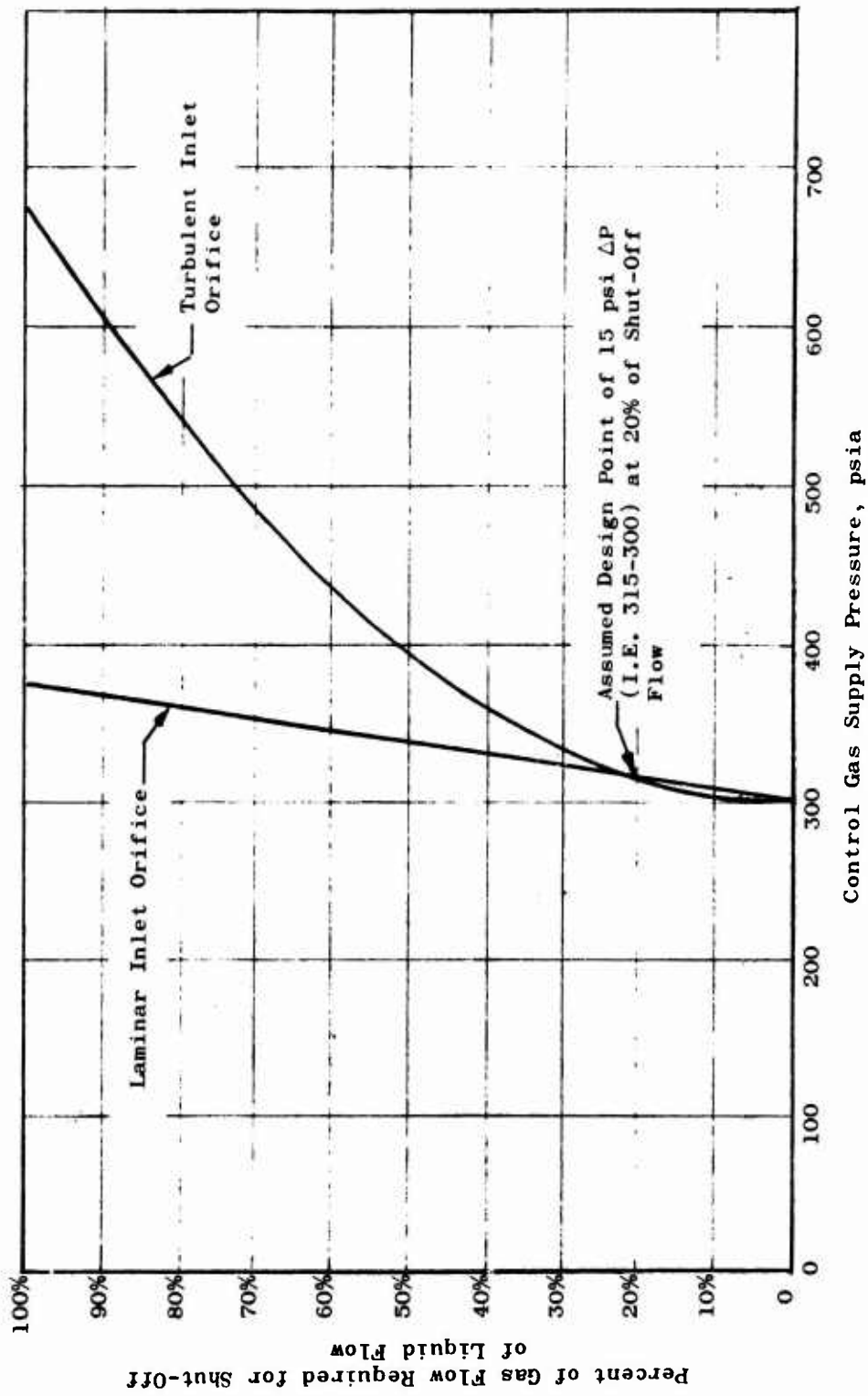


Figure 21. Comparison of Laminar and Turbulent Control Gas Inlet Orifice Characteristics

UNCLASSIFIED

UNCLASSIFIED

Report AFRPL-TR-69-88

III, C, ACS Engine Fluidic Controls Evaluation (cont.)

Initial analysis of this approach showed that with laminar flow, the gas flow rate would be much higher than with turbulent gas flow. This condition would significantly decrease the turndown ratio for the throttle. Recognizing this performance loss precluded any further effort.

(4) Response Time

The analysis accomplished with respect to response time was concentrated upon thermal effects. In the engine application, the control gas would be 1300°F and with extended off times, the vortex throttle would become hot. When liquid flow is initiated after an extended off period, the heat transfer from the throttle to the liquid could produce vaporization of the propellant. This vaporization would affect response time in that the time to reach full liquid flow would become a function of the temperature, mass, and contact area of the vortex throttle.

Two vortex throttle designs were considered in the thermal analysis conducted; a large mass design and a thin wall design, with N_2O_4 as the propellant. A temperature of 1300°F was assumed for both designs at the time that liquid flow was initiated. This analysis showed that for the thin wall design, the possibility of boiling in the throttle exit would exist for 200 millisec. With the large mass design, this condition would exist for 1 sec. The tests conducted in the previous program (Contract -11614) with hot gas and MMH confirmed this basic thermal problem.

b. Fabrication of Evaluation Model

A vortex throttle was fabricated from Plexiglas to the modified internal dimensions supplied by Bowles Engineering. This vortex throttle was made in sections and the same type of clamping retention was used to facilitate easy substitution of sections. The basic assembly shown on Figure No. 22 was used for the initial tests as well as for comparison with the ACS vortex throttle from the -11614 contract.

c. Test Evaluation

(1) Test Description

The tests conducted were directed toward an evaluation of stability and throttling performance of both the modified dimension vortex throttle and the ACS throttle from the -11614 contract. The major difference in configuration between these throttles is that the previous program throttle had a conical liquid chamber with flow straightening vanes. Figure No. 11 shows the ACS throttle that was tested with all tests being run using ambient GN_2 and water. The same basic test set-up shown previously on Figures No. 17 and No. 18 was used for the Aerojet-General tests. An additional

UNCLASSIFIED

UNCLASSIFIED

Report No. AFML-TR-69-166

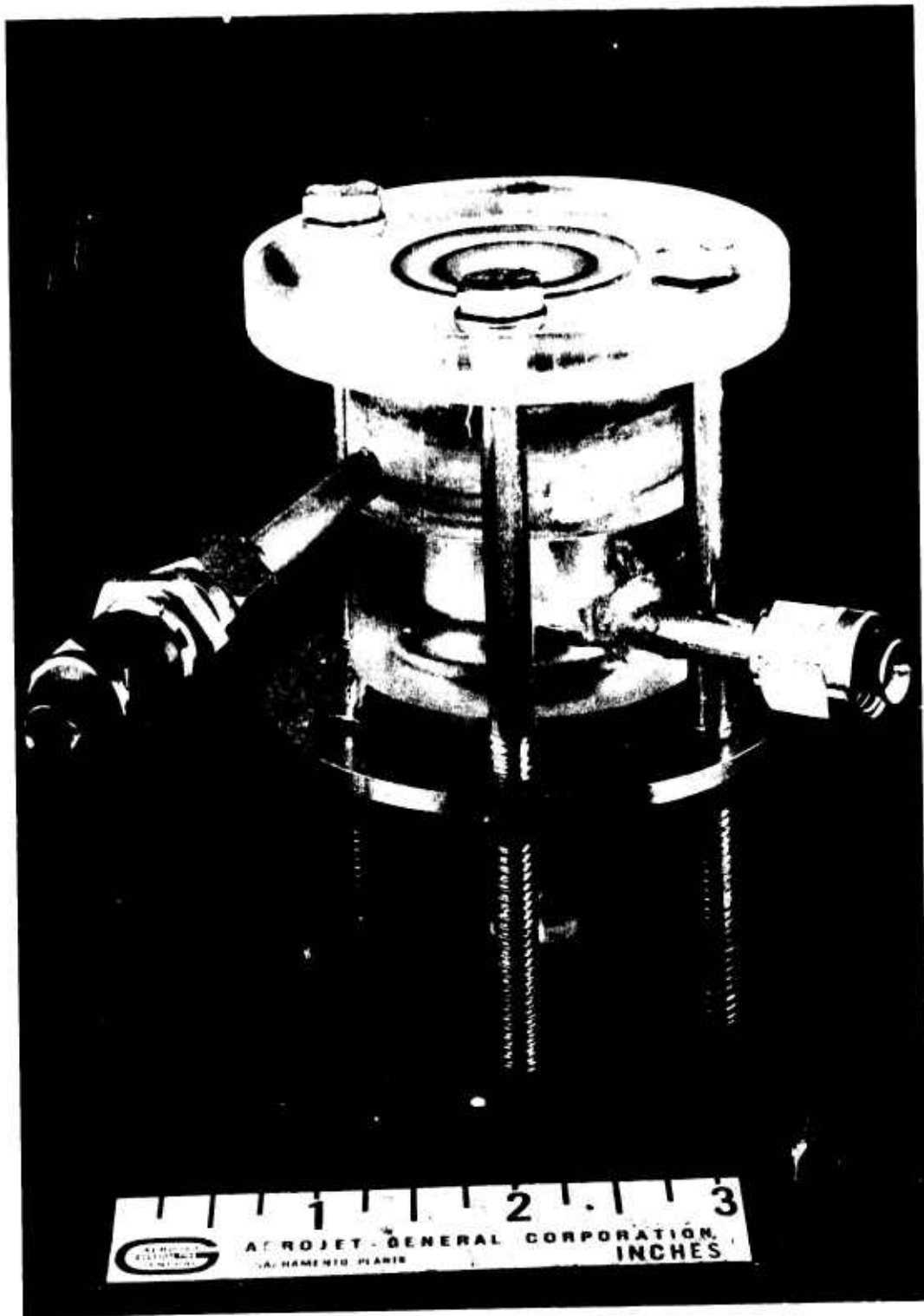


Figure 22. Modified Vortex Throttle Assembly

Page 45

UNCLASSIFIED

UNCLASSIFIED

Report AFRPL-TR-69-88

III, C, ACS Engine Fluidic Controls Evaluation (cont.)

backpressure valve, which is not shown in the photographs, was used to conduct the variable backpressure tests.

The first tests were for the purpose of determining the throttling characteristics of both the conical liquid chamber throttle and the modified dimension throttle with a cylindrical liquid chamber. In these tests, inlet pressure and full flow rate were varied to determine their effect upon the two-phase flow curve, mainly in the region of 50% to 100% liquid flow where the curve is steep. Backpressure was maintained by a valve located in the throttle outlet. Once the full-flow condition was established, the backpressure valve setting remained unaltered during that run. The tests were run by setting the full liquid flow condition and then incrementally throttling the liquid flow by supplying control gas until the no-liquid-flow condition was reached. These tests were monitored using recording instruments to permit an evaluation of instabilities during throttling.

Another test series was run with the plastic throttle to determine the effect of fixed backpressure as compared with a variable backpressure. The backpressure was set at each incremental flow condition to simulate the combustion chamber pressure that would result from that propellant weight flow. The effect of restricting the control gas inlet also was evaluated in this testing.

One test was run to determine whether a hysteresis band existed over the throttling range instead of just at the shut-off condition. This test was conducted with a fixed backpressure using the plastic throttle containing the restricted gas inlet. Incremental readings were taken first for decreasing liquid flow and then for increasing liquid flow. A second objective of this test was to investigate the mid-range curve shape.

(2) Test Results

The main objective of these tests was to evaluate the throttling ability of the vortex throttles with respect to stability and the effect of different parameters upon the two-phase flow curve in the high liquid flow region. In general, the tests confirmed the analysis in that changing parameters had no significant effect upon the basic trend of the two-phase flow curve. All versions of throttles tested exhibited instability in the throttling range.

This instability was indicated by an oscillating flow rate which varied in magnitude but seemed most severe at the lower liquid flow rates. The foregoing results are illustrated by Figures No. 23 through No. 28.

UNCLASSIFIED

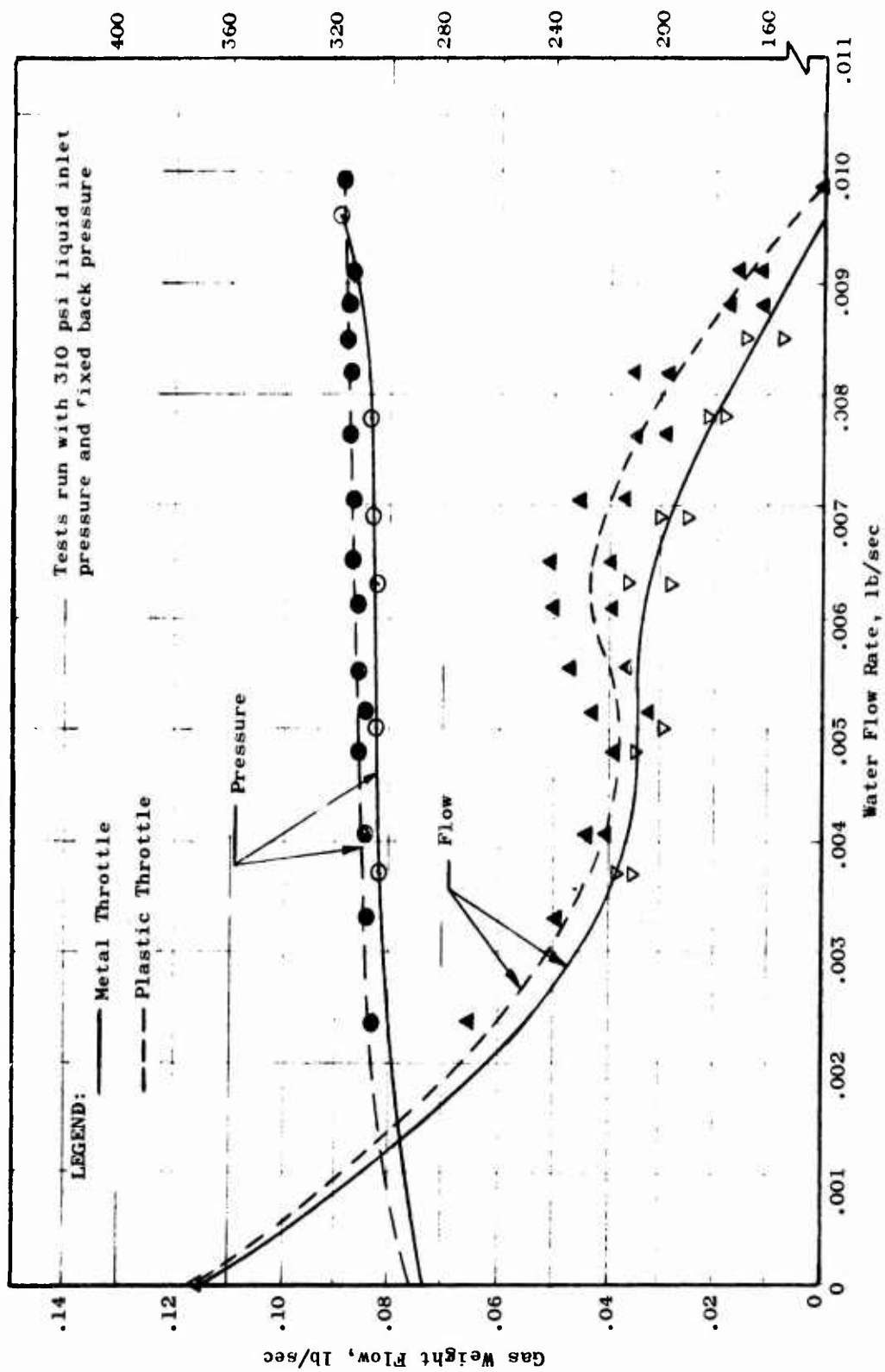


Figure 23. Metal vs Plastic Throttle Performance

FREQUENTLY OF FLOW VARIATIONS IS 4 cps
CONTROL GAS INPUT IS 0.00304 lb/sec GN_2 and STEADY
TURNDOWN RATIO WAS 14:1 at SHUTOFF

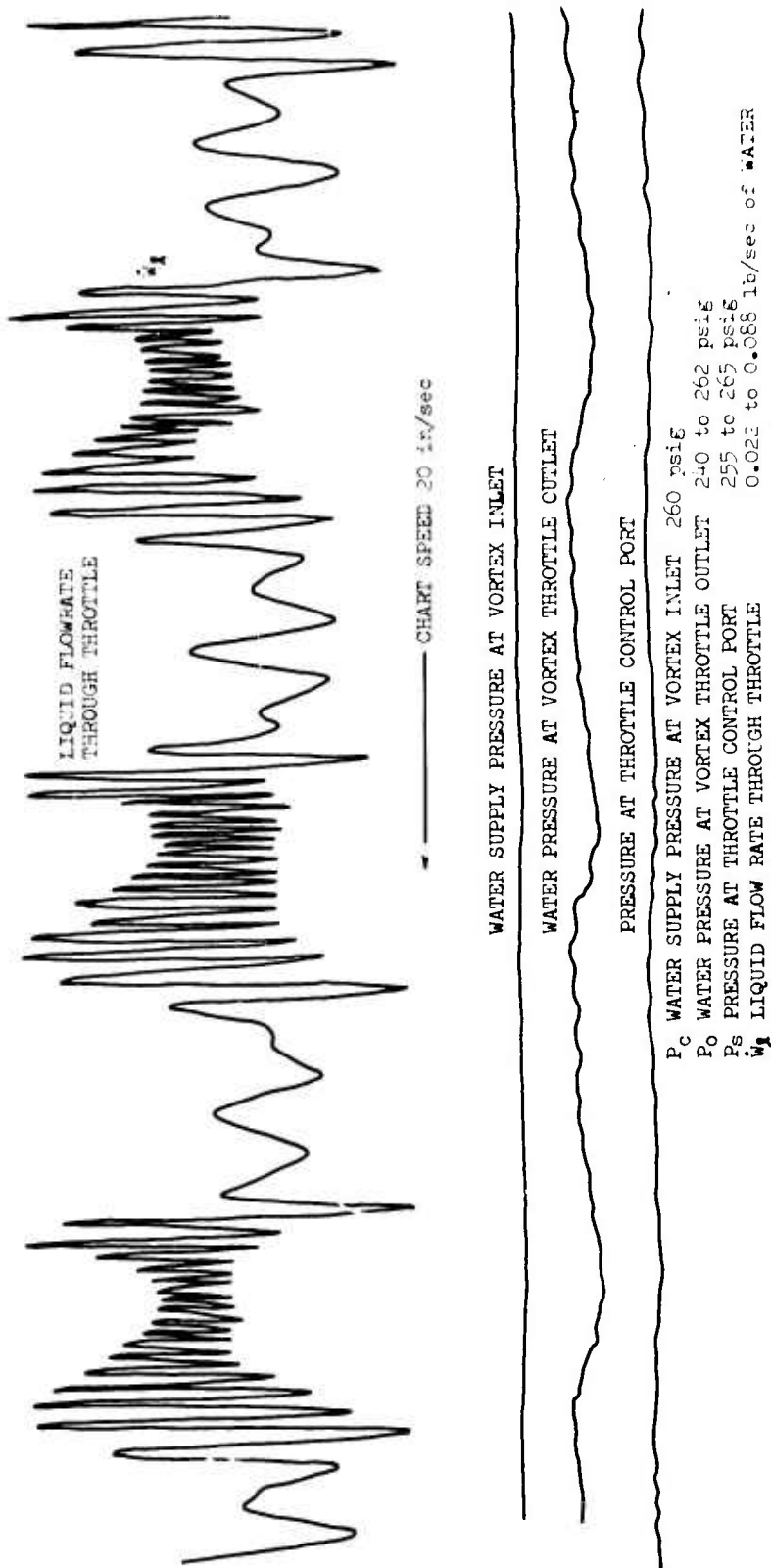


Figure 24. Typical Flow Oscillations

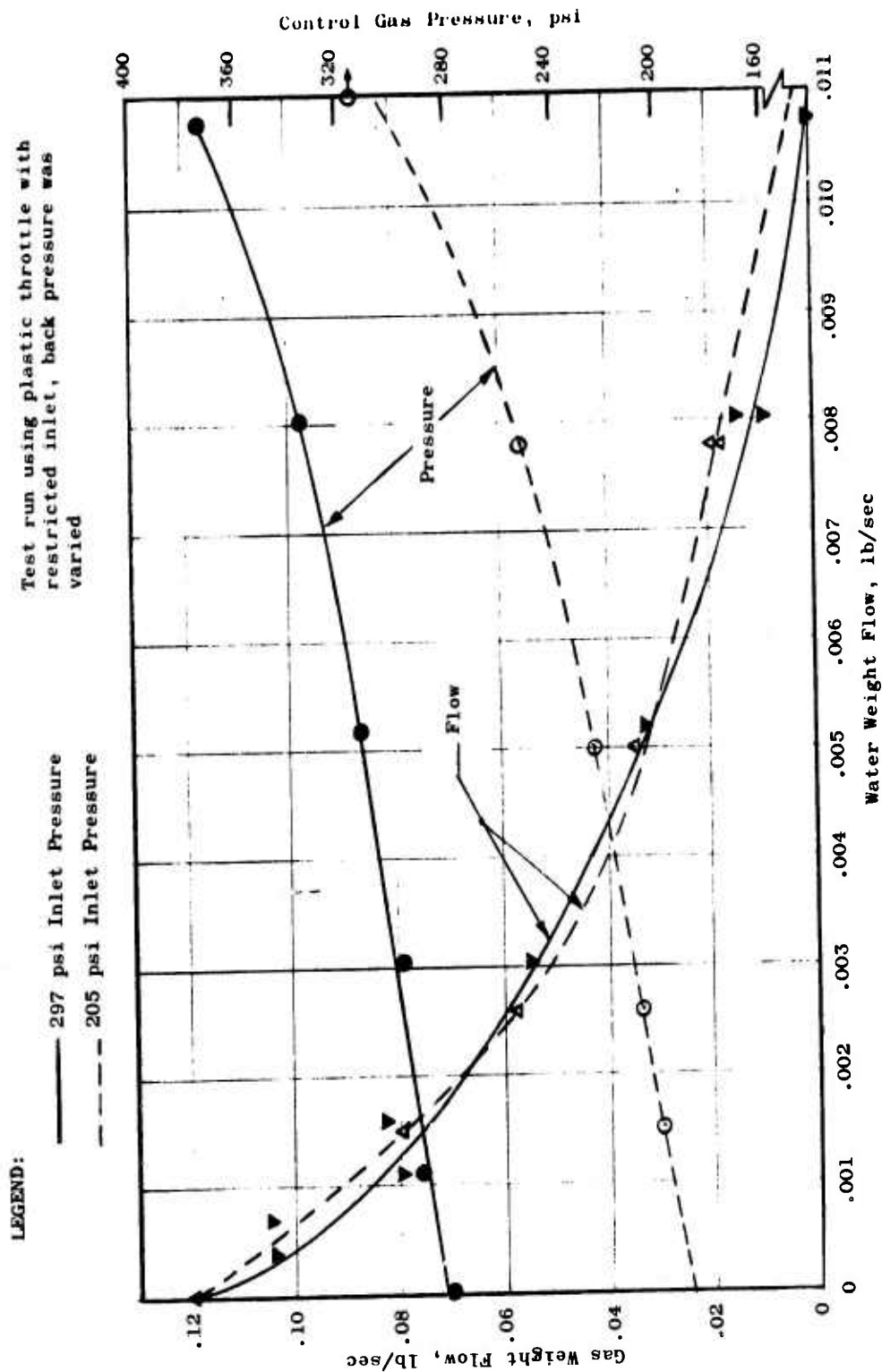


Figure 25. Effect of Inlet Pressure

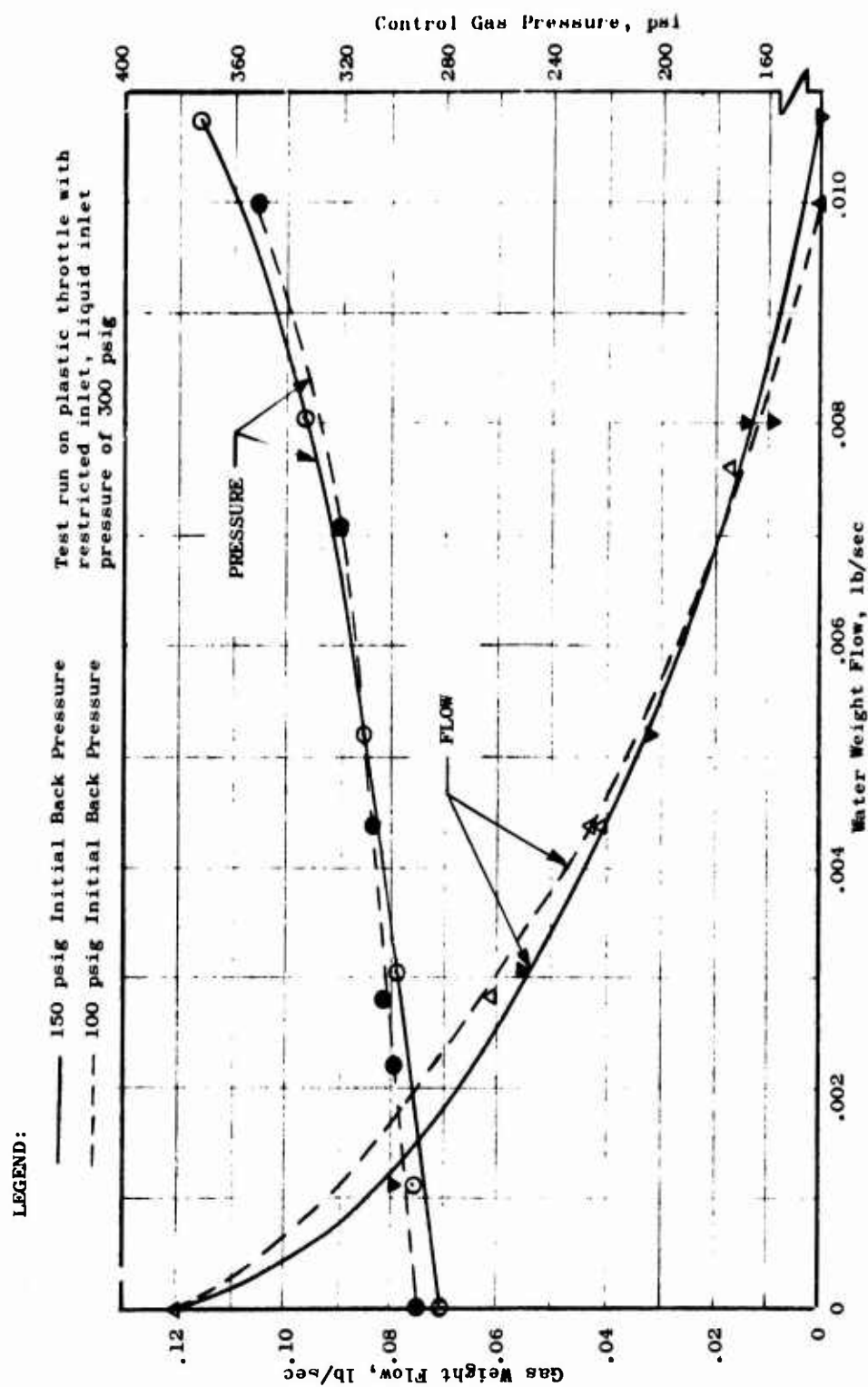


Figure 26. Effect of Backpressure Level

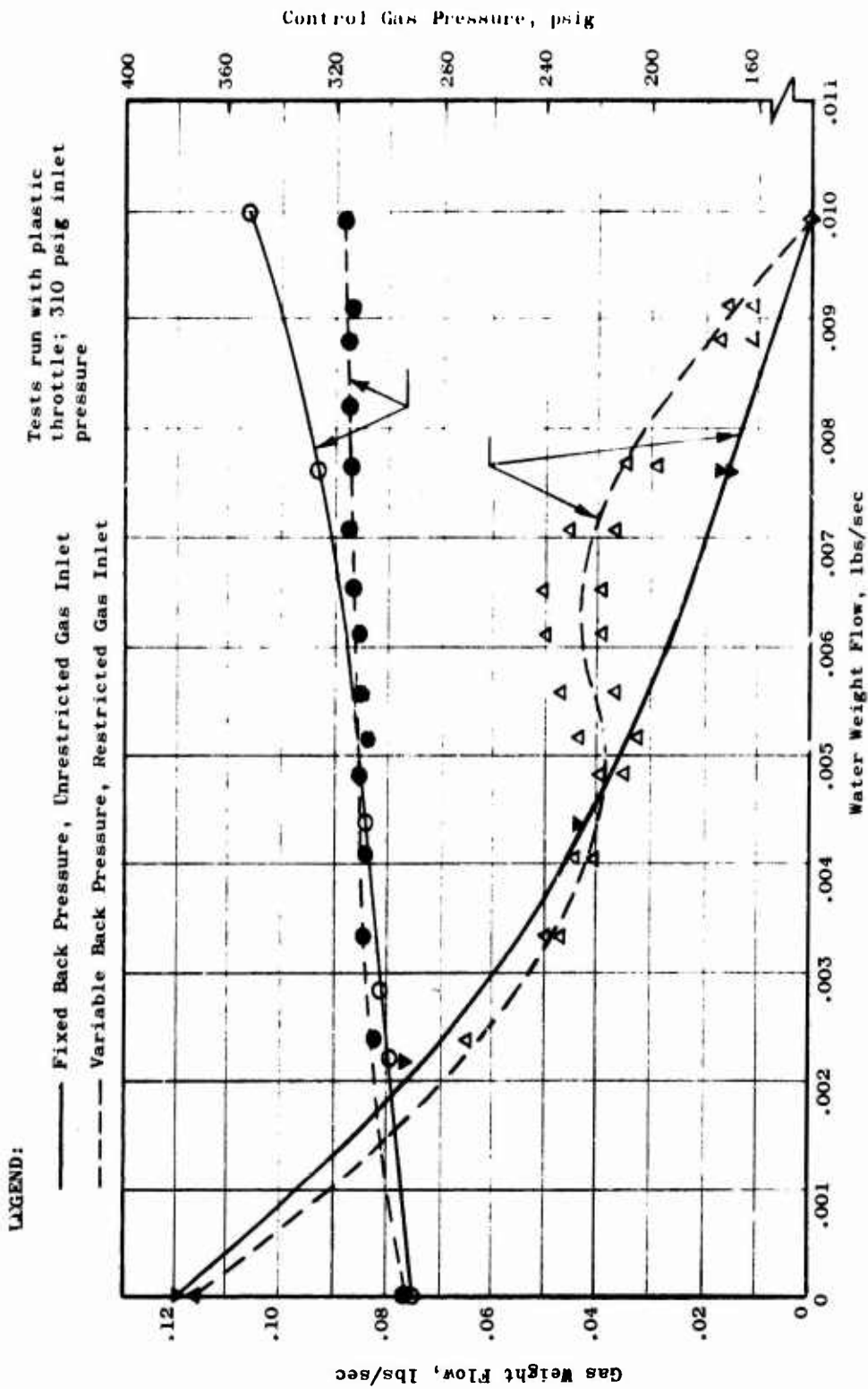


Figure 27. Effect of Fixed vs Variable Backpressure

UNCLASSIFIED

Report AFRPL-TR-69-88

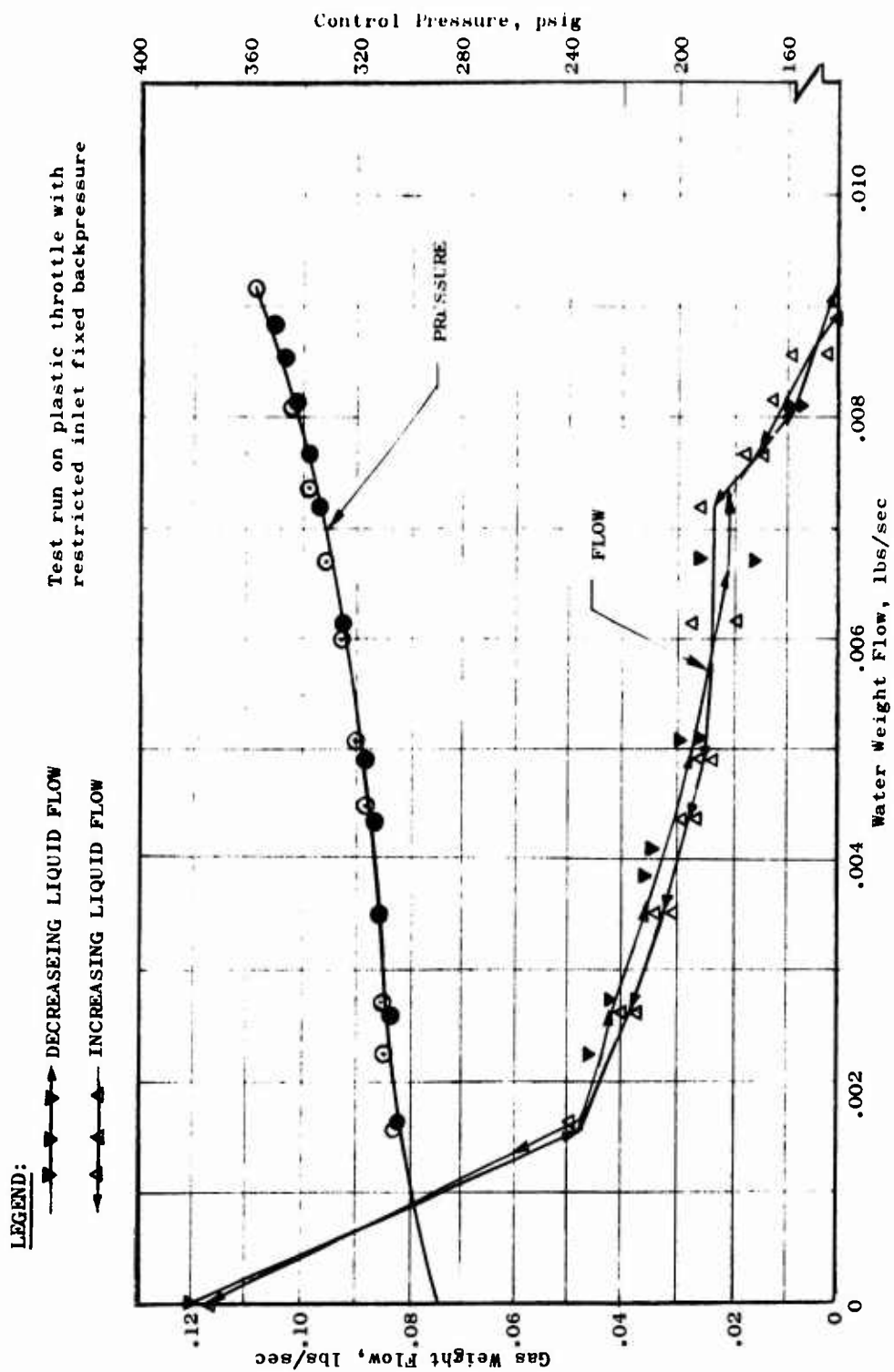


Figure 28. Throttling Operation Hysteresis

UNCLASSIFIED

UNCLASSIFIED

Report AFRPL-TR-69-88

III, C, ACS Engine Fluidic Controls Evaluation (cont.)

Figure No. 23 shows a comparison between the throttle having a conical liquid chamber and turning vanes and the modified dimensions throttle having a cylindrical liquid chamber. The plot of \dot{W}_L versus \dot{W}_g shows that both throttles display the same characteristics. The portion of the curve from full-liquid-flow to approximately 40% flow is steep and then, the slope becomes gradual to the no-liquid-flow condition. These curves also show a peculiarity noted in varying degrees during these tests. The curve flattens out or reverses in the vicinity of 30% flow and this characteristic is not understood at present. The curve inflection could be the result of either or both fluids operating in the transition regime between turbulent and laminar flow.

The curves also show the extent of flow oscillation experienced as defined by the two data points for a set gas weight flow. These points represent maximum and minimum flow rates for that test setting. The variations are quite large when considered in terms of peak-to-peak values as a percentage of mean flow rate. Figure No. 24 shows a typical data tape which reflects the flow oscillations experienced during throttling.

The curve for control gas pressure provides an indication of the flow effects to be expected as a function of pressure variations. If a 300 psi gas supply is assumed, $\pm 2\%$ pressure variations would represent a potential change of 12 psi. On the curve for the plastic throttle, a 12 psi control gas pressure increase from the full on condition would reduce liquid flow almost 30%. This same effect is reflected in varying degrees with all of the throttles tested.

Figures No. 25 and No. 26 show comparisons for the effect of inlet pressure level and different simulated combustion chamber pressure level. The \dot{W}_L versus \dot{W}_g curve essentially is the same. In the region of concern, none of the variations tested significantly altered the steep slope in the range of 50% to 100% liquid flow.

Figure No. 27 is a comparison between performance with a fixed backpressure and a variable backpressure. It also shows the effect of the restricted control gas inlet in relationship to the unrestricted inlet. Here again, the initial portion of the \dot{W}_L versus \dot{W}_g curve essentially is unaffected. The middle section of the curve reflects a difference; however, additional data points for the varied backpressure curve could show the same characteristic tendency of flattening or reversal as displayed by the fixed backpressure curve. In view of the scope of the test objectives as well as schedule requirements, no further investigation of this curve region was attempted. The control gas pressure versus \dot{W}_L curves show the effect of restricting the gas inlet. Inlet restriction provides a wider spread from full-on to off, but it offers no significant gain in the region where more

UNCLASSIFIED

UNCLASSIFIED

Report AFRPL-TR-69-88

III, C, ACS Engine Fluidic Controls Evaluation (cont.)

spread would be most helpful. Thus, the inlet restriction does not aid throttling. There is some evidence that the restricted inlet decreased the amplitude of flow oscillations during throttling.

Figure No. 28 presents the results of a throttling cycle from full-on to off and back to full-on. A precise evaluation is not possible because of the flow oscillation. There is indication that the throttle had a slight hysteresis under the test conditions. This hysteresis is most noticeable in the last 30% of the throttling range. The difference between the decreasing and increasing flow curves is not consistently in the same direction; therefore, this aspect would require further investigation before any conclusions can be made.

Tests conducted at Bowles Engineering were limited to throttling and on-off stability. Several models were run and the following observations made. All models showed instability at approximately 25% flow. The instability was reduced but not eliminated by increasing outlet load. The cylindrical liquid chamber displayed high-frequency instability at all flow rates whereas the conical liquid chamber was smooth down to approximately 25% flow. The addition of the insert in the gas chamber to form a conical annulus did not have a noticeable effect upon throttling stability but did improve stability at shutoff.

3. Conclusions

Several significant indications were noted during analysis and testing of the vortex throttle. Results also showed that some interaction effects have not been isolated and would require additional work to completely define these effects. Within the scope of the work done in this contract and some information available from the previous -11614 contract, the following conclusions are possible.

a. Vortex throttle technology using high pressure and temperature gas on liquid is not sufficiently advanced to be competitive with conventional controls without developing additional basic component technology. The primary comparisons support these conclusions are in the areas of response time, weight, and system stability.

b. On-off operation of the vortex throttle design tested does not seem practical unless some mechanical blocking device or fluidic check valve is used in the fluid inlets. Response time, even if blocking devices were used, is a significant problem. With ambient fluids, response times of 25 to 50 millisec are considered attainable; however, when hot gas is used as the control gas, the thermal effects upon response time are critical. Previous Contract -11614 work with hot gas and MMH showed response times of

UNCLASSIFIED

UNCLASSIFIED

Report AFRPL-TR-69-88

III, C, ACS Engine Fluidic Controls Evaluation (cont.)

180 millisecc after 30 sec of shutoff and 8 sec after 5 min of shutoff. The long response time is the result of slugging at flow initiation which is caused by propellant vaporization as shown on Figure No. 29.

c. Throttling operation offers more potential for a full fluidic system than on-off operation, but stability and controllability must be improved. Stability is a function of throttle geometry, fluid inlet variations, and throttle outlet restrictions. In the throttling range, stability must be achieved before a throttling mode of operation could be seriously considered. The required controllability with respect to the liquid weight flow in relationship to gas weight flow could be attained by operating in a narrow range. This range would be established so that there would be some gas flowing during the "on" condition and some liquid flowing during the "off" condition. This type of operation imposes additional weight penalties because of the extra fluids required. Definition of a specific operation range will depend upon the shape of the \dot{W}_L versus \dot{W}_g curve and the inlet pressure variations expected. Work done in this program indicates little change in the basic curve shape can be achieved in the high liquid flow regime; therefore, prospects of widening the throttling range of operation will depend upon decreasing fluid inlet pressure variations.

d. Many interactions exist between vortex throttle performance characteristics and throttle configuration. These interactions are recognized but have not been defined in specific terms. A more complete understanding of these interactions is necessary to permit design of vortex throttles for specific applications and duty cycles.

e. No specific conclusions with respect to control modules for the vortex throttles can be made. Based upon the proposals received, high temperature, high pressure amplifiers have been made and staged; however, a complete module of the type needed has not been demonstrated.

4. Recommendations

Although fluidic engine controls currently are not competitive in performance and weight with conventional controls, they offer a potential for rocket propulsion applications and continue to have a strong reliability appeal. During the course of work in this program several approaches were conceived which could improve performance, but none have been demonstrated. The interaction effects must be more thoroughly understood before predictable performance gains can be defined with proper consideration of performance trade-offs. The greatest potential for fluidic controls appears to be for small engines having a short duty cycle. Further, pre-development of the various components that comprise an engine control should be undertaken to fully define characteristics before integrating the components into a complete system. Typical incremental studies could be as follows:

UNCLASSIFIED

FOURTH THROTTLE ACTUATION (OFF-ON) AFTER APPROX. 5 MINUTES SHUTOFF

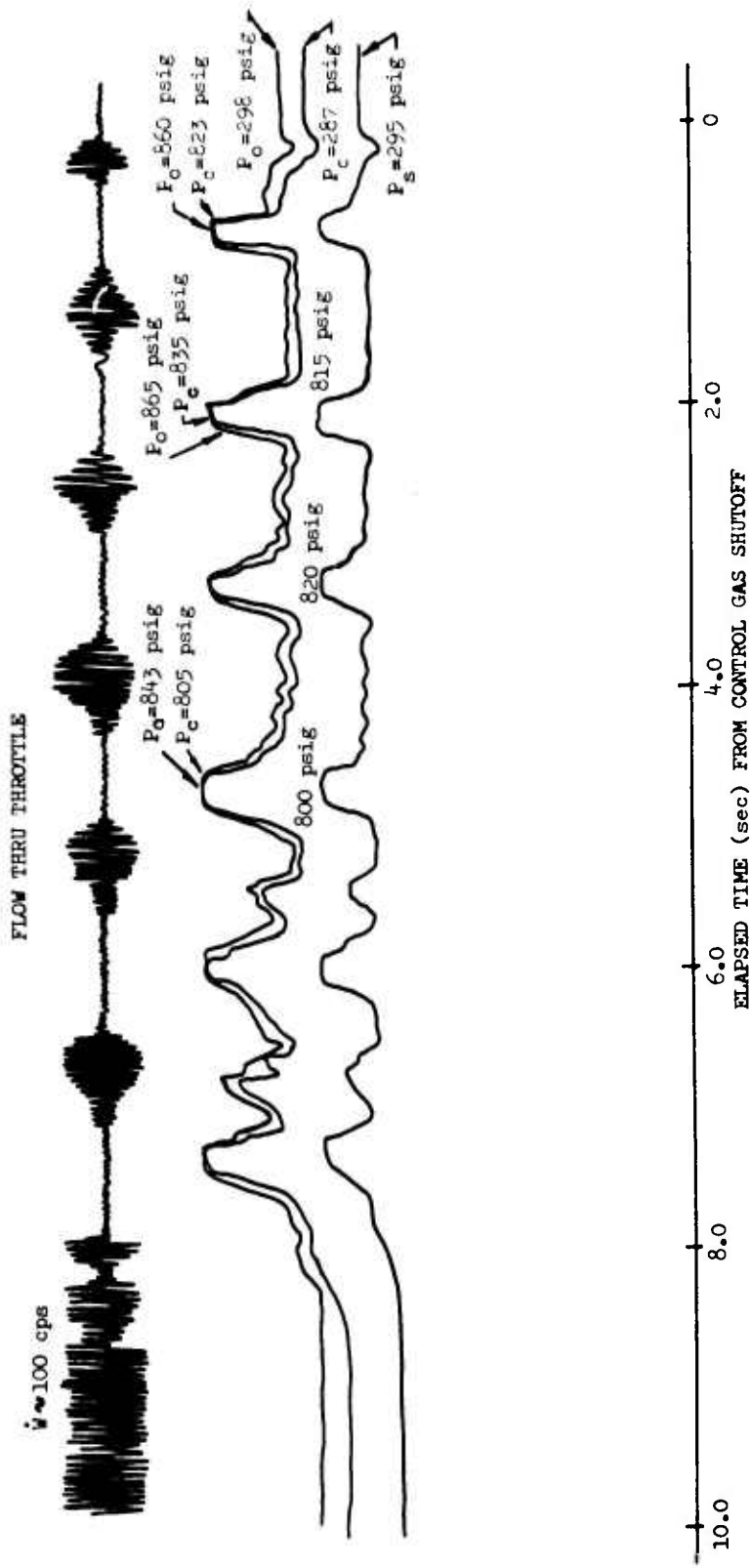


Figure 29. Vortex Throttle Flow Transient

UNCLASSIFIED

Report AFRPL-TR-69-88

III, C, ACS Engine Fluidic Controls Evaluation (cont.)

a. Investigate the possibility of designing a vortex throttle which would have a stable on-off interface and determine the magnitude of the pressure band that could be accommodated without fluid back-up. In conjunction with this effort, explore possible methods to overcome the thermal affects on turn-on response time encountered with hot gas as the control fluid.

b. Conduct analytical and test investigations of a vortex throttle designed solely for use as a throttling device. This effort would include the major objectives of eliminating throttling instability, defining a throttling range to avoid fluid back-up, defining the additional fluid weight required for this type of operation, and the thermal effects in the throttling range.

c. Design and demonstrate a control module using staged, gas-on-gas amplifiers with an electro-mechanical devices for control signal input.

d. Improve staging capabilities demonstrated above and devise as well as demonstrate an electro-pneumatic or all-fluidic interface device to control the staged amplifiers.

UNCLASSIFIED

UNCLASSIFIED

Report AIRPL-TR-69-88

SECTION IV

MINIMUM ACS ENGINE STUDY

A. OBJECTIVE

Determining the required number of ACS engines for PBV control was undertaken in preparation for the final design of a complete Post-Boost Propulsion System. It was identified that the optimum configuration, considering weight and reliability, would be a minimum number of units that would provide the PBV control accuracy. The Minimum ACS Engine Study was initiated to evaluate the effects of reducing the number of ACS engines considering both pulse mode and throttling engine operation.

Figure No. 30 is the basic plan for the Minimum ACS Engine Study, which required the definition of the guidance control logic and capabilities as well as the determination of PBV system accuracy limits. This information was provided to Aerojet-General by guidance supplier and prime airframe contractors. The configurations selected for analysis are listed on Table IV. By evaluating and comparing the effectiveness of these configurations, an optimum attitude control system with a minimum number of engines could be defined.

B. ACS STUDY

The initial study activity was directed toward the evaluation of the throttled, five-engine configuration identified as Configuration 4 on Table IV. The vehicle motion and analog control logic for the five-engine configuration is provided with the guidance and control logic presented as Figure No. 31. It was assumed for the purposes of analysis that the continuous control and error signals are provided. An analog computer simulation of the system was made to determine the controllability, the required engine sizes, and the throttle range.

The guidance and control loop schematic (Figure No. 31) indicates the manner in which the three angular degrees of freedom (ϕ , θ , ψ) are controlled by the attitude control loops and the three translational degrees of freedom (x , y , z) are controlled by the steering loops. All of the feedback control loops include position and rate information to ensure system stability. The steering loops signals (ΔV_x , ΔV_y , ΔV_z) are obtained from accelerometers within the inertial measurement unit (IMU). Processing these signals yields the angular commands (ϕ_c , θ_c , ψ_c) necessary to achieve the proper vehicle location. The vehicle angular rates are sensed by rate gyros within the flight guidance package. These signals then are processed and compared with the angular commands to yield the error signals (ϵ_ϕ , ϵ_θ , ϵ_ψ). The thruster logic results in the activation of select thrusters in response to various combinations of the error signals. Finally, the vehicle motions in response to thruster forces and moments are defined by the vehicle rigid body dynamics.

UNCLASSIFIED

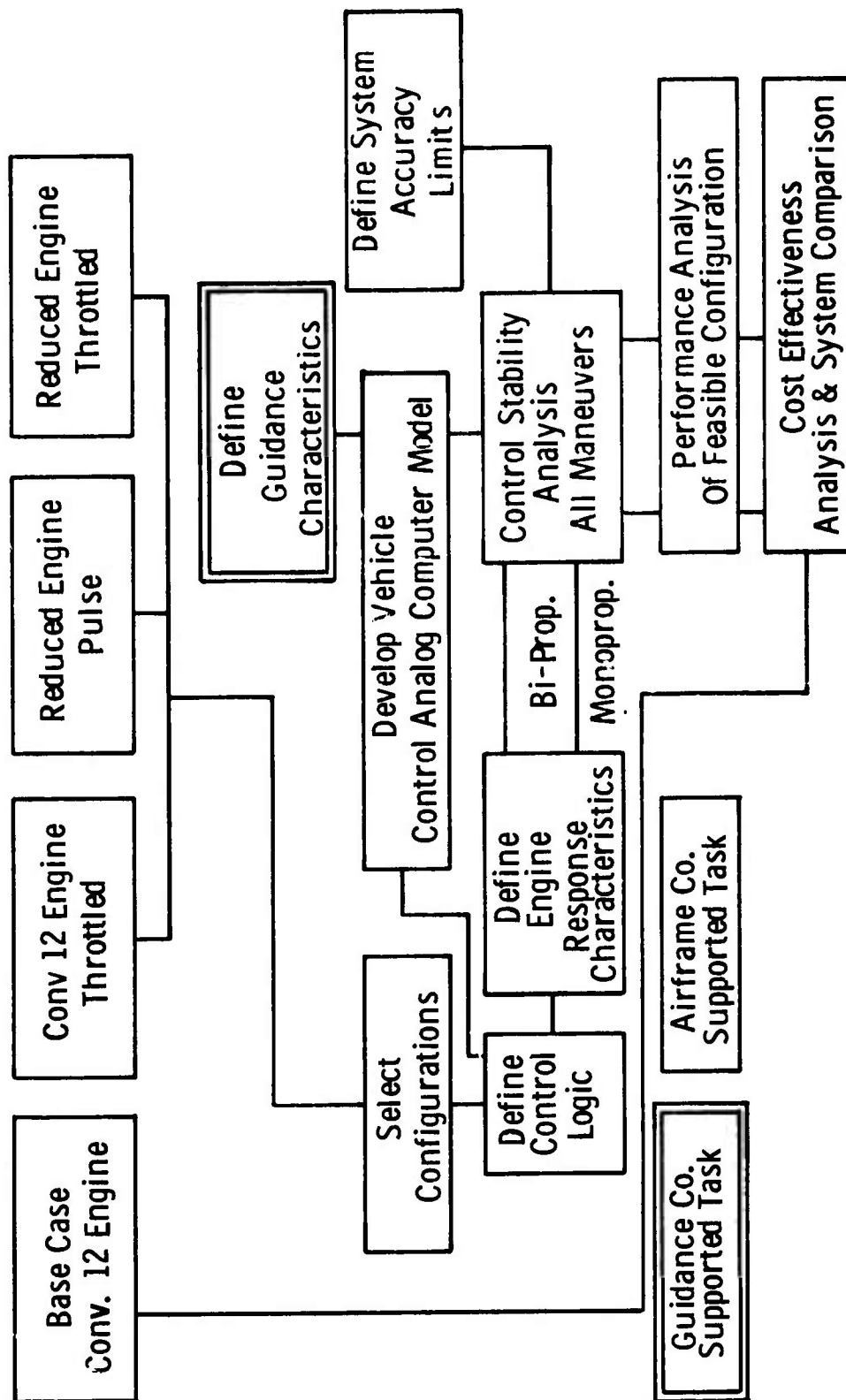


Figure 30. ACS Study Plan

UNCLASSIFIED

Report AFRPL-TR-69-88

TABLE IV

STUDY CONFIGURATIONS

<u>Configuration</u>	<u>No. of Engines</u>	<u>Throttled</u>	<u>Gimbaled</u>	<u>Mode</u>	<u>Pure Couples</u>
1 (base)	12	No	No	Tow	Yes
2	8	No	No	Tow	All but roll
3	8	Yes	No	Tow	All but roll
4	5	Yes	No	Tow	No
5	5	No	No	Tow	No
6	6	Yes	No	Push	No
7	4	Yes	No	Tow	No
8	3	Yes (1 engine)	2 engines (90° total angle)	Tow	Partial
9	6	Yes	No	Tow	Partial
10	6	No	No	Tow	Partial

UNCLASSIFIED

UNCLASSIFIED

Report AFRPL-TR-69-88

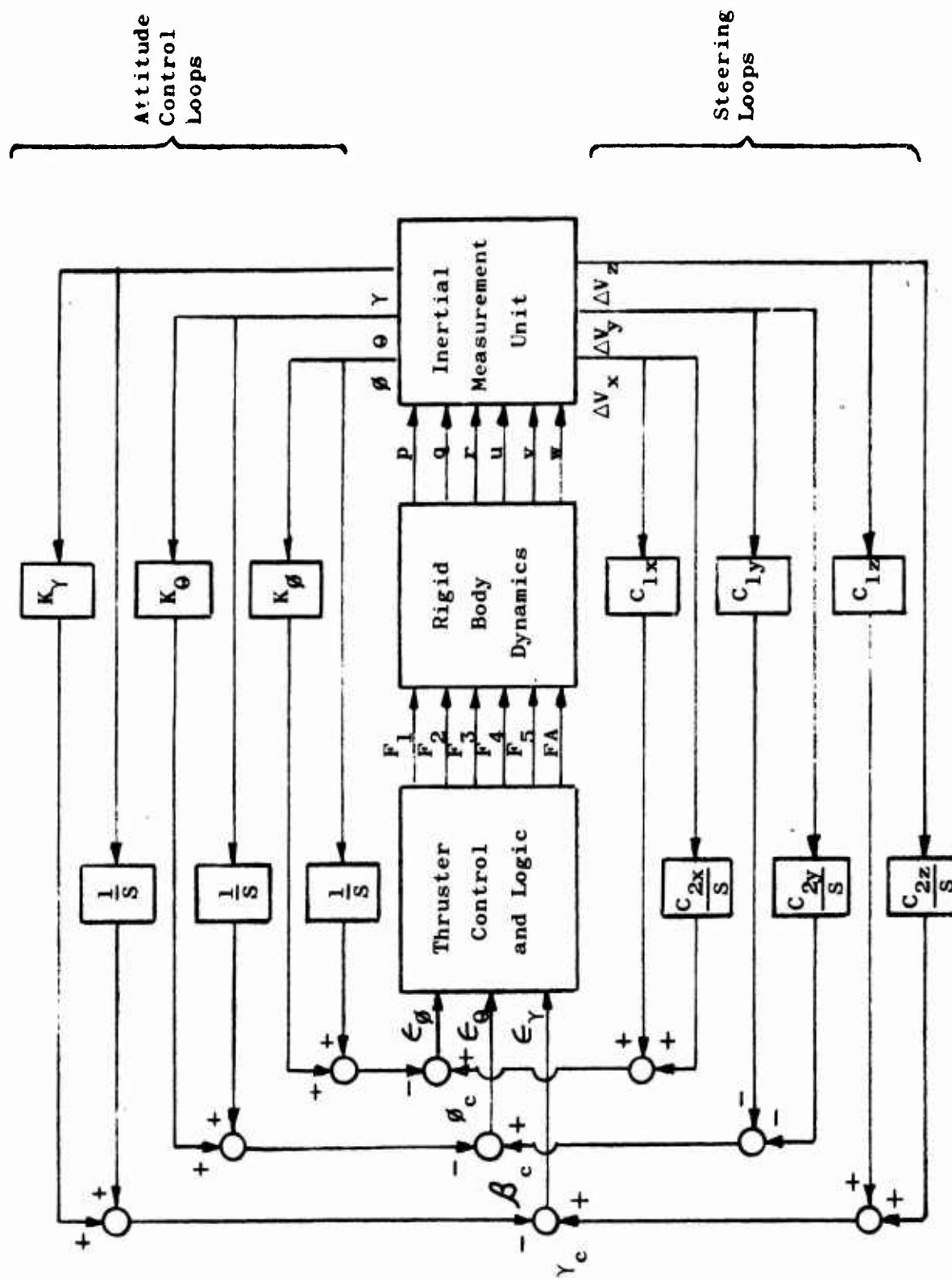


Figure 31. ACS Study Guidance and Control Loop Schematic

UNCLASSIFIED

UNCLASSIFIED

Report AFRPL-TR-69-88

IV, B, ACS Study (cont.)

The five-engine configuration evaluated is sketched on Figure No. 32. There are four primary attitude control engines around the periphery of the Post-Boost Vehicle. These engines are canted outward of the vehicle axis, with each engine providing a roll moment. Engines No. 1 and No. 3 provide a roll moment in the same direction while engines No. 2 and No. 4 are additive. Engine No. 5 provides a thrust vector along the axis of the vehicle.

Preliminary results indicated that the five-engine system has two serious limitations. First, steering maneuvers in the pitch and yaw plane could become quite complicated and/or time-consuming. Secondly, roll controlled by canting four engines results in an extreme propellant consumption.

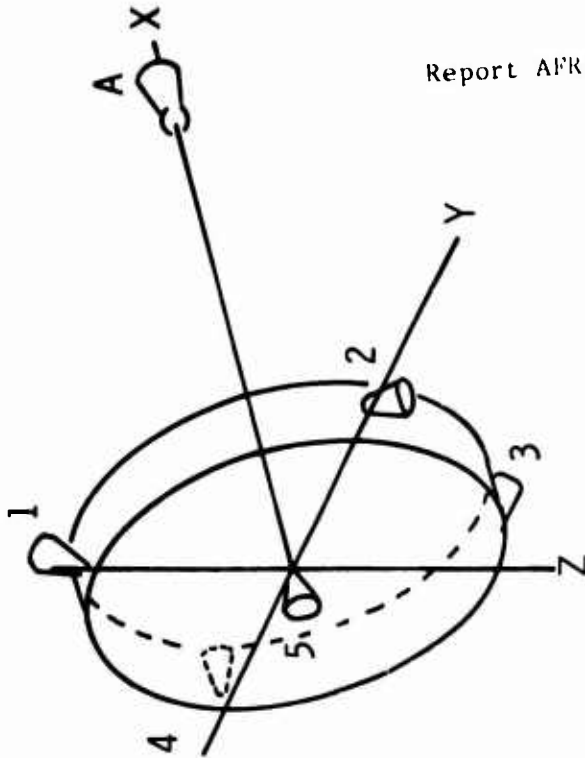
Computer evaluations with the steering loop disconnected show that the five-engine system provides stable attitude control (see Figure No. 33). However, the steering loop was unstable for translation in the pitch and yaw planes with the attitude loop connected because any translation command resulted in a vehicle rotation that was corrected by the attitude loop. This negated the translational impulse. Two options appear possible to correct this condition:

- Modify the control logic to prevent attitude control during a portion of the translation maneuver.
- Rotate the vehicle in such a manner that the bottom engine (No. 5) provides the translational impulse.

The second limitation, high propellant consumption, resulted from canting the engine for roll control. Each pitch or yaw maneuver resulted in roll, which was "bucked-out" by the adjacent pair of engines. For example, as can be seen on Figure No. 33, the total impulse of engines No. 2 and No. 4 equal the impulses of engines No. 1 and No. 3. This propellant utilization rate almost doubled the amount of propellant required for the five-engine scheme as compared to the twelve-engine scheme (see Table V).

These two problems resulted in the definition of a new configuration, the six-engine system. In this configuration, the roll cant from the pitch and yaw engine was eliminated while locating two engines on the vehicle bottom rather than one. Each of the two bottom engines was canted for roll. In this case, when roll control is required, the resultant axial impulse reduces the axial velocity imparted to the vehicle because of pitch and yaw maneuvers. Furthermore, by locating the bottom engine off of the principal axis, partial couples can be obtained when performing pitch and yaw, thereby allowing uncomplicated translation logic.

UNCLASSIFIED



X COMMAND MOTION

O MOTION ALONG AXIS DUE TO FIRED THRUSTER

● REQUIRED THRUSTER TO CORRECT FOR MOTION IN UNDESIREDEGREE OF FREEDOM

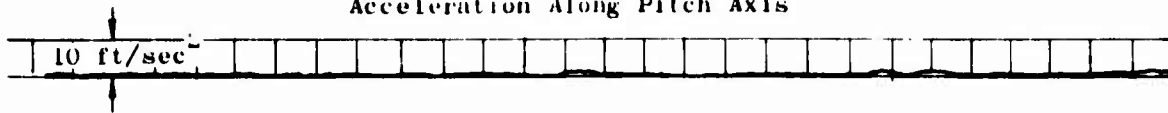
ENGINE	1	2	3	4	5	Ax
<u>TRANSLATION</u>						
+X					O	
-X	O	O	O	O		O
+Y	O			X		
-Y		X	O			
+Z	X			O		
-Z		O	X			
<u>ROTATION</u>						
+ROLL	X		X		●	
-ROLL		X		X	●	
+PITCH	X	●		●	●	
-PITCH		●	X	●	●	
+YAW	●	X	●		●	
-YAW	●		●	X	●	

Figure 32. ACS Study Control Logic (u)

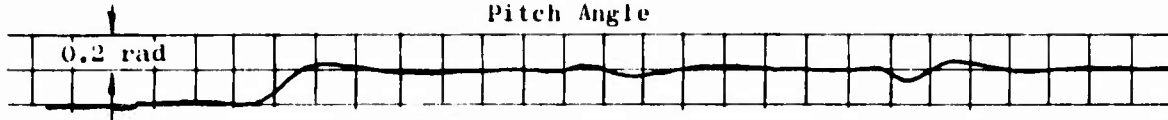
CONFIDENTIAL

Report AFRPL-TR-69-88

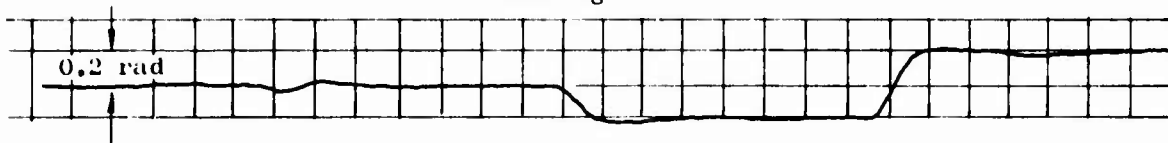
100 lb ACS 45 Degree Cant
Acceleration Along Pitch Axis



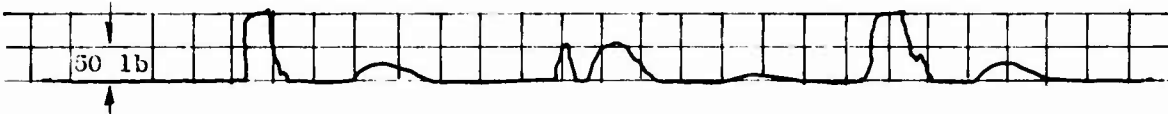
Large Angle Correction
Pitch Angle



Yaw Angle



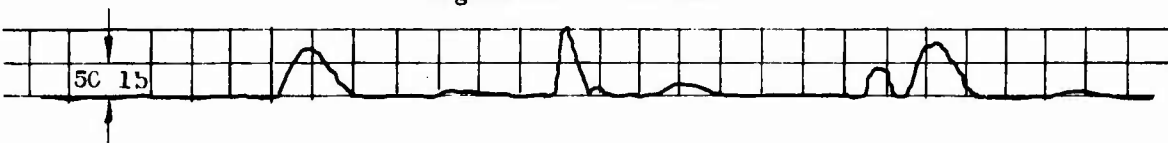
Engine No. 1 Thrust



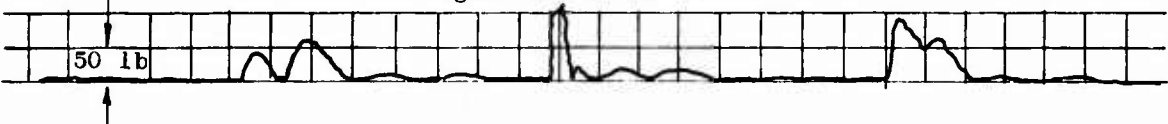
Engine No. 2 Thrust



Engine No. 3 Thrust



Engine No. 4 Thrust



Acceleration Along Roll Axis

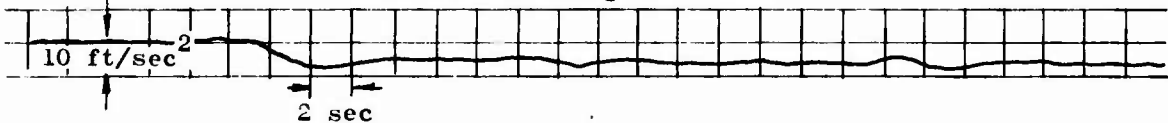


Figure 33. Five-Engine Computer Control Evaluation

Page 64

CONFIDENTIAL

(This page is Unclassified)

UNCLASSIFIED

Report AFRPL-TR-69-88

TABLE V

PRELIMINARY RESULTS

Typical Performance and Weight Values

<u>System</u>	<u>ΔACS Propellant Requirements</u>	<u>ΔTime per Sequence</u>	<u>ΔPropulsion System Inert Weight</u>
12 engine pulses	0	0	0
5 engine throttled no steering (roll cant)	+230%	0	+3%
5 engine throttled with cross steering (roll cant)	+380%	+240%	+6%
6 engine throttled no steering (no roll cant)	+180%	0	+4%

UNCLASSIFIED

IV, B, ACS Study (cont.)

The evaluation of the six-engine configuration was not completed because the contractual program was redirected to provide funding for a propellant tank expulsion demonstration. The Post-Boost Propulsion System Design activity, which included this Minimum ACS Engine Study, was deleted from the contract.

C. CONCLUSIONS AND RECOMMENDATIONS

The following conclusions are based upon that portion of the study that was completed; therefore, they are considered to be preliminary only.

1. Systems operating without any pure couples will provide stable attitude control but probably cannot operate within the operational accuracy limits.
2. Systems operating with partial pure couples might be capable of performing within the prescribed accuracy limits.
3. The five-engine scheme (see Figure No. 32), apparently cannot perform within the accuracy limits without gross steering, which is extremely time and propellant consuming.
4. There is no weight advantage offered by the five-engine scheme.
5. The factors detracting from the five-engine scheme are less significant in the following configurations because vehicle translation capability is improved:
 - Eight-Engine ACS
 - Six-Engine ACS (two on bottom)
 - Six-Engine ACS (120-degree spacing)
 - Five-Engine ACS (gimbaled fifth engine)
 - Three-Engine ACS (two gimbaled)

The configurations identified could offer potential system advantages; therefore, it is recommended that further study be considered to define the limits of each configuration.

CONFIDENTIAL

Report AFRPL-TR-69-88

SECTION V

BIPROPELLANT ACS ENGINE DEVELOPMENT

A. OBJECTIVES AND APPROACH

(U) The bipropellant altitude control engine concept selected to satisfy the operational requirements of a Post-Boost Propulsion System was changed from the integrated fluidic controls configuration to a more conventionally-controlled design when fluidic component technology was determined to be inadequate to provide acceptable engine control.

(C) The N_2O_4/MMH bipropellant engine concept developed in the redirected portion of this program utilized proprietary injector and combustion chamber concepts to provide an extremely rugged engine with a capability for operation over extensive durations and duty cycles. The demonstrated engine, which is shown on Figure No. 34 with the attached thermal test instrumentation, utilizes the stacked platelet "HIPERTHIN" injector concept developed at Aerojet-General. This injector has the unique capability of providing precisely-metered, extremely fine propellant streams. The injector design selected for this application consisted of impinging, like-on-like propellant streams that produce propellant fans. Adjacent fuel and oxidizer fans are produced by the alternate stacking of fuel and oxidizer platelets. Intimate mixing occurs because of the very thin platelets used.

(U) The conductive film cooling concept was used in the chamber to maintain acceptable local temperatures during extended duration firings. The chamber consisted of an Inconel 600 liner with a copper outer jacket which provided the conductive properties needed to cool the throat region. Fuel film coolant was injected so as to impinge upon the forward end of the chamber internal diameter and remove heat from the conductive copper jacket. A thermal balance between the fuel film coolant flow and the heat conducted from the throat resulted in a low equilibrium temperature which, in conjunction with the bimetallic construction, provided a rugged chamber with unlimited duration capability. A test exceeding 1000 sec in duration was conducted to demonstrate the thermal stability of the design.

(U) The valve selected was a torque-motor-operated bipropellant valve manufactured by Moog Inc. of East Aurora, New York. This valve provided on-off operation using the torque motor actuation to deflect torque tubes and mechanically displace the rigid steel flappers from the teflon valve seats.

(C) The engine was designed to meet the goals specified on Table VI. Three injector designs were evaluated; two were HIPERTHIN and the third was a drilled-orifice, eight-element, unlike impingement doublet injector. Two chordal baffles were used for combustion stabilization in first HIPERTHIN

CONFIDENTIAL

CONFIDENTIAL

Report AFRPL-TR-69-88

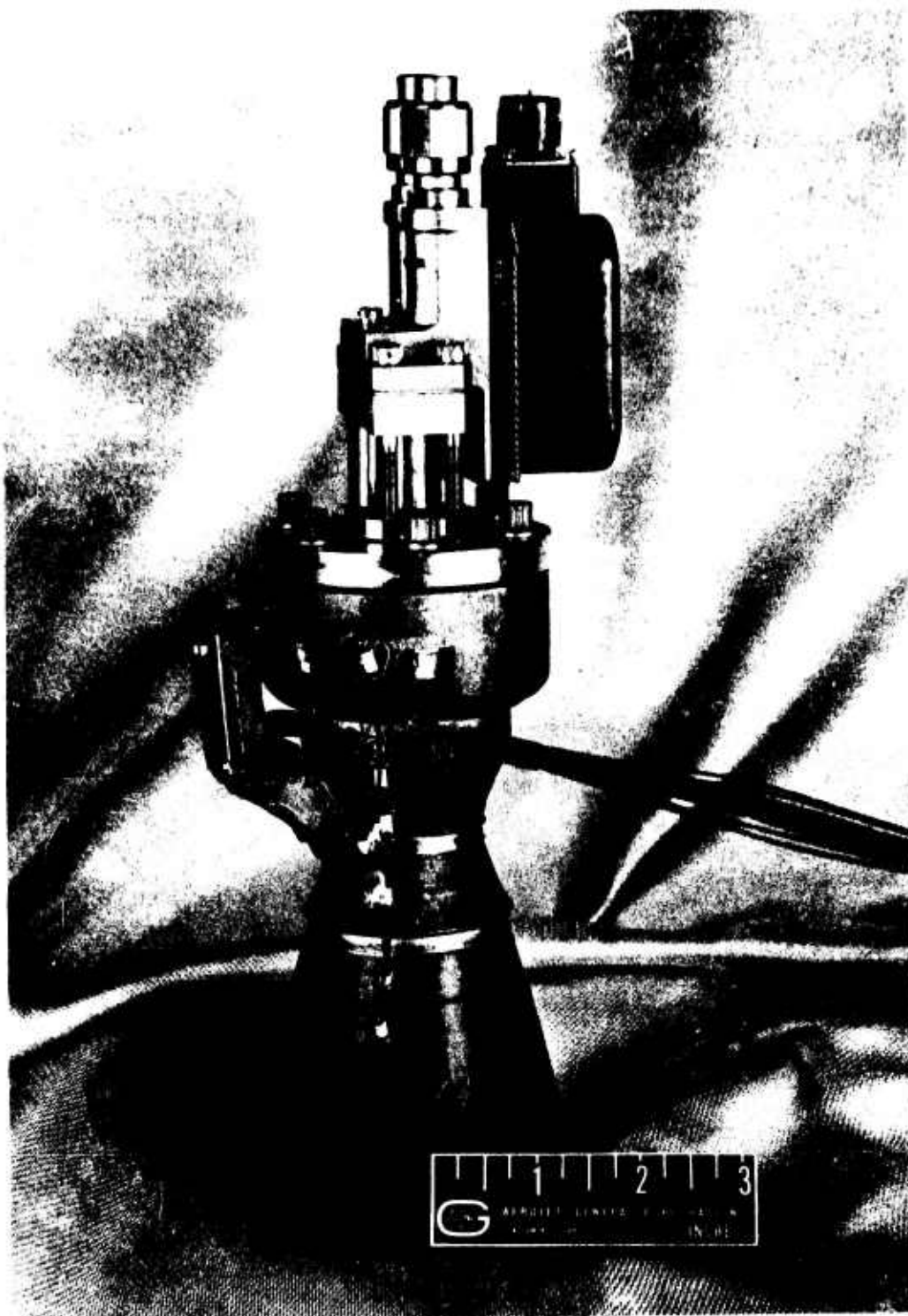


Figure 34. Bipropellant ACS Engine

Page 68

CONFIDENTIAL

(This page is Unclassified)

CONFIDENTIAL

Report AFRPL-TR-69-88

TABLE VI

BIPROPELLANT ACS ENGINE DESIGN GOALS (U)

<u>Parameter</u>	<u>Goal</u>
Thrust	75 lbs \pm 10% (3 sigma)
Specific Impulse	270 sec min
Response:	
Start signal to 90% thrust	.020 sec
Shutdown Signal to 5% thrust	.020 sec
Duty Cycle:	
Worst case thermal duty cycle within 900 second mission	

CONFIDENTIAL

CONFIDENTIAL

Report AFRPL-TR-69-88

V. A. Objectives and Approach (cont.)

injector design. The baffled HIPERTHIN and the eight-element doublet were evaluated through sea-level ambient tests using a bimetallic chamber with a 1.4:1 divergent nozzle expansion ratio. Various fuel film coolant flow rates were utilized with each injector to determine chamber cooling requirements. These tests demonstrated that the HIPERTHIN injector concept provided the more favorable chamber cooling. Excessive coolant flows, which were accompanied by erratic operation, were necessary to approach stable thermal conditions with the doublet injector.

(C) An unbaffled HIPERTHIN injector and a bimetallic chamber with a 40:1 expansion ratio were used in the second thruster design. This combination was initially tested with externally-supplied fuel film coolant to identify the specific requirements for chamber cooling. After modifying the injector to incorporate an internal flow passage for the fuel coolant, a series of tests were satisfactorily conducted at altitude conditions to demonstrate the durability and pulsing characteristics of the engine.

(U) The sequence of the preliminary design, development, and demonstration testing which provided the resultant engine are identified in the following sections.

B. ENGINE PRELIMINARY DESIGN AND ANALYSIS

1. Bimetallic Combustion Chamber

(U) The thrust chamber is a one-piece unit consisting of an Inconel 600 liner and an integral, copper, outer shell. Chamber temperatures are maintained within acceptable limits by conducting heat from the throat area of the thrust chamber to the forward end where the impinging fuel removes heat from the hot chamber wall. In this design, the Inconel acts as a thermal and chemical shield for the copper while the copper provides an efficient path for the conduction of heat from the high temperature throat area to the low temperature forward end of the thrust chamber. The thrust chamber geometric parameters are listed on Table VII.

(U) The internal dimensions of the two thrust chambers differed only in area ratio. In the flight version, an expansion ratio of 40:1 was used with a Rao contour while in the sea-level version, an expansion ratio of 1.4 was used. Variables in a design of this type are the thicknesses of the copper and the Inconel at the various axial locations along the chamber. The sea-level chamber design was used to acquire thermal data for use in the design of the altitude configuration thruster. These data were obtained to define chamber thermal conditions at various coolant flow rates which, along with the theoretical nozzle heat loads, provided a basis for configuring the liner and the conductive jacket.

CONFIDENTIAL

UNCLASSIFIED

Report AFRPL-TR-69-88

TABLE VII

COMBUSTION CHAMBER GEOMETRIC PARAMETERS

Chamber Diameter at Injector	1.25
Throat Diameter	0.518
Contraction Ratio	5.85
Area Ratio (ϵ) Flight Version	40/1
Prototype Version	1.4/1
Copper Heat Sink Ends	20/1
L^*	8.7
L'	2.25
Contour-Nozzle	Rao

UNCLASSIFIED

V, B, Engine Preliminary Design and Analysis (cont.)

Temperature data were obtained from numerous thermocouples on the injector and chamber during both test firing and heat soak periods. Combustion chamber temperatures were provided by thermocouples located at the gas-side surface of the chamber and throat, at the interface between the chamber metals, and on the external surface of the chamber.

a. Altitude Expansion Chamber

The initial design of the bimetallic thrust chamber for altitude use is shown on Figure No. 35. This chamber design has a 40:1 expansion area ratio nozzle and was based upon thermal data extrapolated from tests conducted using different injector types or operating conditions. It was used as the basis for configuring the sea-level chamber and test program.

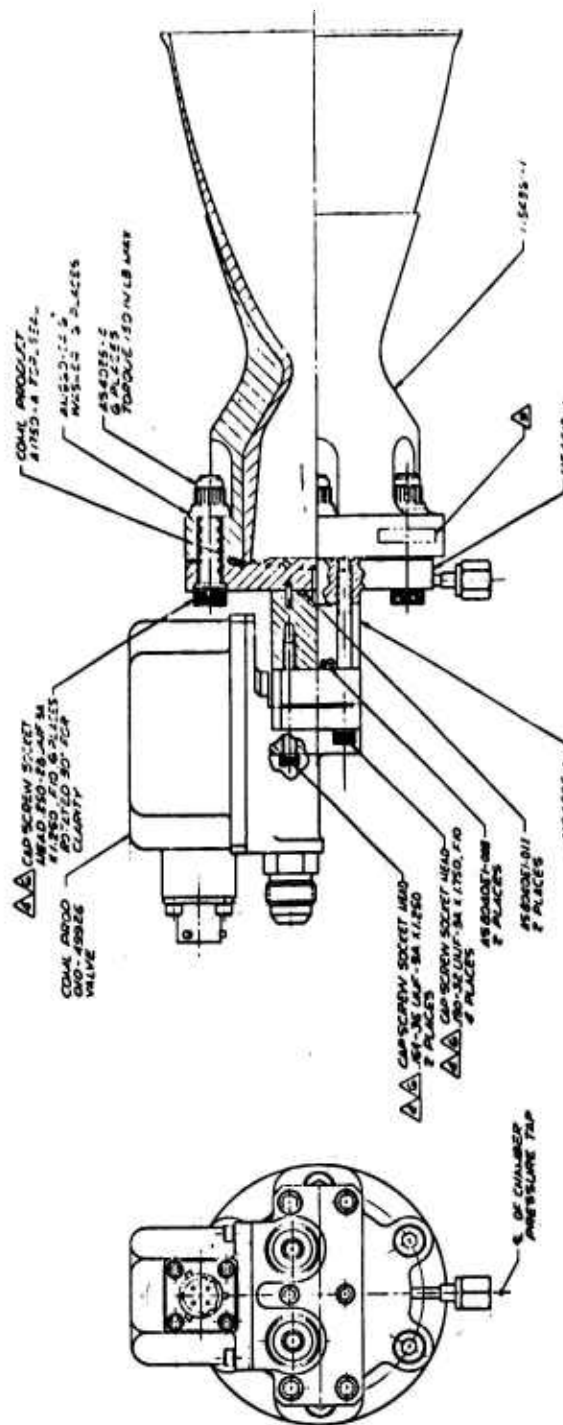
b. Sea-Level Expansion Chamber

The prototype chamber for the sea-level demonstration testing had the same copper and Inconel profile thicknesses as the previously described altitude expansion design. The prototype chamber was designed with an area ratio of 1.4 and was identical to the 40:1 chamber from the injector flange to the axial location of the 1.4 area ratio. The measured throat area temperatures obtained with this chamber were expected to be 20% lower than those of the 40:1 chamber because the heat, which would be conducted from the nozzle extension, would be absent. The thermal design of the flight chamber would be verified by adding the theoretical nozzle heat loads (identified by the thermal model discussed in Section V,4,c) to the chamber heat loads measured during the prototype test series.

2. Injector Design

Two injectors were designed for the evaluation of the sea-level chamber. The primary configuration was an eight-element doublet of the type previously demonstrated with this chamber cooling concept at a lower chamber pressure. It was designed with a core consisting of eight, unlike, impinging, doublet elements and a periphery consisting of 16 orifices nominally designed to flow 35% of the fuel for film cooling. The core elements were designed to mix and then impinge the resultant streams upon the chamber wall. This wall impingement would serve to promote atomization and mixing with the film coolant which impinged at an upstream station on the wall. The film coolant manifold was designed with an inlet that was independent of the core manifold to permit the film coolant flow rate to be varied during testing. The flight configuration injector would have a single inlet and use an internal flow passage for the fuel coolant.

Report AFRPL-TR-69-88



CONFIDENTIAL

Report AFRPL-TR-69-88

V, B, Engine Preliminary Design and Analysis (cont.)

(C) An alternative injector concept which had been successfully demonstrated in other programs with the bimetallic combustion chamber at lower chamber pressures was selected to provide comparative data at the higher operating pressure of this application. The HIPERTHIN injector concept selected for this application was an impinging element design which incorporated integral stabilization baffles. The HIPERTHIN injector was designed to interface with the same chamber as the doublet injector and to operate with a 30% fuel film cooling flow rate. The film coolant manifold was independent of the core circuit to allow performance and thermal data to be obtained at various coolant flow rates. The core manifolds of the injector were designed for minimum volumes to provide an optimum pulse mode operation.

a. Conventional Orificed Injector

(U) The primary injector featured an eight-element, unlike doublet, orifice pattern plus fuel film cooling. It was fabricated from 304L stainless steel components joined by electron-beam welding. The injector manifold volumes were minimized to provide fast response within the limits of the PBPS pressure schedule. Figure No. 36 shows this injector and the design parameters are summarized on Table VIII.

(U) The eight, doublet elements were arranged in a circumferential pattern with the oxidizer orifices located inboard and the fuel orifices radially outboard from the oxidizer. The elements were designed to operate at a momentum ratio $W_o/W_f \times V_c/V_f$, of 2.45. The momentum ratio and the angular orientation of the streams produced a resultant vector directed toward the chamber wall at an angle of 20-degrees to the chamber centerline. The resulting outboard vector directed the mixing propellants to strike the wall 1-in. downstream from the injector face to promote atomization of the core propellants and mixing with the fuel coolant. The film coolant was injected into the combustion chamber through 16 orifices located at an outboard angle of 30-degrees to the axis of the combustion chamber. Impingement of the coolant with the wall occurred at a station 0.225-in. from the injector face.

(U) The injector manifolding consisted of a central oxidizer manifold and two coaxial manifolds for the core fuel and the film coolant. The oxidizer entered the injector body through a drilled hole from the back side. The drilled hole led directly to the eight oxidizer orifices. This provided a low volume circuit which was simple to manufacture and made efficient use of the oxidizer for cooling the central area of the injector face.

(U) The fuel entered the injector through a drilled hole in the injector flange. This drilled hole intersected an annular channel designed with decreasing cross-sectional area to maintain constant manifold velocity. The variable area was used to reduce volume in both the core fuel manifold and

CONFIDENTIAL

UNCLASSIFIED

Report AFRPL-TR-69-88

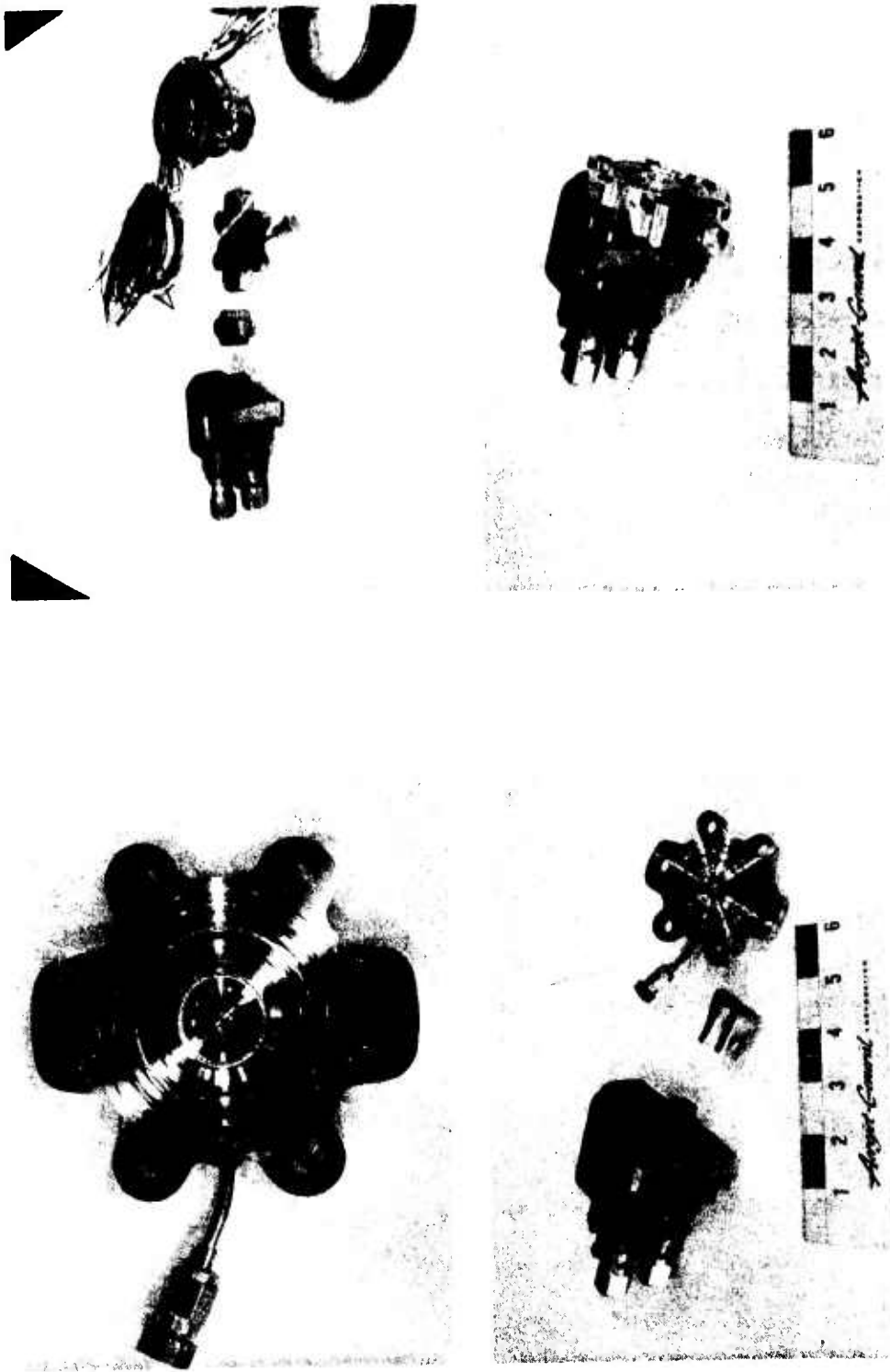


Figure 36. 75 lb Thrust ACS Engine

UNCLASSIFIED

UNCLASSIFIED

Report AFRPL-TR-69-88

TABLE VIII

PBPS DOUBLET INJECTOR PARAMETER SUMMARY

	<u>Oxidizer</u>	<u>Fuel</u>	<u>Fuel Film Cooling</u>
\dot{w} , lb/sec	0.1709	0.1068	35%
Diameter Orifice, in.	0.0236	0.0188	0.0368
Pressure Orifice, psi	95	60	0.0096
Pressure Manifold, psi	24.0	33.0	60
Pressure Total, psi	119	93	33.0
Volume, in. ³	0.00455	0.018	93
V_o/V_f =		1	
MR System =		1.6	
MR Core =		2.45	
$\frac{W_o \times W_o}{W_f V_f}$ =		2.45	

Calculated Injector Weight 0.58 lb
 Calculated Valve Adapter Weight 0.20 lb

UNCLASSIFIED

CONFIDENTIAL

Report AFRPL-TR-69-88

V, B, Engine Preliminary Design and Analysis (cont.)

the film cooling manifold while maintaining a low manifold pressure drop. In the workhorse injector, the fuel film cooling manifold was independent of the core circuit. The separation of the film cooling circuit from the core fuel circuit permitted variation of the coolant flow to optimize the coolant requirements before the flight version was designed.

b. Baffled Injector

(C) The alternative injector tested during the prototype phase of this program was the baffled HIPERTHIN shown on Figure No. 37. The HIPERTHIN injector is formed by assembling platelets which are thin sheets of metal containing patterns of flow channels. Fundamentally, there are two types of platelets used in making this type injector; metering platelets and separator platelets. To assemble an injector, the platelets are placed in a stack and bonded into a single, integral unit. The fuel and oxidizer metering platelets in the stack are separated by a platelet which provides manifolding for the metering platelets. This is shown in the conceptual illustration, Figure No. 38.

(C) The PBPS HIPERTHIN injector was composed of three sub-assemblies that were joined by brazing; the platelet stack, the coolant flange, and the manifold cover. The platelet stack contained nine fuel metering platelets, eight oxidizer metering platelets, 34 plenum spacers, and 54 blank separators. The injector core was fabricated by stacking the platelets in a particular sequence and brazing the platelet subassembly. Two chordal injector face baffles were made by locally recessing the injector face in the areas without baffles. The platelet subassembly then was machined to fit the fuel film coolant flange.

(C) The resulting design provided five rows of alternating oxidizer and fuel impinging pairs. There were 37 impinging fuel pairs and 32 impinging oxidizer pairs over the injector face. Each oxidizer pair consisted of two injection slots which were 0.003-in. wide by 0.0027-in. long. The fuel pairs had 0.003-in. by 0.014-in. slots.

(C) The fuel film coolant flange consisted of a ring surrounding the injector core which had 15 drilled orifices designed to impinge coolant fuel against the chamber wall. The coolant fuel was fed through the platelet stack from an external inlet which was welded to the manifold cover to permit control of film coolant. The flight configuration injector was converted to an internal fuel coolant feed system by drilling through to the top fuel manifold and plugging the external inlet.

CONFIDENTIAL

CONFIDENTIAL

Report AFRPL-TR-69-88

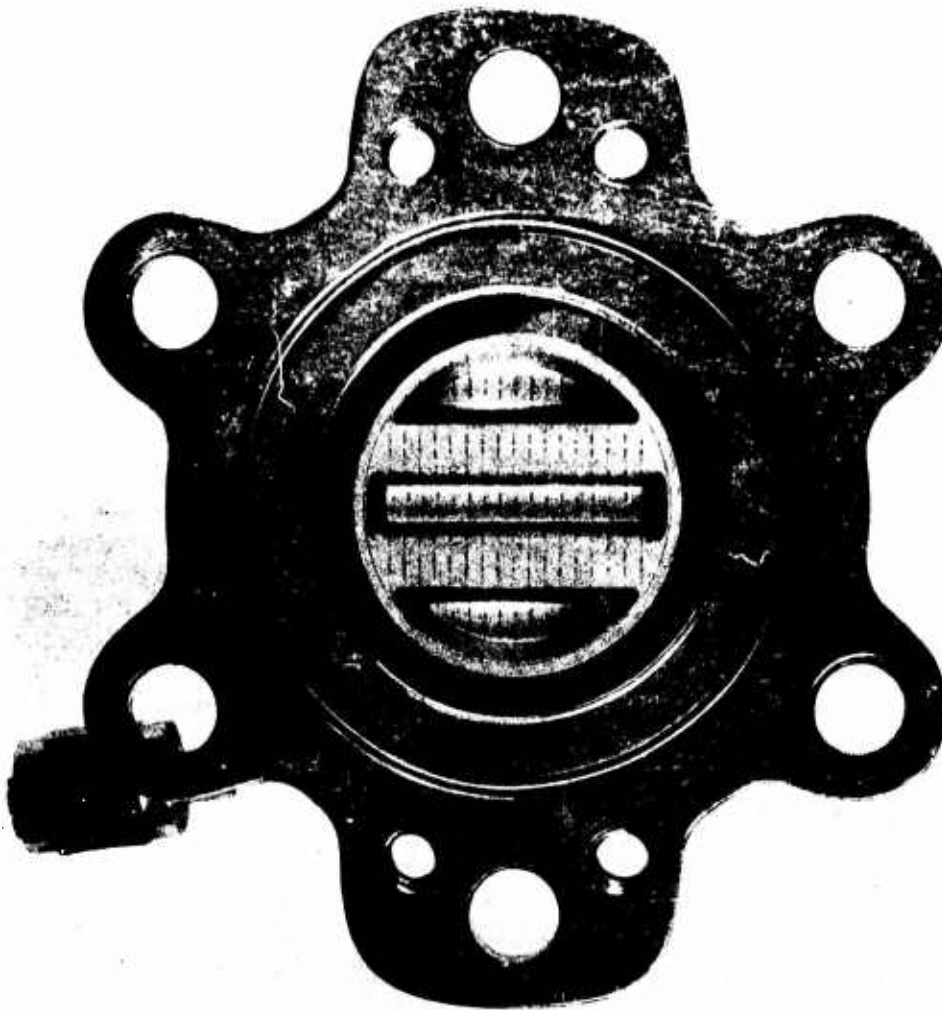


Figure 37. Baffled Alternative Injector (u)

Page 78

CONFIDENTIAL

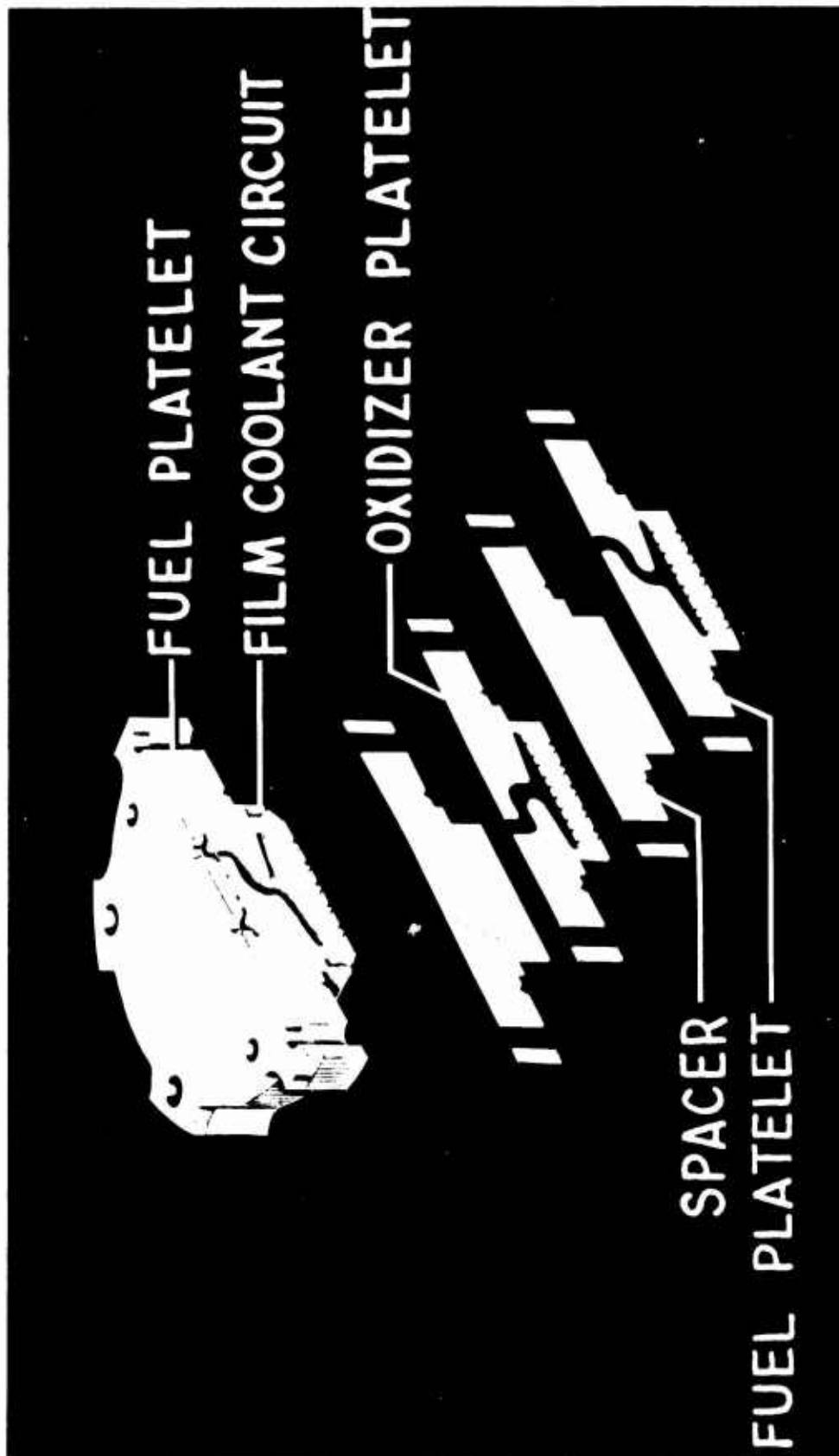


Figure 38. Injector Assembly Sequence (u)

CONFIDENTIAL

Report AFRPL-TR-69-88

V, B, Engine Preliminary Design and Analysis (cont.)

c. Flat-Faced Injector

(C) A second HIPERTHIN injector design was evolved by redesigning the first design to remove the chordal baffles. This resulted in a flat-faced unit. The configuration of the fuel and oxidizer orifices was unchanged; the impingement point of all element pairs was in a single plane. The plane of the face was at the same elevation that the tops of the baffles had been. This design was used to replace the injector with baffles when problems were encountered in cooling the exposed side walls of the fuel film coolant manifold which had been exposed when the baffles were machined.

3. Torque Motor Bipropellant Valve

(U) The thrust chamber valve used was a torque-motor-operated bipropellant valve manufactured by Moog Inc., East Aurora, New York. This valve provided a reproducible and fast response and had been thoroughly demonstrated during testing in another Aerojet-General program.

(U) The valve was very similar to the bipropellant valves built by Moog for the C-1 Program (NASA-funded). The only significant change between the valves built for the C-1 Program and the one used in this program was that the C-1 valve had an all-welded configuration. Metallic seals were used to replace a weld at the interface of the valve body and the valve manifold to reduce costs.

(U) The valve was designed to be fail-safe in the event of a power failure. The armature/flapper was magnetically pre-loaded against the valve seat so that an electrical power failure would result in an "off" condition for both the propellant orifices.

(U) Synchronization of fuel and oxidizer flow was achieved by mechanically-coupling both poppet control flappers to a single armature. Rigid flappers were used in this design to ensure simultaneous opening and closing of both poppets.

4. Pre-Test Analyses

a. Performance

(C) Analyses were conducted to predict the performance of the eight-element doublet and the baffled HIPERTHIN injector designs to be used in the initial evaluations at sea-level conditions. The film coolant flow rate for both injectors was assumed to be 30% for the performance analysis.

CONFIDENTIAL

CONFIDENTIAL

Report AFRPL-TR-69-88

V, B, Engine Preliminary Design and Analysis (cont.)

(C) The HIPERTHIN injector was evaluated using conventional vaporization analysis techniques. The doublet injector, on the other hand, was less amenable to accurate performance analysis using conventional vaporization techniques; therefore, a semi-empirical analysis was conducted to augment the vaporization analysis.

(C) The technique used in the analysis of the doublet injector was to apply empirical bias factors obtained from hot firing data of similar injector-chamber combinations which also impinged propellants onto the chamber wall. These empirical data were correlated with reduced drop size generated by mechanical fragmentation. Test data from two designs were analyzed and good data correlation was achieved when the reduction in drop size was approximately 75% of the original propellant drop diameter. The results of these studies were applied to the doublet injector to provide an upper limit performance prediction.

(C) The first analysis treated the doublet injector as if no wall impingement effects were present. A two-stream tube model was assumed with the core operating at a vaporized mixture ratio of 2.66. The specific impulse contribution of the film coolant was assumed to be the monopropellant specific impulse expanded to a 40:1 area ratio. The net energy release loss was 16.3%, which was consistent with the short, high contraction ratio chamber. In the second method of evaluation, it was assumed that the droplet size was reduced by 78% after the impingement. To account for this mechanism, a two part vaporization analysis was conducted to assess conditions before and after propellant impingement upon the chamber wall. From the injector face to the wall impingement point, the vaporization analysis was handled in a conventional manner. An increased vaporization rate was assumed after chamber wall impingement and droplet size reduction. Then, the total vaporized propellant operating at a local mixture ratio was utilized to predict the performance of the core doublets. The performance contribution from the coolant fuel was added to the core performance to provide the upper limit predicted performance. The delivered performance predictions were obtained by subtracting the individual performance losses resulting from kinetics, geometry and boundary layer effects.

(C) Table IX is a summary of the predicted performance for the HIPERTHIN injector and for the two analytical approaches used with the doublet injector. As the second analysis of the doublet was based upon only two sets of empirical data, the high delivered specific impulse predicted using method two, was considered a performance upper limit.

CONFIDENTIAL

CONFIDENTIAL

Report AFRPL-TR-69-88

TABLE IX

PREDICTED PERFORMANCE SUMMARY (U)

	<u>HIPERTHIN</u>	<u>Doublet Assumption One*</u>	<u>Doublet Assumption Two*</u>
No. of Elements	44 fuel 39 oxidizers	8	8
Impingement Angle	60	90	90
Percentage of Fuel Film Coolant \dot{w}_{fc}/\dot{w}_f	30	30	30
I_{sp} theoretical $\frac{\text{lb-f-sec}}{\text{lbm}}$	330	330	330
Film Coolant Loss, $\frac{\text{lb-sec}}{\text{lbm}}$	4	4	4
Energy Release Loss, $\frac{\text{lb-sec}}{\text{lbm}}$	19	54	12
Finite Rate Loss, FRL $\frac{\text{lb-f-sec}}{\text{lbm}}$	14	12	14
Geometry and Boundary Layer Loss $\frac{\text{lb-f-sec}}{\text{lbm}}$	10	10	10
Delivered I_{sp} $\frac{\text{lb-f-sec}}{\text{lbm}}$	$283 \pm 2\%$	250	290
Percentage of Delivered I_s	$85.7 \pm 2\%$	75.8	87.9

*Assumes no performance improvement because of wall impingement.

**Assumes a 78% decrease in spray drop size after wall impingement

CONFIDENTIAL

UNCLASSIFIED

Report AFRPL-TR-69-88

V, B, Engine Preliminary Design and Analysis (cont.)

b. Stability

During the preliminary design phase of the program, analyses were conducted to assess the relative stability characteristics of two chamber diameters when used with the eight-element doublet injector. A 1.5-in. internal diameter design was found to have marginal stability and a reduction to 1.25-in. was recommended.

Two methods were used to assess the expected stability characteristics of two different chamber quantities. In the first, the conventional Sensitive Time-Lag Theory was used and it indicated that the 1.25-in. chamber diameter would result in a system which was linearly stable with regard to high-frequency instability. Figure 39 shows the predicted operating regime for this design. The second method was to make an empirical comparison of three engines of a similar size to support the theoretical stability predictions. The results of this comparison, which are shown on Figure No. 40, supported the analytical conclusion that stable operation would be achieved with the smaller diameter chamber.

c. Thermal

The design of the conductively-cooled, bimetallic combustion chamber shown on Figure No. 35 was based upon the results of a two-dimensional, radial-axial conduction network thermal analysis. The principle of operation of the conductively-cooled chamber is illustrated on Figure No. 41. Steady-state temperatures were achieved by the transfer of heat to the film coolant from the combustion gases and from the chamber wall adjacent to the injector. The heat transferred from the chamber wall to the coolant was conducted from the high temperature areas (the throat) of the chamber through the copper jacket surrounding the Inconel liner. Nozzle temperatures were transient until a heat balance was established. The high conductivity copper was used to transfer heat with a minimum cross-sectional area (minimum nozzle weight) for a reasonable axial temperature gradient. Radiation cooling was used to cool the nozzle extension.

Fuel film temperatures were calculated in the analysis by including the film as part of the thermal model. Heat was transferred to the film from the combustion gas and also was exchanged between the film and the nozzle wall with the direction of the exchange depending upon the relative temperatures. Convection was considered the mechanism of heat transfer between the combustion gas and the film coolant. A turbulent simplified Bartz (Ref. 4, pp 49-51) heat transfer coefficient was used up to the point at which laminarization was predicted (Ref. 5). Coefficients are shown as a function of chamber length on Figure No. 42.

UNCLASSIFIED

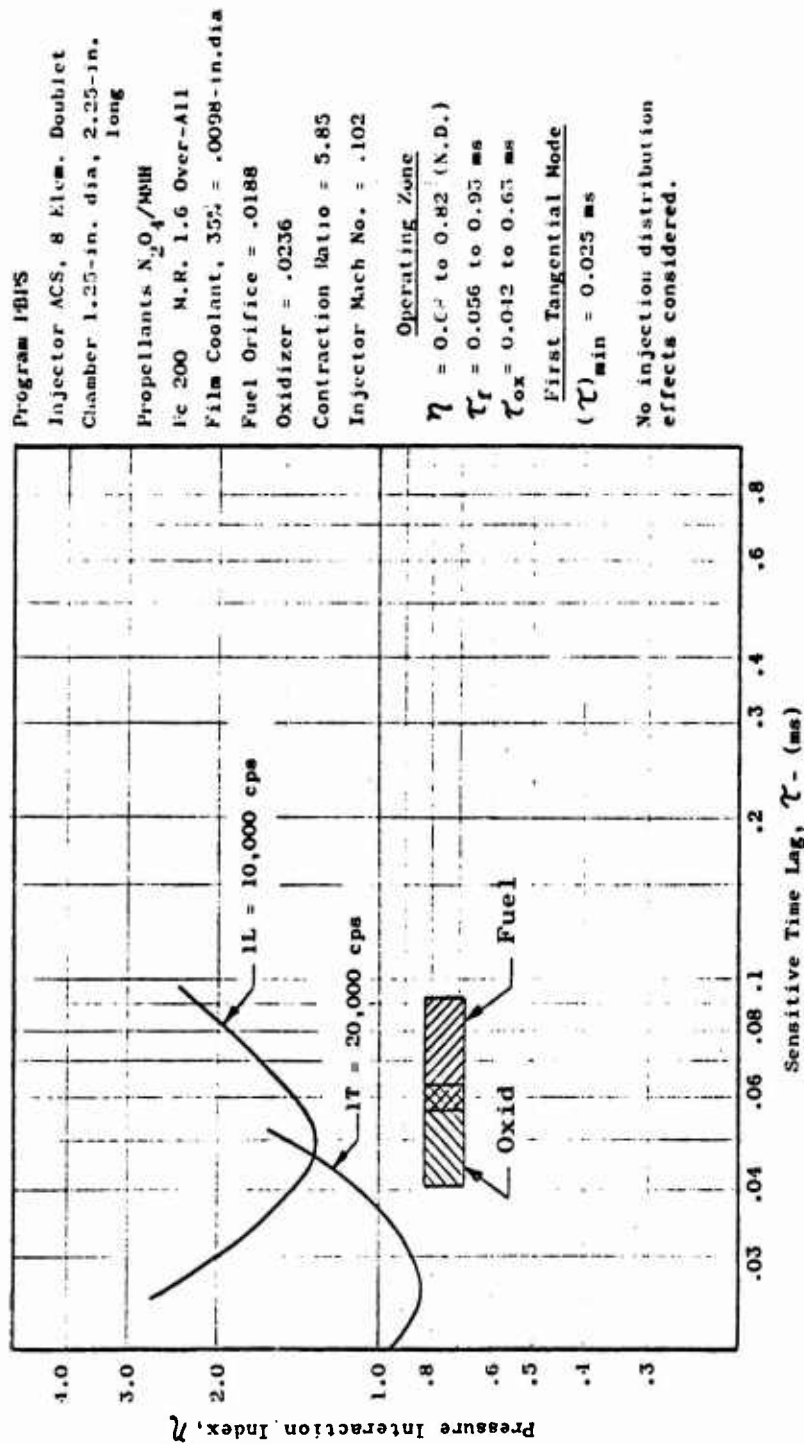


Figure 39. Sensitive Time-Lag Injector Evaluation

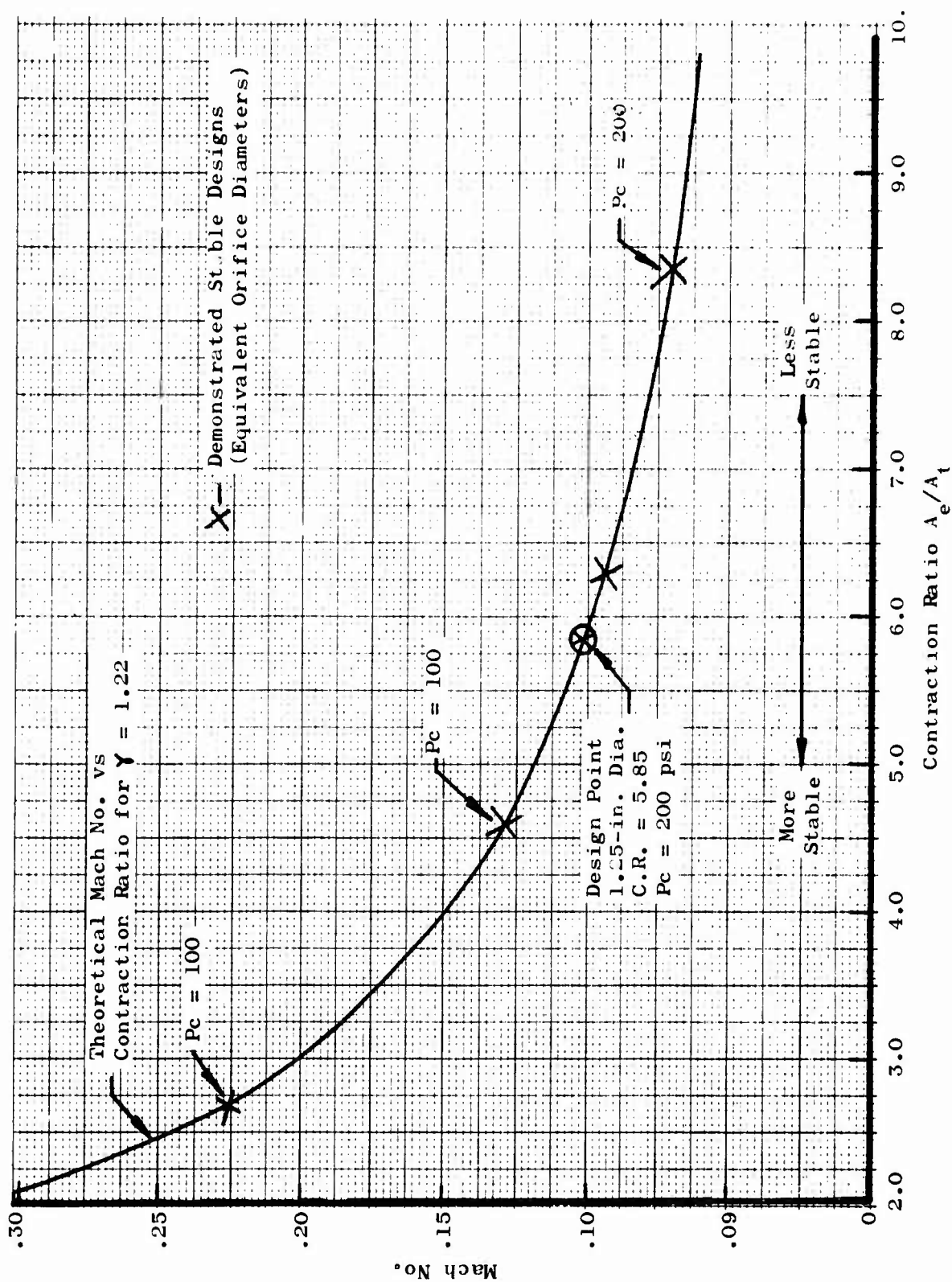


Figure 40. Empirical Stability Study Results

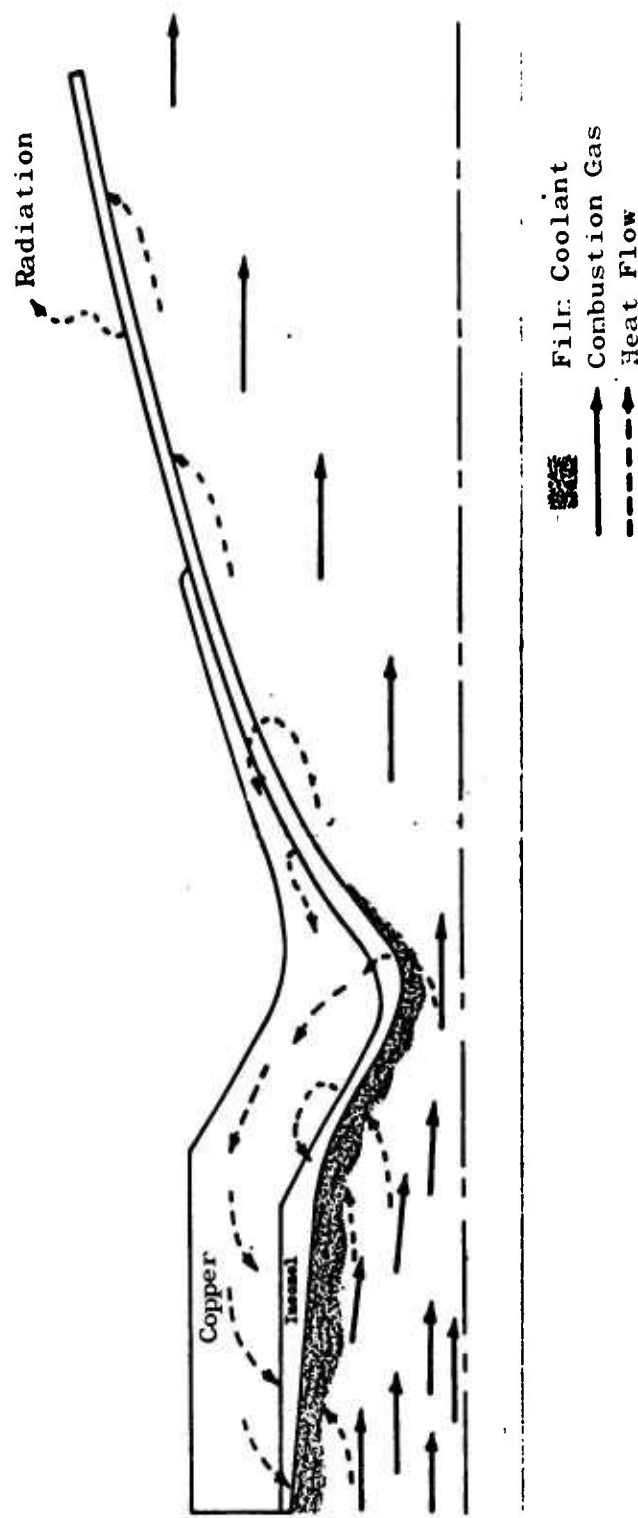


Figure 41. Principle of Operation of Bimetalllic Heat Pump Nozzle

UNCLASSIFIED

Report AFRPL-TR-69-88

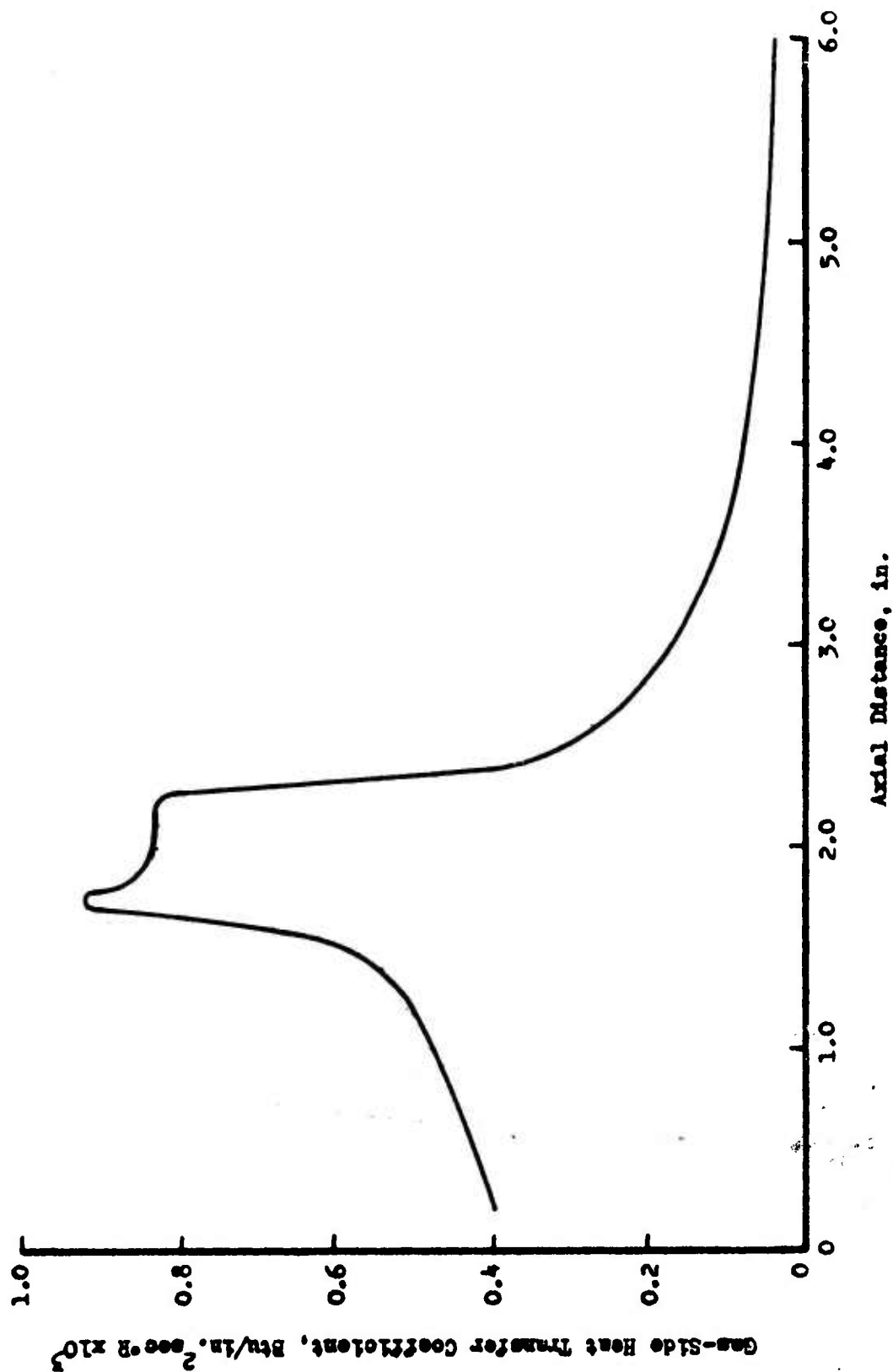


Figure 42. Gas-Side Heat Transfer Coefficient vs Axial Distance

UNCLASSIFIED

UNCLASSIFIED

Report AFRPL-TR-69-88

V, B, Engine Preliminary Design and Analysis (cont.)

Nozzle temperature transients were predicted for a 300 sec firing followed by a 400 sec coast (Figure No. 43) as well as for a continuous 700 sec firing (Figure No. 44). The chamber isotherms predicted for the chamber after 700 sec of continuous firing are shown on Figure No. 45. All predictions were for 30% fuel film cooling. These figures show the maximum temperature experienced (1800°F) was to be at the radiation-cooled nozzle extension. The maximum Inconel temperature, excluding the nozzle extension, was found at the throat, 1300°F after a 300 sec firing and 1400°F after a 700 sec firing.

A thermal evaluation of the 1.4:1 expansion ratio chamber used for the sea-level test evaluation was conducted to determine the expected temperature profiles when the nozzle heat loads were not applied to the chamber. The resultant thermal profile, shown on Figure No. 46, was used as a basis for evaluating thermal data from sea-level tests.

UNCLASSIFIED

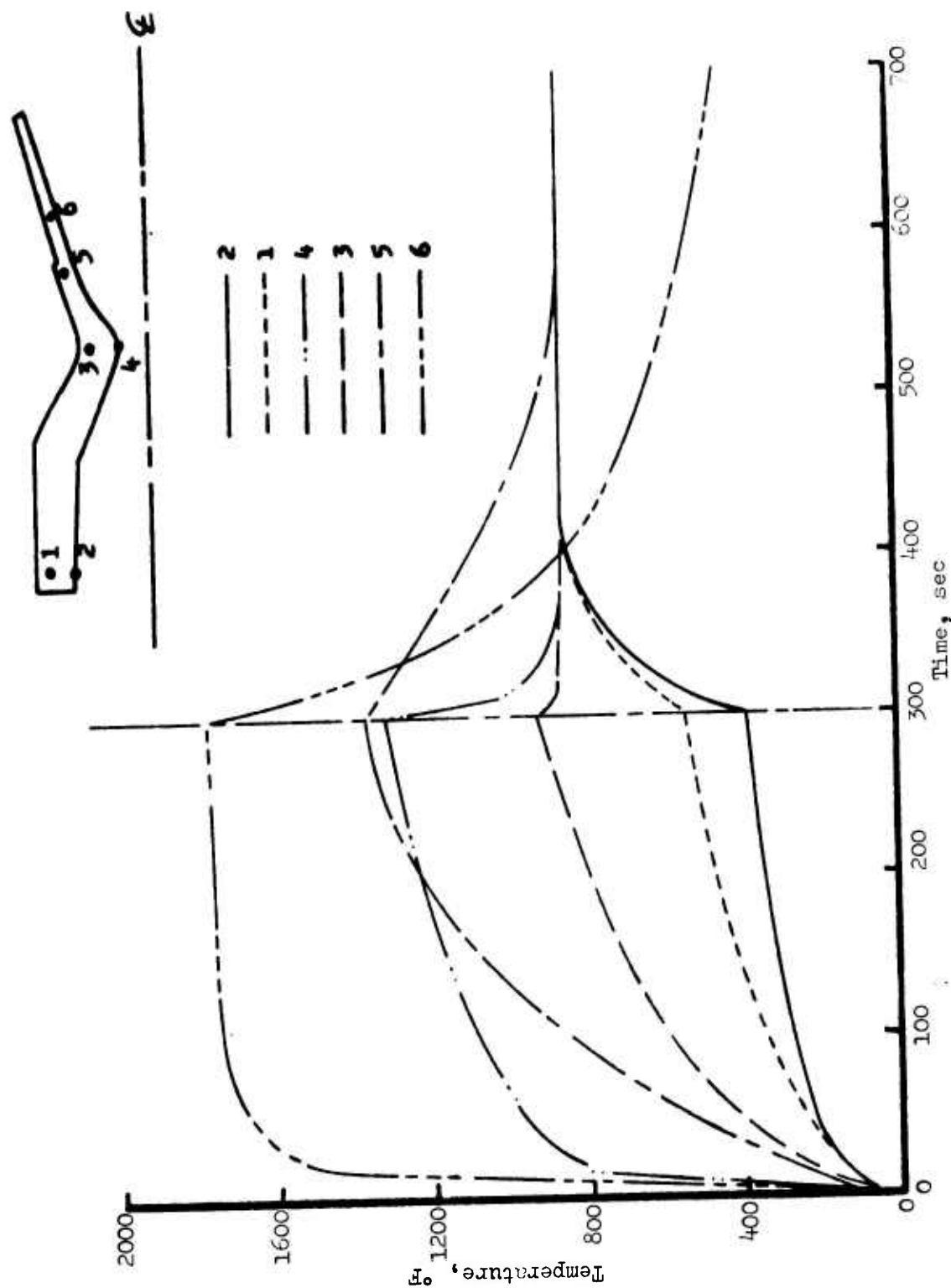


Figure 43. Predicted Nozzle Temperature Transients

UNCLASSIFIED

Report AFRPL-TR-69-88

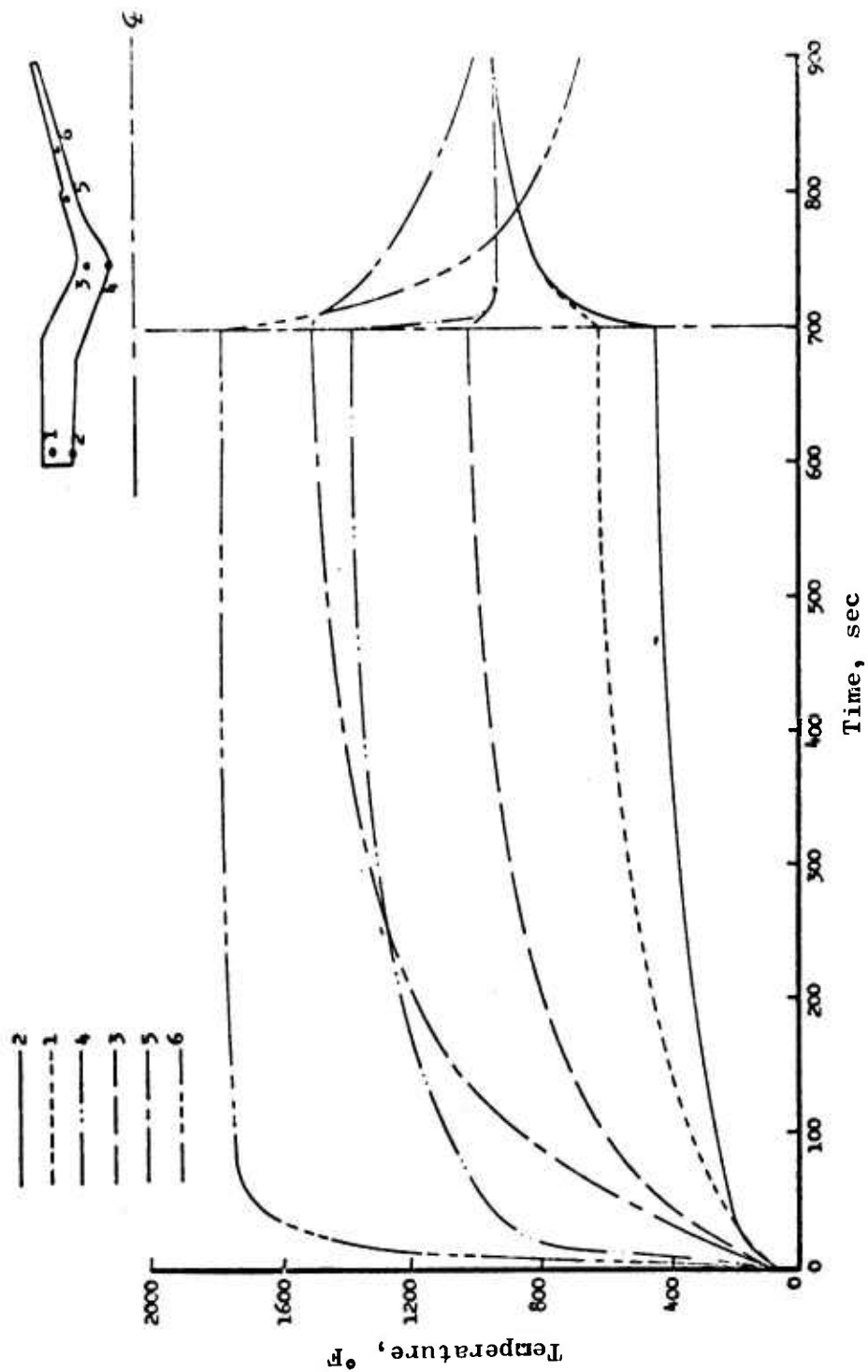


Figure 44. Predicted Nozzle Temperature Transients

UNCLASSIFIED



Figure 45. Predicted Nozzle Isotherms at 700 sec of Firing

UNCLASSIFIED

Report AFRPL-TR-69-88

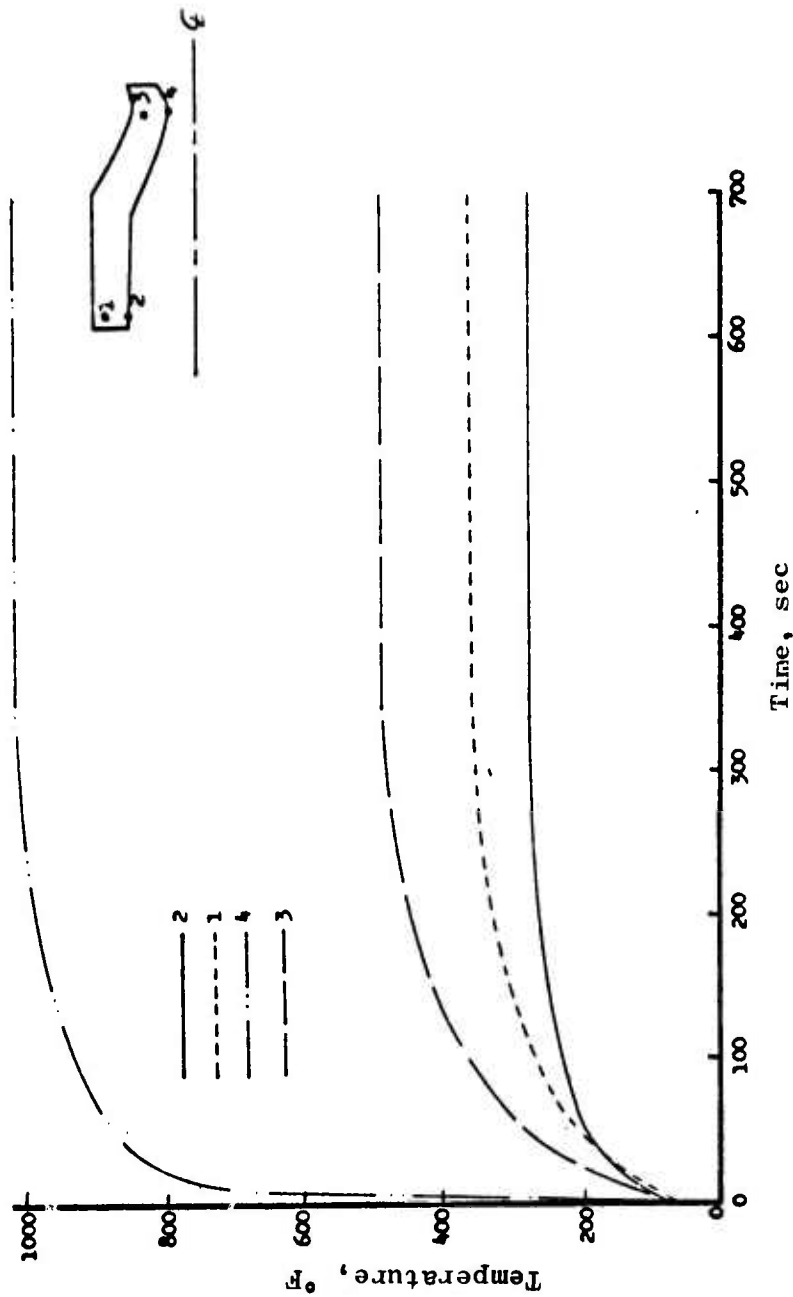


Figure 46. Predicted Nozzle Temperature Transients - Sea-Level

UNCLASSIFIED

V, Bipropellant ACS Engine Development (cont.)

C. ENGINE SEA LEVEL TEST EVALUATION

1. Fabrication

(C) The hardware fabricated for the sea-level expansion ratio test phase included an eight-element, unlike, doublet injector; a baffled HIPERTHIN injector; and a copper/inconel, conductively-cooled combustion chamber which had a 1.4:1 expansion ratio. These components, along with a Moog torque motor bipropellant valve, are shown on Figure No. 47.

(U) The thermal instrumentation used to obtain combustion chamber temperature data also is shown on Figure No. 47. Twenty thermocouples were brazed into 0.0225-in. diameter holes to measure gas-side and copper-inconel interface temperatures. Five thermocouples were staked onto the surface of the chamber for external temperature measurement.

(U) A hydraulic flow check of the valve and each injector was conducted to determine the flow coefficients as well as to verify that the proper pattern characteristics were achieved. All orifices of the doublet injector flowed very clean with direct impingement of the unlike elements as shown on Figure No. 48. The radial outward momentum of the oxidizer flow is shown in the lower left view. The momentum provided by the oxidizer flow carried the combined oxidizer and fuel flow toward the chamber wall as shown in the upper left view. The fuel film coolant flow characteristics are shown in the lower right view.

(C) The first of the two HIPERTHIN injectors fabricated is shown on Figure No. 37. A water flow check of the injector with the oxidizer, fuel, and fuel film coolant circuits flowing is shown on Figure No. 49. The axially-directed flow of the main injector core propellants within the fuel film coolant spray is illustrated.

2. Doublet Injector Evaluationa. Sea-Level Testing

(U) Seventeen test firings were conducted with the doublet injector. These tests were divided into three basic test series and are included in the sea-level tests listed on Table X. The first test series consisted of four tests with approximately 35% fuel film coolant flow supplied by a separate coolant feed circuit. The second test series was conducted with fuel film coolant flows of 48%. The injector was evaluated in the third series after redrilling the oxidizer holes to provide reduced radially outward momentum. This final test series included tests with fuel film coolant flows from 40% to 65%.

CONFIDENTIAL

Report AFRPL-TR-69-88

UNCLASSIFIED

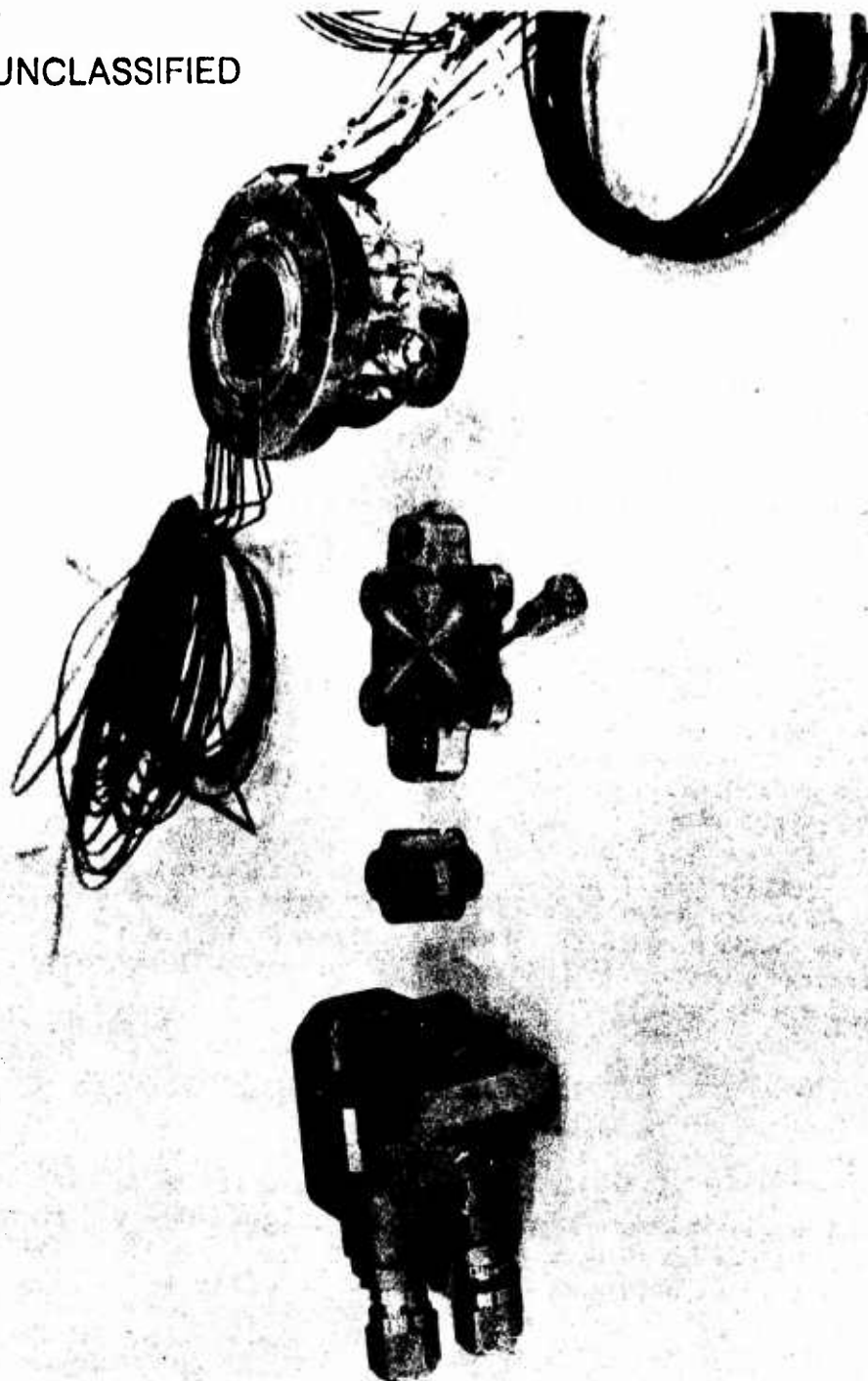


Figure 47. Prototype Engine Components

Page 94

CONFIDENTIAL

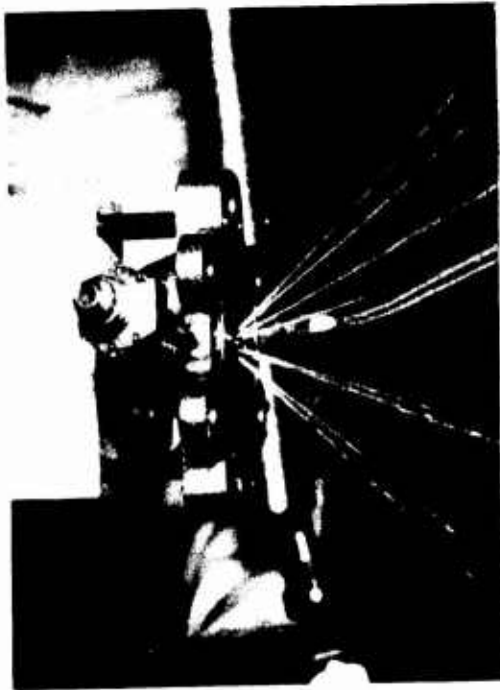
(This page is Unclassified)



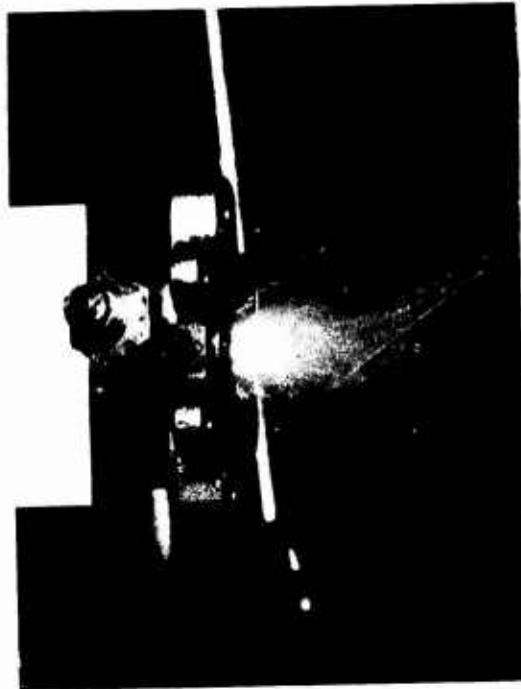
Fuel Circuit



Fuel Film Coolant Circuit



Oxidizer Circuit



Oxidizer and Fuel Core Flow

Figure 48. Doublet Injector Flow Characteristics

CONFIDENTIAL

Report AFRPL-TR-69-38

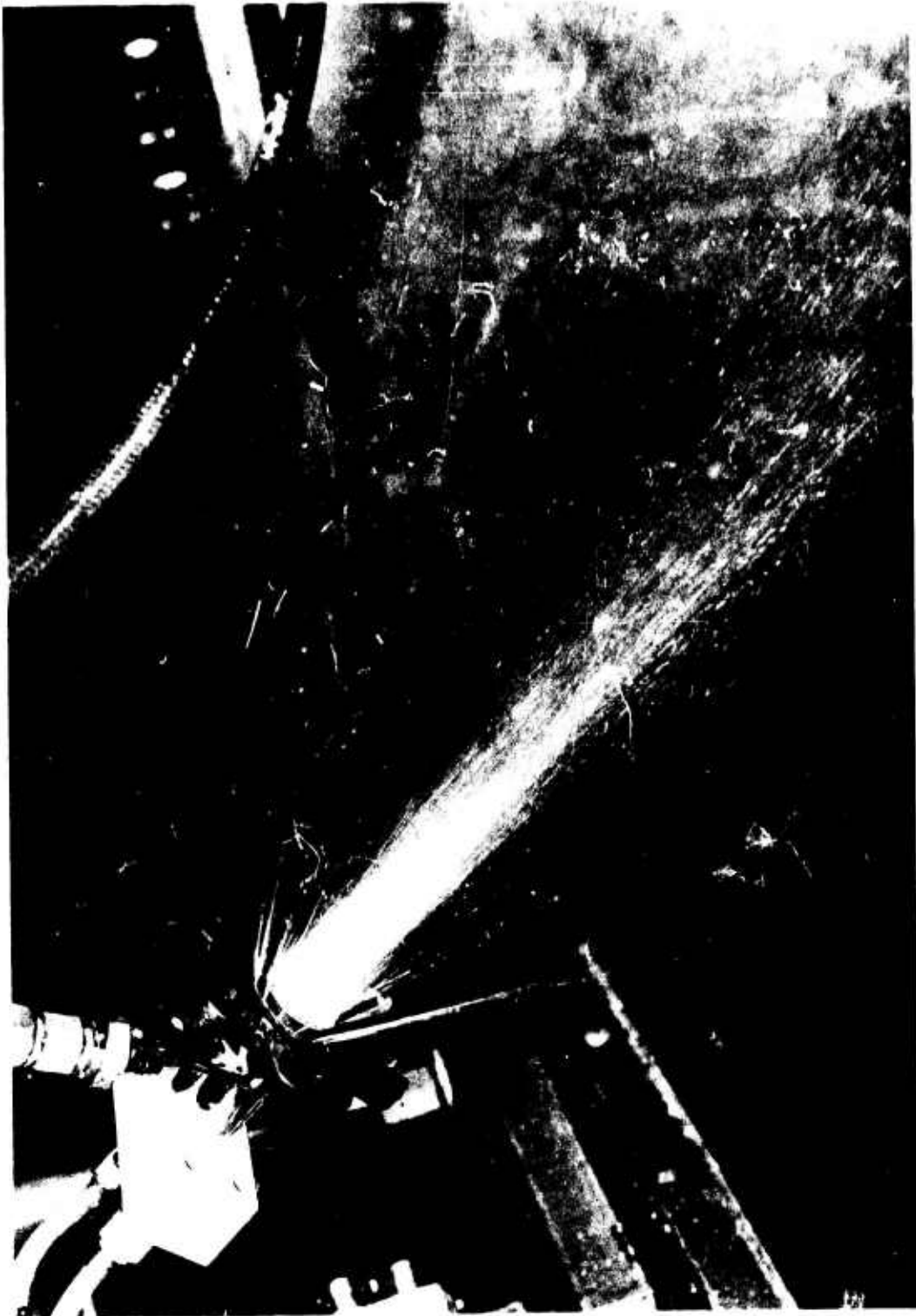


Figure 49. Baffled Alternative Injector Flow Characteristics (u)

Page 96

CONFIDENTIAL

CONFIDENTIAL

Report AFRPL-TR-69-88

TABLE X
SEA-LEVEL ACS TEST SUMMARY

DATE	TEST	TYPE	INJECTOR	CHAMBER	DURATION	M.R. TOTAL	% COOLANT	M.R. GAGE	F _g	REMARKS
	OC-5-									
3-22-68	101	Balance	Doublet	Bi-metallic	5 sec	1.76	34	2.68	234	Thermal shutdown
3-22-68	102	Duration	Doublet	Bi-metallic	3 sec	1.29	34.9	1.97	210	Thermal shutdown
3-22-68	103	Duration	Doublet	Bi-metallic	6 sec	1.4	33.9	2.12	213	Increases wall temp of 15 to 19 to 1900°F.
3-22-68	104	Duration	Doublet	Bi-metallic	13.6	1.42	38.7	2.13	224	12 sec variable coolant flow rate.
5-10-68	105	Balance	HIPERTHIN	Bi-metallic	5 sec	1.525	42.2	2.532	200.2	Steady temp. achieved on visual monitors.
5-10-68	106	Duration	HIPERTHIN	Bi-metallic	162 total (96)	1.755	41.7	3.001	190.6	Thermal shutdown
5-10-68	107	Duration	HIPERTHIN	Bi-metallic	115 total (80) (15)	1.982	33.3	2.973	185.6	Raised kill temps. Restarted at 100°F forward chamber temp. Steady temps. achieved on visual monitor. Thermal shut-down.
5-10-68	108	Duration	HIPERTHIN	Bi-metallic	2.3	1.98	27.4	2.73	191	Restart at peak injector temp. 185°F and a forward chamber temp. 750°F
5-14-68	109	Balance	Doublet	Bi-metallic	4.3	1.25	39.7	2.07	216	Changed orifice to give higher coolant flow rate.
5-15-68	110	Balance	Doublet	Bi-metallic	4.6	1.00	48	1.92	209	Coolant burning past throat. Carbon buildup in chamber.
5-15-68	111	Duration	Doublet	Bi-metallic	32.4	1.08	48.0	2.08	192	Pressure settings for 1.6 system M.R.
5-16-68	112	Balance	Doublet	Bi-metallic	4.6	1.72	48	3.31	220	Sequencer shutdown. Restarted for -11.1 immediately.
5-16-68	113	Duration	Doublet	Bi-metallic	4.5	1.68	49	3.31	220	Steady-state temps. nearly achieved.
5-16-68	114	Duration	Doublet	Bi-metallic	46.6	1.66	49	3.26	218	Reset feed pressures for 150 psi chamber pressure. Test terminated due to feed system coupling.
5-16-68	115	Duration	Doublet	Bi-metallic	4.85	1.77	50	3.52	161	

CONFIDENTIAL

CONFIDENTIAL

Report AFRPL-TR-69-88

TABLE X (cont.)

DATE	TEST	TYPE	INJECTOR	CHAMBER	DURATION	M.R. TOTAL	COOLANT	M.R. TIME	REMARKS
6-6-68	00-5-116	Balance	Doublet	Bimetallic	5	1.1	-0.8	1.67	Balance test after oxidized surface removed
6-7-68	117	Balance	Doublet	Bimetallic	4	1.63	52	3.32	Recheck tank settings
6-7-68	118	Duration	Doublet	Bimetallic	4	1.58	19.5	3.12	Thermal shutdown
6-7-68	119	Balance	Doublet	Bimetallic	7	1.38	62.1	3.66	Reset tank pressure for higher coolant flow
6-10-68	120	Duration	Doublet	Bimetallic	109	1.3	67.9	4.1	Thermal shutdown
6-10-68	121	Duration	Doublet	Bimetallic	5		invalide		Reduced rate M.R. test terminated due to tank leakage
6-12-68	122	Balance	HIPERTWIN	Bimetallic	3		invalide		Balance test interrupted. Oxidized surface removed. Operation.
6-12-68	123	Balance	HIPERTWIN	Bimetallic	3	1.39	39.3	2.28	
6-12-68	124	Balance	HIPERTWIN	Bimetallic	3	1.5	37.9	2.4	Recheck of new tank settings.
6-12-68	125	Duration	HIPERTWIN	Bimetallic	100% (115) (125) (52) *		37.2 35.5 33.4		While data lost at 29L sec. Thermal shutdown after 100 sec.
6-17-68	126	Balance	HIPERTWIN	Bimetallic	3	1.51	36.6	2.52	
6-17-68	127	Duration	HIPERTWIN	Bimetallic	120 (105) *	total 1.47	37.4	2.35	Reset of test tank speed after test. ON "slow" display
					(75) (47) (80) (19)	1.57 1.60 1.7 1.72	33.4 31.2 28.5 27	2.36 2.38 2.36 2.36	" " " " Thermal shutdown
6-17-68	128	Duration	HIPERTWIN	Bimetallic	160	1.63	29	2.3	Test at 1.63 system M.R. and lowest coolant flow. Flow which allowed steady state temp. at test. No tank heat soak. Thermal shutdown occurred.

CONFIDENTIAL

CONFIDENTIAL

Report AFRPL-TR-69-88

TABLE X (cont.)

DATE	TEST	TYPE	INTECTOR	CHAMBER	DURATION	M.R. TOTAL	COOLANT	M.R. SCORE	P ₂	REMARKS
6-18-68	OC-5-									
6-18-68	129	Balance	HIPERTHIN	Bimetallic	1.5	1.58	36.8	2.51	202	
6-18-68	130	Duration	HIPERTHIN	Bimetallic	270	1.59	35.1	2.45	202	Test at 1.6 system M.R. and nominal coolant fraction. Monitor heat soak. Steady temperatures achieved.
6-18-68	131	Duration	HIPERTHIN	Bimetallic	280	1.62	35.5	2.72	198	Test at 1.6 system M.R. and nominal coolant fraction. Monitor heat soak. Steady temperatures achieved.
6-24-68	132	Pulse	HIPERTHIN	Bimetallic	10 pulses		---	---	---	10 pulses, 10 sec. off. Recorded on graph only.
6-24-68	133	Pulse	HIPERTHIN	Bimetallic	20 pulses		---	---	---	10 sec. off, 10 sec. on. Recorded on graph only.
6-24-68	134	Balance	HIPERTHIN	Bimetallic	7	---	---	---	---	P2 tap leaked near end of test.
6-25-68	135	Balance	HIPERTHIN	Bimetallic	8	1.44	37.8	2.35	205	Coolant valve sequence changed to provide simultaneous coolant and main tube flow.
6-25-68	136	Restart	HIPERTHIN	Bimetallic	287	1.6	35.2	2.5	190	Hot restart - 15 sec. fire - 2 sec. coast. 30 sec. fire
6-27-68	137	Balance	HIPERTHIN	No Data Listing Prepared						
6-27-68	138	Restart	HIPERTHIN	Bimetallic	290	1.6	34.9	2.44	203	Hot restart - 200 sec. fire, 5 sec. coast and 90 sec. fire.
6-27-68	139	Restart	HIPERTHIN	Bimetallic	490	1.6	35.2	2.48	200	Hot restart - 200 sec. fire, 13 sec. coast and 240 sec. fire.
6-27-68	140	Restart	HIPERTHIN	Bimetallic	401	1.6	34.9	2.48	202	Hot restart - 200 sec. fire, 5 sec. coast and 200 sec. coast and 200 sec. fire.
6-27-68	141	Duration	HIPERTHIN	Bimetallic	1030	1.59	34.5	2.43	202	Six 5-sec. fire starts after 1000 sec. continuous operation. A-2 converter failure between 900 and 240 sec. fire at 0.15 sec.

CONFIDENTIAL

V, C, Engine Sea Level Test Evaluation (cont.)

The first four tests (OC-5-101 through 104) were conducted at film coolant flow rates of 35% and 40%. The first test was a checkout of the entire system while the next three tests were for the purpose of evaluating film coolant effectiveness and engine performance at varying coolant flow rates. Sixteen thermocouples on the chamber and injector were monitored to provide heat flux and temperature data. Three thermocouples were monitored via visual meters to allow the tests to be terminated if excessive chamber temperatures were measured. The temperatures noted on the meters were 200°F to 300°F higher than anticipated and the last three tests were terminated prematurely as a result of these high temperatures.

Performance data acquired during these tests were analyzed and used to predict performance at 35% coolant flow with a 40:1 expansion area ratio nozzle. The coolant flow was stopped one second before FS2 in two tests to obtain performance data both with and without coolant flow. These data showed that nearly all of the fuel coolant had reacted with the core gas, resulting in very small film cooling losses. The start transient time from FS1 to 90% thrust was 14 millisecc.

The thermal data acquired from tests -101 through -104 with the doublet injector were reviewed to assess the thermal characteristics of the chamber design and to provide a basis for planning subsequent tests. The thrust chamber achieved nearly steady-state thermal conditions in most locations by the end of the 12 sec test. A notable exception was a gas-side thermocouple located at the start of the nozzle convergence which experienced a 270°F temperature rise between 9.3 sec and 12.3 sec and finally reached 1400°F, the maximum recorded temperature. A 100°F temperature rise was noted from 6.3 sec to 9.3 sec. From adjacent thermocouples, the temperature of the inside surface of the throat was calculated to be 1650°F at 13.2 sec. The measured temperatures were 200°F to 600°F higher than predicted.

This injector underwent minor rework to correct a weak flowing orifice on the fuel film coolant ring. Then, it was hydrotested to verify that uniform distribution had been achieved. Following this, the second series of tests (-109 through -115) was conducted to evaluate higher fuel film coolant flow rates. The longest test duration achieved was 45 sec using 49% of the fuel for chamber cooling. The test was terminated automatically when the measured temperatures exceeded the pre-set limits.

Tests -109, -110, and -111 were conducted with the same core mixture ratio conditions but with higher coolant flows than were used in tests -102 through -104. The core mixture ratio and hence, element momentum ratio, was maintained at the previous level to prevent a variation in the wall impingement location from influencing the thermal response of the combustion

UNCLASSIFIED

Report AFRPL-TR-69-88

V, C, Engine Sea Level Test Evaluation (cont.)

chamber. With a normal 45% fuel coolant flow, some combustion was observed beyond the throat station. Inspection of the hardware after the test showed carbon deposits on the chamber wall.

Tests -112, -113, and -114 were conducted with the previous coolant flow rates (45% to 49%) and a 1.6 system mixture ratio. Combustion was normal and chamber temperature rise was slow but continuous. Steady-state temperatures were not achieved and a thermal shutdown occurred after a maximum 45 sec in test -114.

For test -115, the system feed pressures were reduced to provide a chamber pressure of 150 psi at the same coolant fraction as test -114 to evaluate the influence of chamber pressure upon chamber heating. The lower injector pressure drop at the reduced propellant flow resulted in a low-frequency (chugging) instability. The test was terminated after 5 sec of operation.

From the first eleven tests, it was apparent that the coolant fraction required for extended duration operation at a chamber pressure of 200 psi would not be achieved with the existing doublet injector design. An injector modification was made to increase the oxidizer orifice area by 40%, which would provide a more axially-directed resultant vector from the core propellants.

The final test series with the doublet injector included six tests with increasing fuel coolant flows. After two tests to provide oxidizer circuit flow resistances and a firing to verify new tank pressure settings, test -118 was made using nearly 50% of the total fuel flow as coolant. The test was terminated after 44 sec because of high temperature. The data from this test are shown on Figure No. 50. Thermocouple locations are identified on Table XI and shown on the cross-section view of Figure No. 51. The system was rebalanced for a high coolant flow rate and test -120 was initiated using nearly 68% of the total fuel as coolant. The longest operating duration obtained with this injector was achieved under these conditions, but a temperature shutdown occurred after 109 sec of operation. A final test was attempted with a reduced core mixture ratio to provide a more axially-directed vector to the core propellants in an attempt to achieve thermal equilibrium. This test was terminated after 5 sec because of a chamber pressure tap failure.

Seventeen tests were conducted with this injector at coolant fractions of up to 68% of the total fuel and with reduced core mixture ratios to improve the effectiveness of the coolant. Steady-state operating temperatures were approached only during tests at injector core mixture ratios so low that a portion of the propellants were burned beyond the chamber throat plane.

UNCLASSIFIED

UNCLASSIFIED

Report AFRPL-TR-69-88

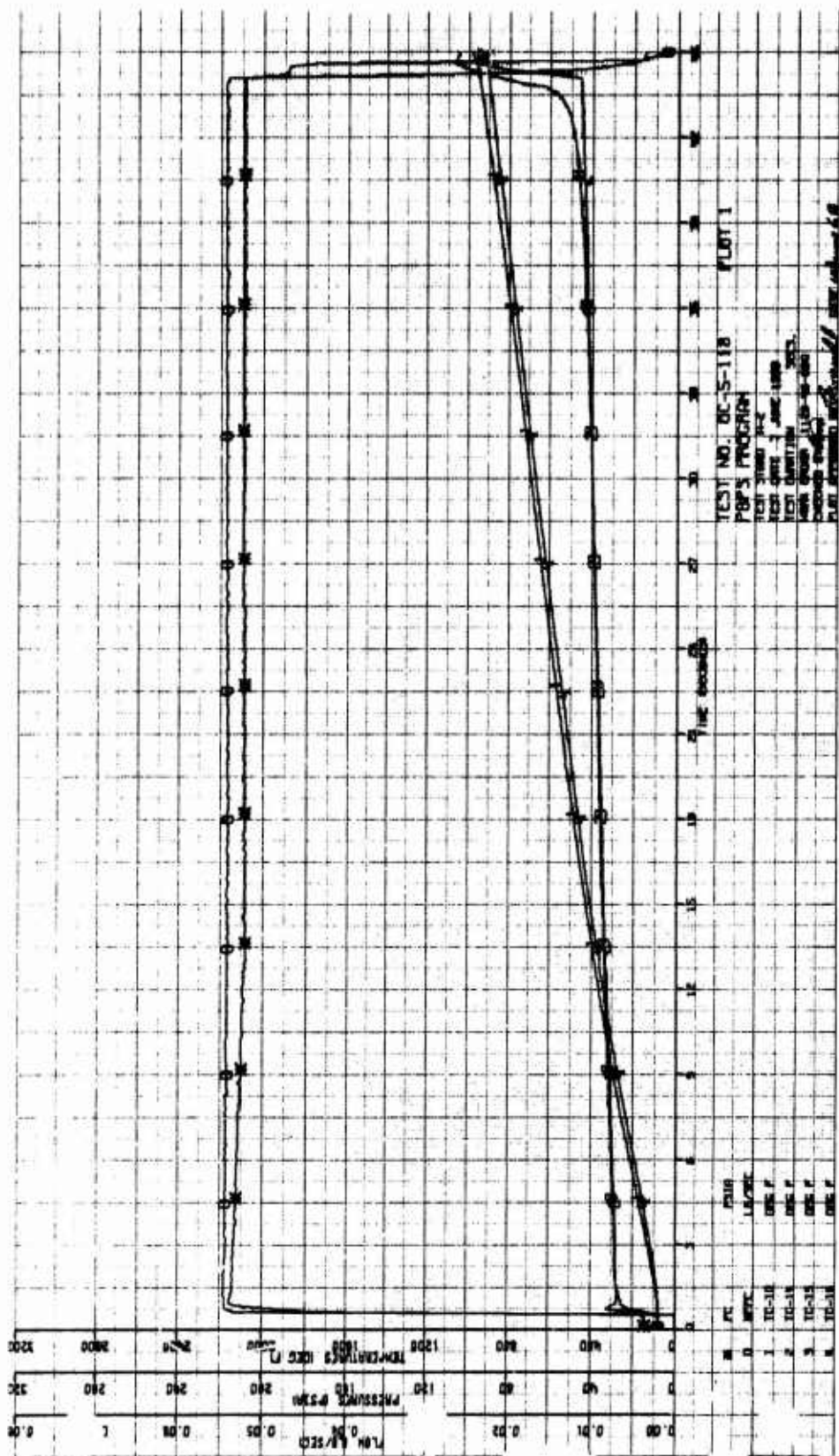


Figure 50. Prototype Engine Test Data (Sheet 1 of 5)

UNCLASSIFIED

UNCLASSIFIED

Report AFRPL-TR-69-88

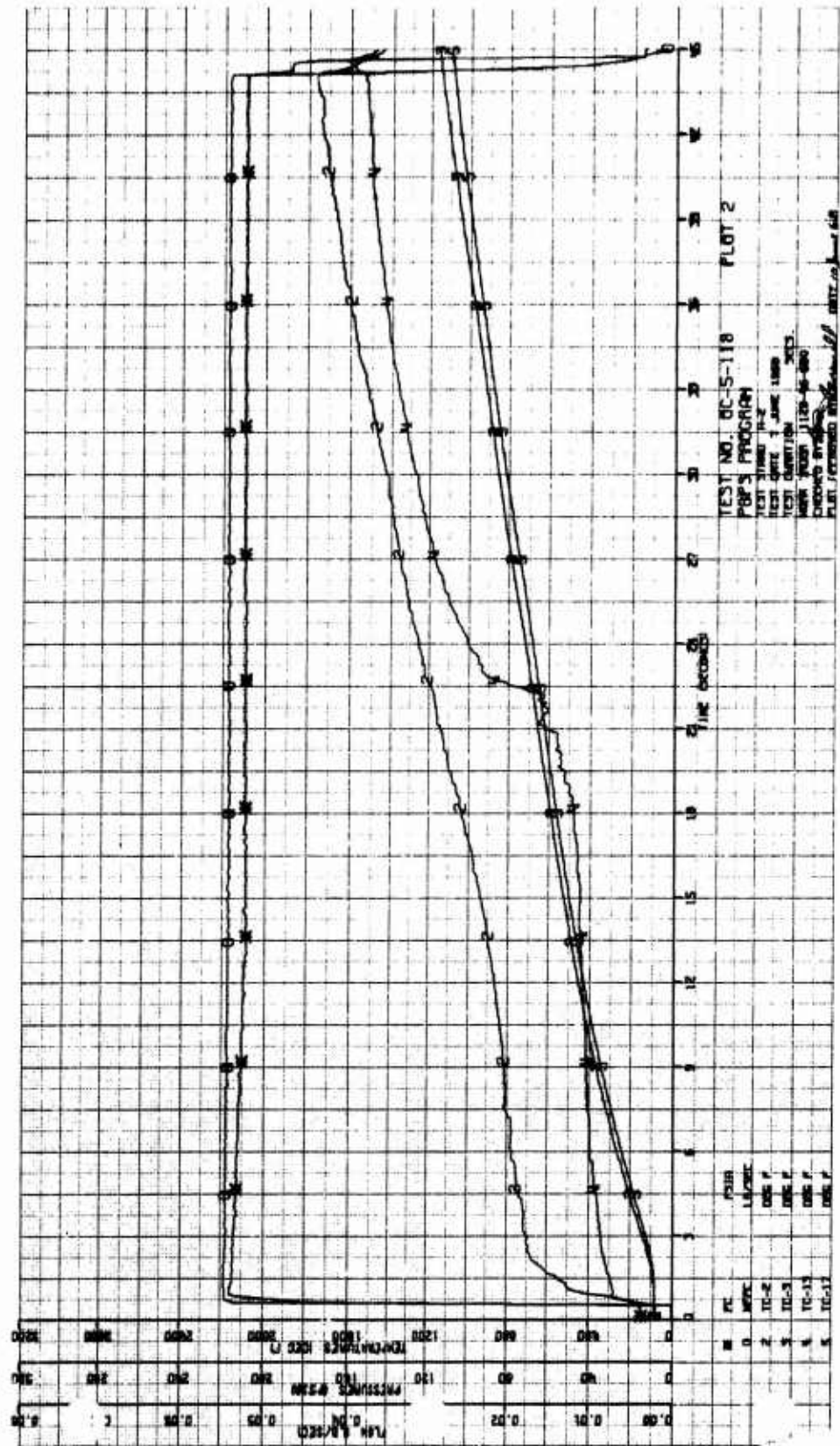


Figure 50. Prototype Engine Test Data (Sheet 2 of 5)

UNCLASSIFIED

UNCLASSIFIED

Report AFRPL-TR-69-88

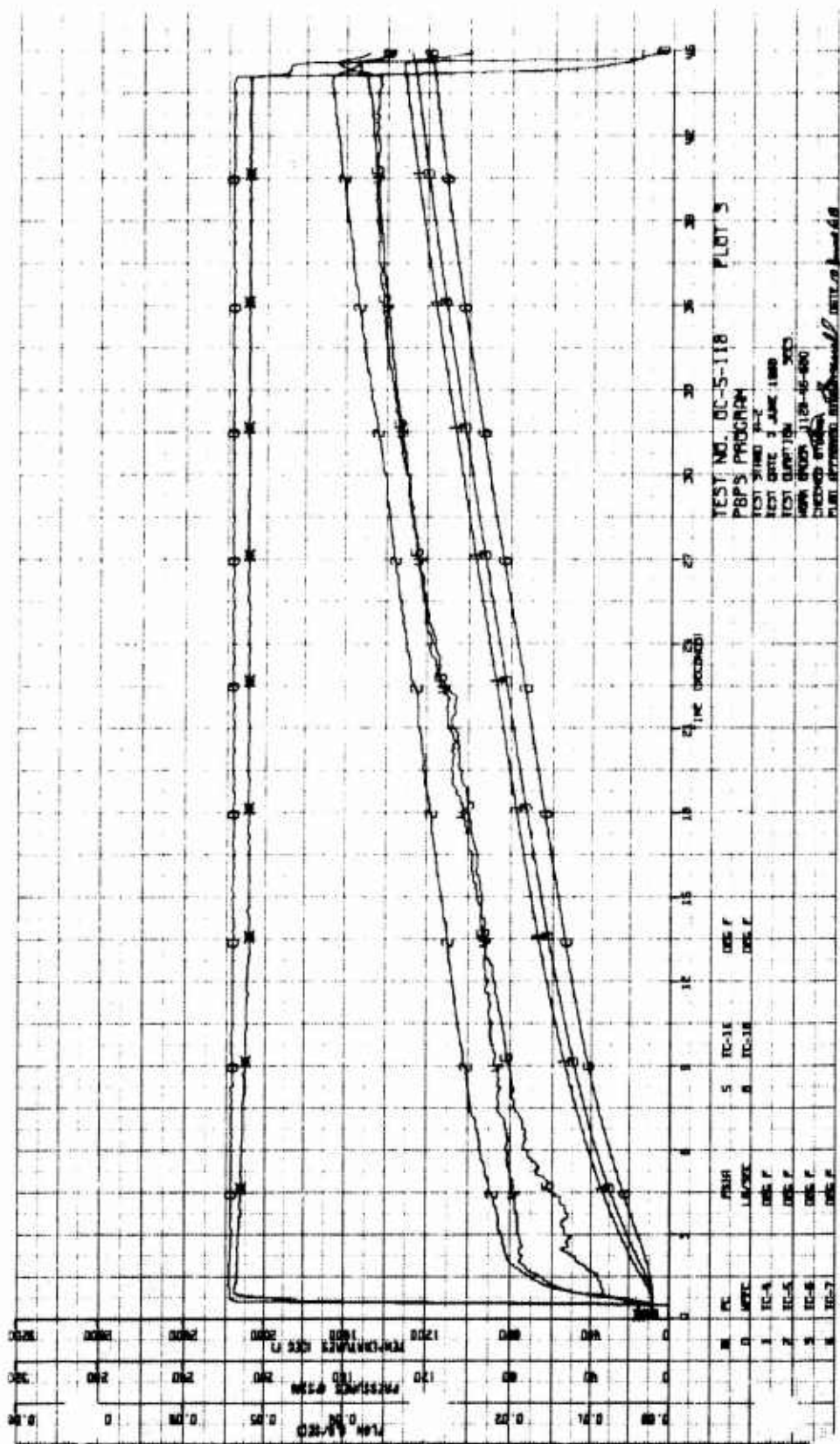


Figure 50. Prototype Engine Test Data (Sheet 3 of 5)

UNCLASSIFIED

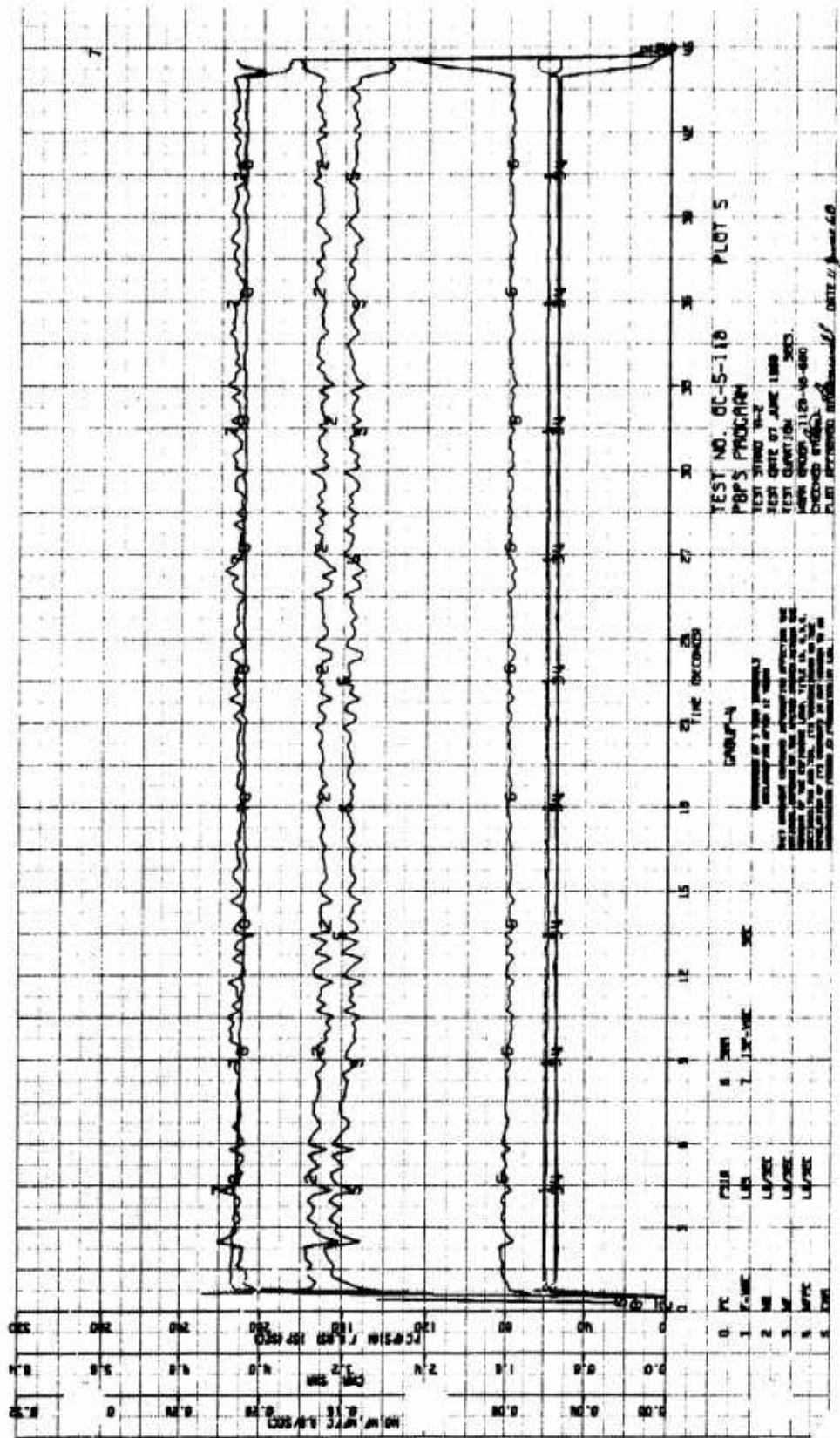


Figure 50. Prototype Engine Test Data (u)
(Sheet 5 of 5)

UNCLASSIFIED

Report AFRPL-TR-69-88

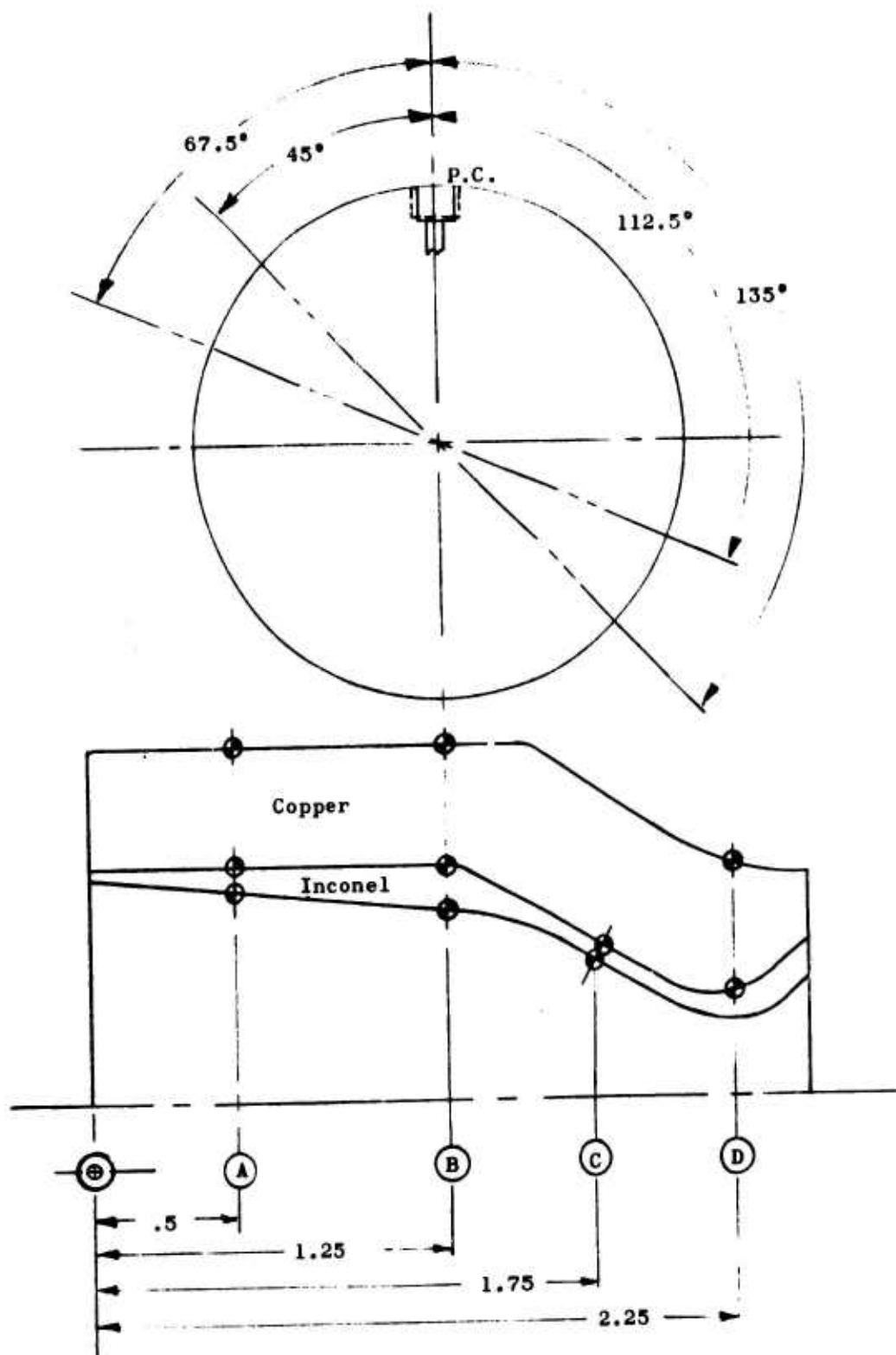


Figure 51. Sea-Level Chamber Thermocouple Location
(Cross-Section)

UNCLASSIFIED

UNCLASSIFIED

Report AFRPL-TR-69-88

TABLE XI

IDENTIFICATION OF SEA-LEVEL CHAMBER-THERMOCOUPLE LOCATION

T/C #	HOT GAS	C/I IN-TERFACE	OUTSIDE SURFACE	ANGULAR LOCATION	VISUAL DISPLAY	DATA PLOT (A-D)	GALVO
1							
2	B			67½°		#2	X
3		B		45°		#2	X
4		C		67½°		#3	
5	C			67½°	X	#3	X
6		C		45°		#3	X
7	C			45°		#3	X
(A) 8			D	67½°		#4	X
9		A		67½°			
10		A		45°		#1	
11	C			135°		#3	X
12	B			112½°		#2	X
13	B			135°	X	#2	X
14	A			112½°		#1	X
15	A			135°	X	#1	X
16			A	135°		#1	
17			B	135°		#2	
18			C	135°		#3	
(A) 19			C	112°	X	#4	
20			O	135°			
(A) 21	Injector Flange			Tc		#4	
(A) 22			D	135°			
(A) 23			D	45°			

NOTE: Plot #1 to include: F_1, P_{c1}, W_o, W_f & W_{ffc}

UNCLASSIFIED

CONFIDENTIAL

Report AFRPL-TR-69-88

V, C, Engine Sea Level Test Evaluation (cont.)

b. Doublet Injector Test Conclusions

(U) The prototype engine tested at sea-level with the eight-element, doublet injector did not achieve a thermal steady-state of operation at the design point mixture ratio. Of the doublet injector tests, test -118 most closely approximated the design operating conditions of mixture ratio and chamber pressure. However, the test was terminated at 44 sec because of excessive chamber wall temperatures. Subsequent doublet tests were made with higher coolant flow rates and at lower over-all mixture ratios. These tests yielded lower performance but still did not achieve thermal steady-state.

(C) The performance values obtained during tests -114 and -118 are as follows:

Test	Data Time	P_c (psia)	MR-Tot.	MR-Core	% FFC	I_{sp}	% I_{sp}	c^*	% c^*
-114	31-32	218.4	1.66	3.26	49.2	205.3	84.6	5040	88.1
-118	39-42	208.6	1.57	3.12	49.6	204.7	84.7	5012	87.7

Test -118 sea-level performance provides an altitude (40:1 expansion ratio) performance of 274 sec of specific impulse for 83.5% of specific impulse at altitude.

(C) From these doublet tests, it was concluded that a substantial program evaluating orifice sizes and impingement angles would be necessary to achieve the proper combination of core flow momentum ratio and the fuel film coolant flow for a thermally-stable design. Therefore, it was decided to proceed with the alternative HIPERTHIN injector concept which had demonstrated thermal compatibility in other programs.

3. Baffled Injector

(C) Four tests were conducted with the baffled HIPERTHIN injector. A system balance test (-105) was followed by a 162 sec test (106) during which three, gas-side chamber wall thermocouples and a thermocouple on the outside of the copper at the throat station were monitored using a visual display. Steady operating temperatures were achieved and after 96 sec of operation at a 41% coolant fraction, the coolant flow was reduced to 33% of the total fuel flow by a remotely-operated variable venturi. The test continued for an additional 34 sec. At the end of 34 sec of firing at a 33% coolant fraction, the test was terminated by a trip system that was initiated when the thermocouple (Tc19) on the back side of the throat station exceeded the pre-set limit of 1000°F.

CONFIDENTIAL

CONFIDENTIAL

Report AFRPL-TR-69-88

V, C, Engine Sea Level Test Evaluation (cont.)

(U) The other monitored thermocouples were observed to be operating below the established shutdown limits, indicating that the throat station temperature limit was somewhat conservative. The shutdown limit of Tc19 was immediately raised to 1300°F and the test was reinitiated as test -107 at the same operating conditions. At the time of restart, the forward chamber temperature was 400°F.

(U) Test -107 continued for a total burn time of 115 sec, of which 80 sec were at 33% coolant fraction. Steady temperature conditions were observed at the end of this period, whereupon the coolant was reduced to 27% over a 20 sec time span. Operation continued for 15 sec until a temperature shutdown occurred.

(C) During the ensuing heat soak period, the temperature response of the thermocouple mounted on the valve-to-injector adapter was monitored using a digital voltmeter. When the peak injector temperature of 485°F was observed, a scheduled hot injector restart was attempted as test -108. Excessive temperature rise rates were observed immediately and the test was terminated after 2.3 sec. Upon inspection of the disassembled injector, the film coolant ring was found to be eroded along the sides of the baffle pockets as shown on Figure No. 52. The metal eroded from these areas was deposited on the combustion chamber flame surface causing some localized minor erosion which was subsequently removed by polishing. As shown, the erosion was limited to the coolant ring in the areas away from the interfaces with the baffle ends. No damage to the injector platelets was noted.

(U) The valve control sequence used to terminate a test was to shut off and briefly purge the film coolant circuit prior to closing the bipropellant valve. The engine start-up sequence included a delay of approximately 0.4 sec between full chamber pressure and the initiation of coolant flow. At the initiation of test -108, the coolant manifold temperature was somewhere between the 485°F recorded for the valve adapter and the 750°F recorded on the forward chamber. It was concluded that the combined effect of the high initial manifold temperature and the 0.4 sec delay in coolant flow contributed to the failure of the coolant manifold. It is not clear whether the coolant fuel flashed to vapor because of the high initial temperature or because the exposed coolant ring surface area was excessive.

(U) Prior to the second test series with the doublet injector described earlier, the test procedure was modified to minimize the coolant flow delay and an insulating gasket was used to replace the metal O-ring used as the injector-to-chamber seal.

CONFIDENTIAL

CONFIDENTIAL

Report AFRPL-TR-69-88

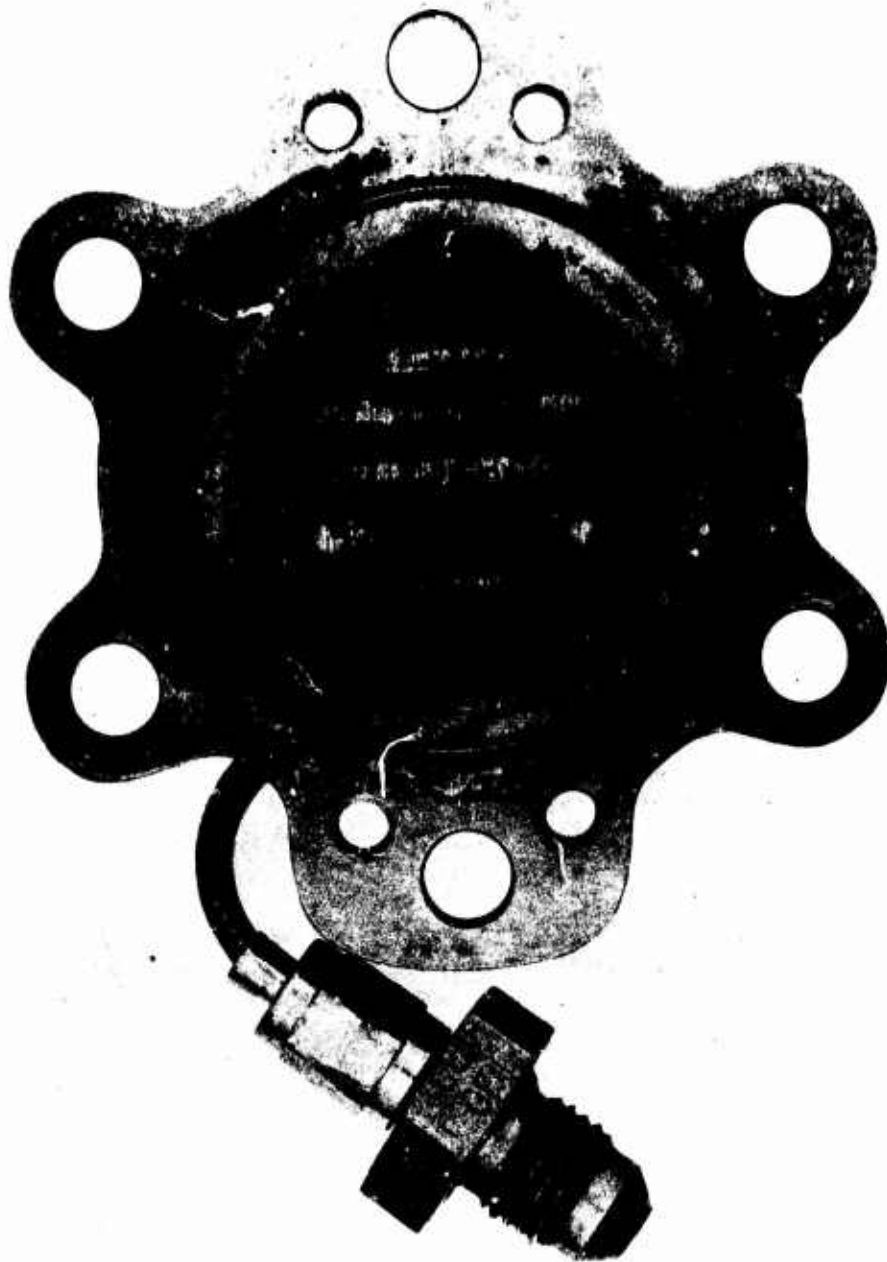


Figure 52. Eroded Alternative Injector (u)

CONFIDENTIAL

V, C, Engine Sea Level Test Evaluation (cont.)

4. Injector Evaluation

a. Sea-Level Testing

(C) An unbaffled HIPERTHIN injector design with the same type of like impingement injection orifices as were used in the baffled injector was designed, fabricated, and tested. The baffles were eliminated to reduce the surface area of the coolant ring exposed to the combustion gases. An insulating gasket was used as the injector-to-chamber seal to reduce injector heating. Other features of this injector were identical to the previously described baffled design which had demonstrated the desired performance and thermal characteristics. The injector as well as its flow characteristics is shown on Figure No. 53.

(C) The evaluation testing of the unbaffled HIPERTHIN injector consisted of 20 test firings which ranged from 30 millisecc pulses to 1000 sec of continuous firing. All used the 1.4:1 expansion ratio chamber. Coolant flow rates were varied from 27% to over 40%. Successful hot restarts were made with injector back flange temperatures of 400°F and forward chamber temperatures of 775°F.

(U) After the initial checkout and balance tests were completed, test OC-5-125 was initiated using 37.2% of the total fuel as coolant. After 115 sec of operation, steady chamber temperatures were achieved. The coolant flow then was throttled to 35.5% and the test continued for 125 sec at this coolant fraction. The visual temperature monitors again indicated that thermal equilibrium of the thrust chamber had been achieved, whereupon the coolant flow was further reduced to 33.4%. A temperature shutdown, which was approximately 400 sec after the test was initiated, occurred shortly after the final coolant flow reduction.

(U) Test -127 was made as a repeat of test -125 when it was learned that a malfunction had occurred in the data link so that the digital data was not recorded. During this test, steady-state temperatures were achieved at coolant fractions of 37.4%, 33.4%, 31.2%, and 28.5% over approximately 400 sec of test firing. A thermal shutdown occurred at 424 sec, 19 sec after the coolant fraction had been reduced to 27%.

(U) Tests -128, -130, and -131 were made with a 1.6 over-all mixture ratio at the lowest, nominal, and higher coolant fractions demonstrated in test -127 to determine the influence of core mixture ratio upon chamber heating as well as upon subsequent heat soak temperatures. The earlier tests were initiated at a 1.6 over-all mixture ratio which increased as the coolant flow was reduced. When steady operating temperatures had been displayed for an extended period, the test was terminated and injector/chamber soak-out temperatures were monitored for 4 min to 5 min.

CONFIDENTIAL

Report AERPL 12 69 83

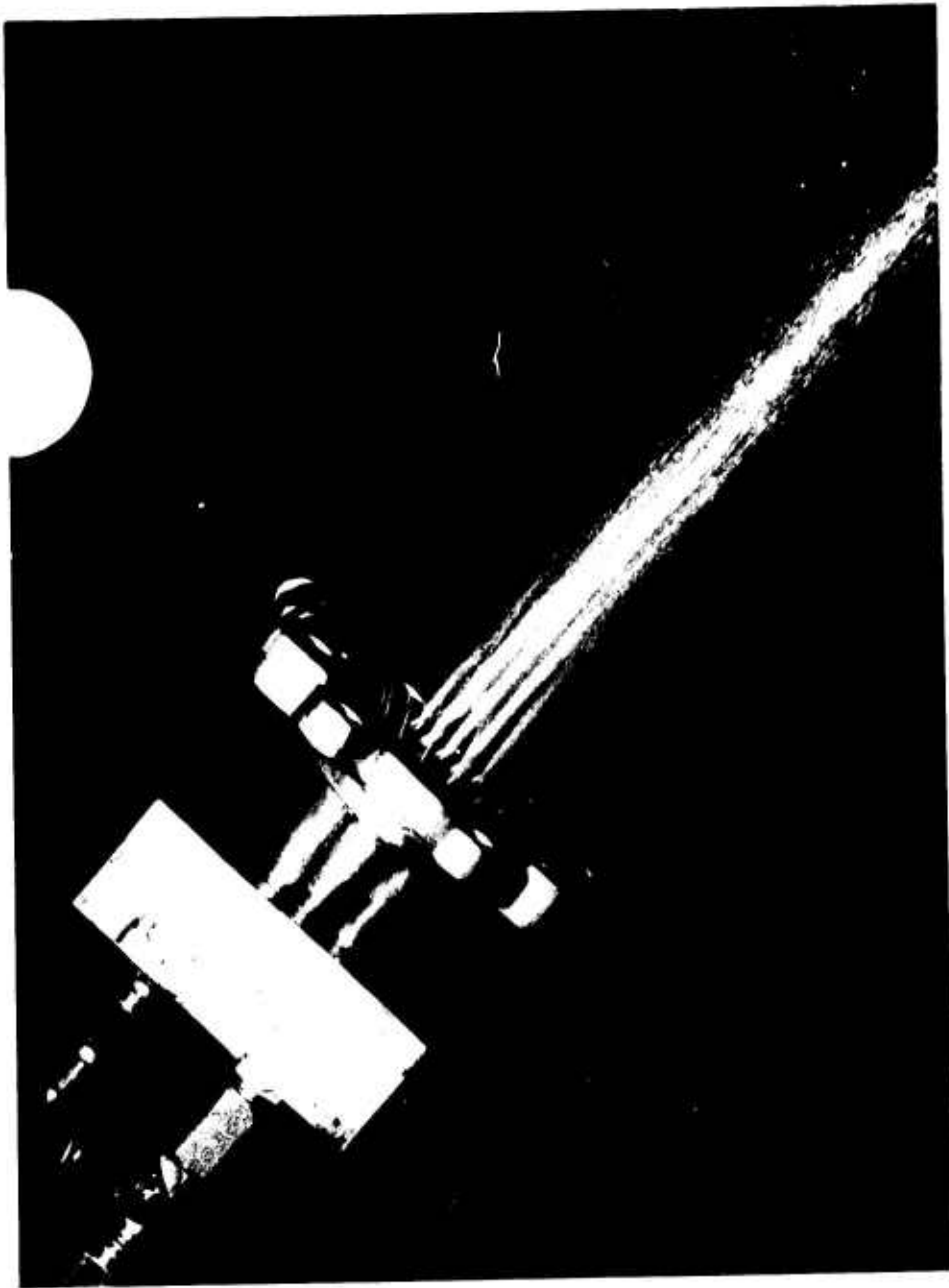


Figure 53. Injector Flow Characteristics

Page 113

CONFIDENTIAL

CONFIDENTIAL

Report AFRPL-TR-69-88

V, C, Engine Sea Level Test Evaluation (cont.)

Pulse testing was conducted as tests -132 and -133 to evaluate the pulse mode response and repeatability of this injector. Response times to 90% of chamber pressure were 0.015 sec for the first pulse and 0.013 sec for subsequent pulses.

Tests -136, -138, -139, and -140 were made to determine performance and thermal characteristics of hot restarts using a 35% coolant fraction. After steady operating temperatures were achieved, the engine was stopped for different soak periods to provide various injector and forward chamber temperatures at restart. The goal of these tests was to establish temperature limits to be used in the design of the engine with the altitude nozzle.

Test -136 was the first of the hot restart tests designed to evaluate chamber temperature response when it was started hot. After firing for 257 sec to achieve thermal equilibrium, the chamber was soaked for 5 sec and then restarted at a 260°F injector flange temperature and a 620°F forward chamber temperature. After restart, the chamber temperature increased above previous levels and continued to increase when the test was terminated because oxidizer supply had been depleted. The 29 sec of operation following restart was too short to achieve steady-state thermal conditions.

Test -138 was a repeat of the heat-soak period used in test -136 for the purpose of evaluating chamber thermal recovery during hot restart. The sequence of this test was: 200 sec fire, 5 sec heat-soak, followed by a 90 sec test. At restart, the forward chamber temperature was 775°F and the injector temperature was 300°F. Wall temperatures did not become steady and were significantly higher (by 30°F to 300°F) than the previous steady values. The test was terminated by an erratic thermocouple which was a "kill" parameter (Tc15); however, there is evidence that the film coolant heat transfer mechanism was degrading and that the onset of film boiling heat transfer was imminent in the forward chamber region.

A longer heat-soak period was used during test -139 to provide a different thermal profile at restart. After steady-state temperatures had been achieved, the test was stopped for 15 sec and restarted with a 300°F injector temperature and a 700°F forward chamber temperature. The test continued for 200 sec with wall temperatures that were only 10°F to 30°F higher than those achieved in the first firing. The coolant flow rate was reduced from 35% to 32.4% and the test continued for 100 sec. Steady thermal conditions were not achieved. After a 15 sec soak period, a second restart was attempted at 975°F forward chamber temperature. The test was terminated after 0.5 sec of steady chamber pressure when the temperature exceeded the pre-set maximum limit of 1000°F on the gas-side at the forward end of the chamber.

CONFIDENTIAL

(This page is Unclassified)

UNCLASSIFIED

Report AFRPL-TR-69-88

V, C, Engine Sea Level Test Evaluation (cont.)

Test -140 was designed to provide high injector temperatures at restart by increasing the heat-soak period. A 200 sec firing was followed by a 40 sec soak and an additional 200 sec firing. The forward chamber was 700°F and the injector was 360°F at restart. Steady wall temperatures were achieved which were 10°F to 30°F higher than previous steady values. After a 90 sec soak, the engine was restarted again at 400°F injector temperature and a 665°F forward chamber temperature for a 2 sec firing. Wall temperature response was normal.

Test -141 consisted of a 1000 sec continuous firing followed by five, .5 sec firings with a 2 sec coast period between them. Steady temperatures were achieved during the firing and no abnormalities were noted during restart. The digital data link malfunctioned at 945 sec and only oscillograph data were recorded after this time.

b. Test Results and Evaluation

Steady-state operation was achieved with film coolant flow rates of 35% and 40% of the fuel flow at a 1.6 system mixture ratio. Steady conditions generally were evidenced after a duration of approximately 200 sec as demonstrated by the typical wall temperature data shown on Figure No. 54. Total test durations of up to 1000 sec were achieved (test -141).

Wall temperature distributions measured during steady operation with 35% and 40% film cooling are shown on Figures No. 55 and No. 56. These data show that, as expected, the wall temperature levels decrease with increasing film coolant flow rate.

The measured wall temperatures are somewhat higher than previously predicted and the thermal model of the 75 lb thruster was re-evaluated in light of these measurements.

The objective of the hot restart tests conducted with the sea-level expansion chamber was to define acceptable design limits for restart operation. The results indicate the following design criteria:

- (1) 700°F Maximum Chamber Temperature,
15 sec Minimum Coast

The 700°F temperature and 15 sec coast were shown to be acceptable in test -139 wherein the steady temperatures achieved after the restart were only 10°F to 50°F higher than the values observed after the cold start. The data from this test are summarized on Figure No. 57.

UNCLASSIFIED

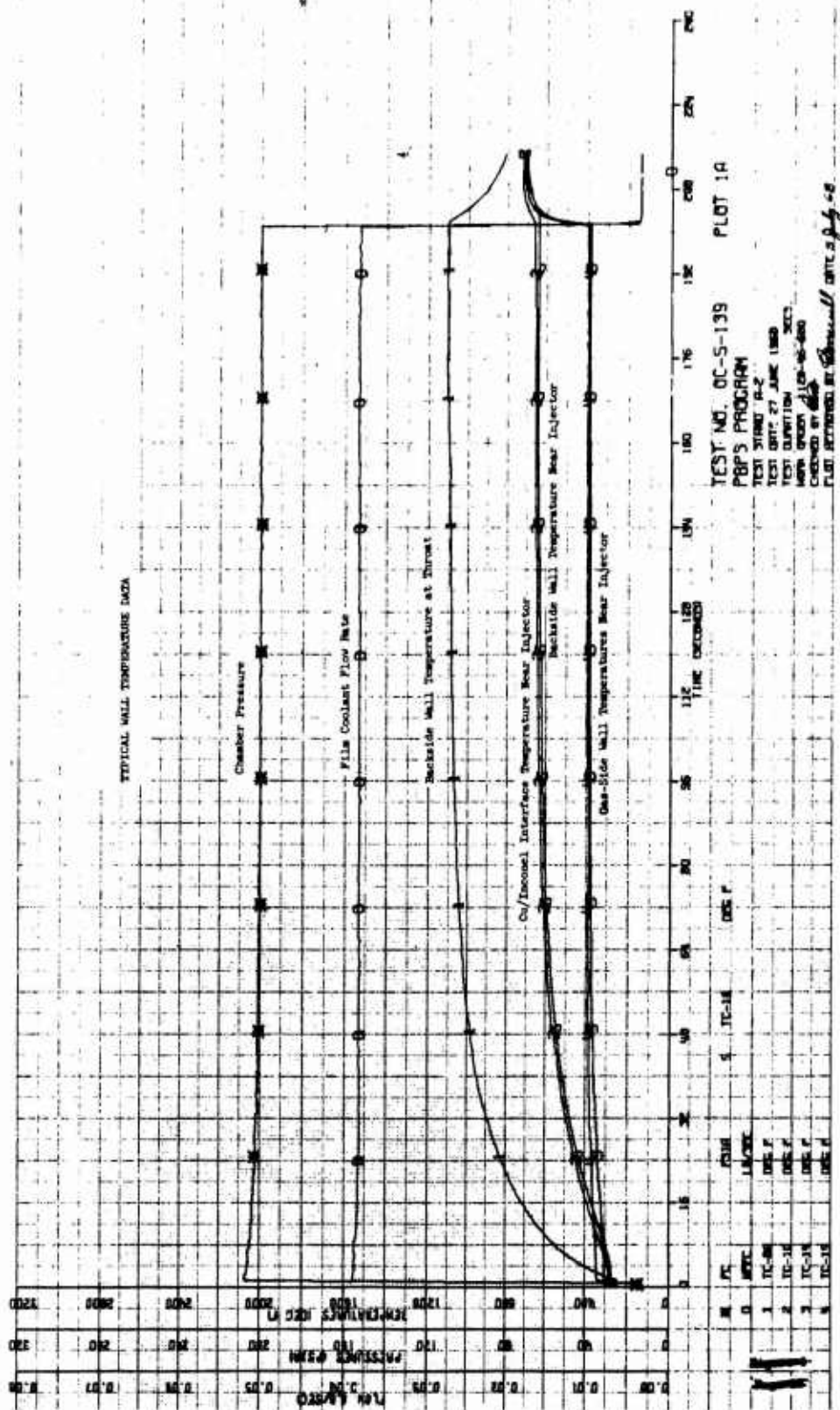
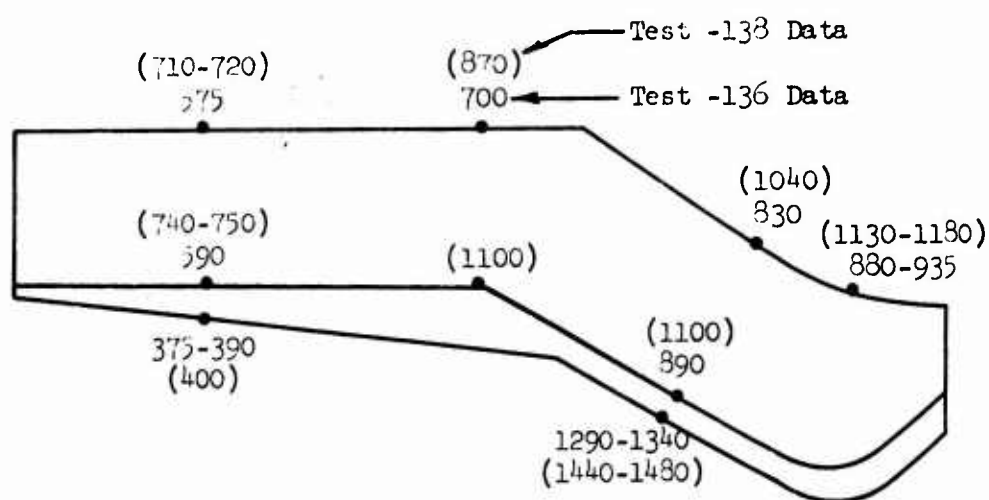


Figure 54. Typical Wall Temperature Data

UNCLASSIFIED

Report AFRPL-TR-69-88

<u>Test</u>	<u>Duration, sec</u>	<u>MR</u>	<u>P_c</u>	<u>% Film Cooling</u>
OC-p-133	257	1.6	196	35.2
OC-b-138	200	1.6	203	34.9

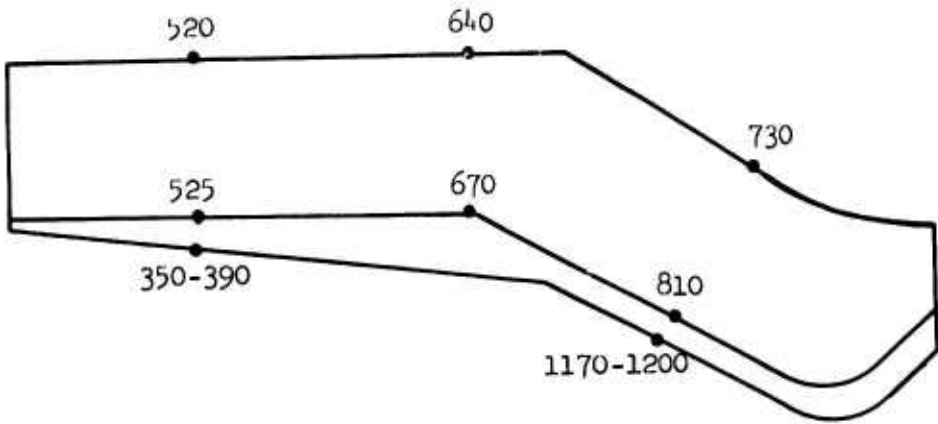


Temperatures in °F

Figure 55. Steady-State Wall Temperatures at 35% Film Cooling

UNCLASSIFIED

<u>Test</u>	<u>Duration, sec</u>	<u>MR</u>	<u>P_e</u>	<u>Δ Film Cooling</u>
OC-5-131	280	1.62	193	40.5



Temperatures in °F

Figure 56. Steady-State Wall Temperatures at 40% Film Cooling

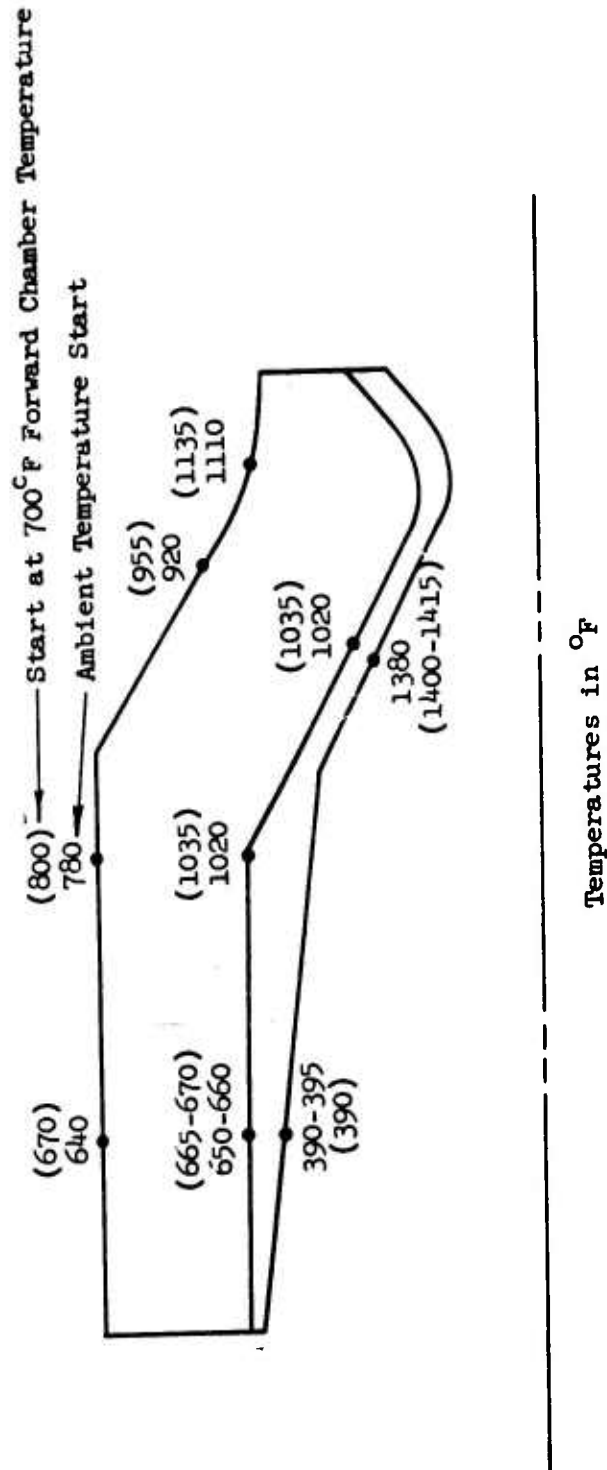


Figure 57. Steady-state Wall Temperatures for Cold and Hot Starts

CONFIDENTIAL

Report AFRPL-TR-69-88

V, C, Engine Sea Level Test Evaluation (cont.)

(U) An unsteady condition and significantly higher wall temperatures (by up to 300°F) occurred after hot restart in test -138 (5 sec coast, 775°F chamber temperature) and test -136 (5 sec coast, 620°F chamber temperature).

(2) 400°F Maximum Injector Temperature

(C) Successful hot restarts were achieved at injector temperatures of 300°F (tests -138 and -139), 360°F (test -140) and 400°F (test -140). In a test previously conducted with a similar injector (test -108), injector failure occurred when a restart was attempted at a 485°F injector temperature. Therefore, the maximum value tested safely, 400°F, is believed to be an appropriate design criteria for N_2O_4 /MMH propellants and HIPERTHIN type injectors.

D. ALTITUDE TEST EVALUATION

1. Altitude Chamber Redesign and Fabrication

(U) The thermal model for the 40:1 area ratio thrust chamber, which had been configured prior to testing, was changed to provide gas-side boundary conditions which matched the test data. This analysis resulted in a correlation of computed gas-side and mean copper temperatures to measured data as shown for Figure No. 58. This correlation gave confidence that the calculated gaseous and liquid region heat transfer coefficients were accurate.

(U) Design analyses of a 40:1 area ratio thruster operating with 35% fuel film cooling were conducted using the gas-side boundary conditions shown on Figure No. 59. These studies indicated that it was desirable to minimize the Inconel liner thicknesses because lower over-all thrust chamber weight and lower operating temperatures resulted. This led to the thruster design shown on Figure No. 60, which incorporates the minimum practical Inconel liner thicknesses. The predicted wall temperatures for this design were acceptable as shown on Figure No. 59.

(U) The altitude expansion ratio combustion chamber fabrication was completed with the Inconel and copper profile shown on Figure No. 60. The complete bipropellant 75 lb thrust engine for the altitude demonstration testing is shown on Figure No. 61.

CONFIDENTIAL

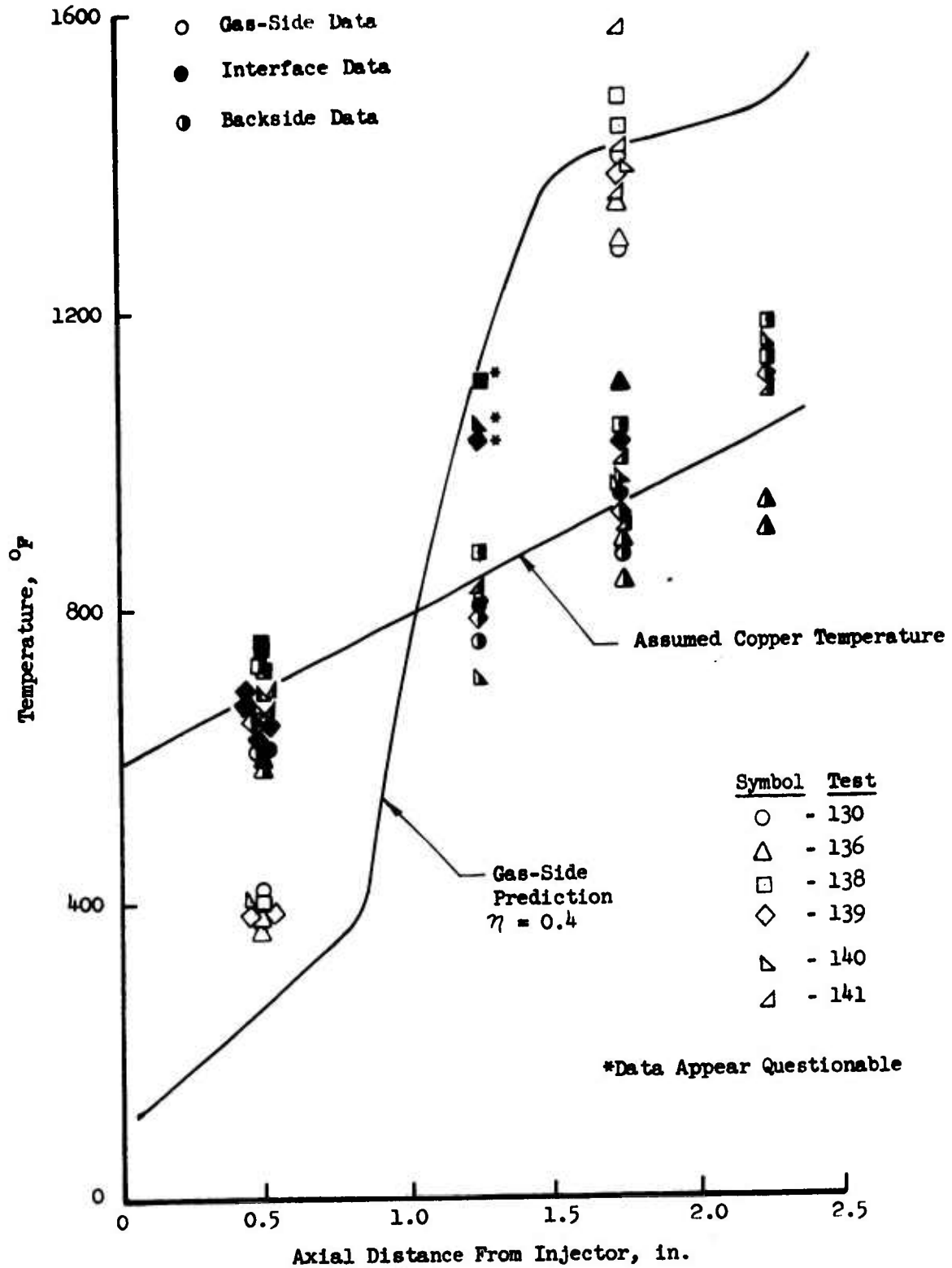


Figure 58. Thermal Data Comparison with Model Predictions

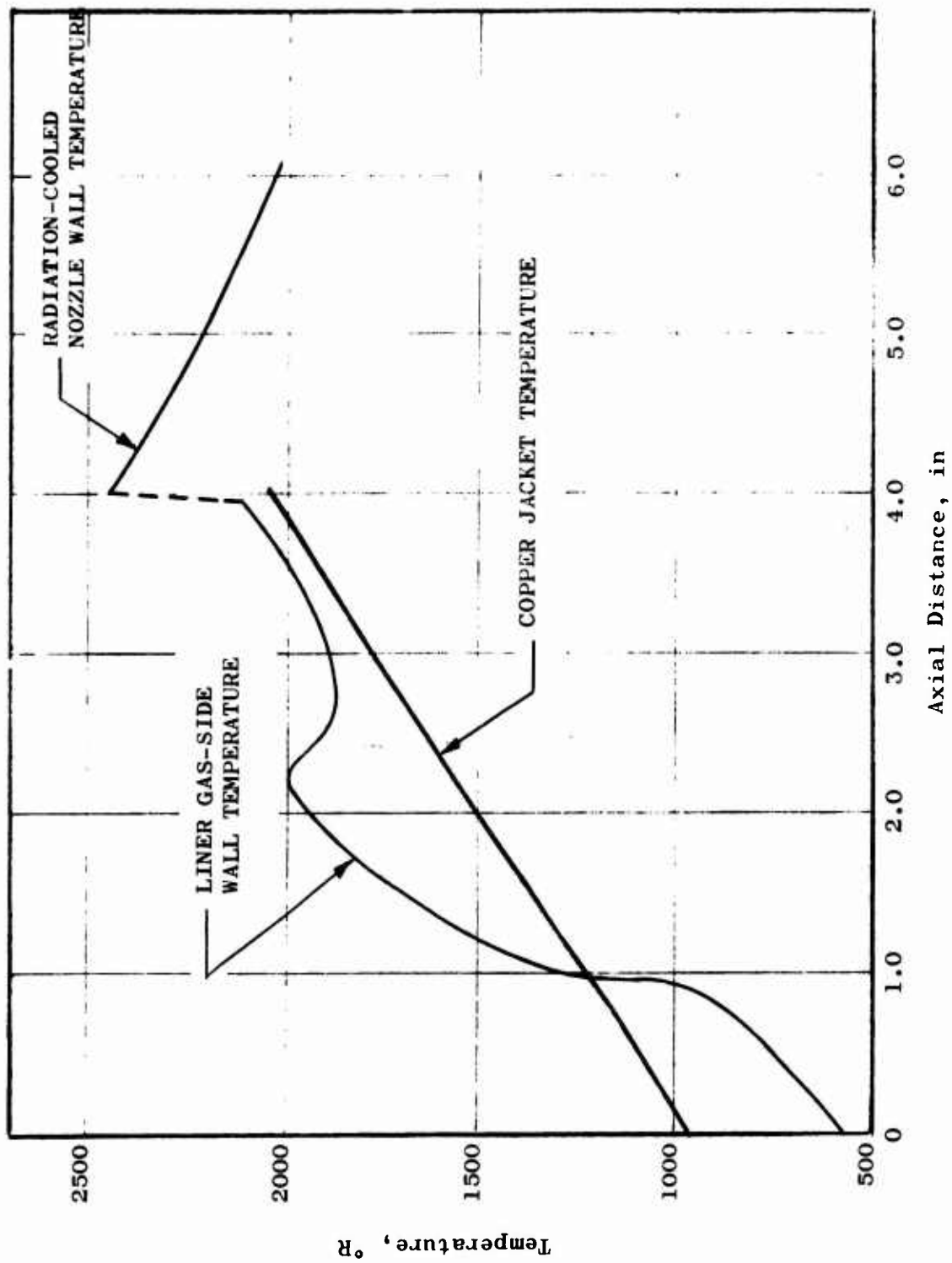


Figure 59. Steady-State Temperature Prediction for 40:1 Thrustor Design

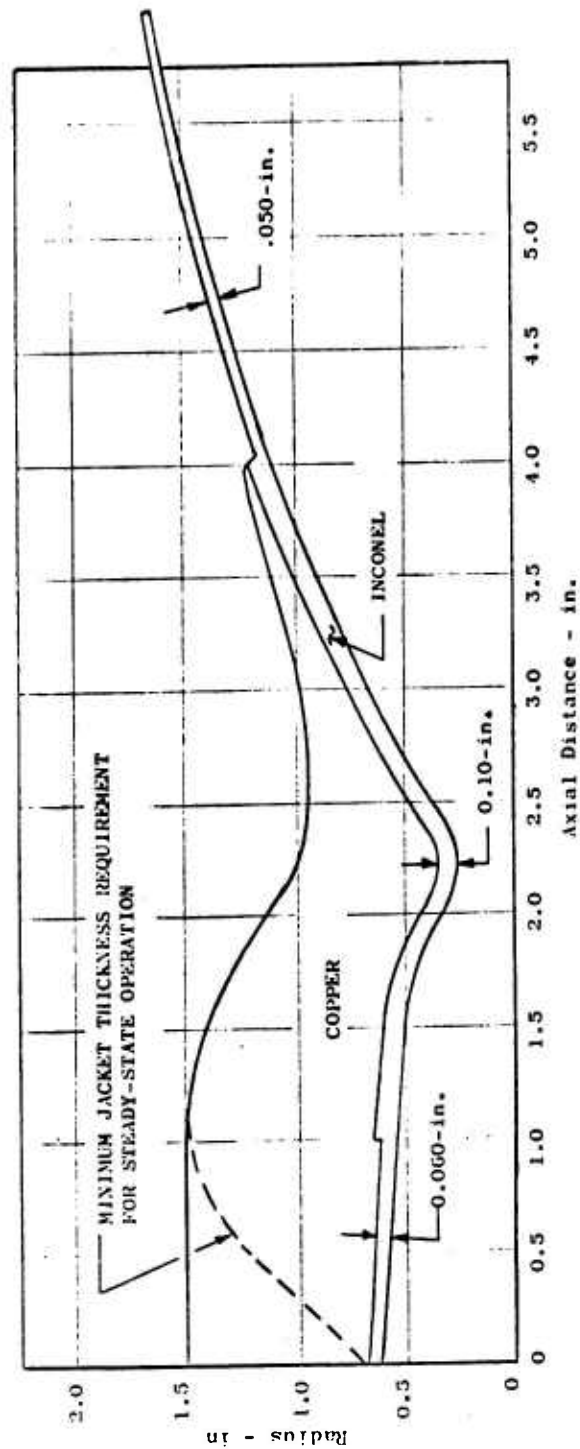


Figure 60. Altitude Chamber Cross-Section

UNCLASSIFIED

Report AERPL-TR-69-88



Figure 61. Bipropellant ACS Engine - Initial Design

Page 124

UNCLASSIFIED

V, D, Altitude Test Evaluation (cont.)

2. Altitude Testing

a. Fuel Film Coolant and Chamber Variations

(C) The attitude control engine with the 40:1 expansion nozzle and the HIPERTHIN injector shown on Figure No. 61 initially was tested with an external fuel film coolant supply. This allowed the engine to be tested at different fuel film coolant flow levels to determine the exact coolant requirements for the new chamber under simulated altitude conditions.

(U) Ten tests were conducted at altitude conditions (tests OC-5-142 through -151) with fuel film coolant fractions of 36% to 43% of the total MMH flow. The tests were run at simulated altitude conditions by firing within a large evacuated chamber in the Aerojet-General Research Physics Laboratory. Extended test durations were not possible with this test simulation because of the resultant pressure build-up in the large test vessel. The maximum test duration reached prior to exit nozzle separation was 158 sec.

(U) The two primary tests in this series were tests -146 and -151. Test -146 ran a duration of 150 sec with a film coolant flow of 37.9% total fuel flow as shown on Figure No. 62. A thermal shutdown occurred at 150 sec. Test -151, with a film coolant of 42.5%, attained a duration of 158 sec as shown on Figure No. 63. The test was terminated when thrust fluctuations indicated that increasing altitude cell pressure was causing nozzle separation to occur.

(U) Higher than expected chamber forward end temperatures were experienced in these initial long duration tests with the 38% and 43% fuel film coolant flows. The thermal data review showed that the wall temperatures near the radiation skirt attachment point tended to steady out and compared favorably with predictions. However, the wall temperatures upstream of the throat were higher than expected by approximately 300°F and transient in nature. The thermal analysis of the data indicated that the relatively-thick copper jacket allowed too much heat to be conducted to the liquid film coolant. This reduced the liquid-cooled length of the chamber to approximately one-half that observed during sea-level testing. The increased fuel coolant flow in test -151 did delay the decomposition of the MMH boundary at the gas-side thermocouple location from 80 sec after start during test -146 to approximately 120 sec. This condition is shown by the abrupt rise in T-5 (gas-side thermocouple) in Figures No. 62 and No. 63 at the stated times.

(U) An analysis then was conducted to assess the influence of removing copper from the chamber throat location upon the chamber temperatures. This analysis showed that the copper thickness could be trimmed to

CONFIDENTIAL

Report AFRPL-TR-69-88

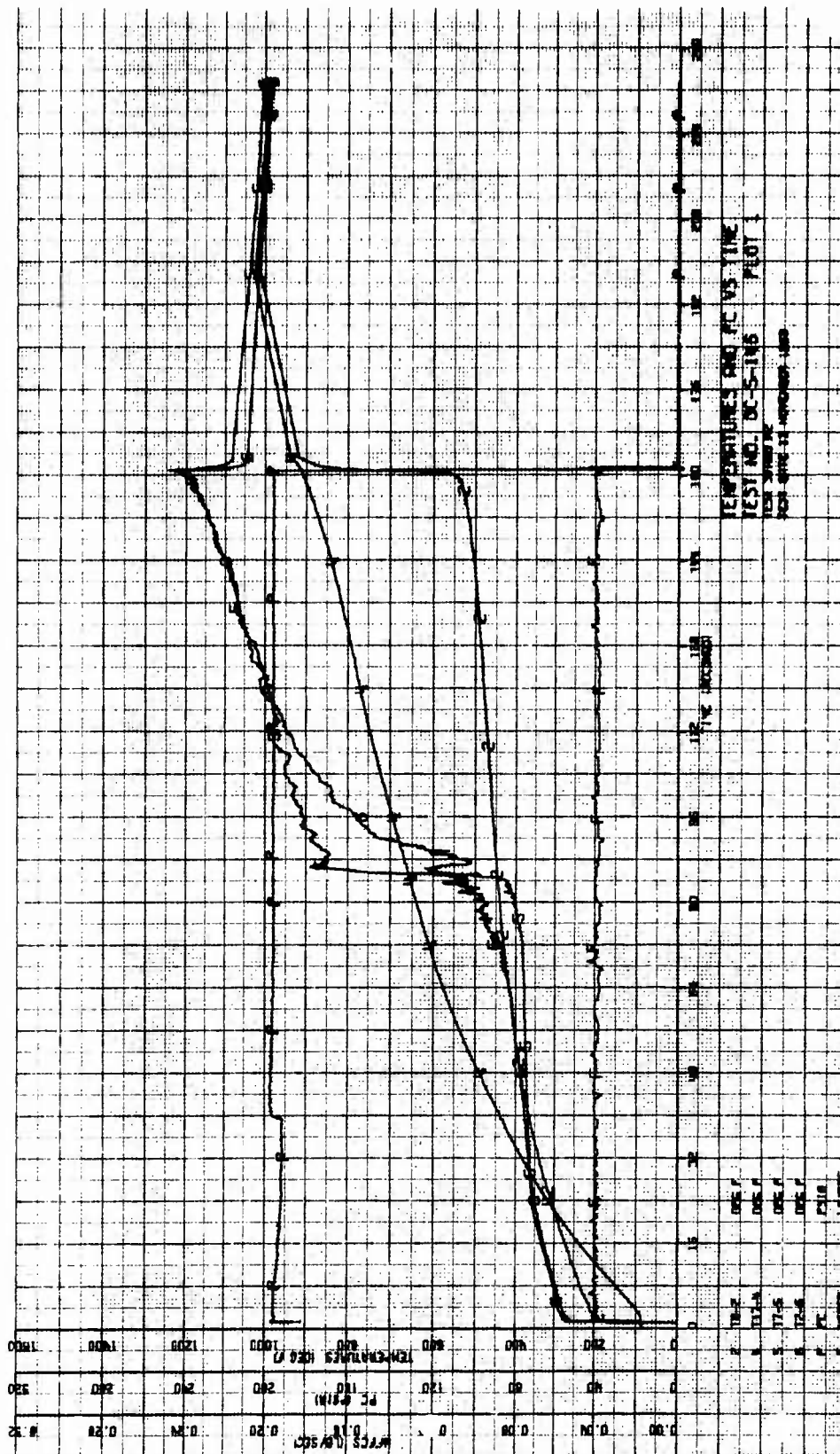
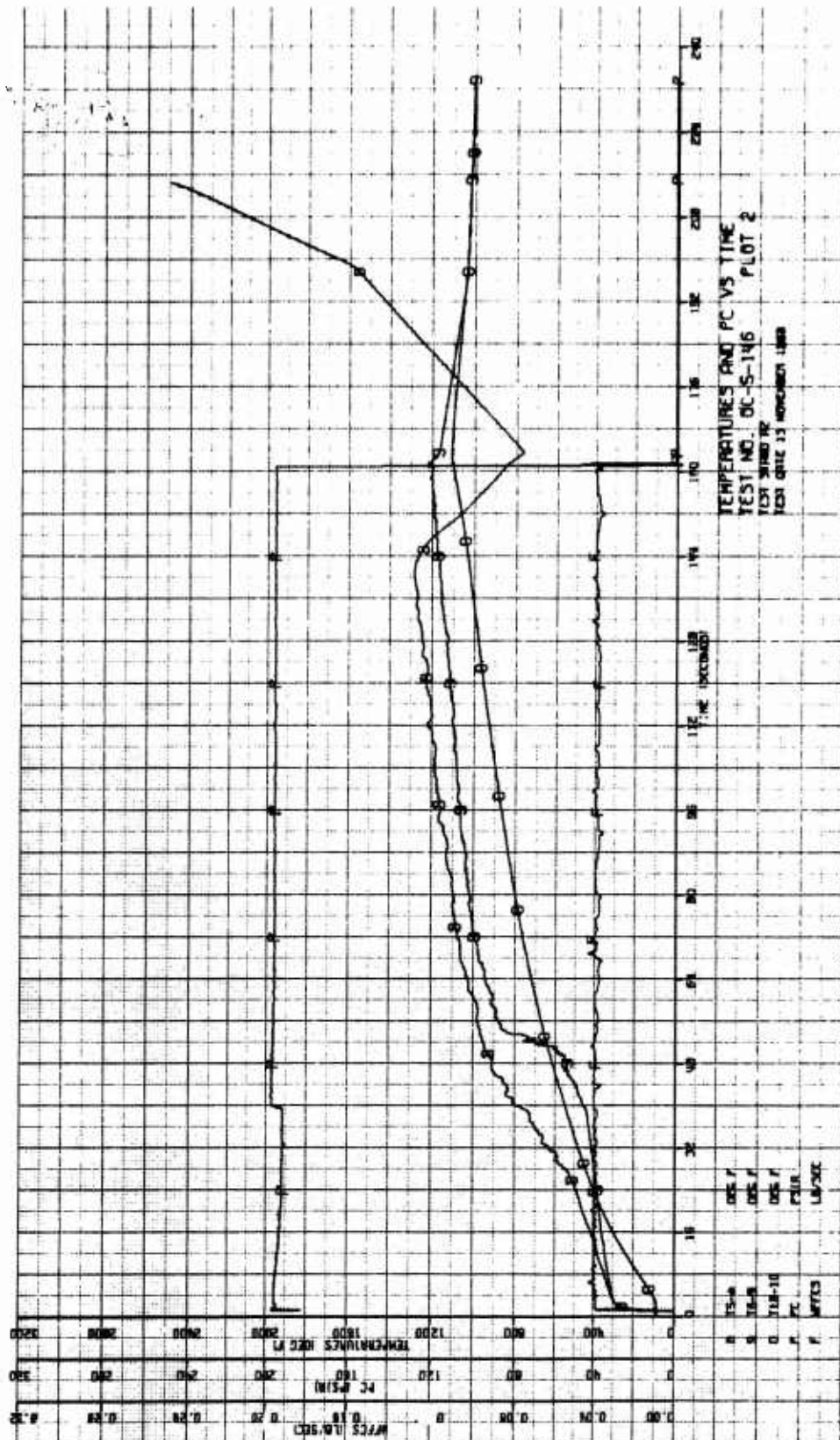


Figure 62. Altitude Engine Test No. OC-5-146 (Sheet 1 of 5)

CONFIDENTIAL

(This page is Unclassified)

Report AFRL-TR-69-88



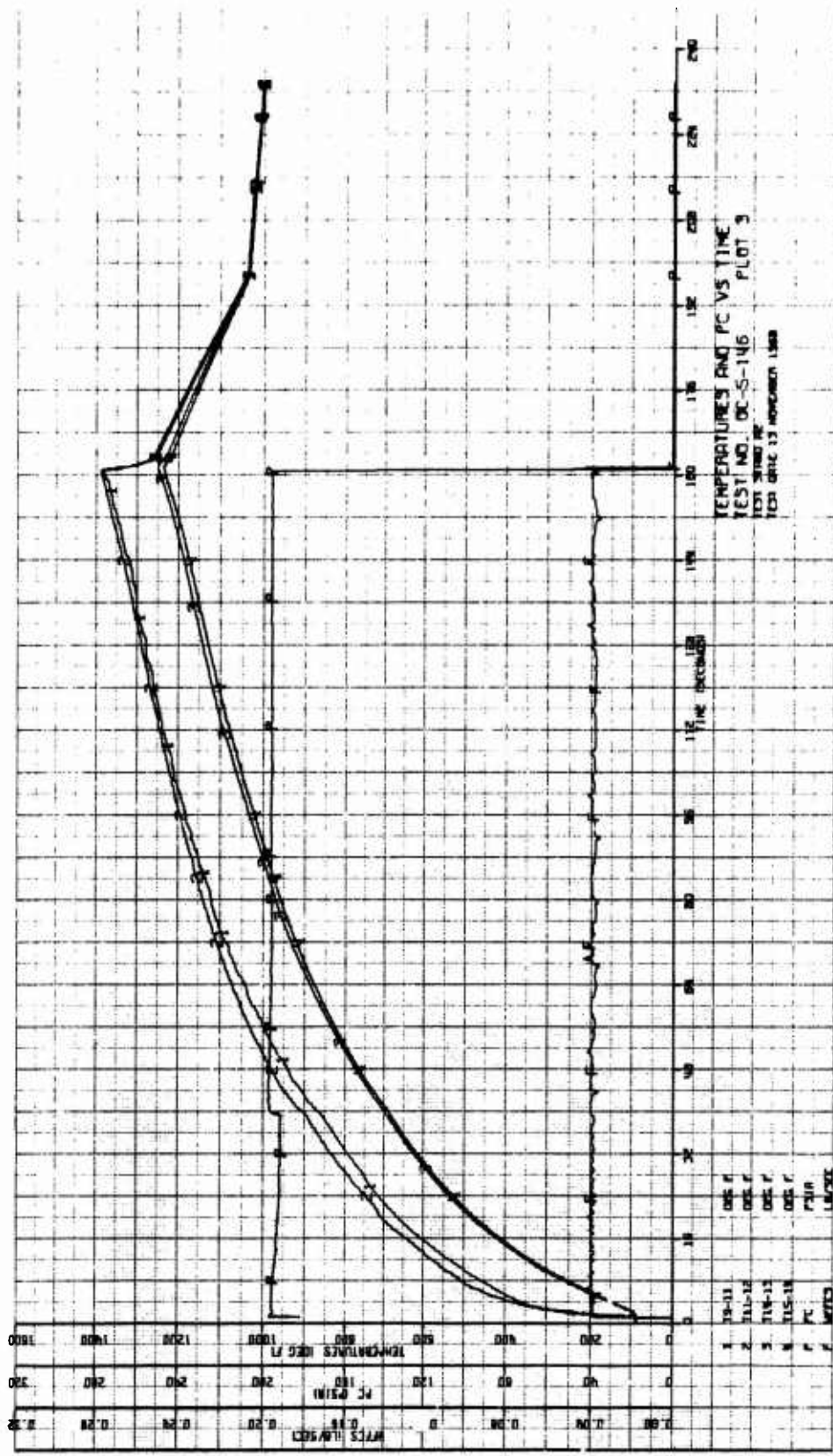


Figure 62. Altitude Engine Test No. OC-5-146 (Sheet 3 of 5)

CONFIDENTIAL

Report AIRPL-TR-69-88

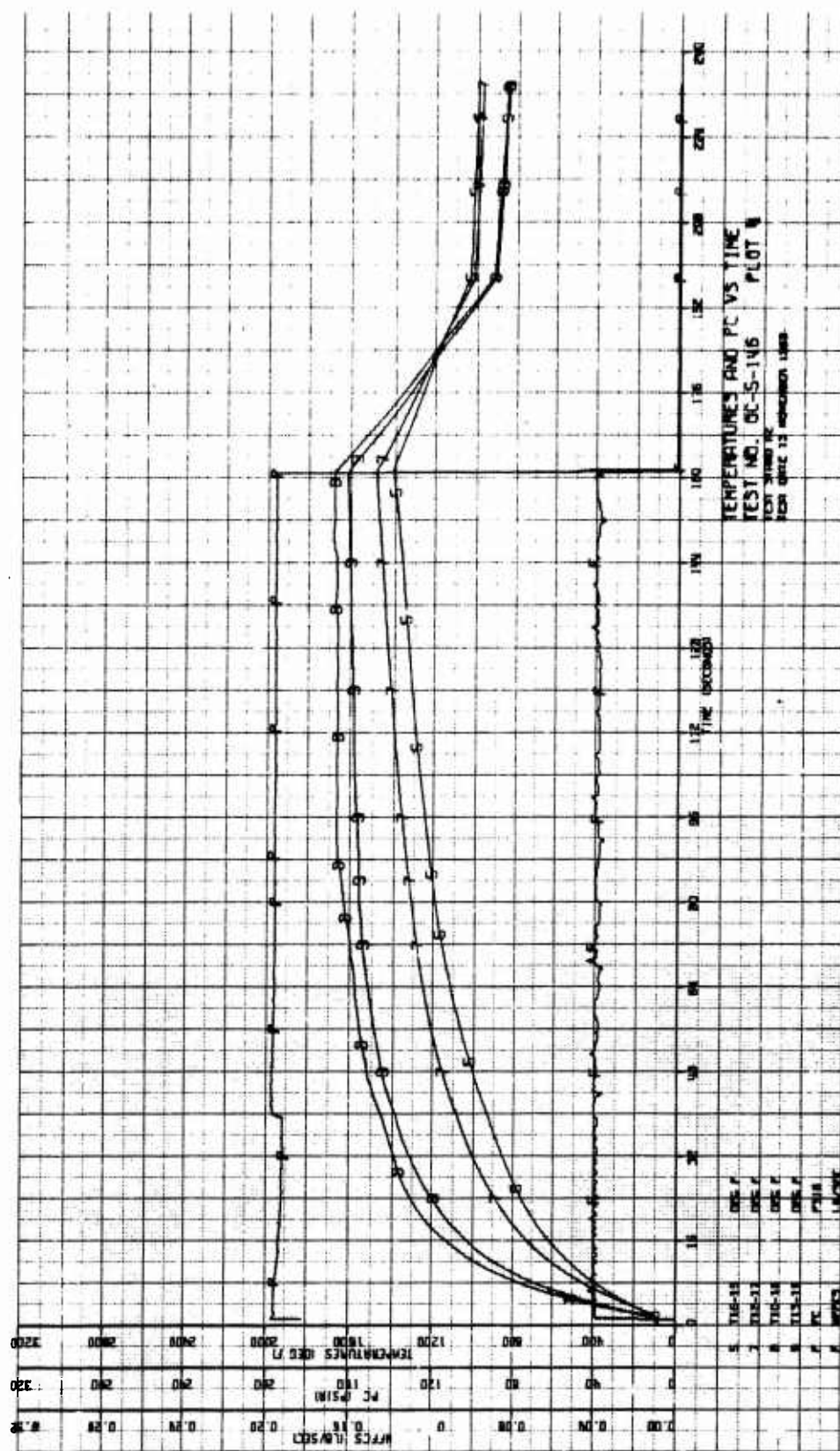


Figure 62. Altitude Engine Test No. OC-5-146 (Sheet 4 of 5)

CONFIDENTIAL

(This page is Unclassified)

UNCLASSIFIED

Report AFRPL-TR-69-88

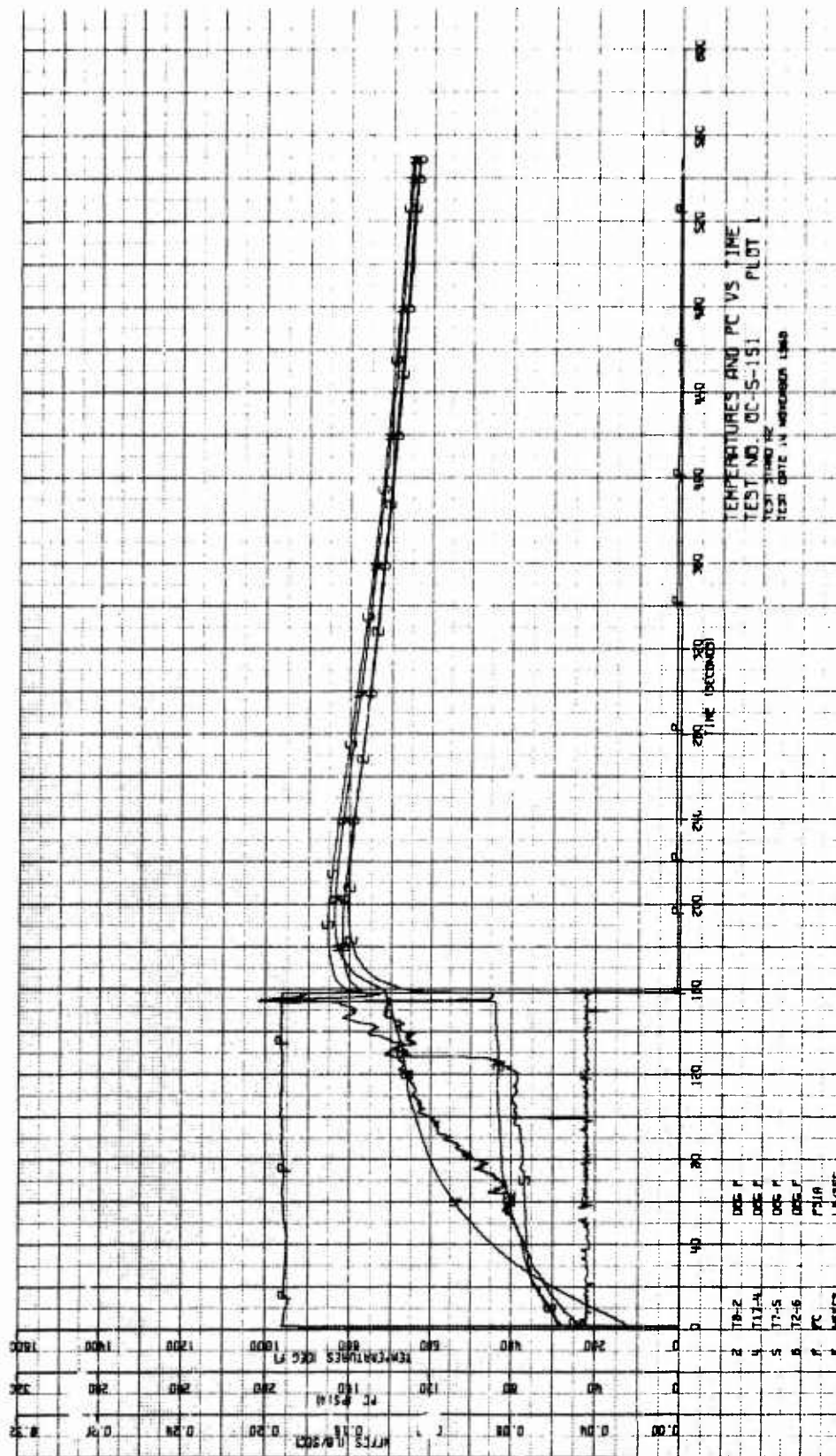
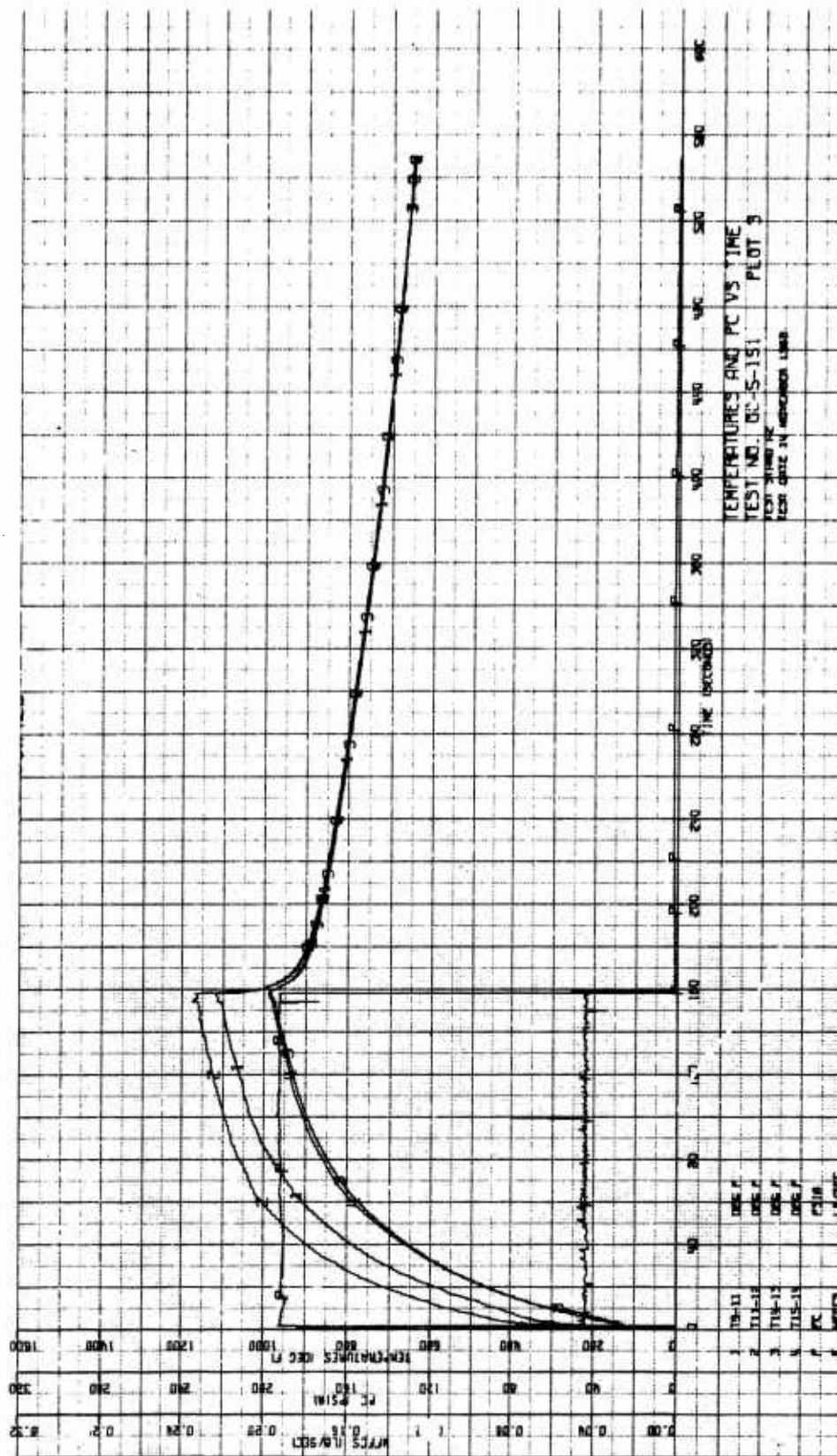


Figure 63. Altitude Engine Test No. OC-5-151 (Sheet 1 of 5)

UNCLASSIFIED

UNCLASSIFIED

Report AFRPL-TR-69-88



UNCLASSIFIED

Report AFRPL-TR-69-88

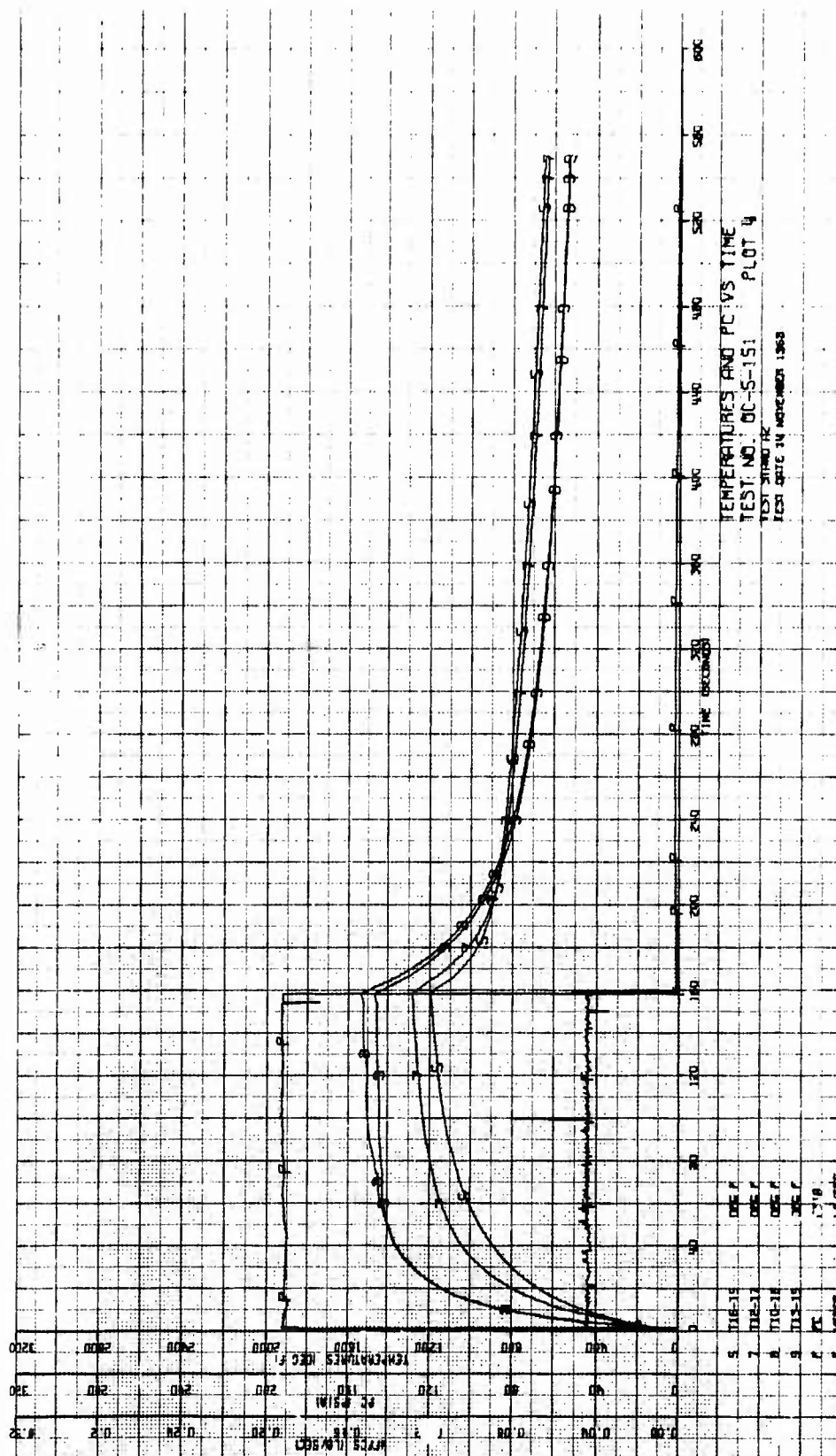


Figure 63. Altitude Engine Test No. OC-5-151 (Sheet 4 of 5)

UNCLASSIFIED

CONFIDENTIAL

Report AFRPL-TR-69-88

V, D, Altitude Test Evaluation (cont.)

provide an acceptable thermal profile with 38% fuel film coolant flow. The modification to the combustion chamber reduced the thickness and the axial length of the copper jacket to lower the heat transfer to the forward end of the chamber. Thermal instrumentation and the nozzle emissivity coating, which were damaged during the chamber machining, were repaired. The re-installation of the thermocouple leads and connectors was completed. An outline of the revised external geometry of the chamber and the location of thermal instrumentation are shown schematically on Figure No. 64.

The injector modification to integrate the film coolant circuit with the core fuel circuit also was accomplished. The design point for coolant flow was 38% of the fuel. Final flow calibration tests of the injector were conducted using fuel (MMH) and were as follows:

<u>Pressure Drop</u>	<u>Coolant Flow</u>
<u>psi</u>	<u>Percentage of Fuel</u>
217	38.5
250	37.0
300	36.2

The above coolant flow rates were used for tests -152 through -162 which included a sufficient range of test conditions to reveal that the coolant flow was higher than was needed for adequate chamber cooling. Prior to test -163, the injector was modified to reduce the coolant flow by approximately 10%. At this time, 0.020-in. was removed from the face to clean up the injector orifices which had been slightly damaged when the residue from a Teflon-filled injector-to-chamber gasket had been removed. Hydraulic testing after this modification showed that the oxidizer element impingement point had been displaced away from the injector face. The oxidizer and fuel were not mixing as well as previously observed in earlier hydraulic tests.

b. Altitude Demonstration

A final, simulated altitude demonstration of the bipropellant ACS engine was conducted with the modified 40:1 expansion ratio combustion chamber and the injector modified for internal fuel flow to the fuel film coolant manifold. This engine was shown on Figure No. 34 and another view of it installed in the altitude facility of the Aerojet-General Research Physics Laboratory is shown on Figure No. 65. Ten altitude tests were conducted at chamber pressures from 150 psia to 240 psia and at total mixture ratios ranging from 1.27 to 1.8.

CONFIDENTIAL

(This page is Unclassified)

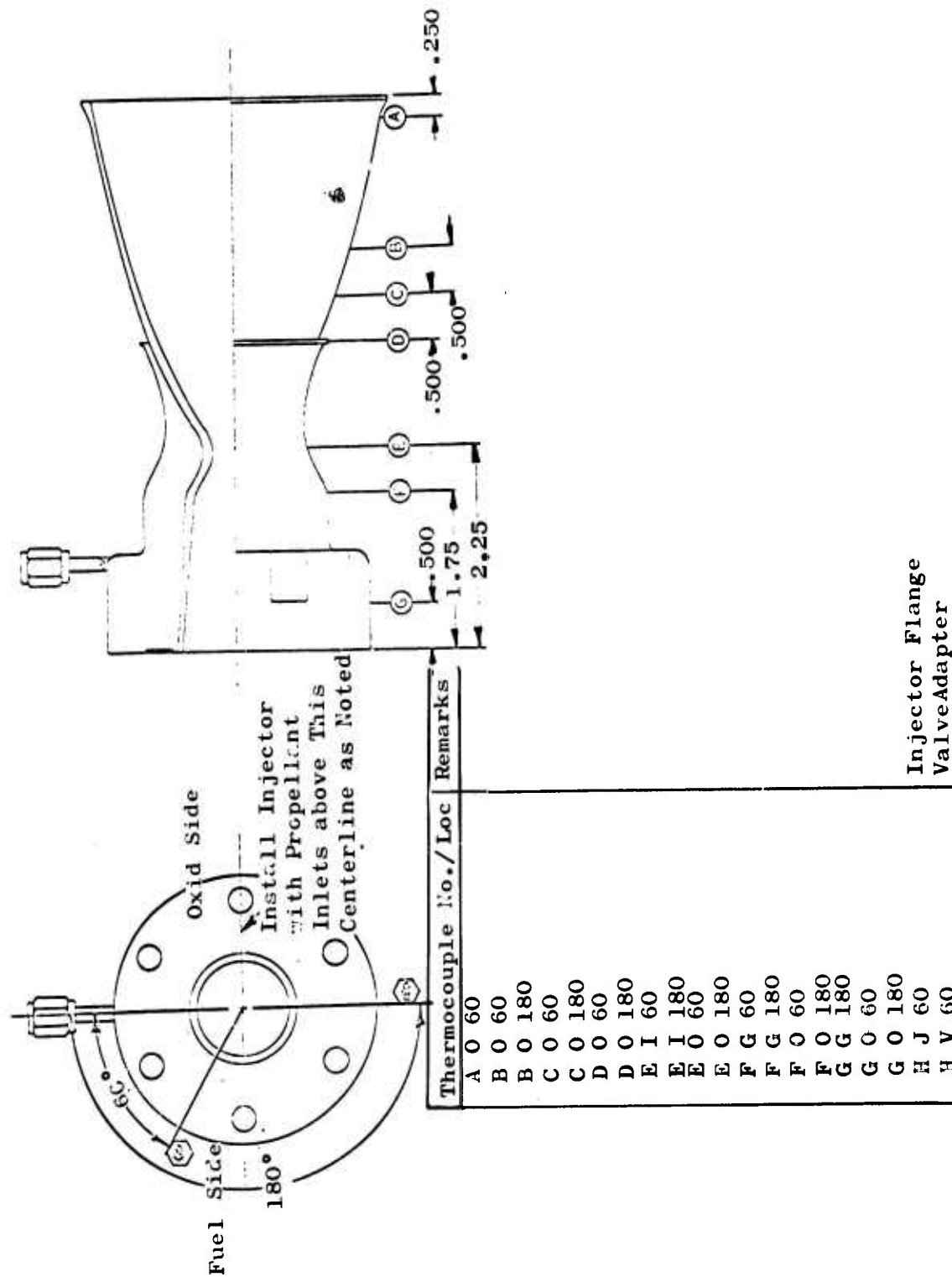


Figure 64. Chamber Modifications and Thermocouple Location

UNCLASSIFIED

Report AFRPL-TR-69-88



Figure 65. ACS Engine in Altitude Facility

Page 138

UNCLASSIFIED

CONFIDENTIAL

Report AFRPL-TR-69-88

V, D, Altitude Test Evaluation (cont.)

(U) A test was conducted following the duration demonstration to evaluate the worst case thermal duty cycle of the combustion chamber. Plots from this test (-169) are included as Figure No. 66 and include a repetitive cycle of 10 sec of engine firing followed by a 5 sec coast. This was selected because the maximum soak-out temperature of the forward end of the chamber is reached approximately 5 sec after shutdown. A question existed as to whether the chamber forward temperature could be "pumped up" thermally so a satisfactory restart would not occur. The engine successfully completed ten cycles. However, the engine was shut down during the eleventh pulse when an excessive thermal condition was reached at the convergent section of the chamber. Thermocouples No. 1 and 2 in Plot A of Figure No. 66 show the sequentially increasing chamber forward end temperatures. A high-frequency pressure transducer located in the fuel feed system recorded a continuous 20 Hz oscillation during this pulse.

(U) A series of pulsing tests were conducted after the thermal cycle test -169 to determine the engine pulsing characteristics. These tests were conducted for the purpose of evaluating both varying engine electrical pulse widths (EPW) with constant electrical coast widths (ECW) and varying the coast width with a constant pulse width.

(U) The influence of electrical pulse width upon the engine pulse characteristics was evaluated in the three test duty cycles of tests -171, -172, and -173. Each test consisted of 14 pulses with a constant electrical coast width of 0.150 sec. The pulses were of 0.010, 0.015, 0.025, 0.050, 0.100, and 0.150 sec duration and were in the sequence shown in the oscillograph traces of test -172, which are presented as Figure No. 67. The recorded chamber pressure had a slow response because of the length and internal diameter of the line to the chamber pressure transducer. The pulse profile is best represented by the measured thrust on Figure No. 67 and the bit impulse characteristics of Figure No. 68. The recorded temperatures, flows, and pressures for the three tests are shown on Figure No. 69, No. 70, and No. 71.

(C) A series of three test pulse cycles were conducted to evaluate the influence of electrical coast width upon pulsing characteristics. These tests (-174, -175, and -176) were the final tests with the engine. Each test included 7 pulses of 0.100 sec duration with increasing electrical coast widths of 0.050, 0.100, 0.150, 0.250, 0.500, and 1.500 sec. A typical test sequence is shown in the thrust traces from test -176 which are included as Figure No. 72. Start transients for each pulse with an electrical coast width greater than 0.150 sec are very similar with a transient time from electrical signal to 90% thrust of from 0.015 sec to 0.016 sec. The transient times to 90% thrust were consistently 0.012 sec after an electrical coast width of 0.050 sec in the second pulse of each test. This 0.003 sec to

CONFIDENTIAL

CONFIDENTIAL

Report AFRPL-TR-69-88

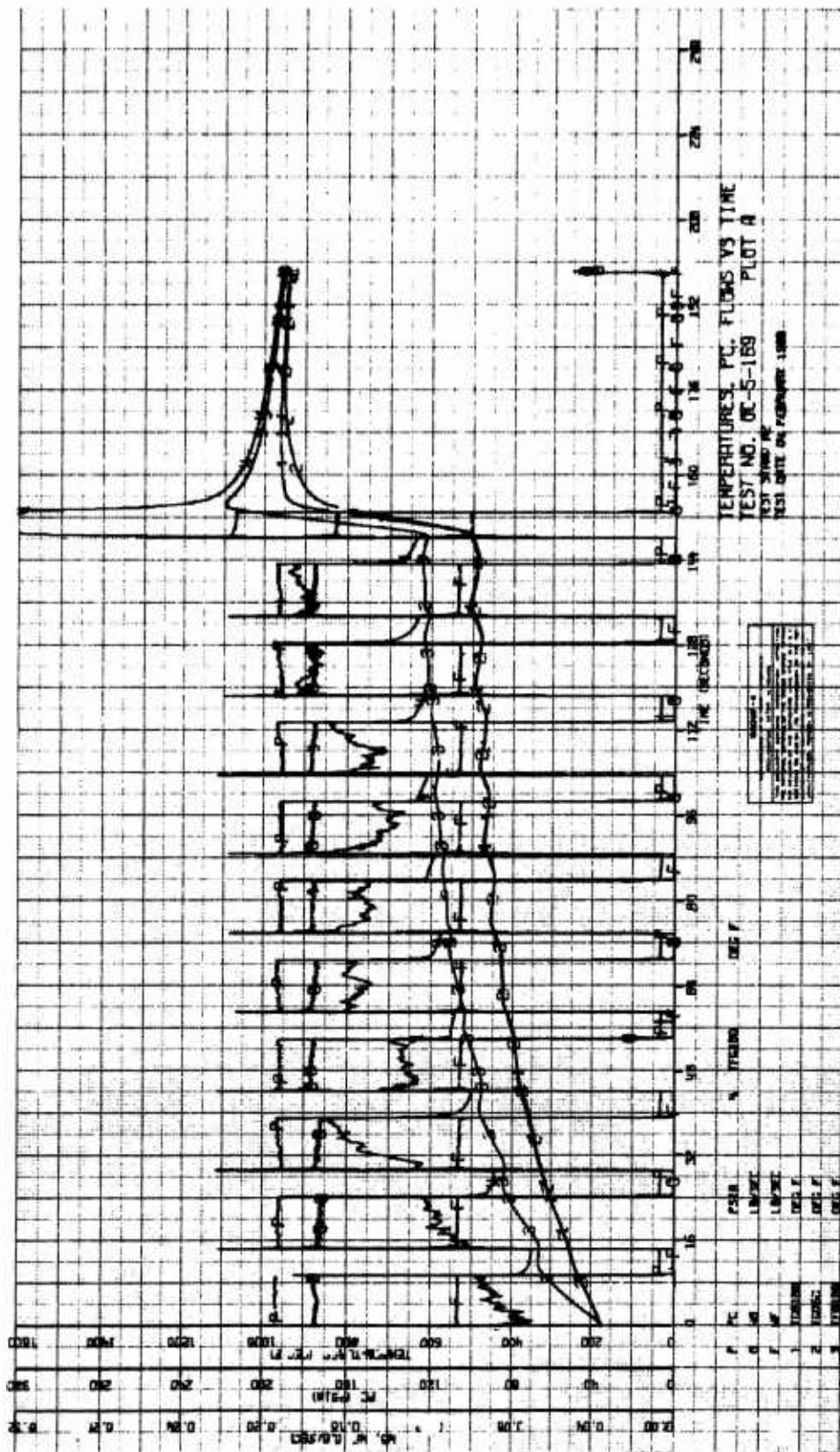


Figure 66. Thermal Soak Duty Cycle Test No. OC-5 (u)
(Sheet 1 of 3)

CONFIDENTIAL

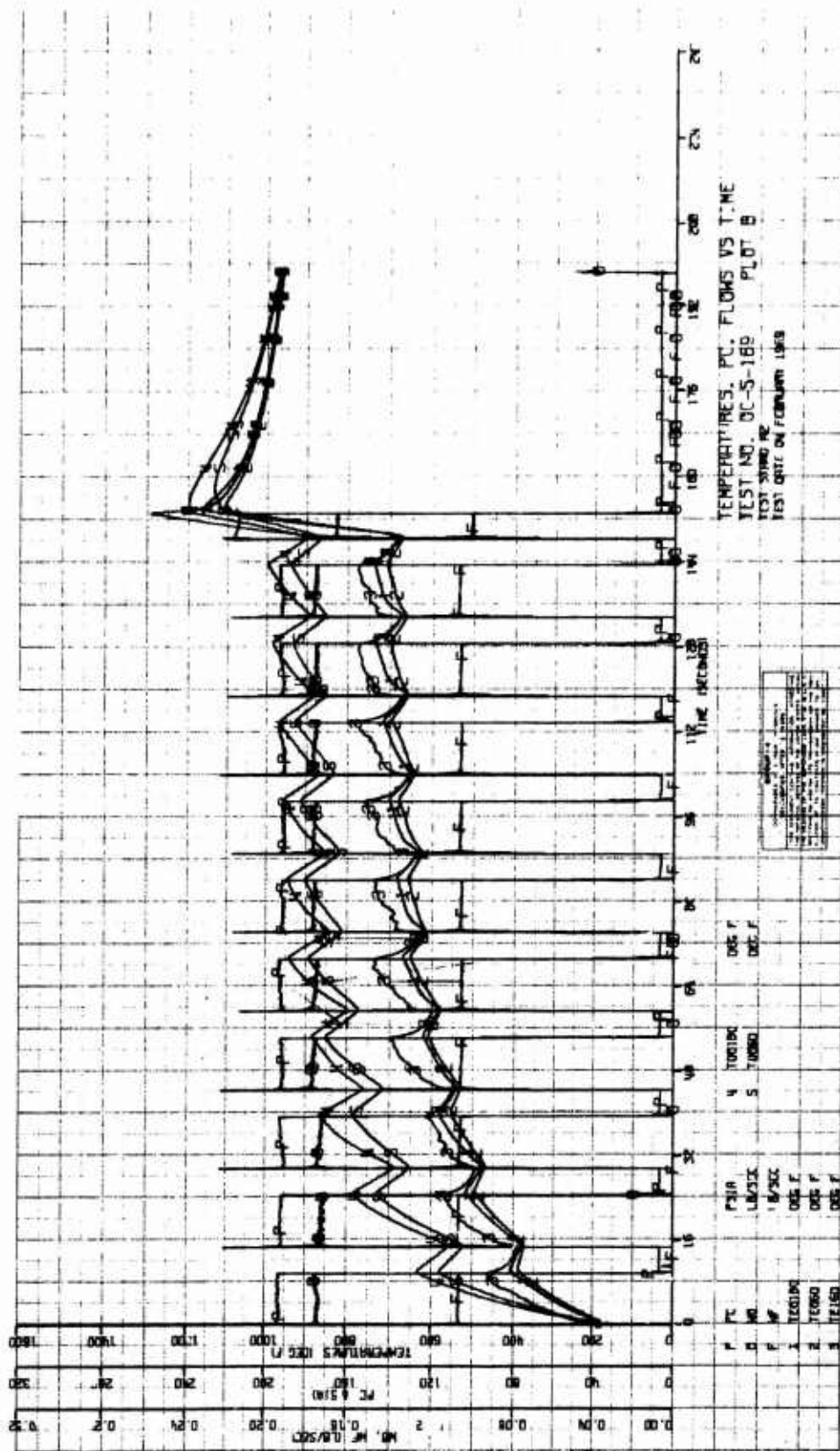


Figure 66. Thermal Soak Duty Cycle Test No. 00-5-169 (u)
(Sheet 2 of 3)

CONFIDENTIAL

Report AFRPL-TR-69-88

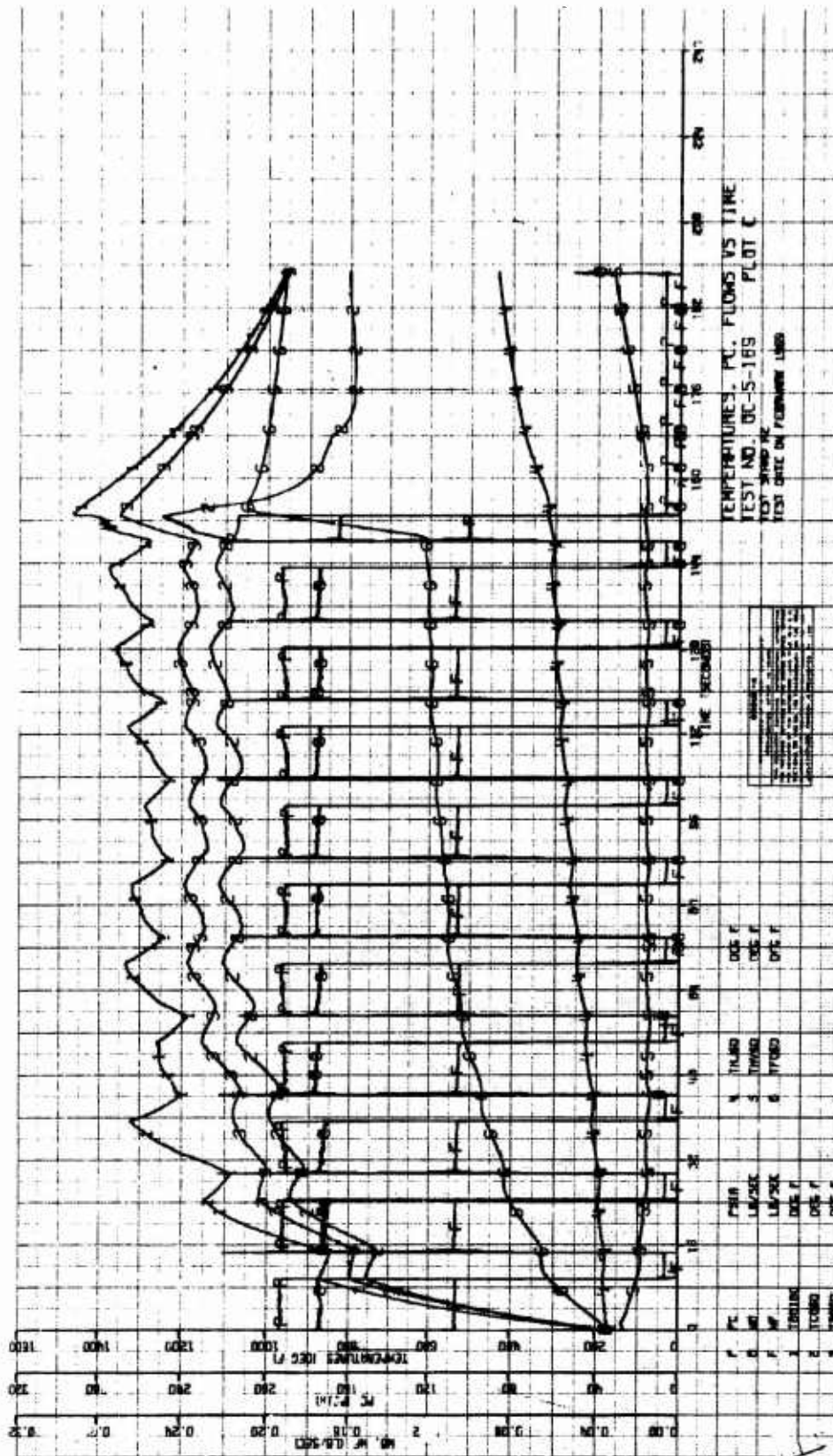


Figure 66. Thermal Soak Duty Cycle Test No. OC-5-169 (u)
(Sheet 3 of 3)

CONFIDENTIAL

UNCLASSIFIED

Report AFRPL-TR-69-88

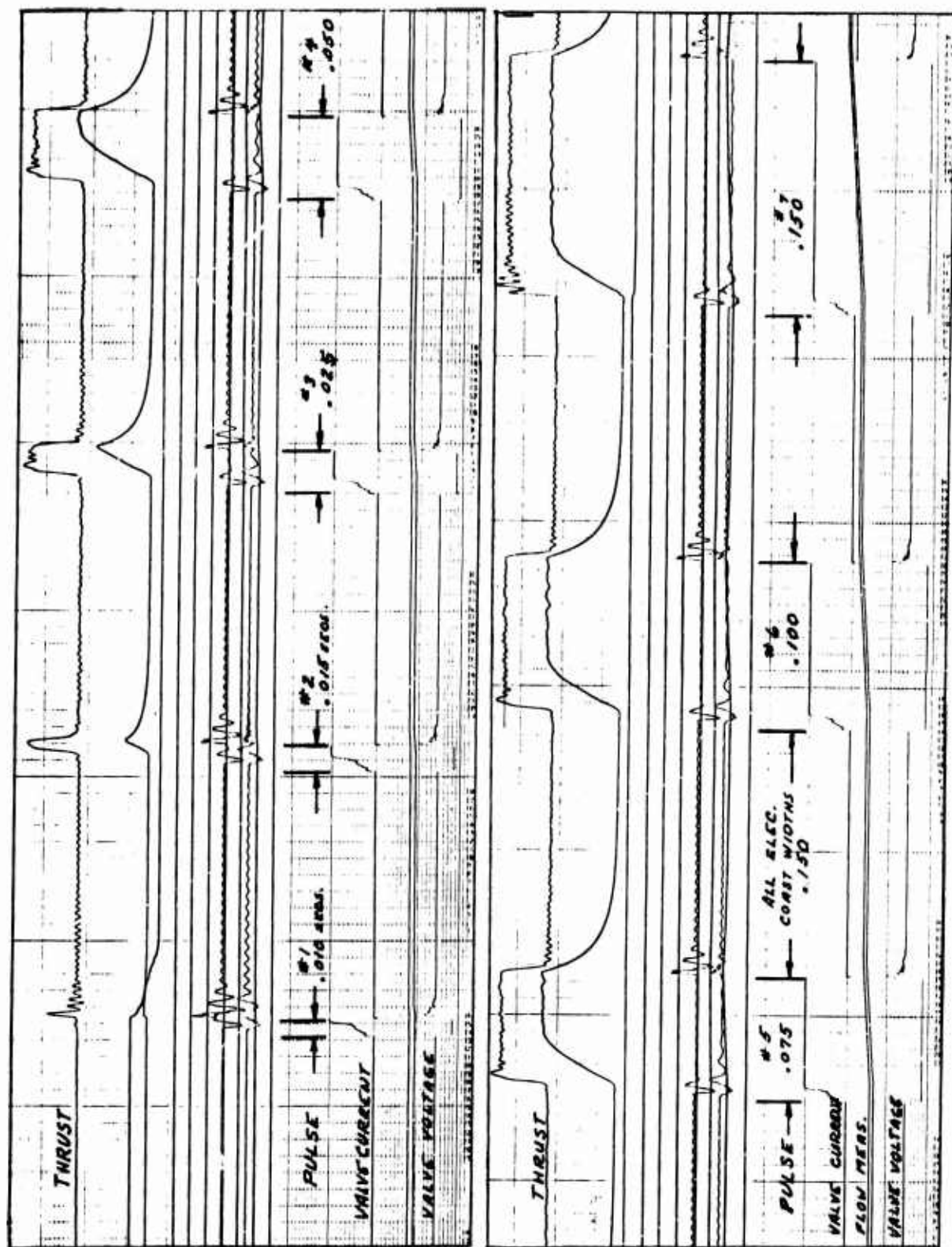


Figure 67. Pulsing Characteristics (Sheet 1 of 2)

UNCLASSIFIED

UNCLASSIFIED

Report AFRPL-TR-69-88

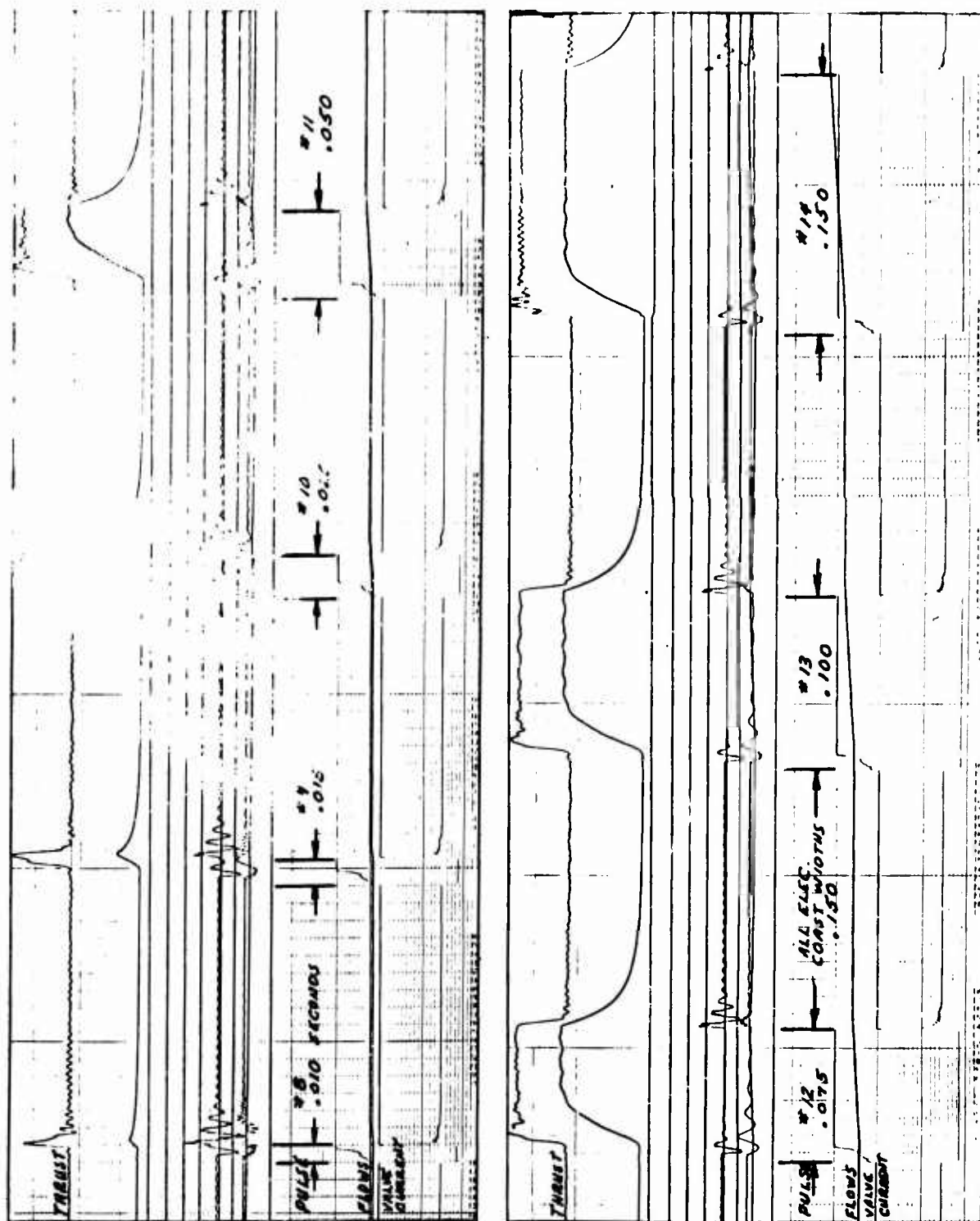


Figure 67. Pulsing Characteristics (Sheet 2 of 2)

UNCLASSIFIED

CONFIDENTIAL

Report AFRPL-TR-69-88

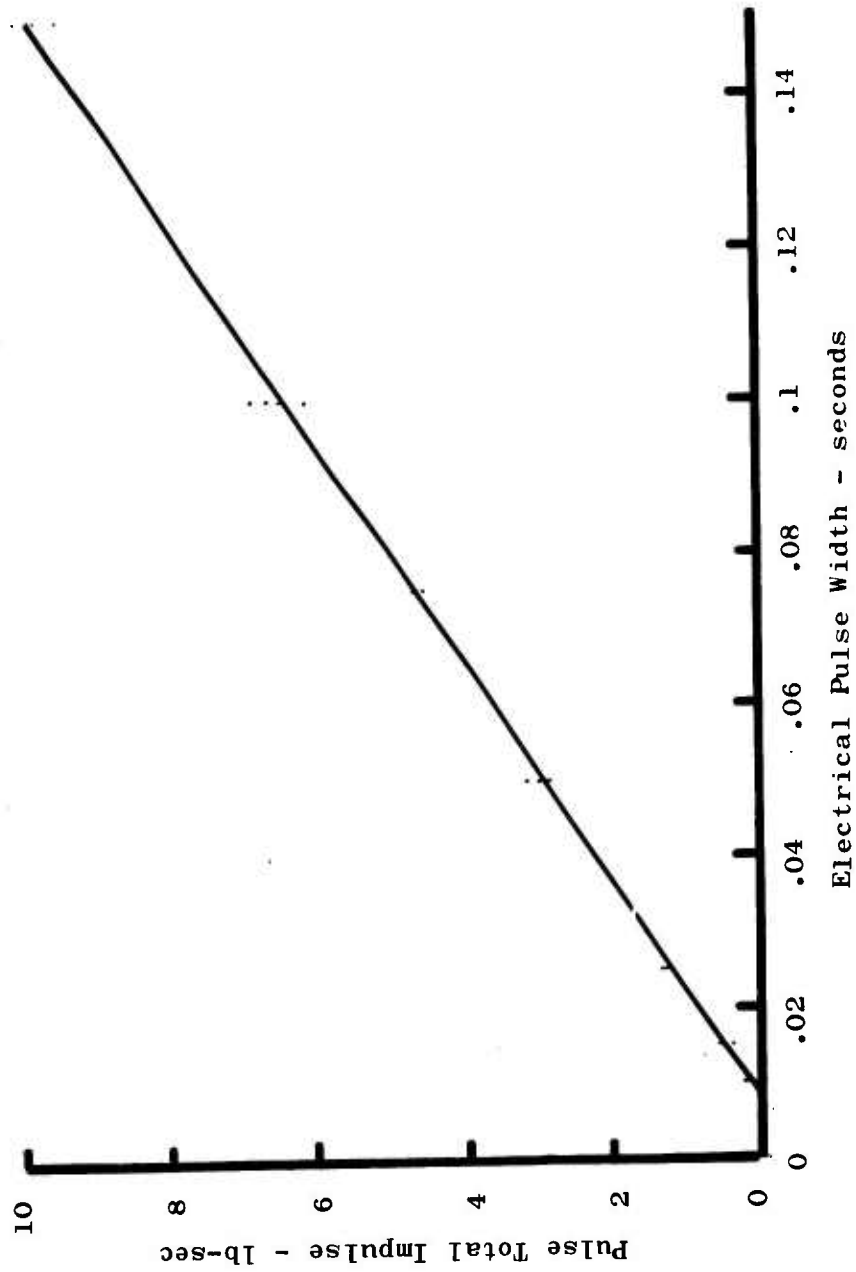
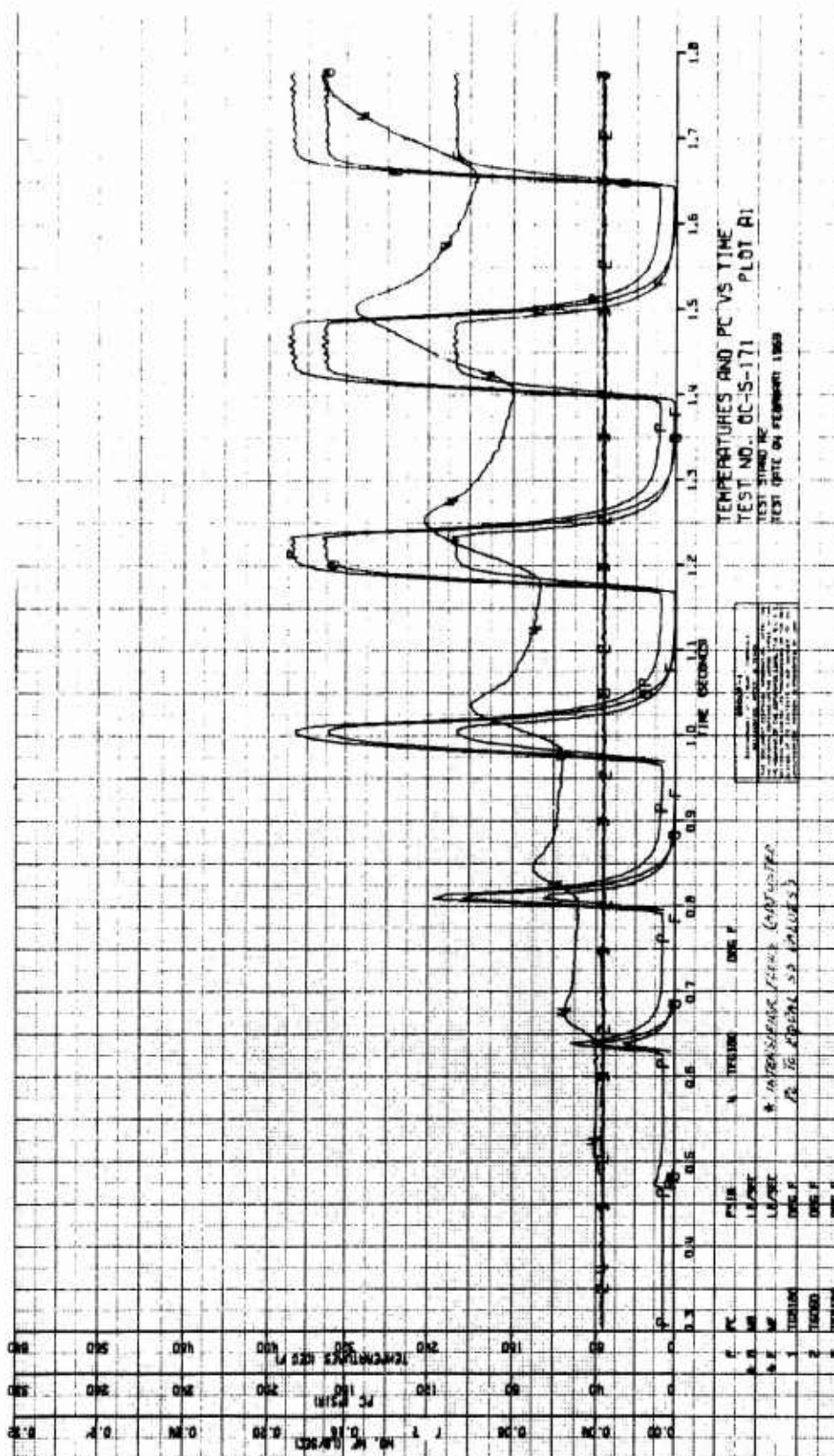


Figure 68. Pulsing Performance - Bit Impulse (u)

CONFIDENTIAL

CONFIDENTIAL

Report AFRPL-TR-69-88



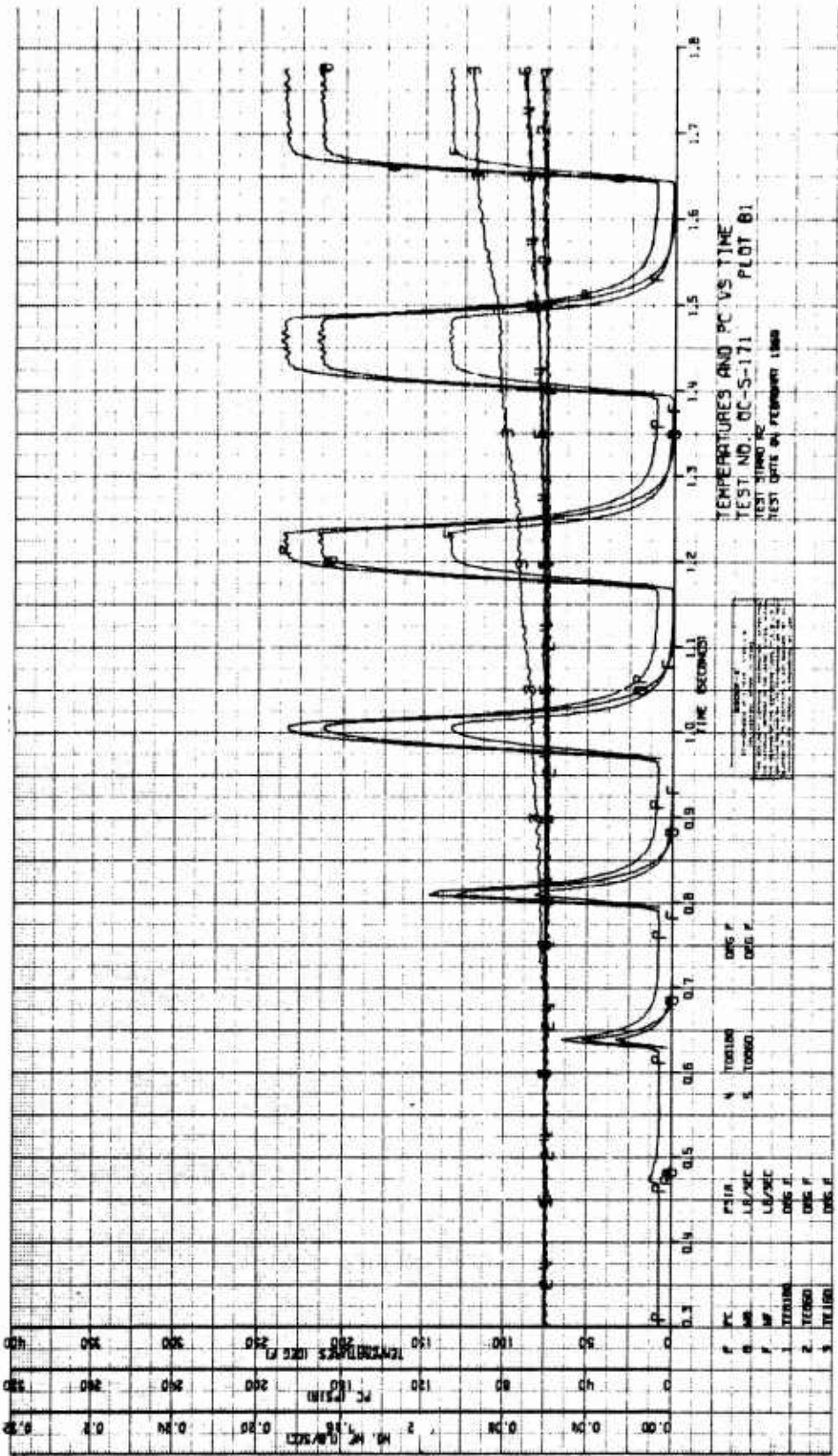


Figure 69. Pulse Data - Test No. OC-5-171 (u)
(Sheet 2 of 6)

CONFIDENTIAL

Report AFRPL-TR-69-88

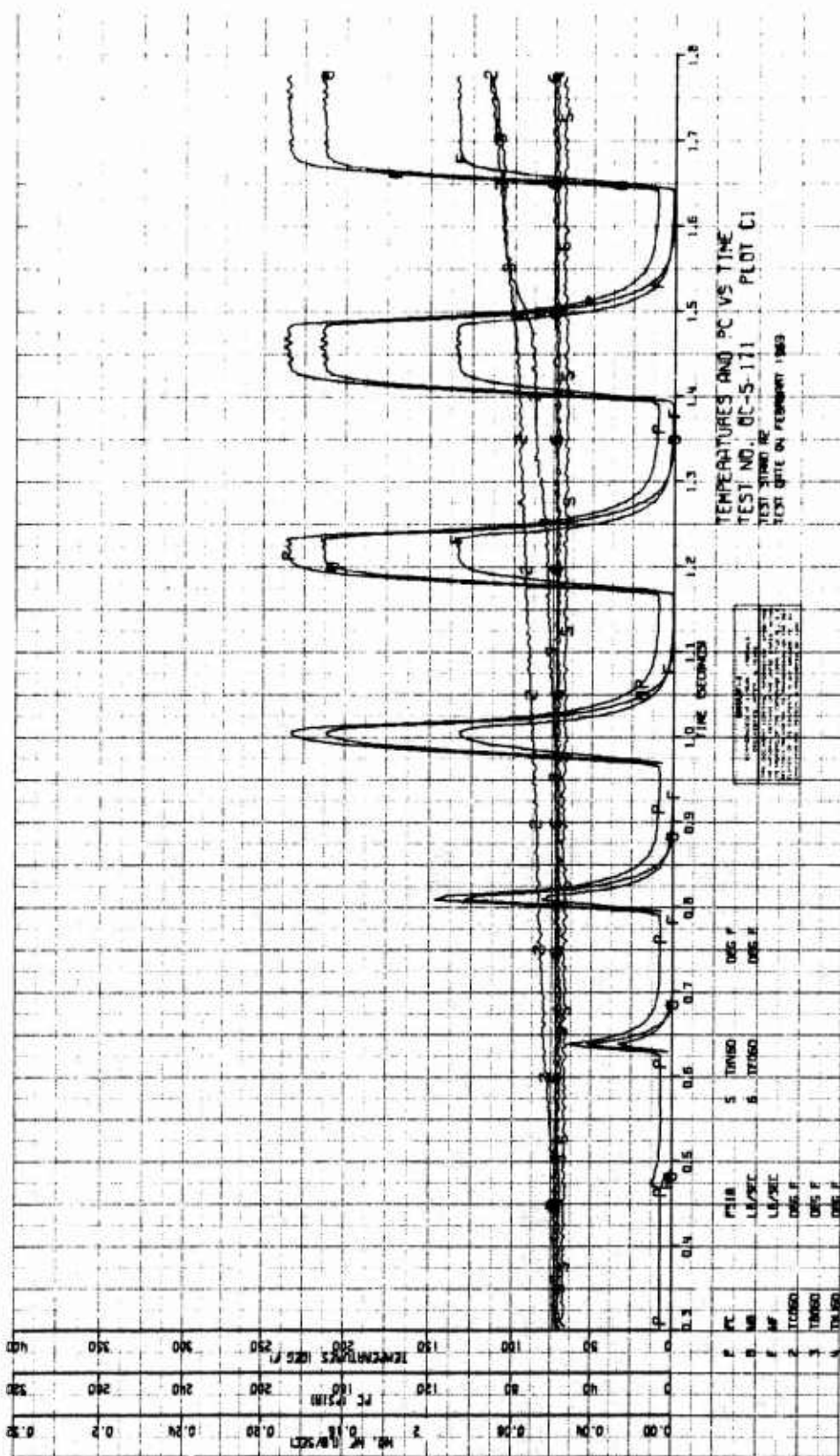


Figure 69. Pulse Data - Test No. OC-5-171 (u)
(Sheet 3 of 6)

CONFIDENTIAL

Report AFRL-TR-69-88

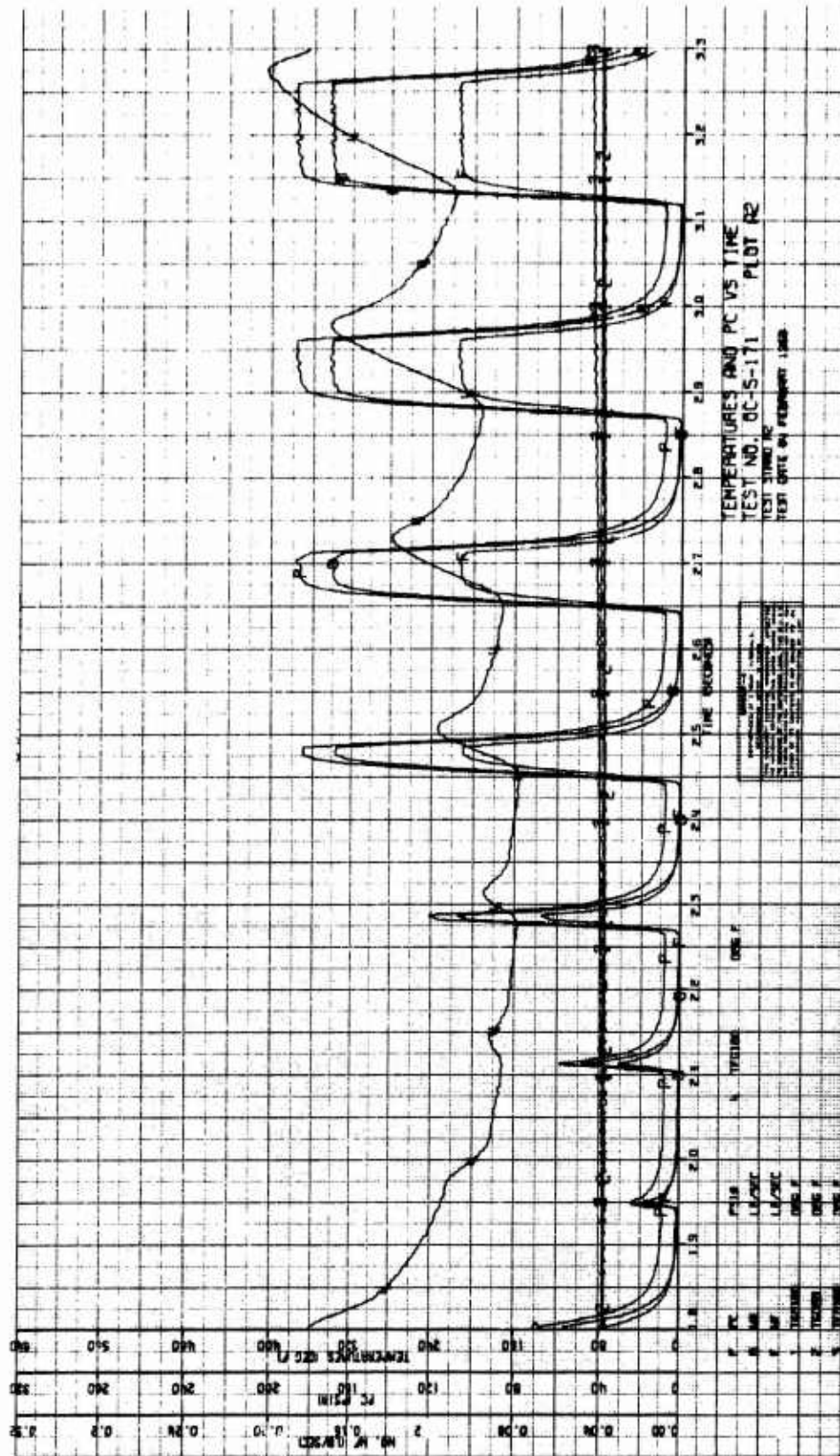


Figure 69. Pulse Data - Test No. OC-5-171 (u)
(Sheet 4 of 6)

CONFIDENTIAL

Report AFRPL-TR-69-88

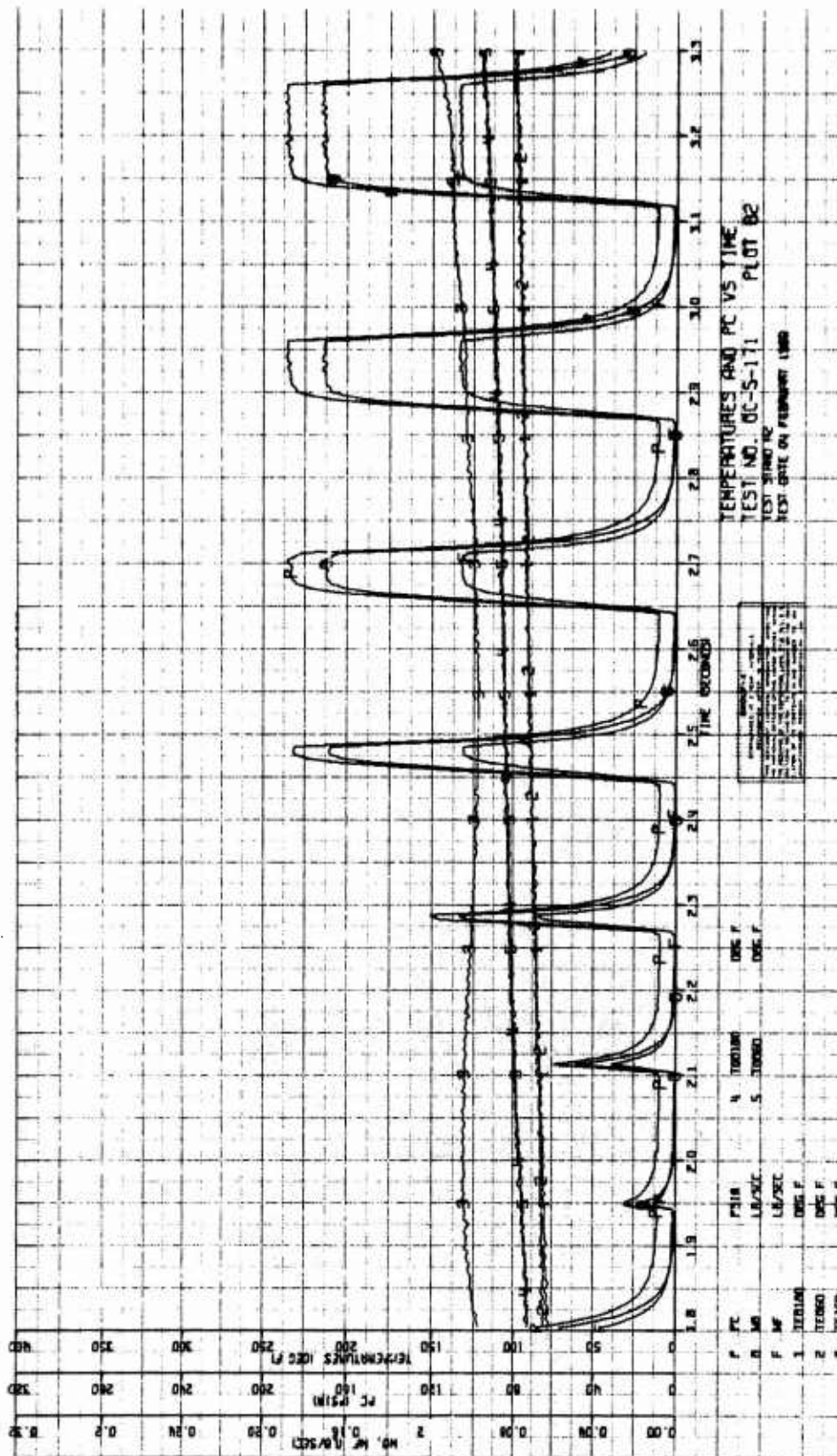


Figure 69. Pulse Data - Test No. OC-5-171 (u)
(Sheet 5 of 6)

CONFIDENTIAL

Report AFRPL-TR-69-88

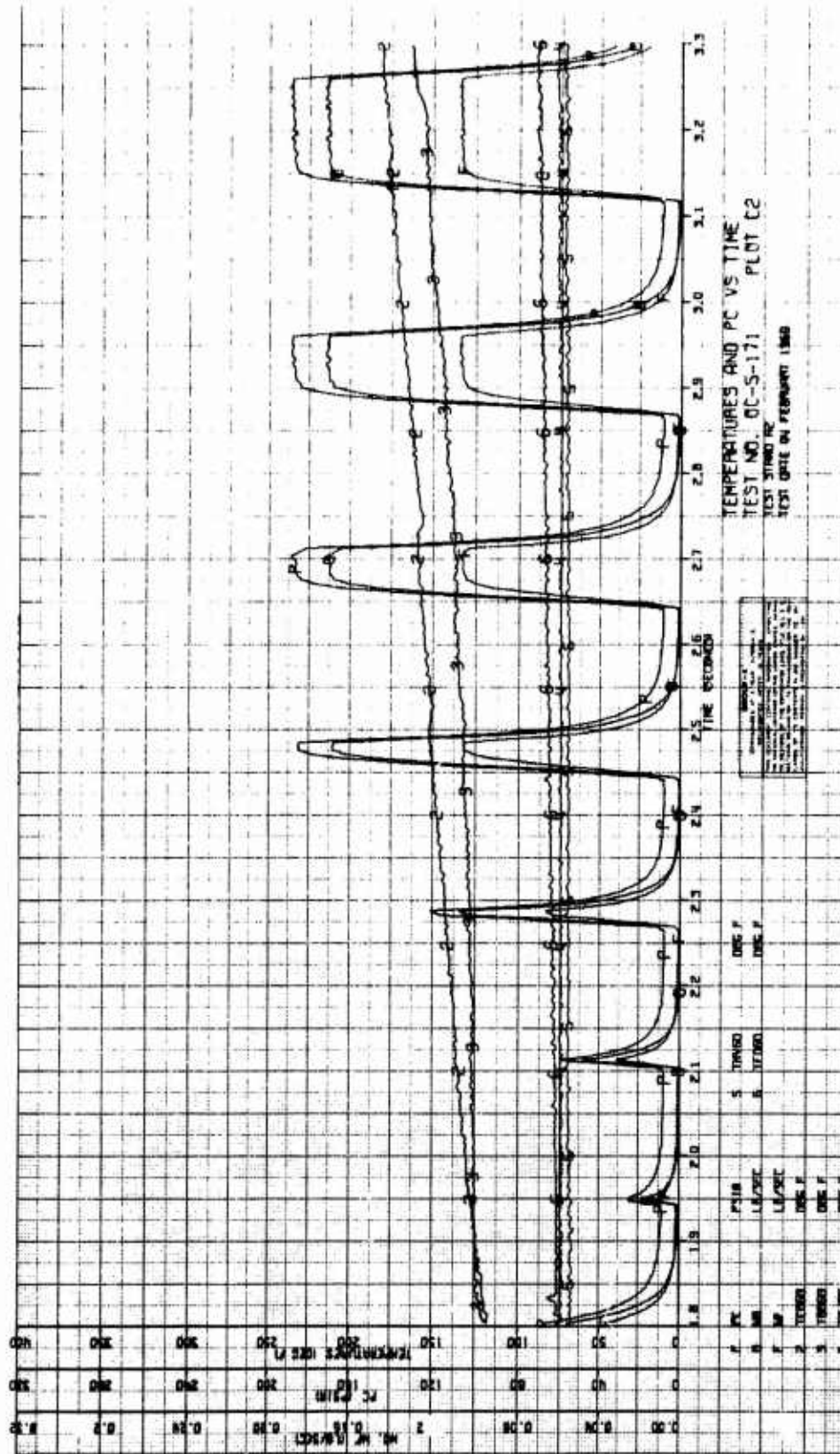


Figure 69. Pulse Data - Test No. OC-5-171 (u)
(Sheet 6 of 6)

CONFIDENTIAL

CONFIDENTIAL

Report AFRPL-TR-69-88

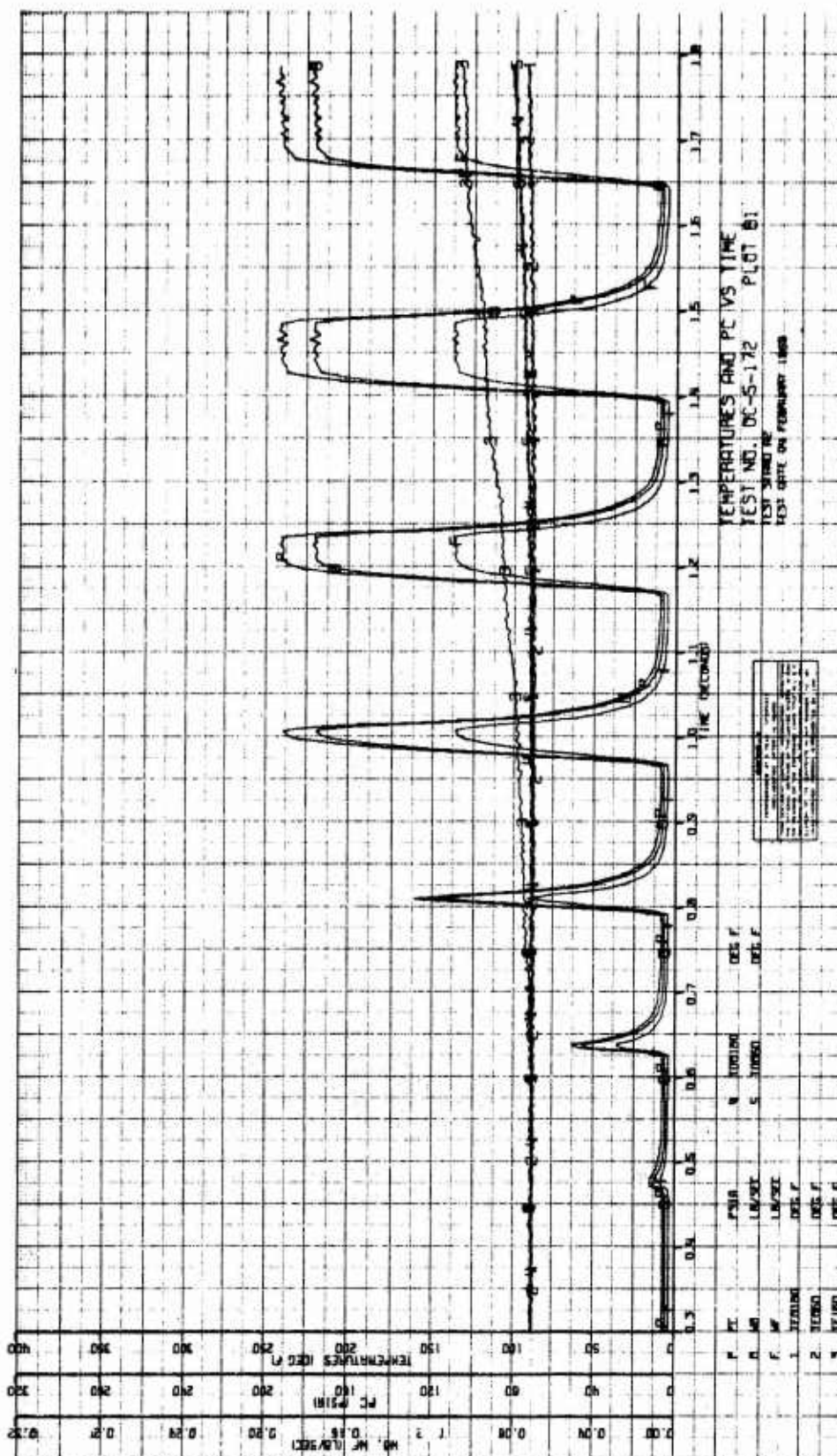


Figure 70. Pulse Data - Test No. OC-5-172 (u)
(Sheet 2 of 6)

CONFIDENTIAL

CONFIDENTIAL

Report AFRPL-TR-69-88

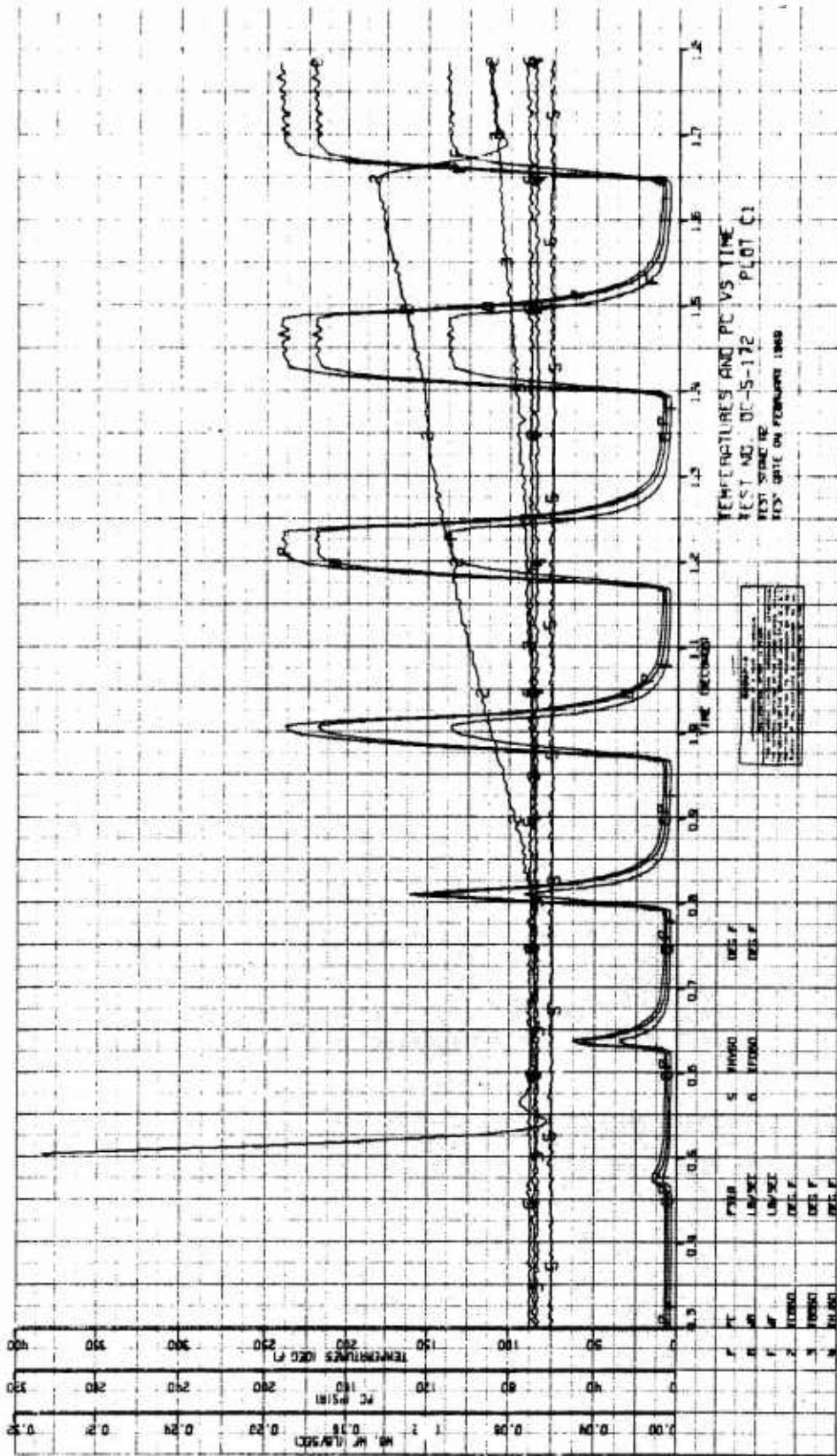


Figure 70. Pulse Data - Test No. OC-5-172 (u)
(Sheet 3 of 6)

CONFIDENTIAL

Report AFRPL-TR-69-88

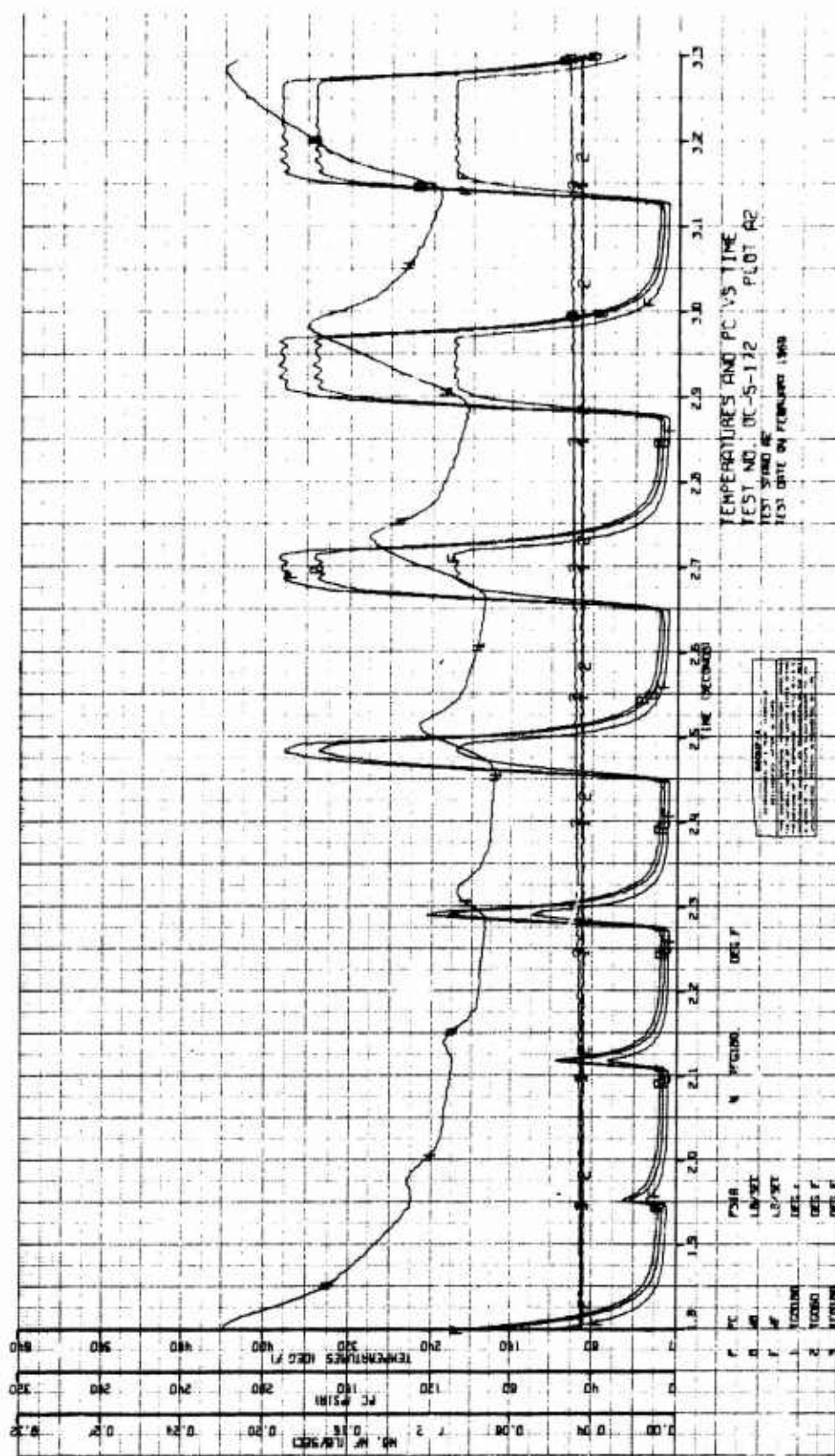


Figure 70. Pulse Data - Test No. OC-5-172 (u)
(Sheet 4 of 6)

CONFIDENTIAL

Report AFRPL-TR-69-88

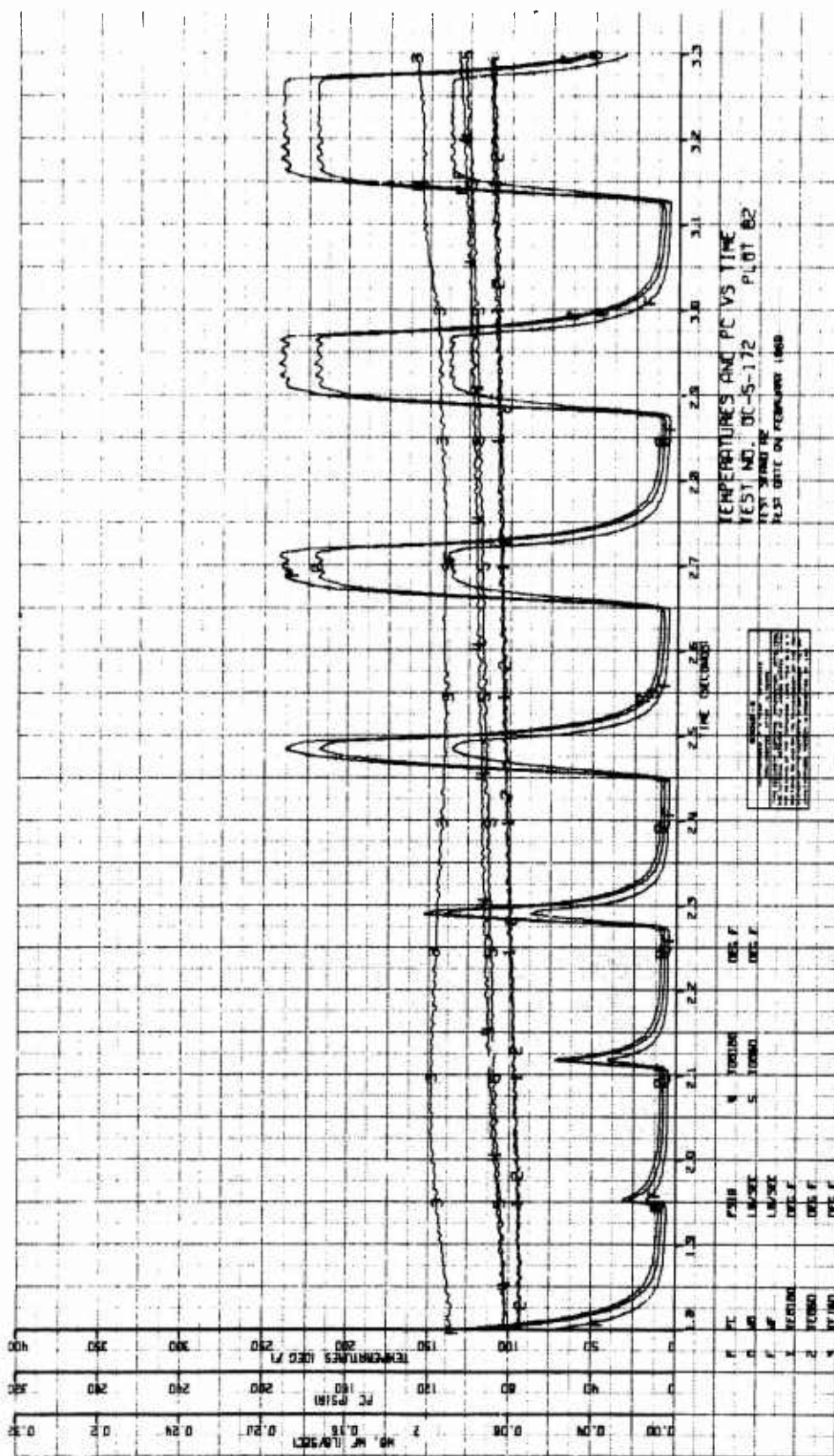


Figure 70. Pulse Data - Test No. 00C-5-172 (u)
(Sheet 5 of 6)

CONFIDENTIAL

CONFIDENTIAL

Report AFRPL-TR-69-88

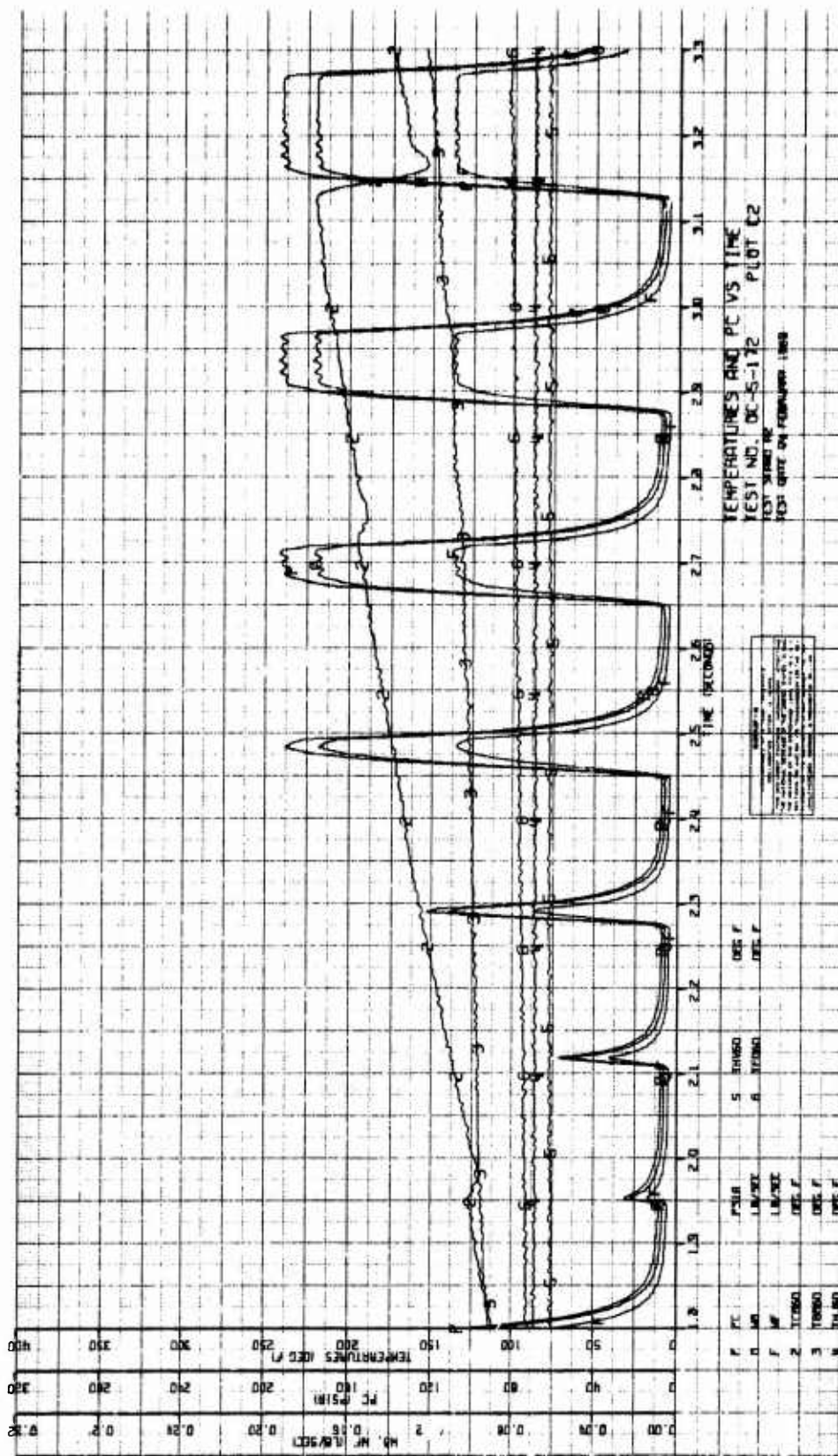


Figure 70. Pulse Data - Test No. OC-5-172 (u)
(Sheet 6 of 6)

CONFIDENTIAL

Report AFRPL-TR-69-88

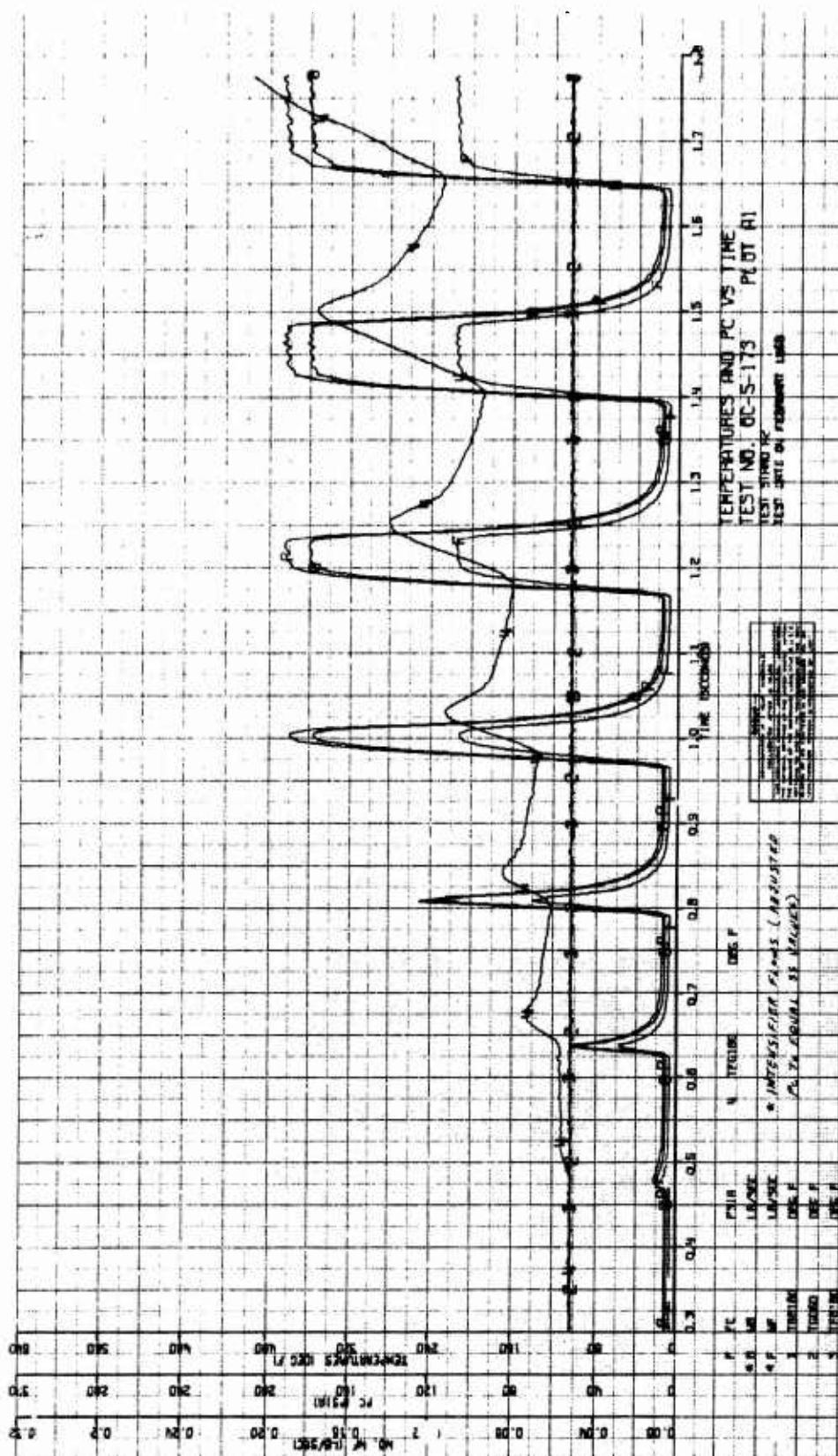


Figure 71. Pulse Data - Test No. OC-5-173 (u)
(Sheet 1 of 6)

CONFIDENTIAL

CONFIDENTIAL

Report AFRPL-TR-69-88

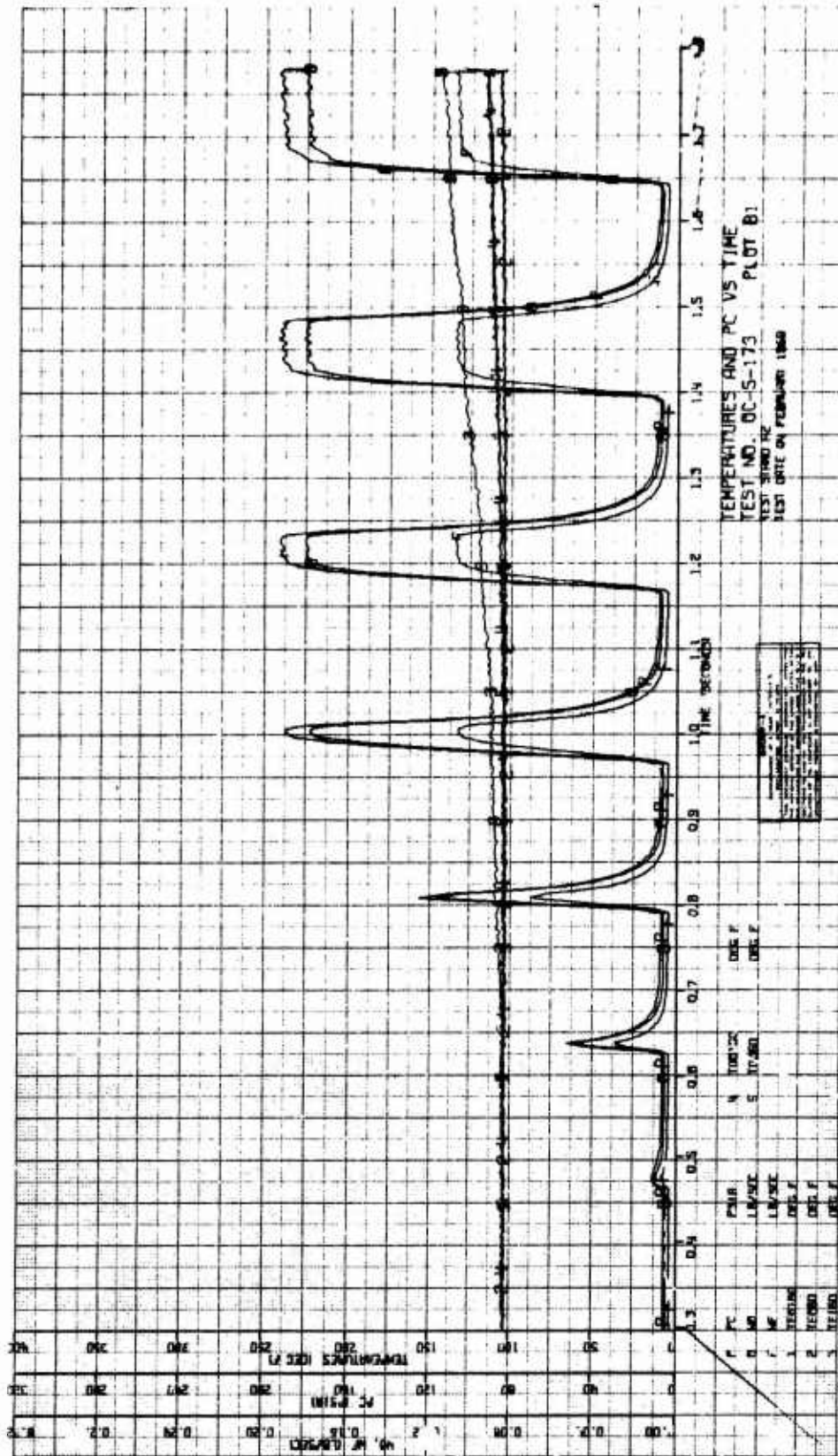


Figure 71. Pulse Data - Test No. OC-5-173 (u)
(Sheet 2 of 6)

CONFIDENTIAL

CONFIDENTIAL

Report AFRPL-TR-69-88

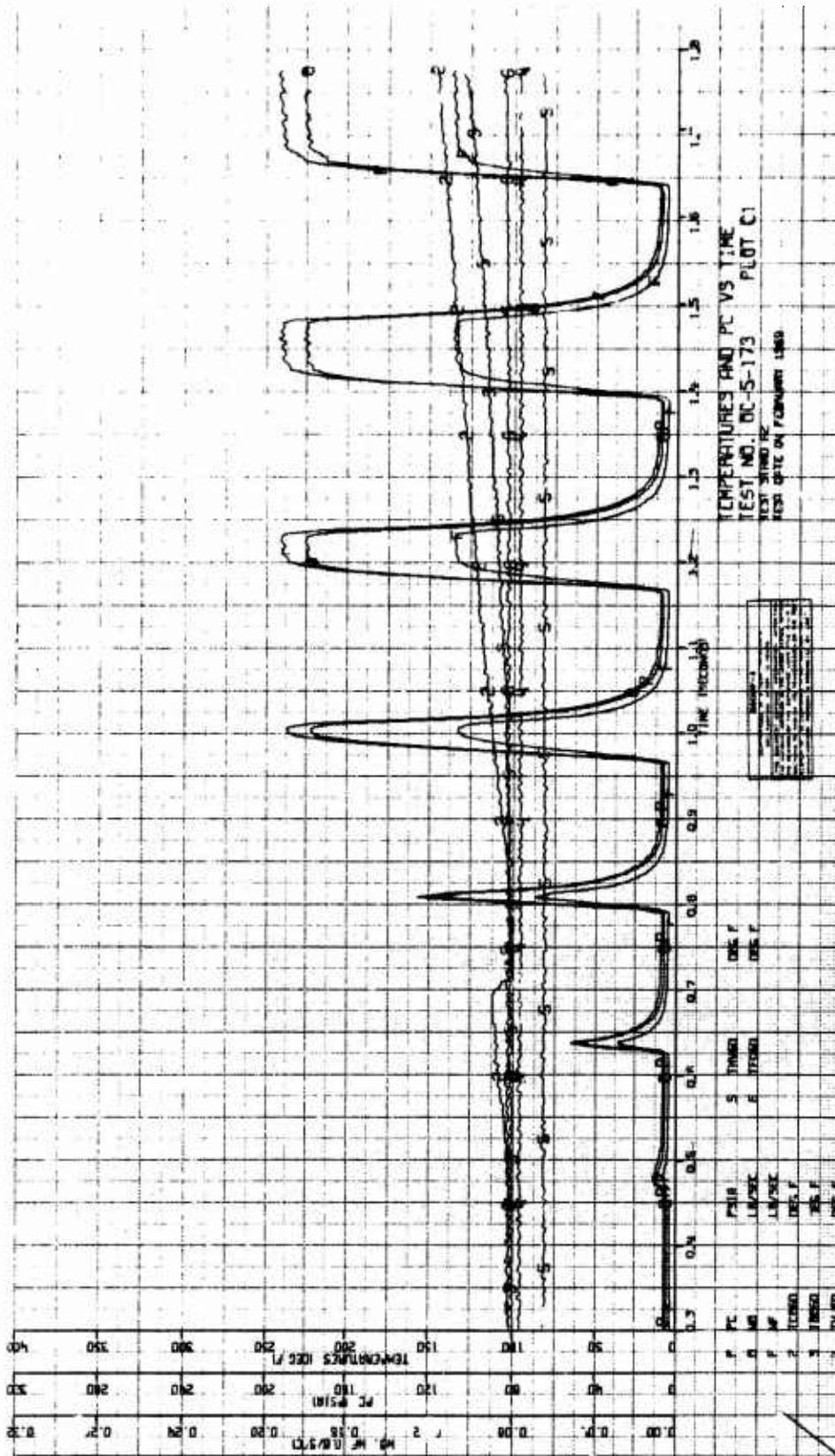


Figure 71. Pulse Data - Test No. OC-5-173 (u)
(Sheet 3 of 6)

CONFIDENTIAL

Report AFRPL-TR-69-88

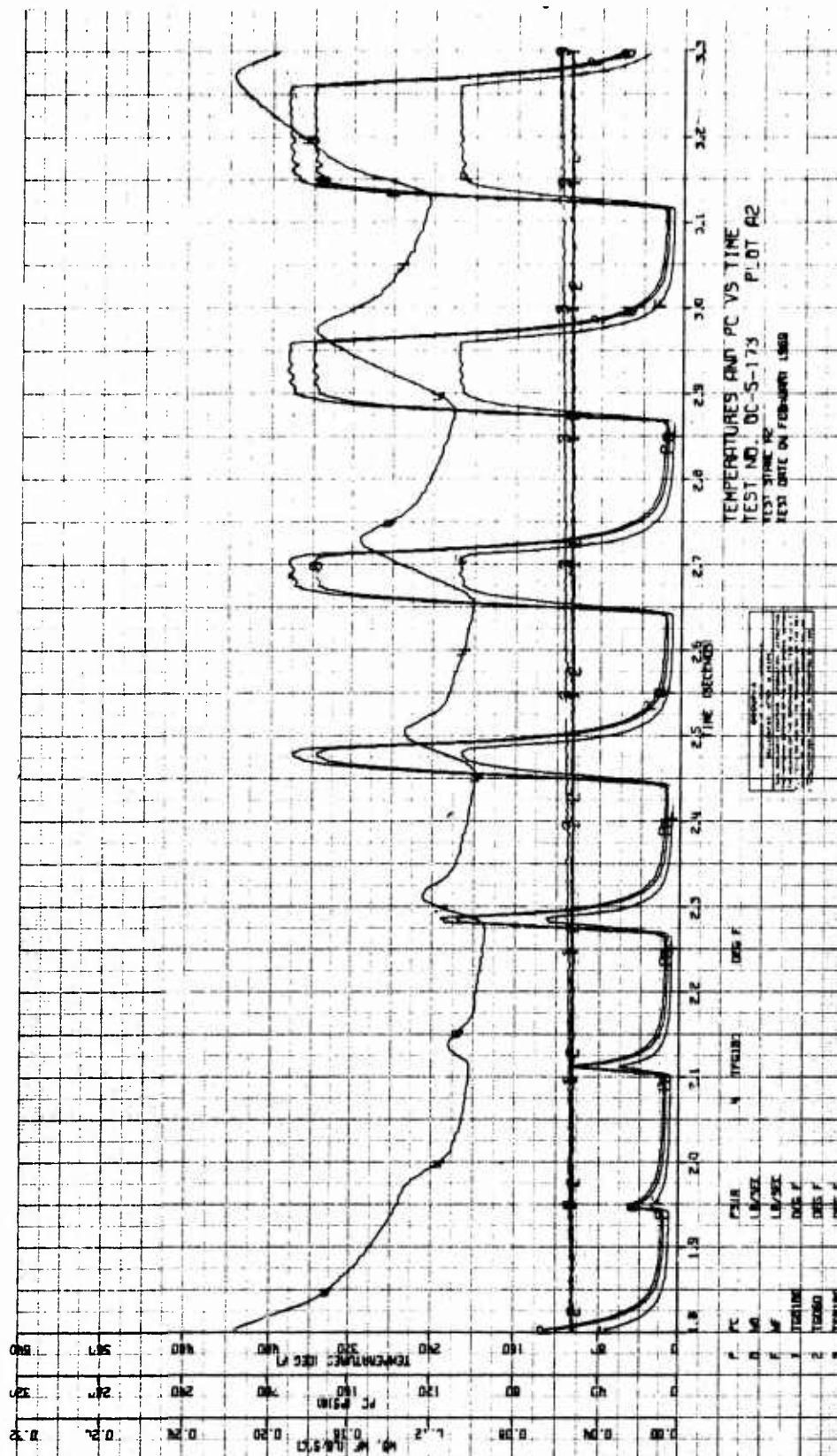


Figure 71. Pulse Data - Test No. OC-5-173 (u)
(Sheet 4 of 6)

CONFIDENTIAL

CONFIDENTIAL

Report AFRPL-TR-69-88

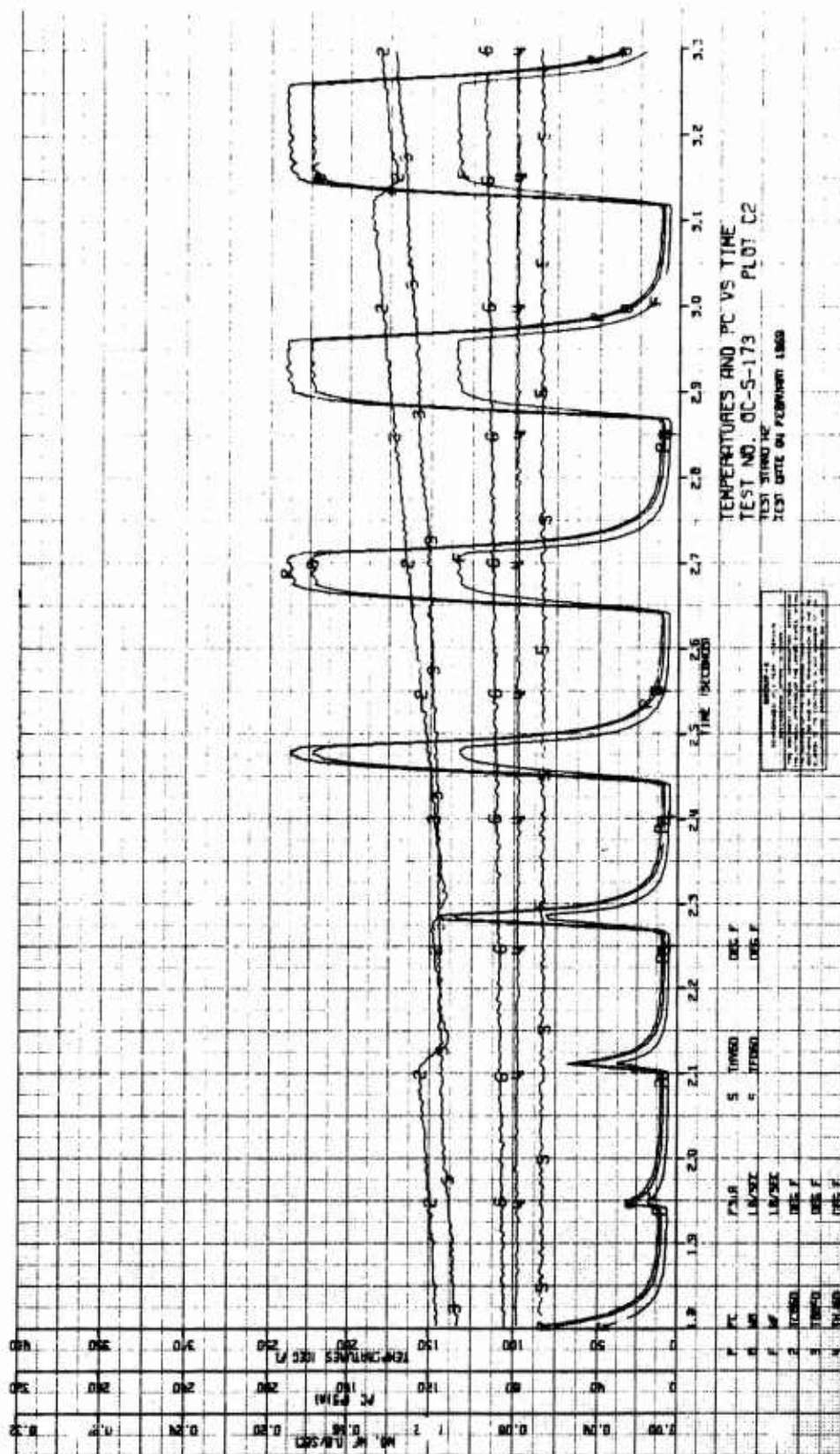


Figure 71. Pulse Data - Test No. OC-5-173 (u)
(Sheet 6 of 6)

CONFIDENTIAL

CONFIDENTIAL

Report AFRPL-TR-69-88

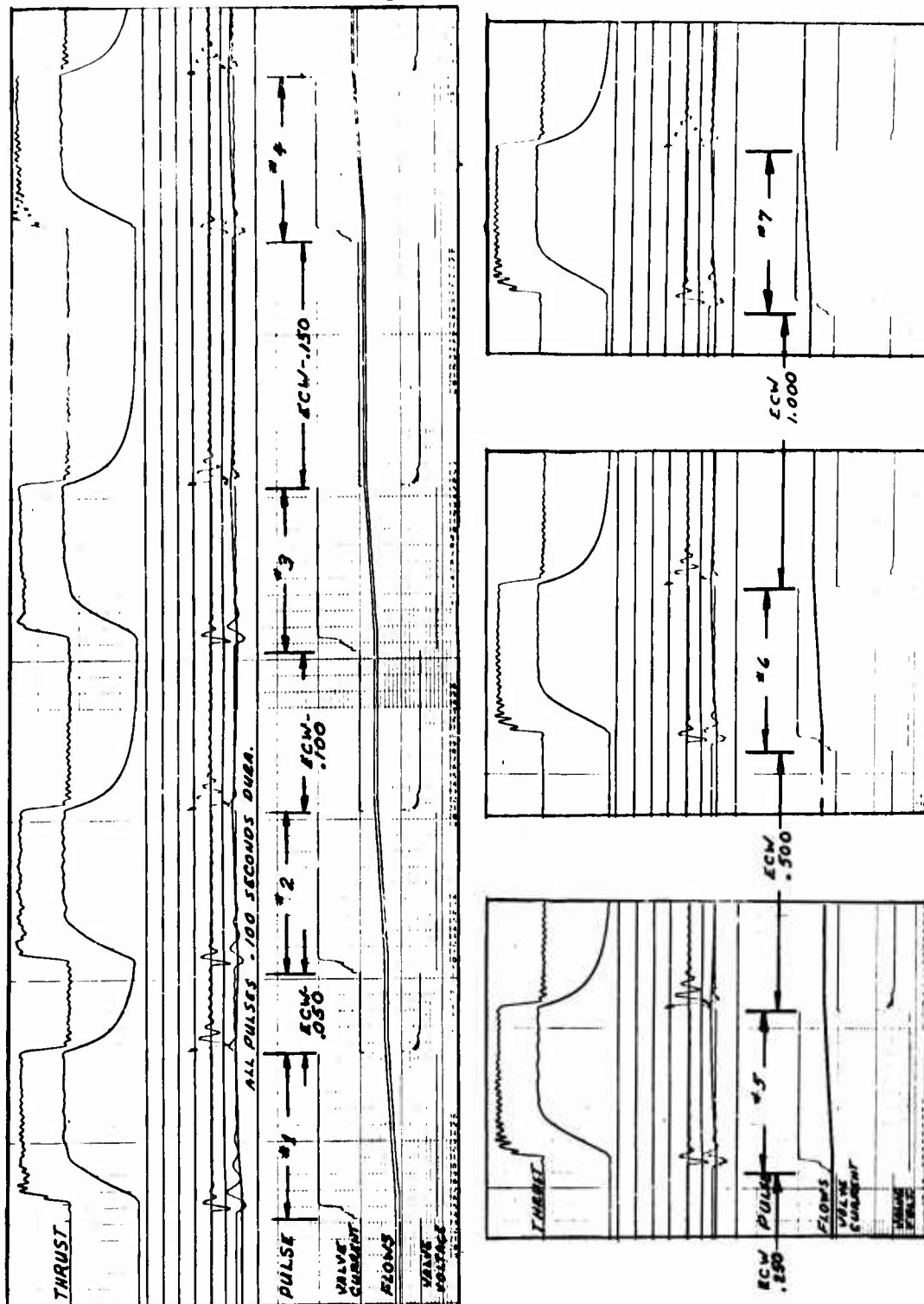


Figure 72. Oscillographs from Varying Electrical Coast Width

CONFIDENTIAL

(This page is Unclassified)

CONFIDENTIAL

Report AFRPL-TR-69-88

V, D, Altitude Test Evaluation (cont.)

0.004 sec difference represents the injector fill time for an evacuated manifold. The shutdown times were consistently 0.008 sec from electrical shutdown signal to 5% thrust. The temperature and flow data for the three tests are presented on Figures No. 73, No. 74, and No. 75.

c. Test Results

The final demonstration test series was conducted to provide a limited thermal, performance, and transient response characterization of the thruster. The thermal evaluation included both steady-state and multiple restart operation to subject the unit to the worst case thermal conditions. Tests were conducted at various chamber pressures and mixture ratios to demonstrate the capability of the thruster at off-design conditions. Pulse mode tests were conducted with pulse durations from 0.010 sec to 0.150 sec. The influence of previous coast duration was evaluated by testing with off-times between pulses ranging from 0.050 sec to 1.00 sec.

(1) Thermal

The wall temperatures measured during steady-state test -164 are shown on Figure No. 76 and compared with the pre-test predictions for the thrust chamber. Test -164 was conducted for a duration of 150 sec and thermal steady-state was achieved. The copper jacket after thrust chamber was designed using gas-side boundary conditions based upon wall temperature measurements from test -146. The measured test data showed wall temperatures in the jacketed portion of the thruster to be 250°F to 300°F lower than predicted. In addition, the radiation skirt temperature at the 4.5-in. axial station was approximately 200°F lower than in test -146. There are three possible explanations for these reduced wall temperatures; the film cooling flow rate in test -164 was higher than in test -146, the film cooling was more effective in test -164 because of reduced heat conduction from the throat, and reduced injector performance produced a lower energy release in the hot gas core with a consequent lowering of core gas and film cooling temperatures.

The multiple restart thermal evaluation was conducted as test -169. This test was terminated during the eleventh of a series of 10 sec duration pulses by a higher than anticipated chamber temperature rise rate. This condition was caused by a combustion instability which, as subsequently discussed, could have been triggered by a monopropellant reaction of the coolant fuel as it was heated by the forward chamber wall. The gas-side thermocouples at the forward end of the chamber were inoperative during this test. Outside surface temperatures and gas side temperatures 1.75-in. from the injector recorded temperatures of 480°F and 630°F, respectively, at

CONFIDENTIAL

(This page is Unclassified)

CONFIDENTIAL

Report AFRPL-TR-69-88

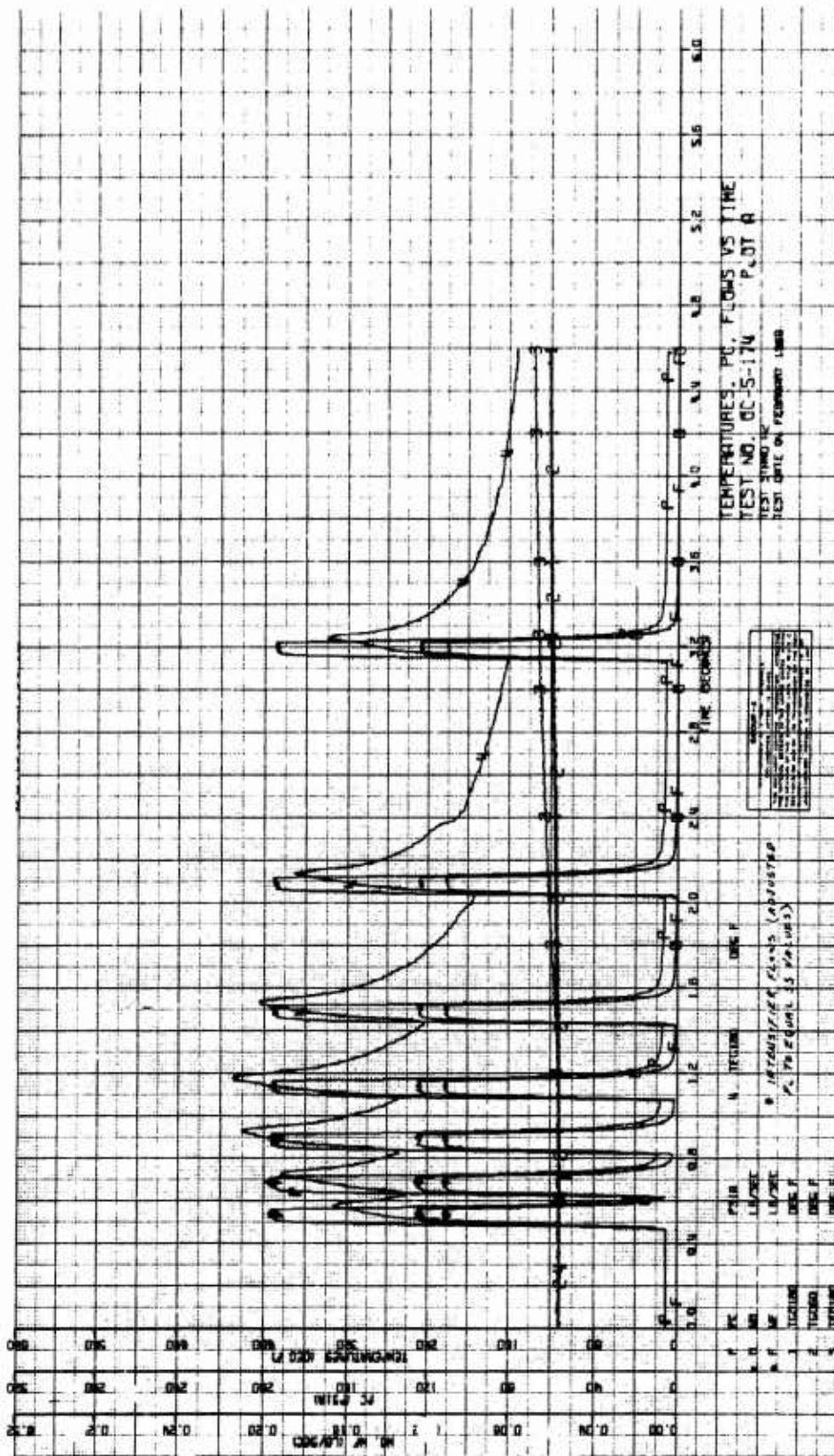


Figure 73. Pulse Data - Test No. OC-5-174 (u)
(Sheet 1 of 3)

CONFIDENTIAL

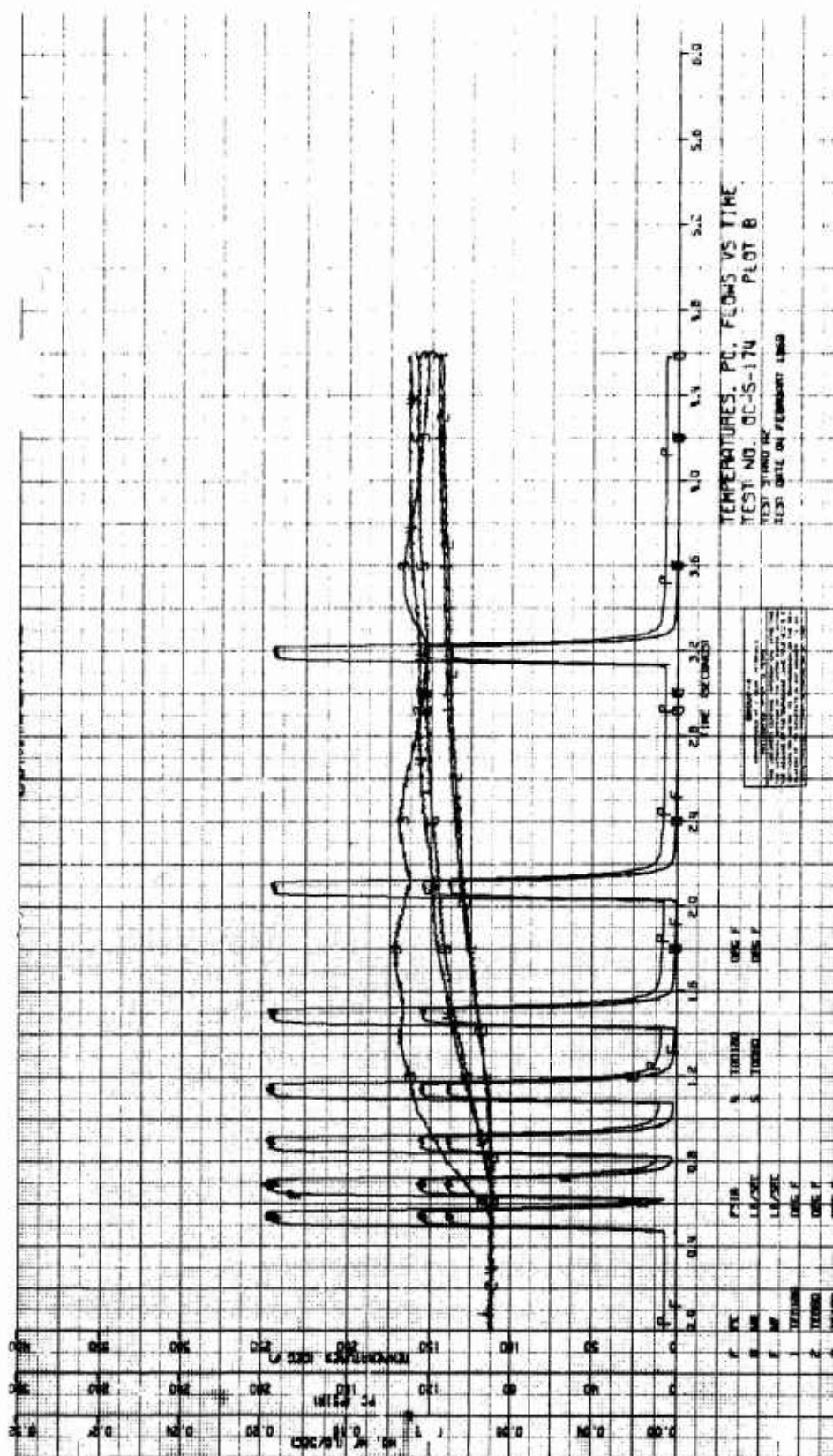


Figure 73. Pulse Data - Test No. OC-5-174 (u)
 (Sheet 2 of 3)

Report AFRPL-TR-69-83

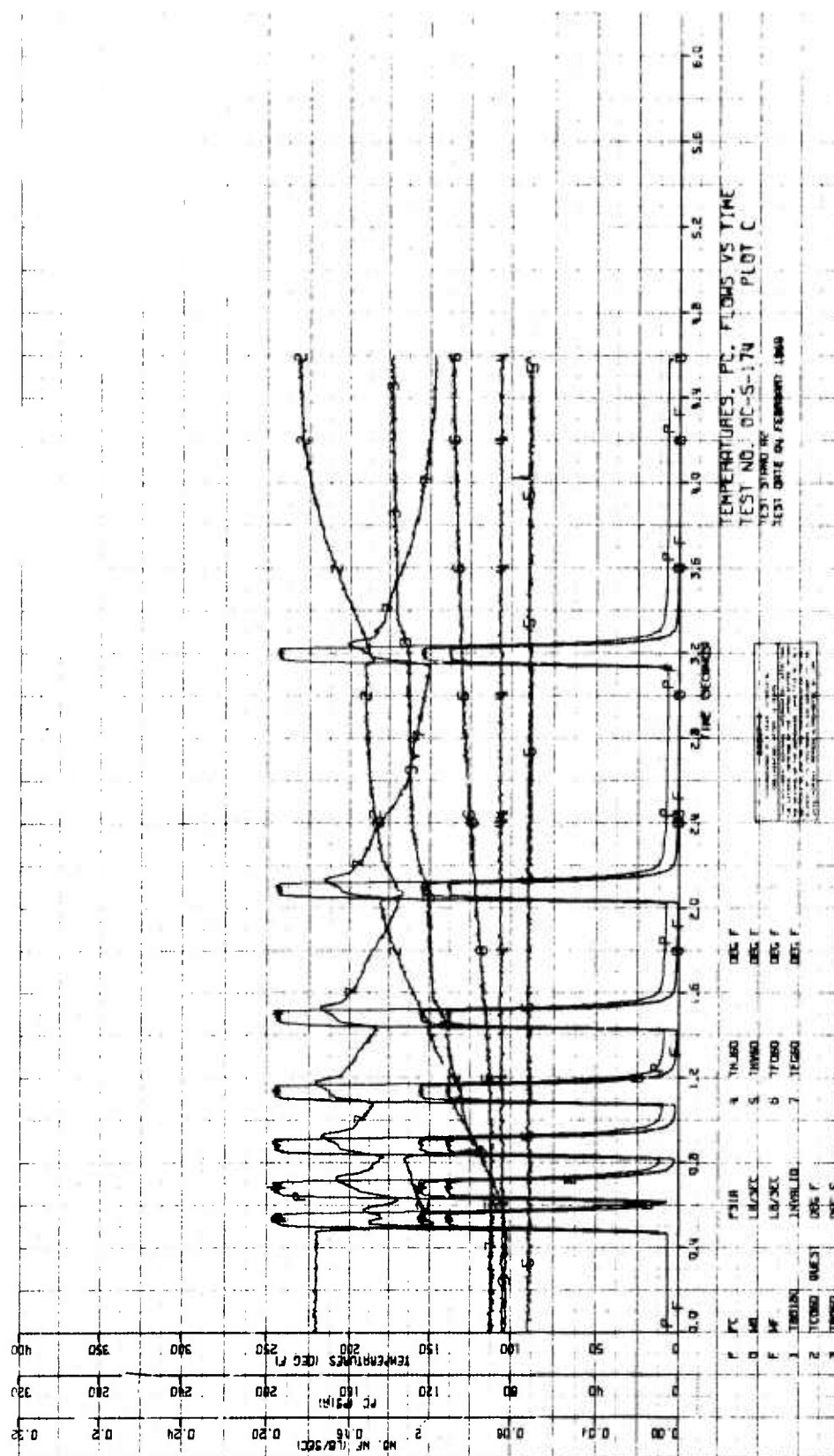


Figure 73. Pulse Data - Test NO. OC-5-174 (u)
(Sheet 3 of 3)

CONFIDENTIAL

Report AFKPL-TR-69-88

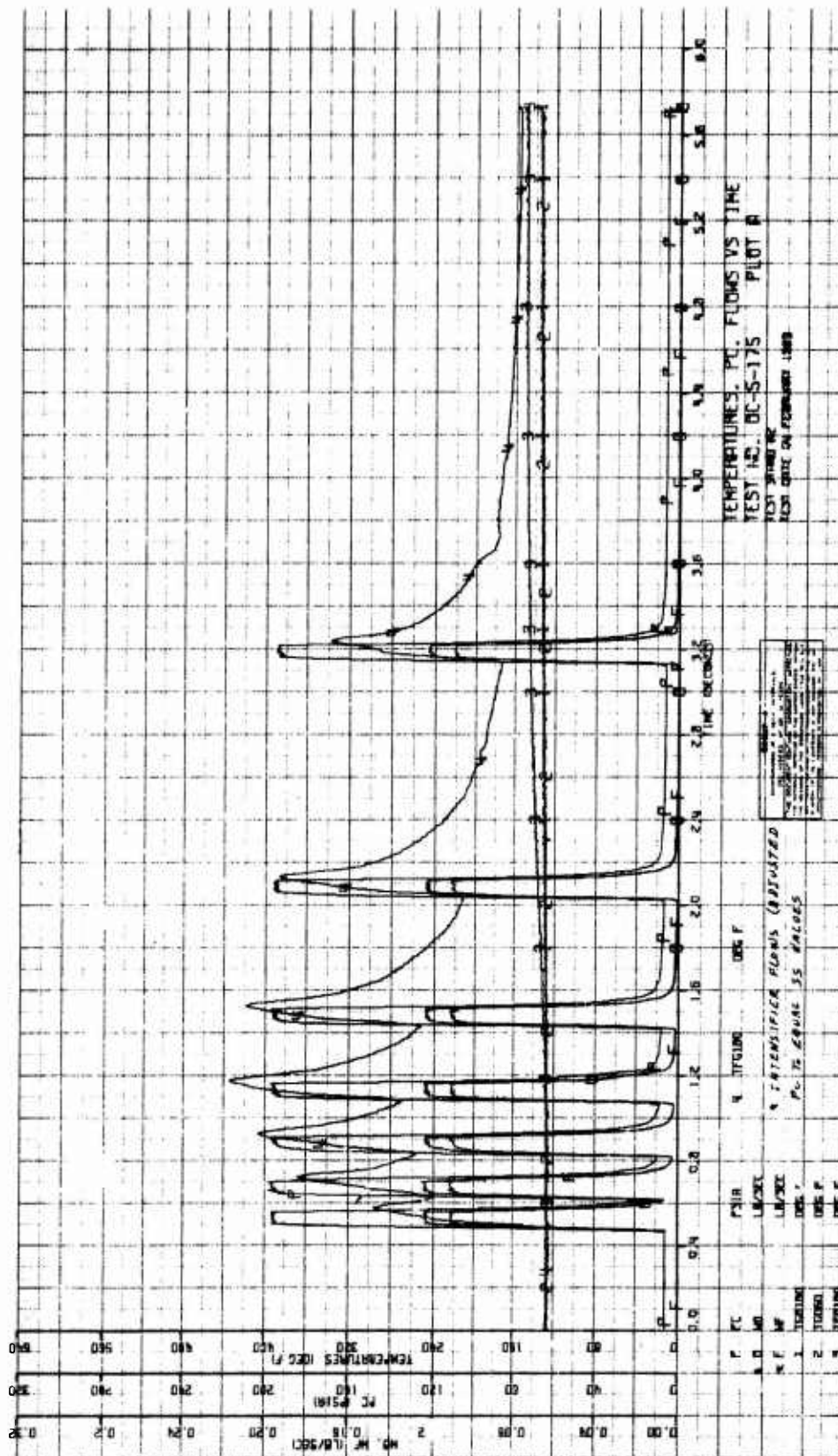
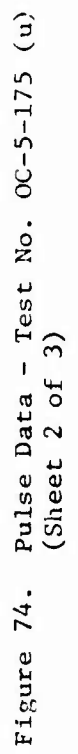


Figure 74. Pulse Data - Test No. OC-5-175 (u)
(Sheet 1 of 3)

CONFIDENTIAL

Report AFRL TR-69-88



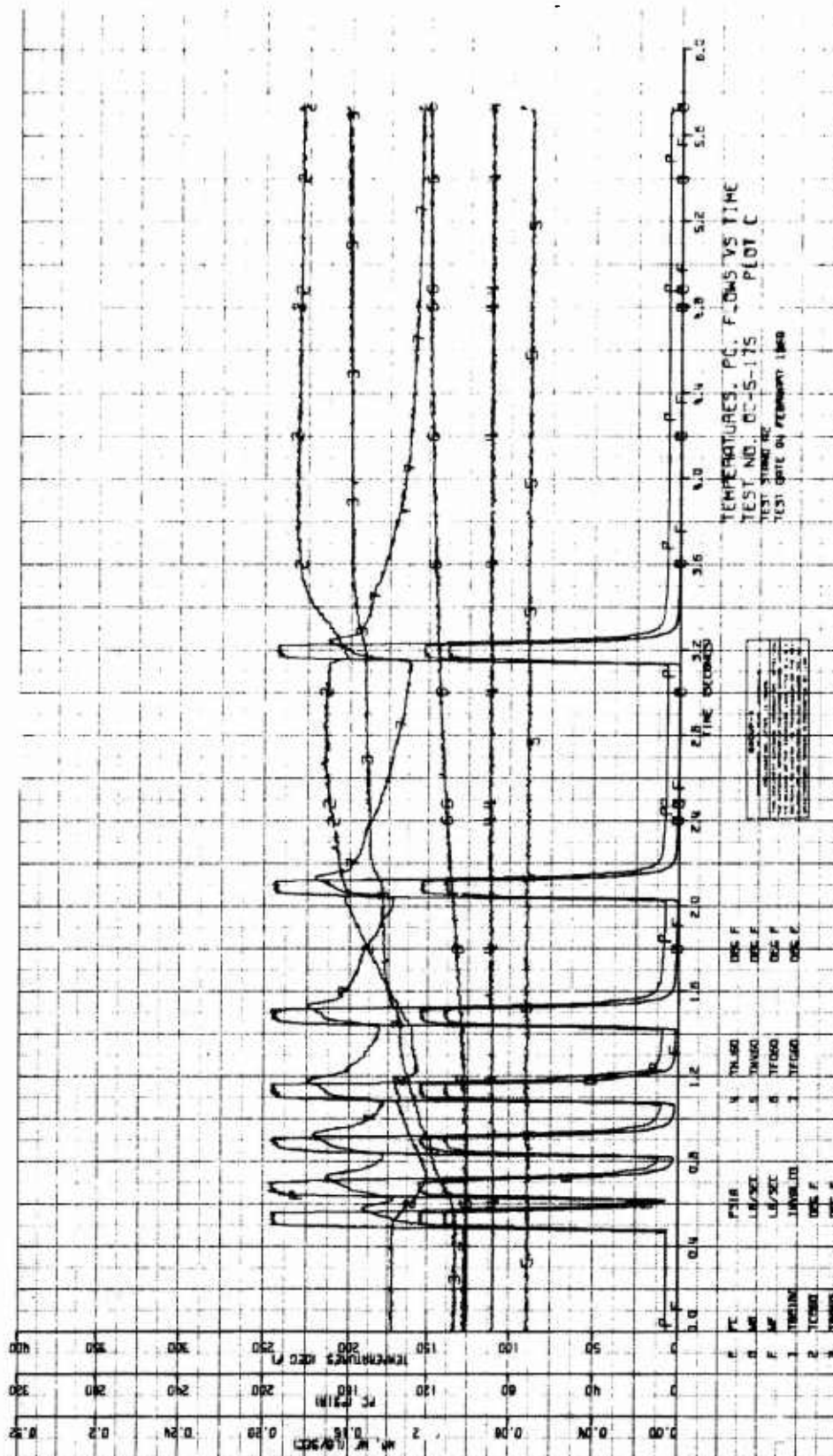
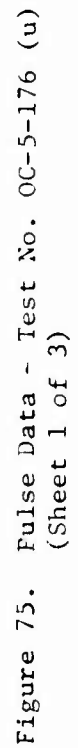


Figure 74. Pulse Data - Test No. OC-5-175 (u)
(Sheet 3 of 3)

Report AFRPL-TR-69-88



CONFIDENTIAL

Report AFRPL-TR-69-88

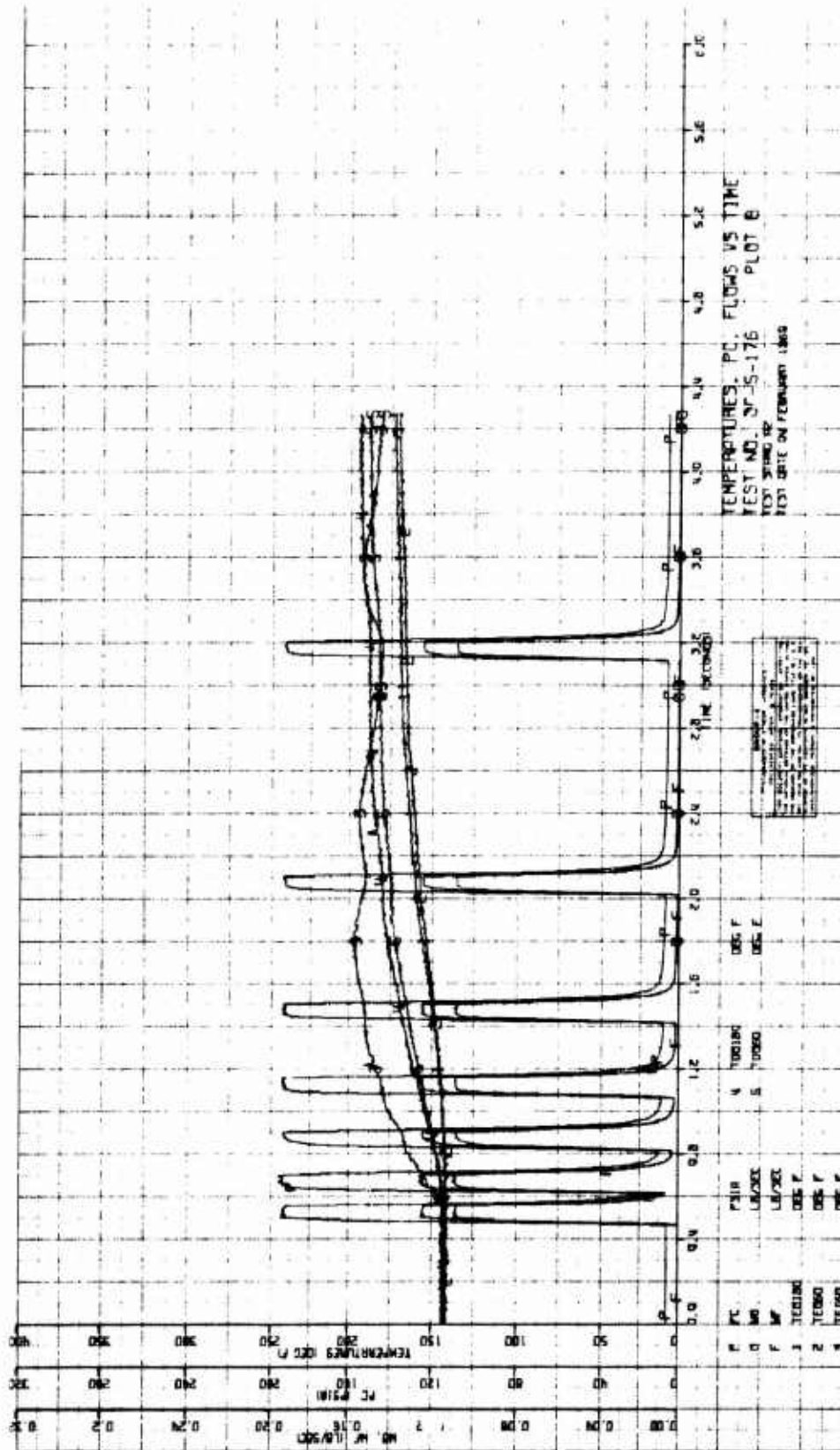
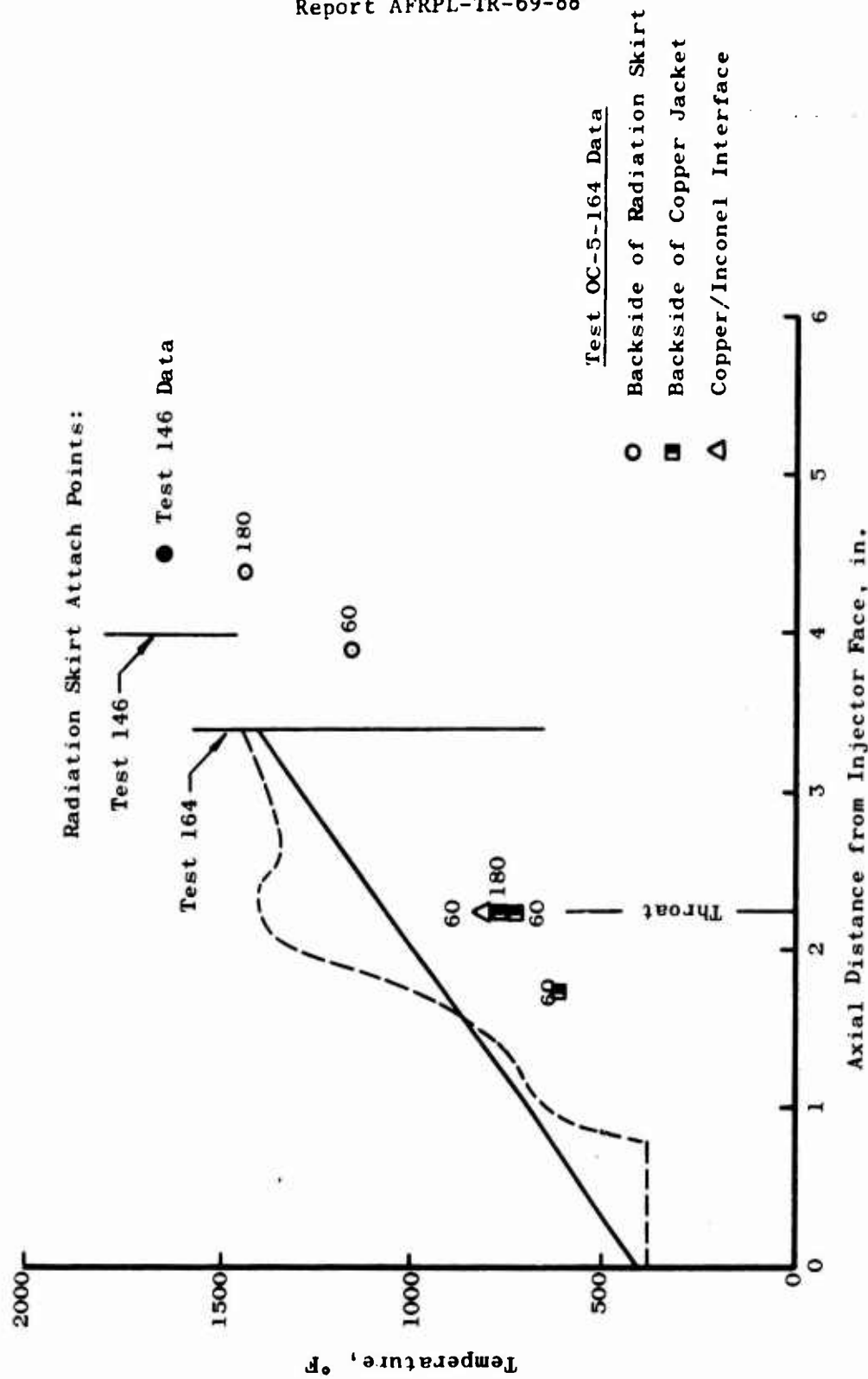


Figure 75. Pulse Data - Test No. OC-5-176 (u)
(Sheet 2 of 3)

CONFIDENTIAL

CONFIDENTIAL

Report AFRPL-TR-69-88



Measured and Predicted Wall Temperatures
75 lb PBPS Thrustor

CONFIDENTIAL

(This page is Unclassified)

Figure 76. Measured and Predicted Wall Temperatures

CONFIDENTIAL

Report AFRPL-TR-69-88

V, D, Altitude Test Evaluation (cont.)

the start of the test. These temperatures were indicative of the gas-side forward chamber temperature and provided a maximum allowable restart temperature for this configuration.

(U) The latest PBPS mission duty cycle is less severe thermally than the "worst case" thermal duty cycle of this demonstration series. The currently defined mission duty cycles can be achieved easily with this thruster design concept.

(2) Performance

(C) The performance of the PBPS engine, which was measured at sea-level and at simulated altitude conditions, is presented in this section. Fifty-five performance and thermal evaluation tests were conducted using the unbaffled HIPERTHIN injector and two different bimetallic chambers. Of these 55 tests, 20 were performed with a 1.4 area ratio chamber operating at sea-level pressures. Thirty-five tests were conducted in the altitude chamber with the 40:1 area ratio chamber. Thermal equilibrium was not achieved with the eight-element doublet injector; therefore, its performance was not considered to be meaningful for comparison purposes.

(U) Nitrogen tetroxide/monomethylhydrazine propellants were used in all tests at a nominal chamber pressure of 200 psia. The mixture ratio was 1.6 and the altitude thrust 75 lb. The combustion chamber length measured from injector face to throat plane was 2.25-in. and the contraction ratio was 5.9 (characteristic length, L^* , was 9.3).

(C) The HIPERTHIN injector tested in this program had baffles and a fuel film cooling circuit designed to allow independent coolant flow control and measurement. Later design modifications resulted in the fabrication of a new unit which eliminated the baffles. This unit subsequently was reworked to incorporate internal coolant flow control and to remove 0.020-in. from the injector face. The following is a summary of the unbaffled injector-bimetallic chamber configurations which were tested along with the pertinent performance parameters:

CONFIDENTIAL

CONFIDENTIAL

Report AFRPL-TR-69-88

V, D, Altitude Test Evaluation (cont.)

<u>Injector</u>	<u>Nozzle Area Ratio</u>	<u>Average % FFC</u>	<u>No. of Tests</u>	<u>Mixture Ratio Range</u>	<u>Specific Impulse Range</u>	<u>Coolant Flow</u>
Unbaffled HIPERTHIN	1.4:1	26-39	17	1.38-1.64	186.5-204.8	External
Unbaffled HIPERTHIN	40:1	37-46	9	1.37-1.74	257.7-281.8	External
Unbaffled HIPERTHIN	40:1	35-42*	5	1.30-1.65	267.7-246.4	Internal*
Unbaffled HIPERTHIN	40:1	30-35**	6	1.31-1.72	254-237	Internal**

*Estimate of internally fed film coolant flow.

**Coolant orifice size reduced and injector face machined back
0.020 in. for these tests.

(U) The above listing excludes short duration balance tests, pulse tests, and some tests wherein measured parameters appeared invalid.

(a) Sea-Level Tests

(C) Performance analysis of the sea-level tests of the unbaffled HIPERTHIN injector indicated that energy release efficiencies of approximately 91% to 92% were achieved. The percentage of measured specific impulse varied from 77% to 84.2%, dependent upon mixture ratio and coolant flow. All sea-level specific impulse values include a 3.5% nozzle curvature loss. At a nominal mixture ratio of 1.6 with approximately 35% fuel film coolant (FFC) 80% to 82% one-dimensional expansion (ODE) specific impulse was achieved. The percentage of characteristic exhaust velocity at these conditions was 83% to 85%. The performance achieved during the steady-state portions of the tests is shown on Figures No. 77 and No. 78 for percentage of specific impulse and percentage of characteristic exhaust velocity as a function of coolant flow. The data scatter was the result of problems encountered with flowmeters and thrust measurements.

CONFIDENTIAL

○ Test No. OC-5-()

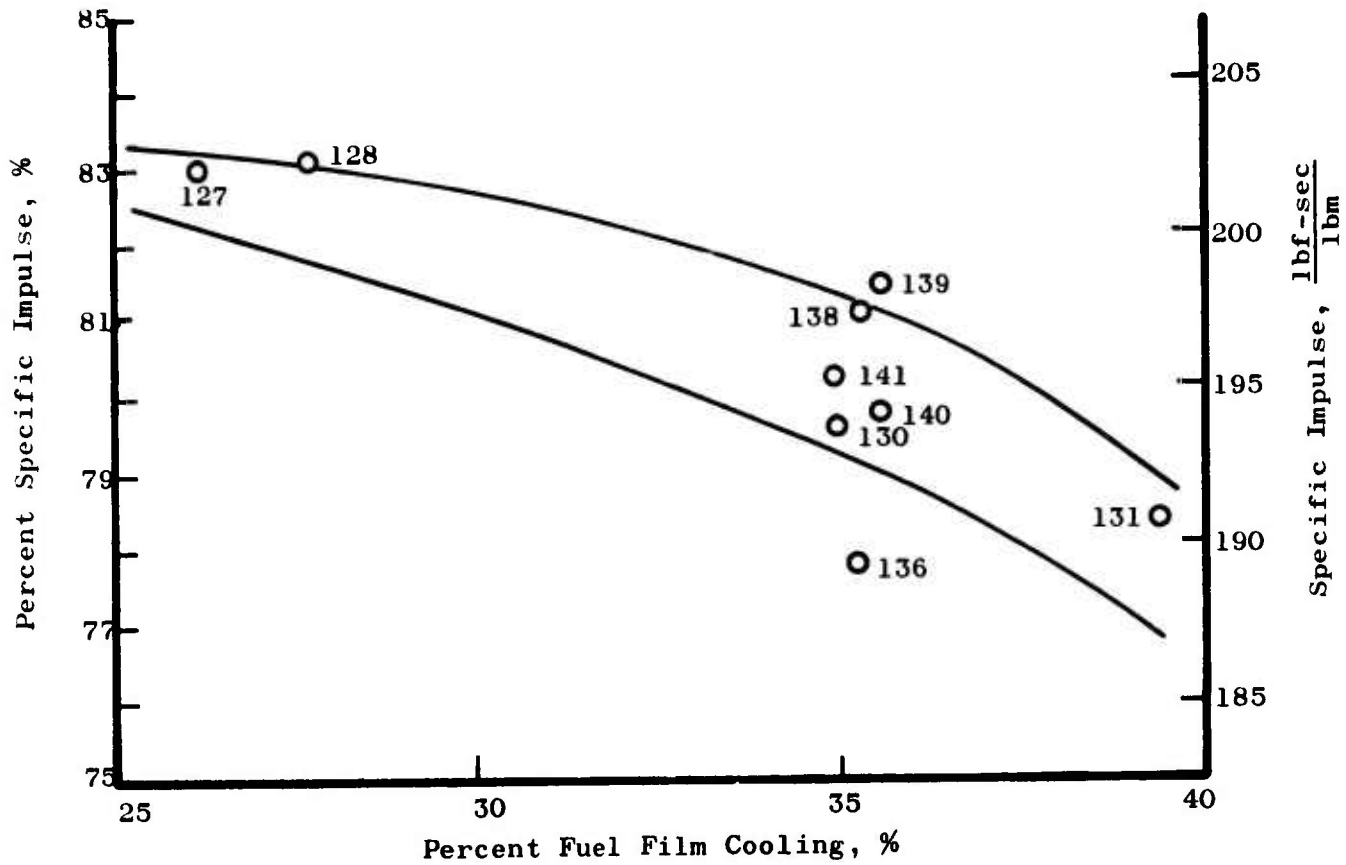


Figure 77. Effect of Percentage of Coolant Flow Upon Percentage of Specific Impulse (u)

CONFIDENTIAL

Report AFRPL-TR-69-88

● Test No. OC-5-()

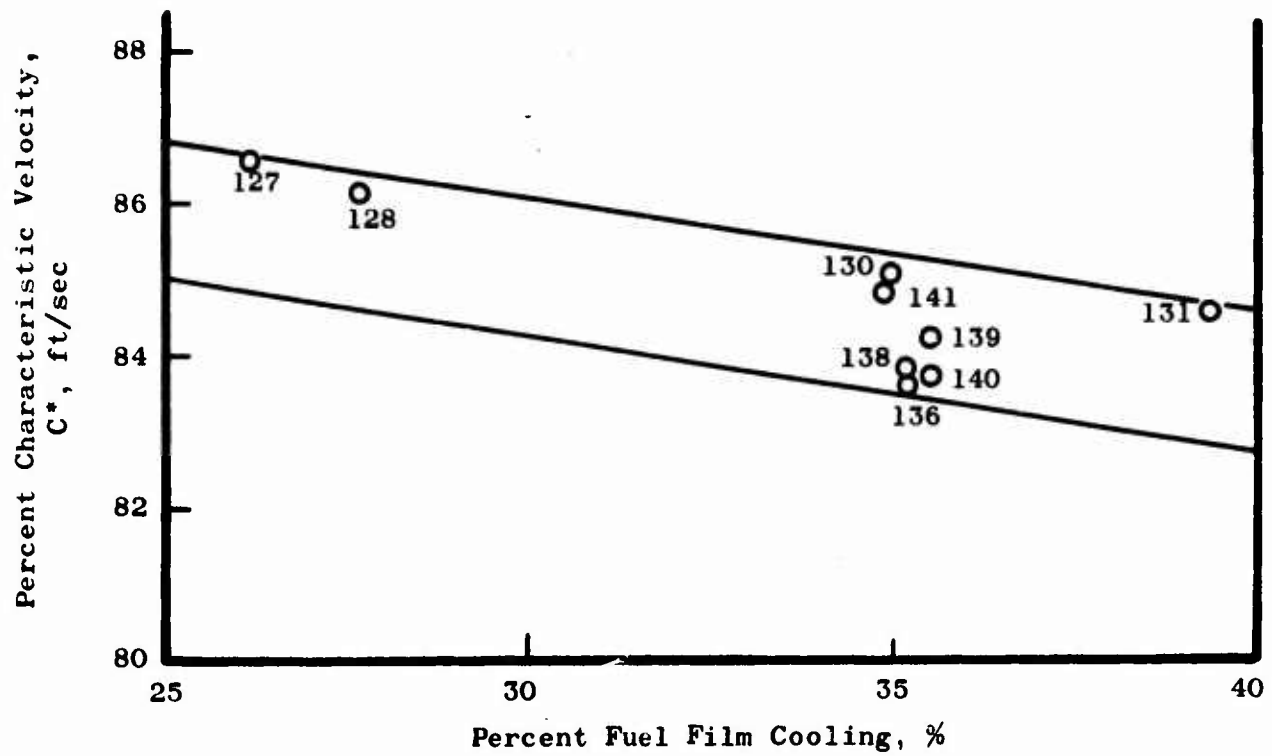


Figure 78. Effect of Percentage of Coolant Flow Upon Characteristic Velocity

CONFIDENTIAL

(This page is Unclassified)

CONFIDENTIAL

Report AFRPL-TR-69-88

V, D, Altitude Test Evaluation (cont.)

(b) Simulated Altitude Tests

(C) During testing at simulated altitude conditions, problems were encountered in determining the true vacuum thrust because the thrust stand used was designed for pulsing and altitude start evaluations. Heating of the test stand and changes in cell pressures during the long tests caused thrust shifts. For these reasons, it is believed that the best estimate of the altitude performance of the engine should be obtained by using the sea-level energy release (ER) efficiency, based upon measured thrust, and the known nozzle losses for the altitude nozzle. Using this technique, possible differences in ER between sea-level and altitude tests were assumed to be proportional to measured percentages of characteristic exhaust velocity changes. Using this method, delivered altitude specific impulse was found to be 267 ± 7 sec at a mixture ratio of 1.6 and 35% fuel film cooling. Variability in the measured percentage of characteristic exhaust velocity was caused by an erratic oxidizer flowmeter reading during some tests. Figure No. 79 shows the effect of mixture ratio on corrected vacuum specific impulse.

(C) Performance improvements for this injector can be achieved by reducing contraction ratio (based upon the injector area) to provide a finer injector pattern. The contraction ratio used was selected to meet the requirements of the doublet injector. Energy release efficiencies of 98% or better have been demonstrated using HIPERTHIN injectors in low contraction ratio, 2-in. long chambers operated with N₂O₄/A-50 propellants at 500 psig. This shows that an additional increase in altitude impulse could be obtained by operating at a mixture ratio of less than 1.6.

(3) Stability

(U) All testing in this program was conducted with a high-frequency pressure transducer located in the oxidizer feed system upstream of the valve. This technique allowed the acquisition of combustion stability data without using chamber-mounted transducers, which disrupt boundary flow and result in erroneous chamber thermal data. Tests have been conducted in other Aerojet-General programs with high-frequency transducers located both through the chamber wall and in the propellant feed system. These showed that the same oscillation frequencies were recorded by each transducer during unstable operation. The amplitudes recorded by the feed-system-mounted transducer were somewhat lower than those recorded at the chamber.

(U) During test -169, which was a multiple restart series to evaluate chamber heating, excessive chamber wall temperatures were noted during the eleventh of the fifteen pulses scheduled. Each pulse was 10 sec on and 5 sec off. Review of the high-frequency records from this

CONFIDENTIAL

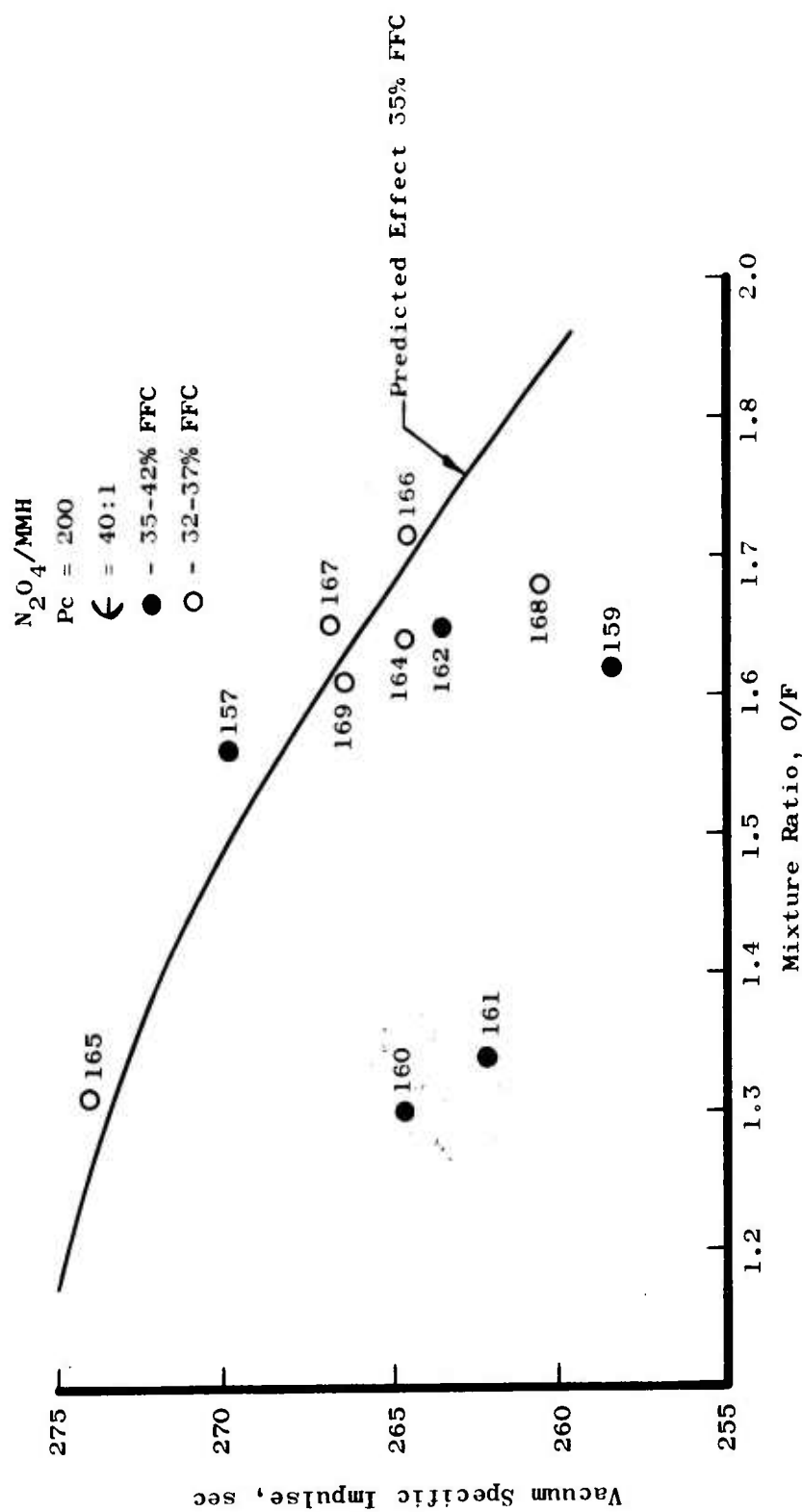


Figure 79. Effects of Mixture Ratio Upon Corrected Specific Impulse (u)

CONFIDENTIAL

Report AFRPL-TR-69-88

V, D, Altitude Test Evaluation (cont.)

test showed the presence of an intermittent 20 KHz oscillation during the start transients of pulses 5, 6, 7, 9, and 10 which lasted for a maximum of 0.063 sec. During pulses 1 through 4 and on pulse No. 8 no oscillations were observed. During pulse 11, the 20 KHz oscillation was sustained for 4.5 sec, which increased the chamber wall temperature to 1600°F causing a thermal shutdown. The calculated frequency of the first tangential mode for this chamber design is 20 KHz. The amplitude of the oscillation ranged from 86 psi during the early portion of the test to 50 psi during steady-state operation.

The combustion gases in the vicinity of the chamber wall are fuel-rich while those in the core are oxidizer-rich. The performance of the unit during stable operation indicates that the fuel-rich gases in the boundary are combusted as a monopropellant.

The steady-state performance data recorded during pulse 11, which was unstable, showed the characteristic exhaust velocity to be 18% higher than was recorded during the earlier stable pulses. This indicates that the entire flow of oxidizer and fuel were reacting as a bipropellant. Based upon these factors, the following mechanism is judged to be the cause of the instability.

The rapid vaporization and improved mixing of the fuel-rich boundary with the oxidizer-rich core is precipitated by the hot wall condition during ignition. This improved combustion results in a higher energy release at the injector periphery which has a destabilizing effect. Once the instability is established for sufficient duration, the chamber wall heats at a rate in excess of that required to rapidly vaporize the incoming propellant. Thus, the instability promotes rapid mixing of the barrier as well as the core and becomes a self-sustaining process.

The implication of these results is that this engine system must include a stabilizing device (i.e., baffles or acoustic absorbers) if it is to operate in an on-off pulse mode which increases chamber wall temperatures as observed during this test.

E. CONCLUSIONS AND RECOMMENDATIONS

The bipropellant ACS engine demonstrated a duration capability in excess of 1000 sec of continuous as well as fast response pulsing operation. The engine pulsing operation demonstrated its capability for performing the expected PBPS mission attitude control duty cycle. The fast response of the engine provides reproducible bit impulses with electrical pulse widths as low as 0.010 sec.

V, E, Conclusions and Recommendations (cont.)

(C) The combination of the conductively-cooled, bimetallic combustion chamber, the HIPERTHIN injector and the fast response MOOG torque motor valve provides a thruster offering some unique advantages.

1. Envelope

The combustion of HIPERTHIN injector and the combustion chamber used in this program provide the capability for producing good engine performance utilizing a short chamber equivalent length (injector-face-to-throat). This results because of the fine propellant atomization and injection density of the injector.

2. Rugged Design

The engine design provides a thruster which is completely insensitive to handling shocks, external loads, vibration, and dents. The assembled unit has the basic structural capability of the parent malleable metals involved. The absence of phenolics, coatings, or exposed propellant passages in the design eliminates any concern for functional capability brought about by the possible mishandling, shock, dents and scratches that normally occur during operational use.

3. Unlimited Life

The conductive film cooling concept, similar to that applied in beryllium chambers, is utilized in the bimetallic chamber. This bimetallic design does not have the operational thermal cycle limitations identified with the beryllium designs.

(C) The engine test program demonstrated what compromises had to be made in design to achieve a universal thruster. The engine fuel film coolant fraction was identified upon the basis of an unlimited mission duty cycle within a 900 sec time period. Therefore, the coolant needed for continuous operation within that time period was identified as ~38%, which reduced the delivered performance of the engine to 271 sec of specific impulse.

(U) The final demonstration tests of the engine resulted in an apparent performance degradation which was not associated with the design. The engine had consistently delivered performance equivalent to the design goal until the injector rework was accomplished to incorporate the fuel film coolant as an internal flow circuit. During that rework, the injector face was machined back approximately 0.010-in. to remove surface irregularities. This affected the oxidizer orifice impingement characteristics and reduced the effectiveness of the bipropellant mixing.

CONFIDENTIAL

Report AFRPL-TR-69-88

V, E, Conclusions and Recommendations (cont.)

For the optimum application of this engine concept, it would be beneficial to more specifically identify the expected duty cycle and provide a fuel film coolant for that expected thermal load. This would result in additional performance capability because the coolant fraction could be reduced.

Page 184

CONFIDENTIAL

(This page is Unclassified)

UNCLASSIFIED

Report AFRPL-TR-69-88

SECTION VI

POSITIVE EXPULSION PROPELLANT TANK DEMONSTRATION

A. OBJECTIVE

The Advanced PBPS Subsystem Development Contract (AF 04(611)-11614 (Ref. 1)) satisfactorily demonstrated the feasibility of two primary subsystems required for an advanced propulsion system of a size equivalent to that needed for the intended weapon system. These demonstrations included the concept evaluation of the ring-stabilized propellant expulsion tank and the development of a monopropellant N_2H_4 generator subsystem which provides hot gas for the expulsion process. The re-direction of this program (Contract F04611-67-C-0095) added the requirement to continue the development of the ring-stabilized expulsion tank through the fabrication of lightweight propellant tank assemblies and the integration of the two subsystems to demonstrate hot gas expulsion of the propellants (N_2O_4 and MMH) from lightweight tank assemblies.

For this demonstration, the components fabricated and developed under Contract AF 04(611)-11614 were utilized. The propellant expulsion tanks were provided by the subcontractor, Arde, Inc. These tanks were a welded 300 series stainless steel construction which then was stretched to the final conospheroid shape and size at cryogenic temperatures to achieve a strength to weight ratio equivalent to titanium. The tank design is shown on Figure No. 80 and the demonstrated characteristics of a lightweight tank are listed on Table XII. A complete lightweight tank assembly is shown on Figure No. 81. The assembly sequence of an expulsion bladder into a lightweight tank, including water expulsion and burst testing is illustrated on Figure No. 82.

The positive propellant expulsion is provided by an integral steel expulsion bladder welded into the tank at the girth weld joint. The controlled reversal of the thin bladder shell provides the positive expulsion of the propellant. The bladder has wire rings brazed to the pressurant side of the one-piece formed steel shell to maintain stability of the reversal process and provide a single cycle capability. A bladder is shown undergoing a satisfactory reversal process in the sequential photographs of Figure No. 83.

The feasibility of the ring-stabilized bladder concept in the large conospheroid shapes was initially demonstrated under the AF 04(611)-11614 contract. Development problems with the fabrication of the bladder shells in that program precluded the completion of the fabrication and demonstration of the lightweight propellant tanks through hot gas expulsion of N_2O_4 and MMH. Therefore, this effort was added as a primary objective of this program and the propellant expulsion demonstrations of both N_2O_4 and MMH over simulated PBPS duty cycles were successfully accomplished. The propellant tanks were fabricated from expulsion bladder shells and tank components that were residual to the AF 04(611)-11614 contract.

UNCLASSIFIED

UNCLASSIFIED

Report AFRPL-TR-69-88

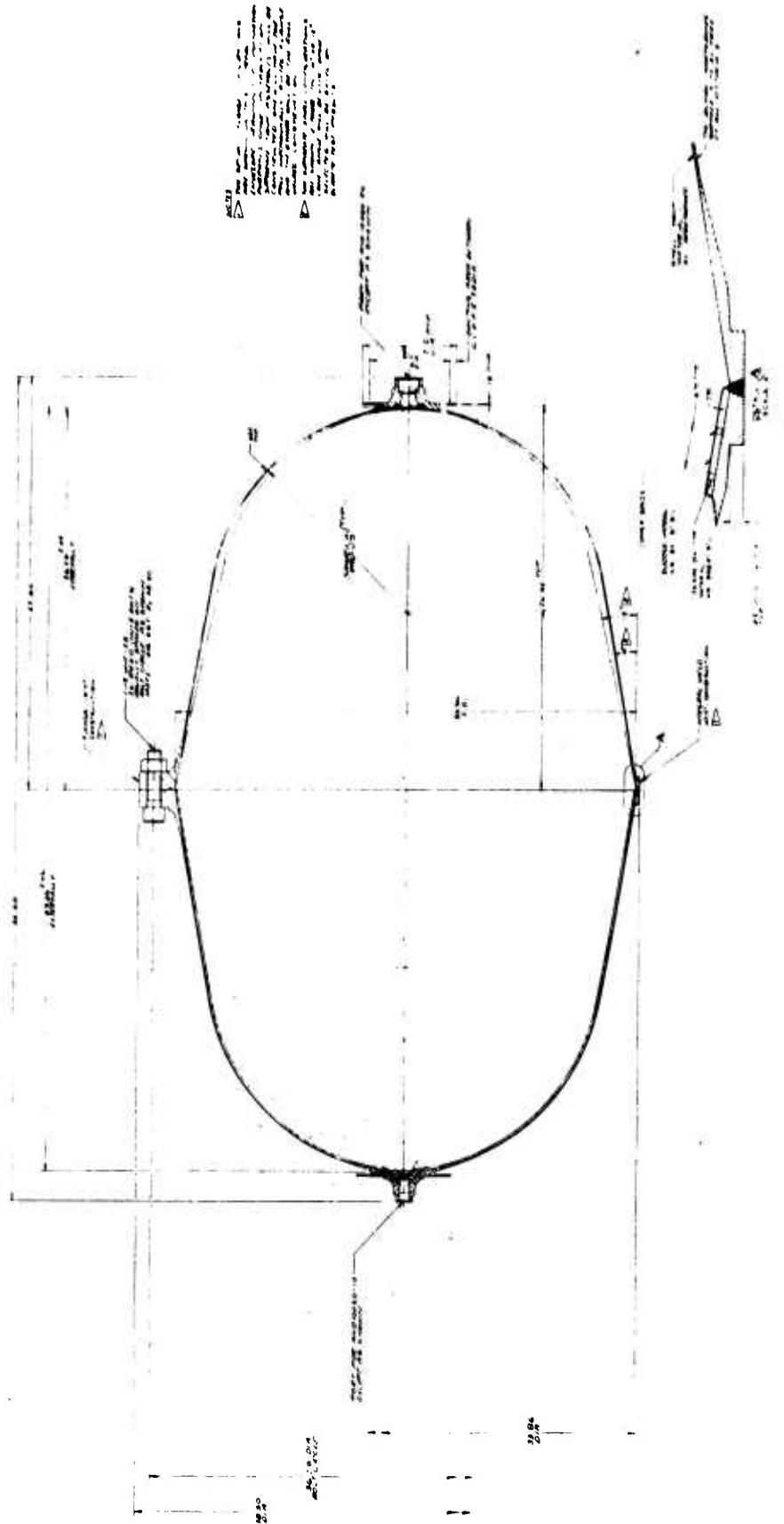


Figure 80. Tankage/Expulsion Subsystem Interface Drawing

UNCLASSIFIED

CONFIDENTIAL

Report AFRPL-TR-69-88

TABLE XII

PROPELLANT EXPULSION TANK DESIGN CRITERIA (U)

	<u>Design Point</u>	<u>Range</u> <u>Parametric Study</u>
Nominal Working Pressure, psia	350	200 -- 800
External (crush) Differential Pressure, psia	14.7	
Safety Factor - Internal Pressure	1.25	
Safety Factor - External Pressure	1.33	
Effective Pressurant Temperature, °F	300°F	200 -- 800°F
Configuration	Conospharoid L/D = 1.6 Taper = 10°	L/D = 0.5 -- 2.0 (including sphere)
Tank Volume (without bladder), in. ³	31,213	1500 -- 50,000
Propellants to be Stored	Nitrogen Tetroxide	Monomethyl- Hydrazine
System Storage Temperature, °F	+20 -- +150	
System Operational Temperature, °F	+40 -- +120	
Storage Life, goal	10 years	
Ambient Pressure, psia	0 -- 15	
Shock	To be defined	
Acceleration (sustained non operating)	14 g perpendicular to tank longitudinal axis -- 33 g along plane of tank axis	
Vibration (sweep) Random, g ² /cps	0.0015--0.05 at 12 db/octave 0 - 35 cps 0.05 35 - 200 cps 0.05--0.16 at 12 db/octave 200 - 300 cps 0.16 300 - 1500 cps	
Sine, g-rms	1.4 0 - 300 cps 3.0 300 - 1500 cps	
Tanks have a maximum of 10% ullage and are unpressurized during launch		
Helium Leakage Requirements	1 x 10 ⁻⁶ scc/sec	

CONFIDENTIAL

CONFIDENTIAL

Report AFRPL-TR-69-83



Figure 81. Flightweight Propellant Expulsion Tank

Page 188

CONFIDENTIAL

(This page is Unclassified)

UNCLASSIFIED

Report AFRPL TR-69-38

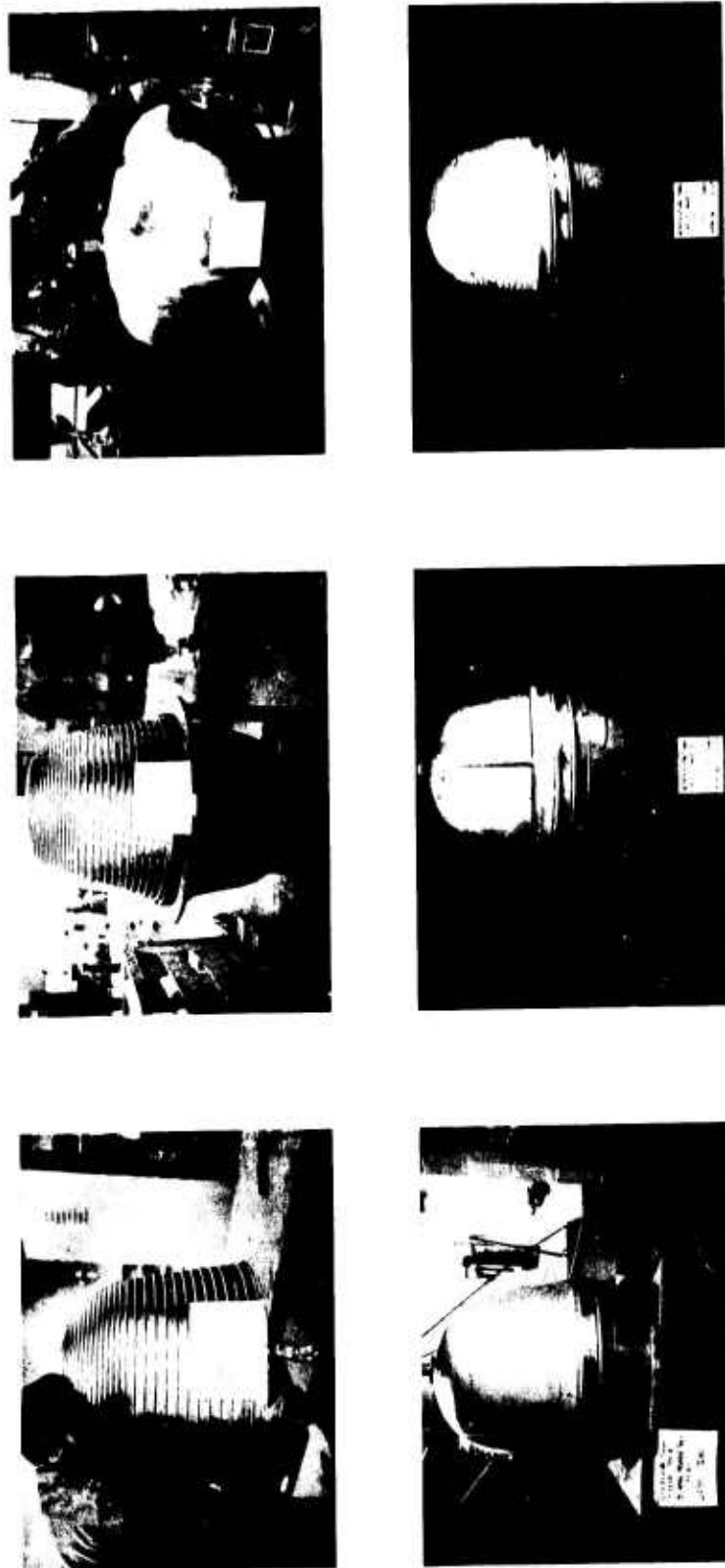


Figure 82. Full-Scale Welded Tank Fabrication and Test

UNCLASSIFIED

UNCLASSIFIED

Report AFRPL-TR-69-88

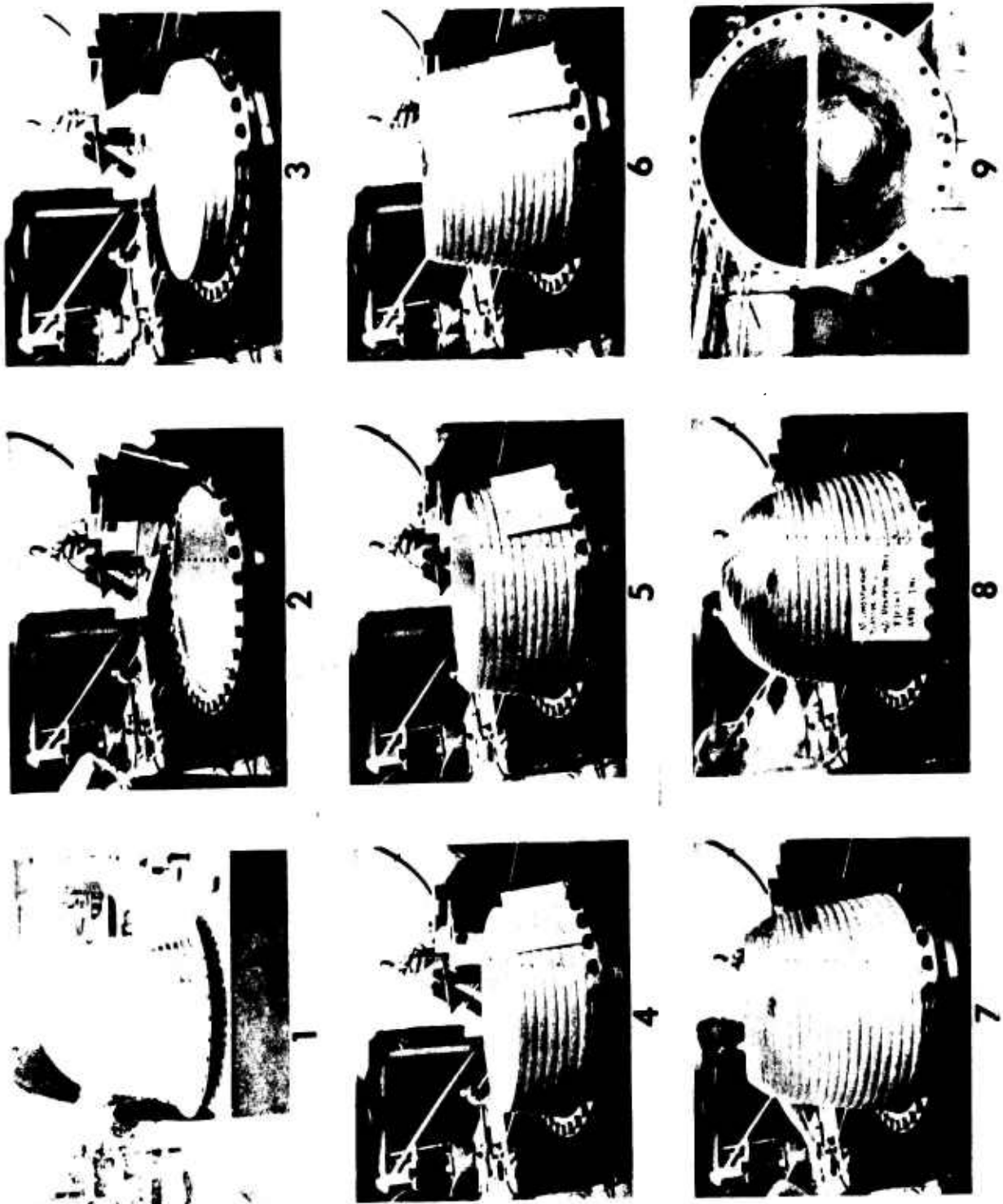


Figure 83. Conospheroid Diaphragm Reversal Test, S/N 61 Bladder

UNCLASSIFIED

UNCLASSIFIED

Report AFRPL-TR-69-88

VI, A, Objective (cont.)

A workhorse pressure switch and solenoid valve control were used in the bootstrap gas generator subsystem to provide a regulated hot gas supply for the propellant expulsion tests. This subsystem also was developed under the AF 04(611)-11614 contract and was originally supplied by the Hamilton Standard Division of United Aircraft.

B. EXPULSION BLADDER DEVELOPMENT

1. Contract AF 04(611)-11614 Bladder Development

The conospherical shape of the positive expulsion bladder resulted in a major fabrication problem during the AF 04(611)-11614 contract regarding the production of the one-piece, steel shells used to make the large-size bladders. The resultant shell forming process was a combination of deep drawing a stainless steel sheet to produce a shell preform and the subsequent hydraulic stretch of that preform into a female die to attain the desired configuration of the shell. This sequence of shell forming resulted in a non-uniformity of shell thickness. The girth or flange area shell thickness was approximately 0.027-in. The uniformity of thickness reduced to a minimum of 0.010-in. to 0.011-in. at the area of transition from the cone to the hemispherical shape. Then, the shell thickness increased to 0.019-in. at the dome apex.

Changes in the bladder shell configuration were identified and incorporated to enhance the probability of the rim roll mode of the bladder during reversal as shown on Figure No. 83. The following changes to the expulsion bladder were made to minimize the possibility of bladder shell collapse in the thin area of the shell at the transition from the cone to the hemisphere.

- Electropolish the diaphragm shell to a thickness of 0.016-in. to 0.018-in. in the critical flange/cone region
- Incorporate a reverse fold "gutter" in the shell at the flange to aid in initiating a rim-roll mode of actuation
- Place the first central wire as close to the gutter as possible
- Provide control wires of 0.188-in. diameter in the region from the flange through the transition of the cone to the hemispherical dome
- Provide 0.156-in. diameter control wires on the dome

UNCLASSIFIED

UNCLASSIFIED

Report AFRPL-TR-69-88

VI, B, Expulsion Bladder Development (cont.)

A successful controlled reversal was demonstrated with this configuration (see Figures No. 82 and No. 83). The reversal of S/N 71 shown on Figure No. 84 was not a full rim-roll mode; however, this test was considered successful because the reversal process was controlled by the wire rings.

2. Expulsion Bladder Fabrication

In this program (Contract -0095), the subcontractor, Arde, Inc., was required to deliver nine flanged bladders for use with the two flanged workhorse tanks for expulsion and subsystem integration testing. In addition, four bladders were required for the four flightweight propellant tank assemblies.

The first six flanged bladders received at Aerojet-General were Serial Nos. 64, 65, 67, 69, 74 and 75. These units were fabricated to the same configuration as the S/N 61 and S/N 71 bladders tested under the prior contract and are shown on Figures No. 83 and No. 84, respectively.

The first bladder tested at Aerojet-General was S/N 67 and this test verified that an additional step had to be taken to provide control of the reversal process. The test was a water expulsion one conducted within a partial acrylic tank so that the reversal process could be observed. The test failed when the bladder collapsed in the thin area of the shell and subsequently reversed with the apex roll mode. The wire spacing had not been designed for an apex roll mode; therefore, the wire subsequently interfered, buckled, and lost control of the shell reversal. Two bladder fabrication changes were implemented to provide an additional margin of shell strength so that the localized buckling in the thin area would be minimized. The following changes were evaluated.

a. Increased Diameter Control Wire Evaluation

An increase in the control wire diameter on bladder S/N 83 was evaluated by the subcontractor, Arde, Inc., to ascertain if sufficient structural margin could be provided to effectively control the reversal process. The S/N 83 bladder was fabricated and delivered to Aerojet-General with the control wire diameters and spacing shown on the right half of the bladder shell cross-section depicted on Figure No. 85. The configuration of the six, flanged bladders previously delivered for Aerojet-General testing is shown on the left half of Figure No. 85.

The reversal of S/N 83 bladder with the 0.250-in. diameter wires was not successful because the shell collapsed again in the thin zone and an apex roll-mode resulted. The test was terminated when control wire interference resulted.

UNCLASSIFIED

UNCLASSIFIED

Report AFRPL TR 69-38

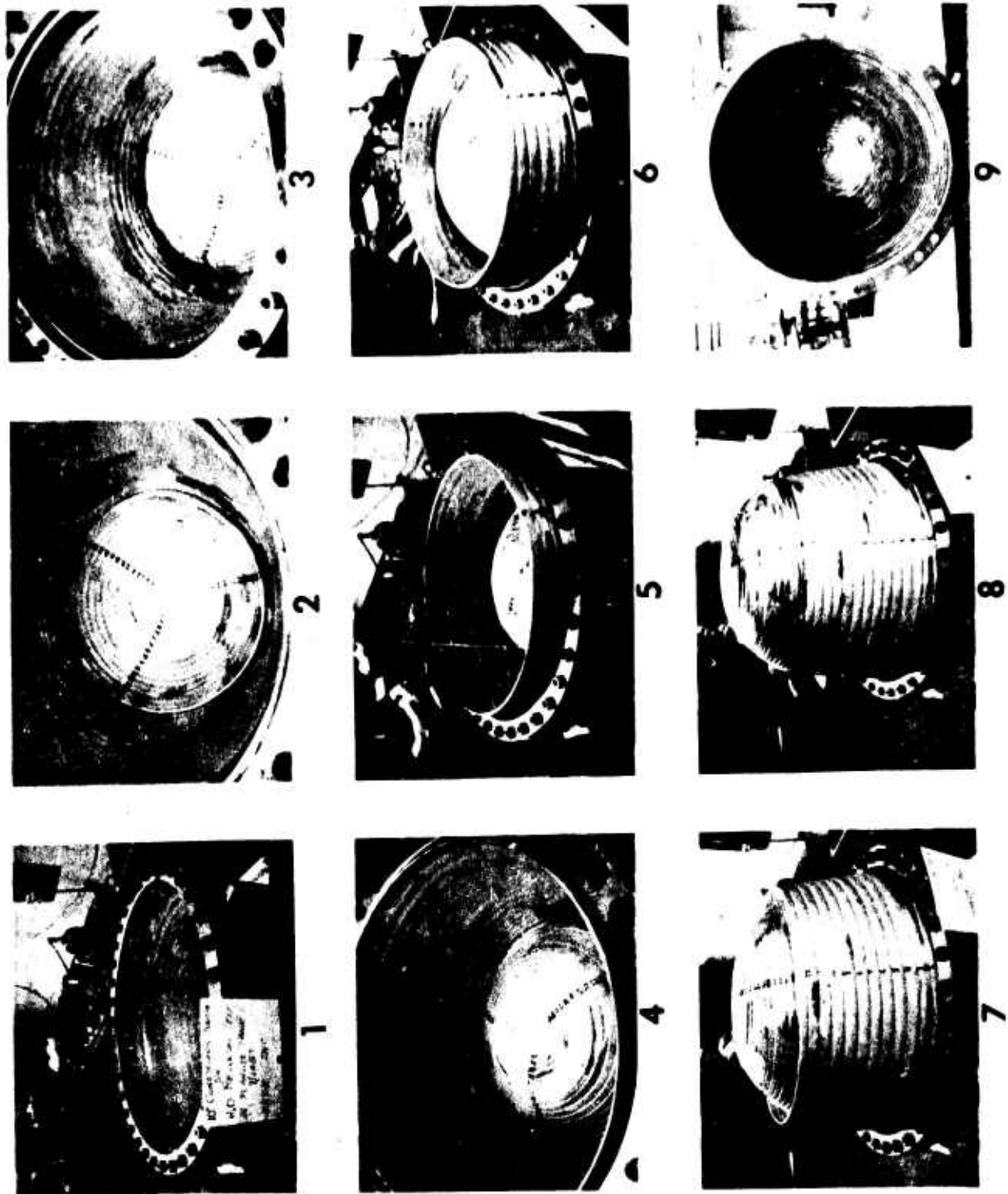


Figure 84. Conospheroid Diaphragm Reversal Test, 8 X 71 Model

UNCLASSIFIED

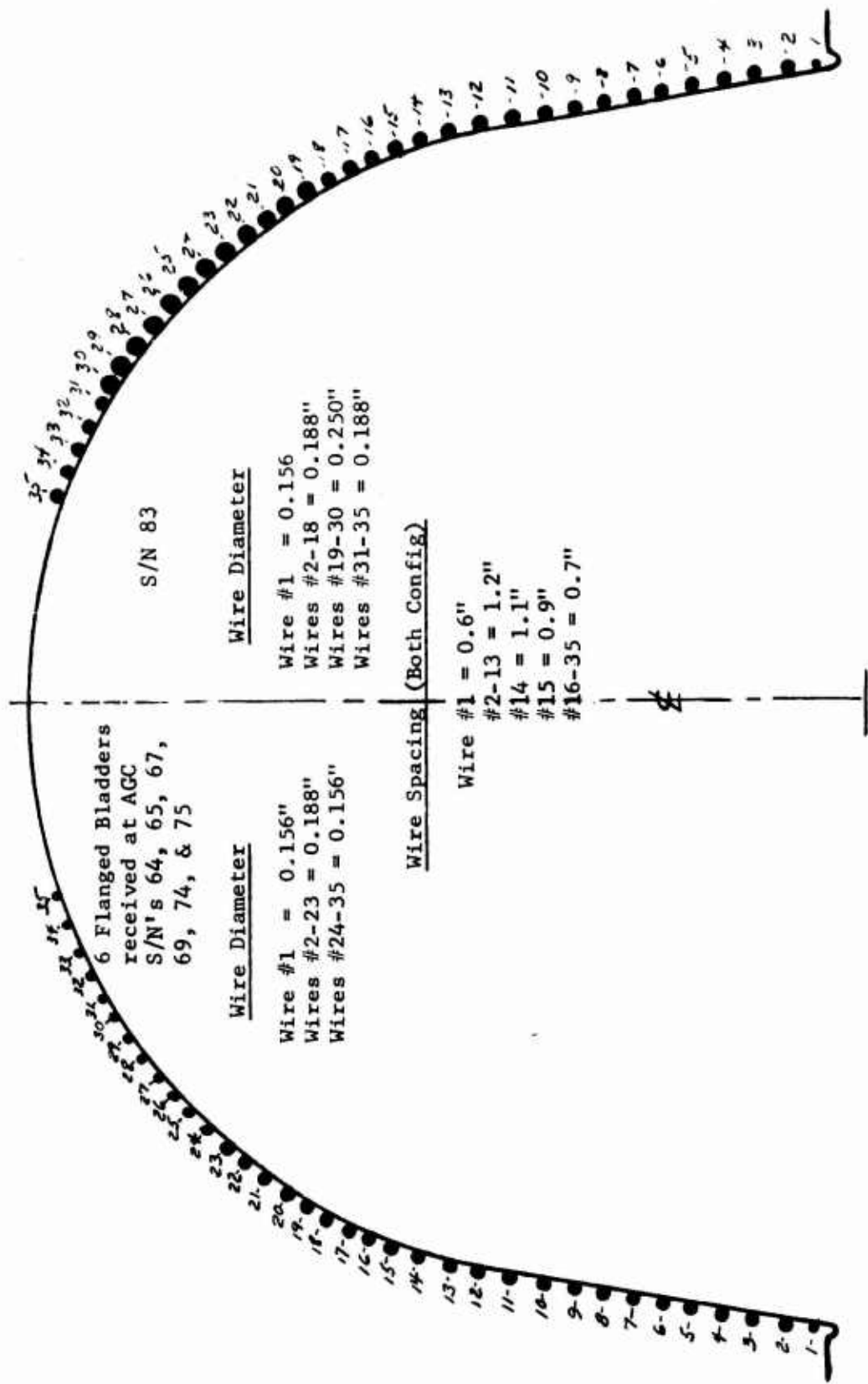


Figure 85. Arde Ring-Stabilized Expulsion Bladder Configurations

UNCLASSIFIED

Report AFRPL-TR-69-88

VI, B, Expulsion Bladder Development (cont.)

b. Flame-Spray Metal Coating of Shell

The unsuccessful tests of the S/N 67 bladder with the 0.188-in. control wires and the S/N 83 bladder with the 0.250-in. wires indicated that additional structural margin must be provided in the shell over the thin zone to prohibit shell buckling in that area. A flame-spray coating of nickel-aluminide (a product of the Metro Company, New York) on the gas-side of the bladder between the wire was evaluated using bladder S/N 65. This coating would increase the effective shell thickness in that area. The coating is applied by first lightly sandblasting the metal surface to increase surface roughness and to provide better metal adhesion. Then, the shell between the wires is flame-sprayed. The reversal test of the S/N 65 bladder was successful. Figure No. 86 is a photomicrograph of the bladder shell cross-section after the reversal test. The photomicrograph verified the actual thickness of the granular metal coating to be approximately 0.10-in.

Based upon the results from the S/N 65 bladder testing, the remaining bladder shells for both the flanged bladder testing and the lightweight propellant tank assemblies were flame-sprayed in a similar manner. The configuration, disposition and use of each bladder fabricated by Arde, Inc. and delivered for evaluation are listed on Table XIII. Braze and flame spraying fabrication problems were encountered with the last six bladders fabricated (S/N's 62, 66, 84, 85, 87 and 88). These problems and the dispositions were as follows.

(1) Braze Problems

The S/N's 84 and 88 bladders exhibited copper leak-through to the propellant side of the bladder which required rework consisting of removing the copper and weld repair of the pinholes. The remaining four bladders had multiple braze voids as shown on Figure No. 87. Arde reworked these shells by pushing the shell from the inside to reduce the gaps between the shell and the wire rings. Then, the shells were rebrazed with a lower melting point braze material (Au-N). Two of the bladders, S/N's 85 and 88, were rejected after this rework because of indentations and shell collapse between the wires in the thin zone.

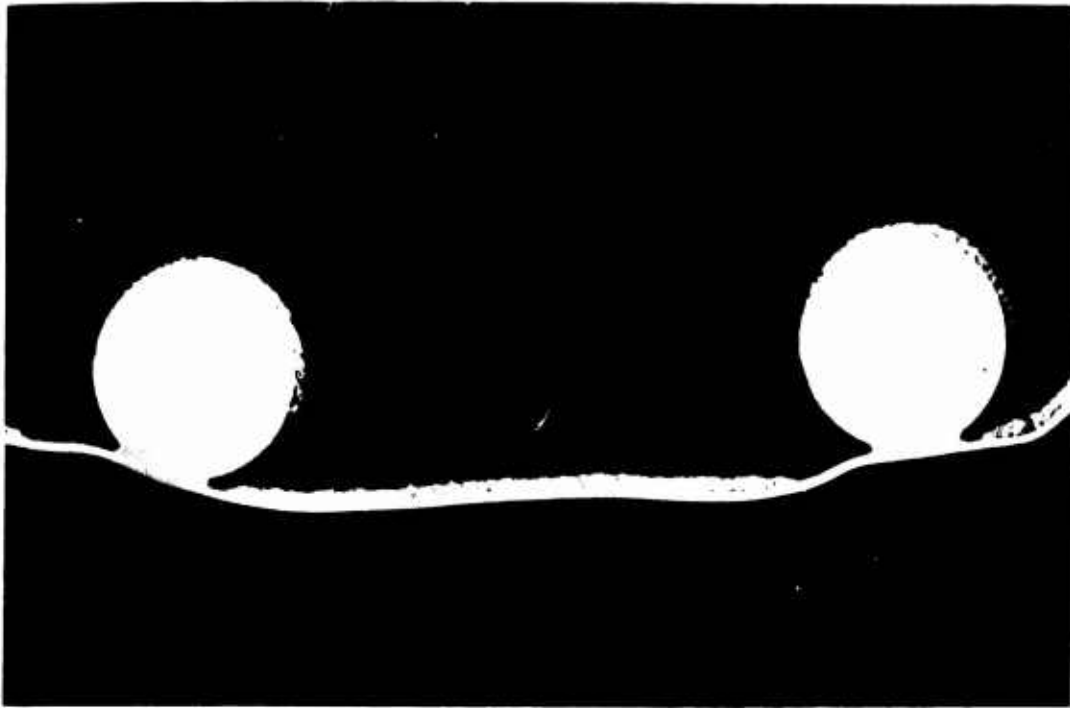
(2) Flame Spraying Problem

The final four bladders subsequently were flame-sprayed with nickel-aluminide to provide additional shell material thickness in the thin zone of the shell. The bladder shells experienced a localized shell buckling condition between the wires in this thin area during the sandblasting and flame spraying operation. This condition is shown on Figure No. 88. It is not known if the rework of these shells (reweld and a second braze cycle) influenced the formation of these deformations. However, the

UNCLASSIFIED

UNCLASSIFIED

Report AIRPL IR 69-53



BLADDER CROSS SECTION AFTER EXPULSION TEST



Figure 86. Flame-Spray-Metal on Bladder Shell

UNCLASSIFIED

UNCLASSIFIED

Report AFRPL-TR-69-88

TABLE XIII

EXPULSION BLADDER SUMMARY

<u>Bladder S/N</u>	<u>Configuration</u>	<u>Condition</u>	<u>Disposition/Results</u>
67	3/16-in. wires	Acceptable	Reversal mode evaluation - shell buckled and pinhole tear
65	3/16-in. wires - flame spray coating	Acceptable	Reversal mode evaluation - good reversal
83	1/4-in. wires	Acceptable	Reversal mode evaluation - terminated due to shell collapse
69	3/16-in. wires - flame spray coating	Acceptable	Rated pressure water expulsion with N ₂ - good expulsion
75	3/16-in. wires - flame spray coating	Acceptable	Hot gas water expulsion - good expulsion
66	3/16-in. wires - flame spray coating	Braze gaps during first braze - indentations after spray	Hot gas water expulsion - completed expulsion with buckling and shell tear
62	3/16-in. wires - flame spray coating	Braze gaps during first braze - indentations after spray	Hot gas water expulsion - terminated expulsion 85% complete due to high ΔP
64	3/16-in. wires - flame spray coating	Acceptable	Flightweight tank - MMH expulsion
74	3/16-in. wires - flame spray coating	Acceptable	Flightweight tank
84	3/16-in. wires - flame spray coating	Copper leak-through - indentations after spray	Flightweight tank
87	3/16-in. wires - flame spray coating	Braze gaps during first braze - indentations after spray	Flightweight tank - N ₂ O ₄ expulsion

UNCLASSIFIED

UNCLASSIFIED

Report AFRPL-TR-69-88

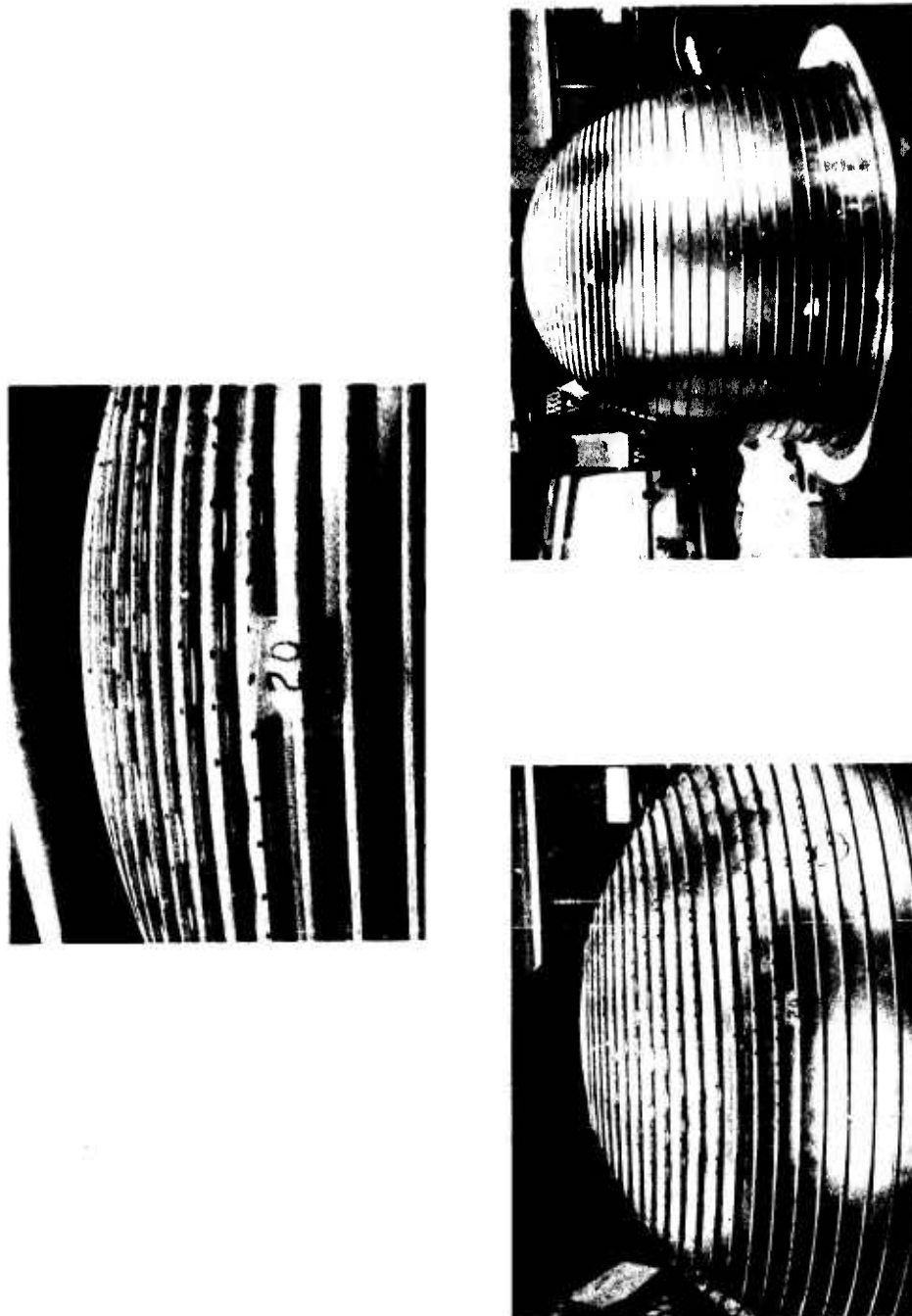


Figure 87. Bladder S/N 62 Braze Joints in Hemispherical Region

UNCLASSIFIED

UNCLASSIFIED

Report C-ATRP-TR-69-83

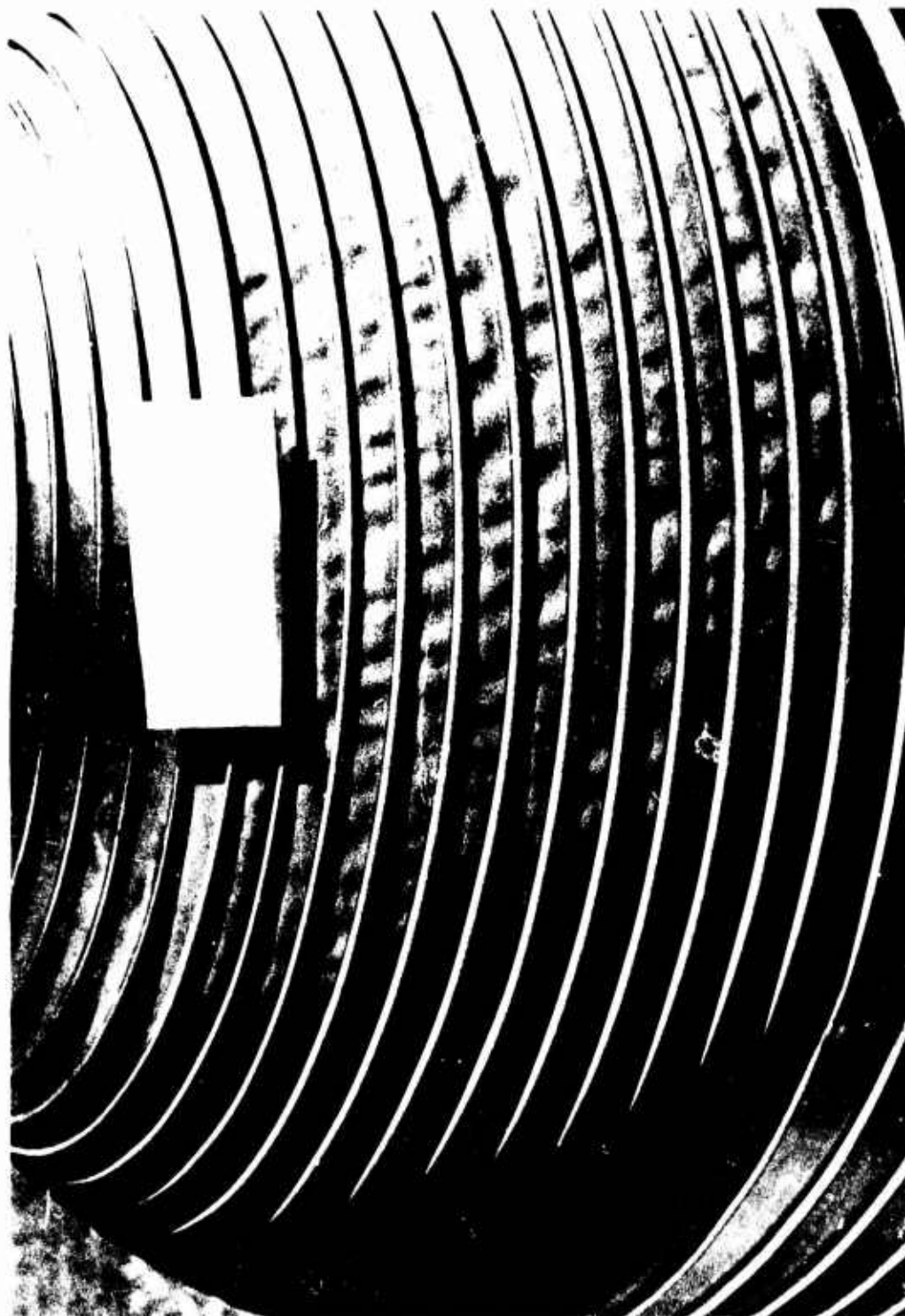


Figure 38. Expulsion Bladder Shell Indentations

Page 199

UNCLASSIFIED

UNCLASSIFIED

Report AFRPL-TR-69-88

VI, B, Expulsion Bladder Development (cont.)

surface irregularities should have been minimized when the bladders were seated into the flightweight tank after welding. The helium leak-check was conducted at a differential pressure of 50 psi across the bladder to simulate the maximum propellant vapor pressure expected to be contained during storage. This pressure should have been sufficient to produce a catenary deformation of the shell between each wire and remove the surface irregularities.

3. Bladder Collapse Mode Evaluation

a. Acrylic Tank Evaluation of S/N 67 Bladder

Expulsion bladder S/N 67 was tested to evaluate the collapse mode through the use of an acrylic tank half. Water was expelled from the acrylic side of the tank. It also was used as a pressurant to provide control because the clear acrylic shell had a marginal pressure capability. The flanged Arde tank half, S/N 1, was used as the other half of the tank. The test setup is shown on Figure No. 89, both before and after reversal.

A detailed review of the test motion pictures verified that the bladder shell initially buckled at the girth on one side of the bladder. This occurred at approximately 3 psi to 5 psi actuation pressure. However, the rolling of the bladder shell was restrained at the girth and the shell differential pressure increased to approximately 7 psi. This resulted in the initial shell roll at the thin area of the junction between the cone and hemisphere (wire ring No. 21, numbered from the girth) and continued bladder shell roll towards the dome. After reaching the dome (wire ring No. 35), the bladder began rolling from ring No. 21 down towards the girth with an apex roll mode until the shell reached wire No. 14. At this point, wires No. 13 and No. 14 interfered and buckled. Then, the unit girth rolled from wire No. 1 through 13. When full rolling of the shell at the girth began, it started in the area of the shell buckling and slowly propagated around the girth. This nonsymmetrical roll resulted in the bladder becoming cocked in the tank. Once girth rolling was established, the bladder straightened itself after rolling two rings. A slight tear in the shell, as shown on Figure No. 90, was noted between wires No. 13 and No. 14 when the roll modes were pulled.

An examination of the bladder shell after the test revealed the shell gutter contacted the tank wall after reversing. This contact, which is shown on Figure No. 91, was in the quadrant of the girth where rolling last occurred. Bladder shell thickness was measured and it was determined that the shell varied from 0.017-in. to 0.022-in. in thickness at the girth. The thicker zone was located in the quadrant where girth buckling and roll last occurred. Subsequent structural analysis indicated the thickness variation would have increased the roll pressure by approximately 25%. This increased actuation pressure caused roll at the transition point between the cone and the hemisphere to occur and it propagated the undesirable apex roll mode.

UNCLASSIFIED

UNCLASSIFIED

Report AFRL TP 69-38

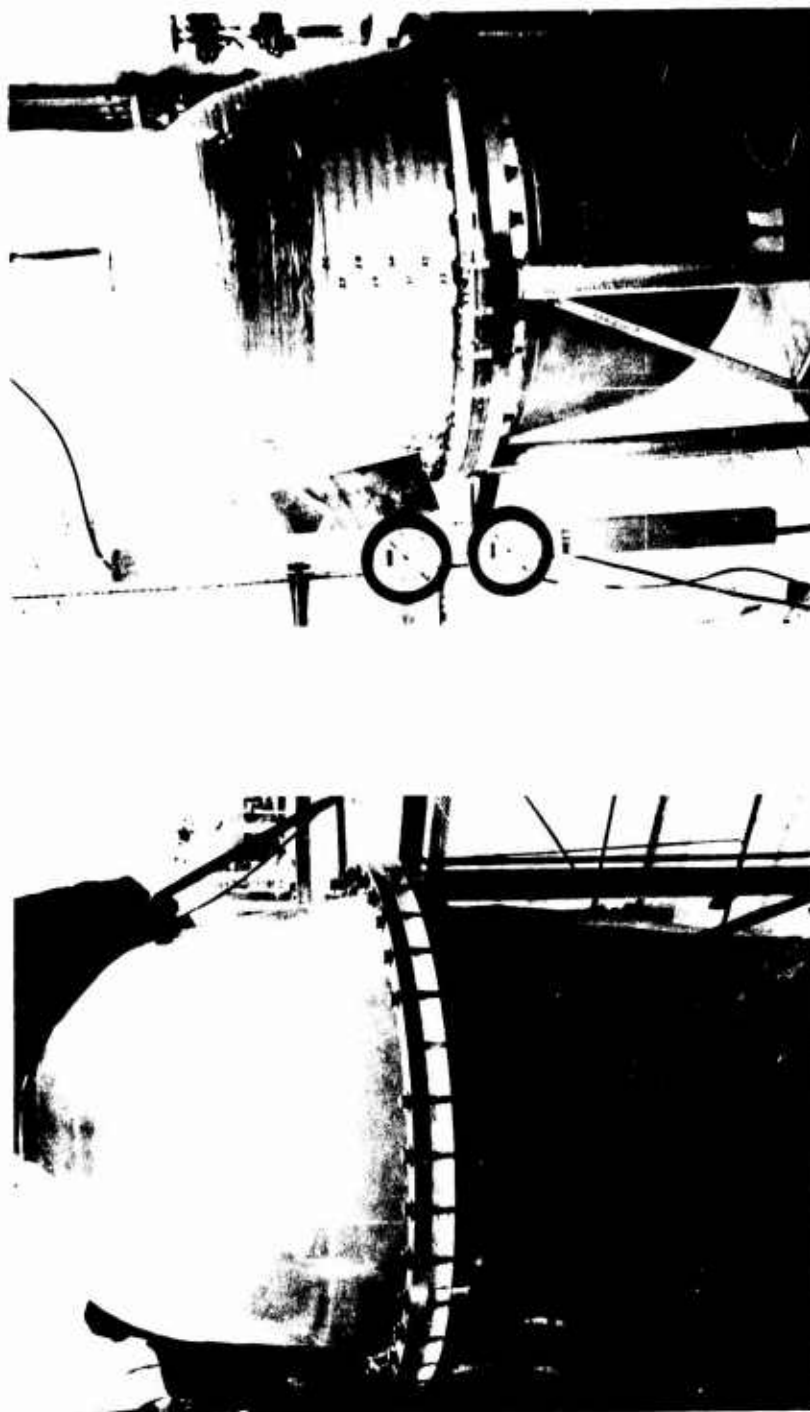


Figure 89. Arde Ring-Stabilized Diaphragm Reversal

UNCLASSIFIED

UNCLASSIFIED

Report AFRPL-TR-69-88

PIN HOLE TEAR DUE TO
SHELL 3 CORNER FOLD

DIAPHRAGM AFTER
REVERSAL

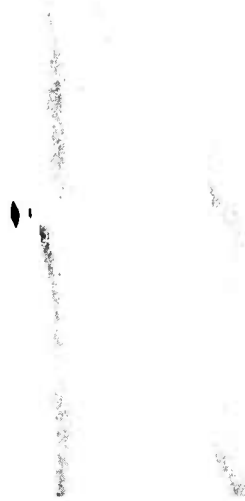
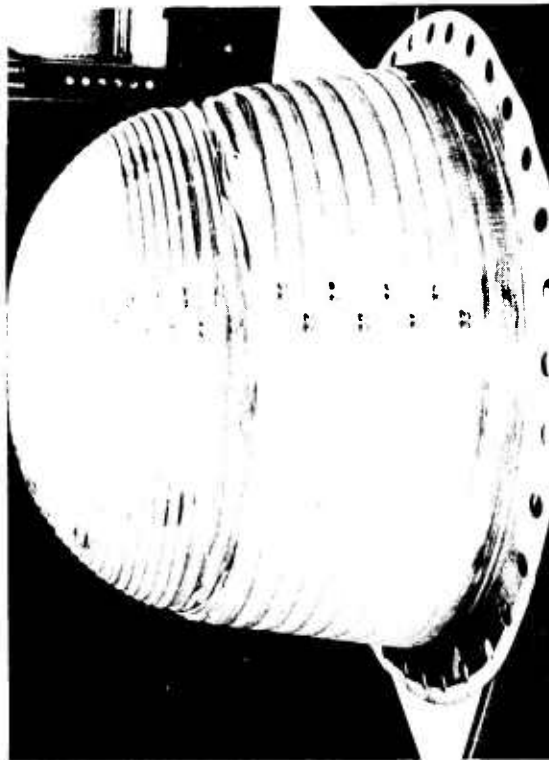


Figure 90. Arde Ring-Stabilized Diaphragm Reversal

UNCLASSIFIED

UNCLASSIFIED

Report AERPL TR 69-33

DIAPHRAGM GIRTH AREAS AFTER REVERSAL
VIEWS 180-DEGREES APART

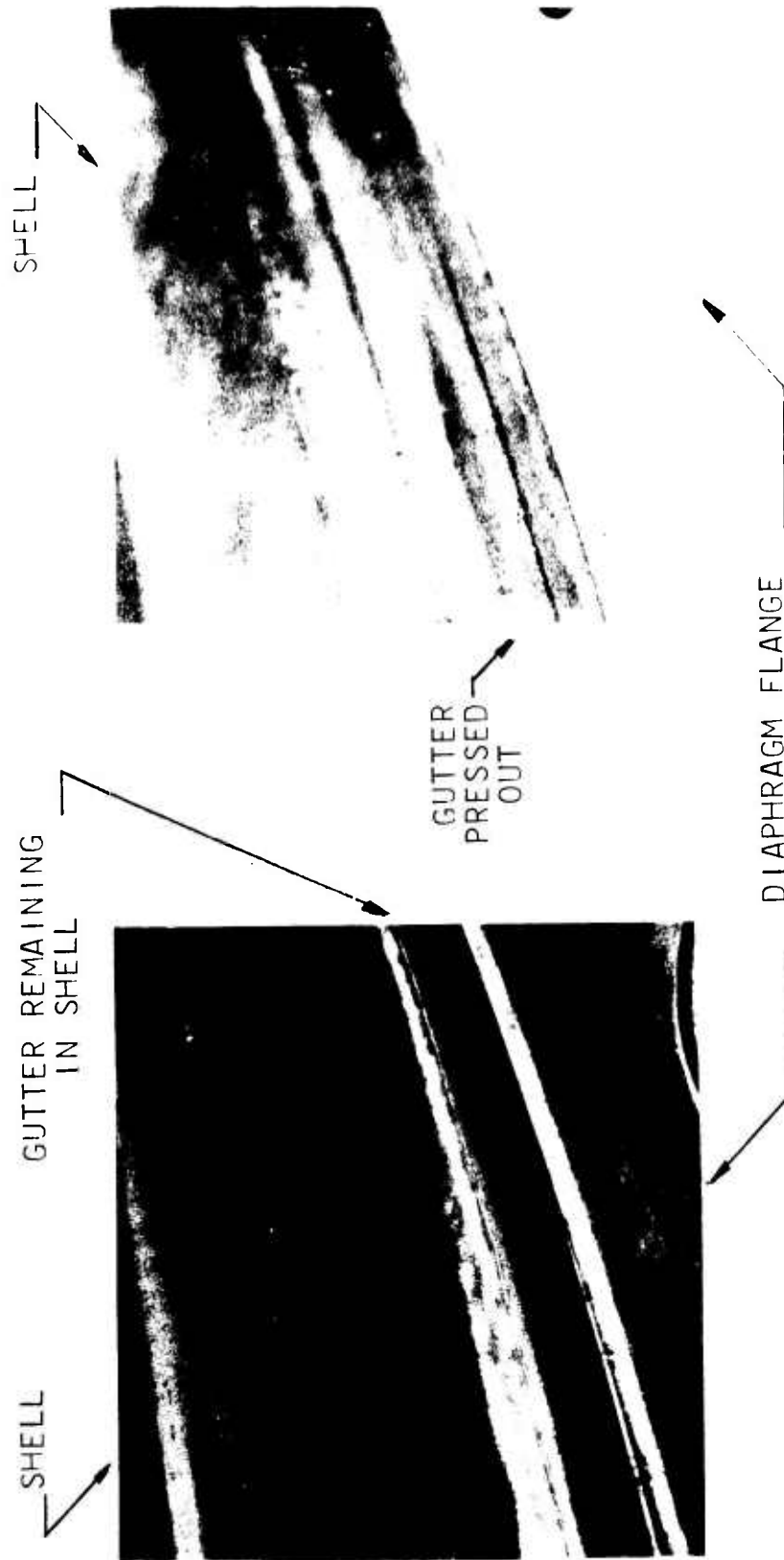


Figure 91. Diaphragm S/N 67 After Expulsion

UNCLASSIFIED

UNCLASSIFIED

Report AFRPL-TR-69-88

VI, B, Expulsion Bladder Development (cont.)

The structural analysis of the bladder was investigated to determine what corrective action could be taken which would result in an increased probability of girth roll for any given bladder. The two corrective actions accomplished for the next bladder shell were chemical milling of the girth area to thin the shell and plasma arc spraying the metal in the transition area between the cone and hemisphere to thicken the bladder shell. It was demonstrated that both techniques were mechanically feasible for demonstration articles and that material removal or addition could be controlled to ± 0.0005 -in. Subsequently, the structural analysis revealed that decreasing the bladder thickness by 0.004-in. at the girth would result in a 50% increase in the probability of buckling while increasing the probability of rolling by only approximately 30%. Therefore, no further thinning of the girth area was attempted.

Arde, Inc., proposed evaluating the possibility of increasing the diameter of those wires covering the shell thin zone. This was intended to provide a greater pressure differential to initiate roll in that zone of the shell and increase the probability of a girth roll mode. This change was implemented on bladder S/N 83.

b. S/N 65 Flame-Spray Coated Bladder Evaluation

Changes were implemented in the test of S/N 65 bladder which minimized the possibility of an apex reversal. Modifications to the flanged test tanks ensured a concentric tank and bladder alignment as well as a larger moment in the bladder at the girth joint to initiate roll at that point. Also, the bladder assembly was flame-sprayed with nickel aluminide*** on the gas-side of the bladder between the wires to increase the effective shell thickness in the thin area. The thickness of the sprayed metal was intended to be 0.006-in. to 0.008-in. The reversal sequence is shown on Figure No. 92. The post-test evaluation of the bladder indicated that the actual thickness of the sprayed metal coating was approximately 0.010-in. as shown on the shell cross-section photomicrograph, Figure No. 86. The structure of the added material was granular as compared to the parent metal of the formed shell. However, it did increase the column strength of the bladder assembly.

The bladder assembly initiated the desired roll mode at the "gutter" in the girth and at an effective actuation pressure of 5 psi differential. A girth roll-mode of bladder reversal continued through a complete expulsion cycle without damage to the bladder integrity. The stabilizing wires did not control the bladder shell reversal uniformly after wire No. 24 was reached. However, this wire is in the hemispherical section and does not pose a major problem for expulsion.

***A product of the Metro Company, New York.

UNCLASSIFIED

CONFIDENTIAL

Report AFRPL-TR-69-88

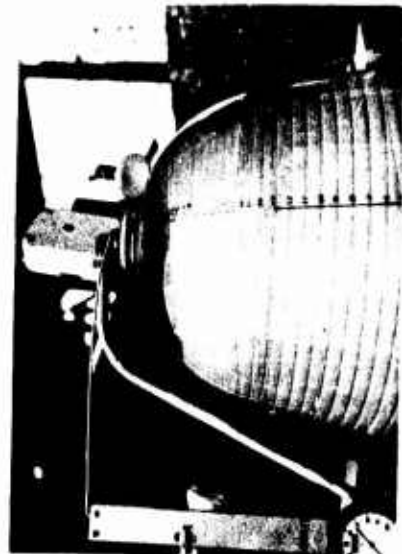
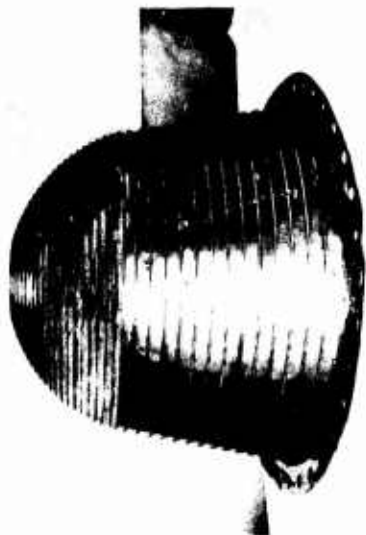
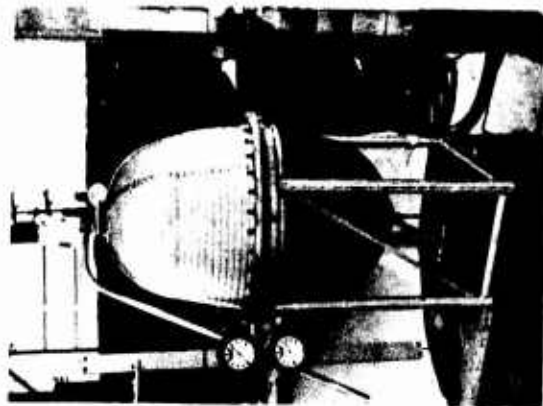
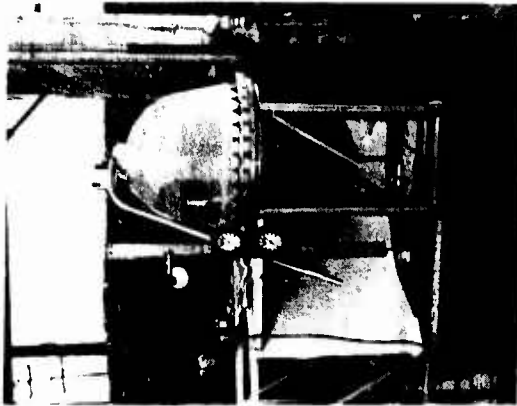
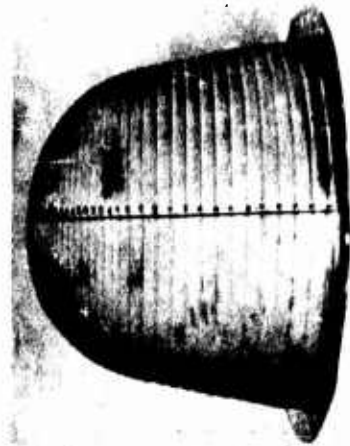
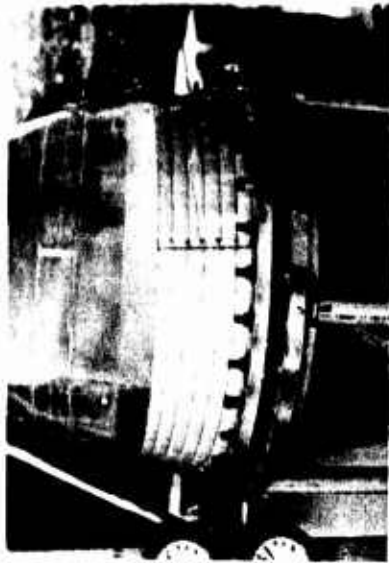


Figure 92. Ring-Stabilized Bladder S/N 65 Water Expulsion

CONFIDENTIAL

(This page is Unclassified)

CONFIDENTIAL

Report AFRPL-TR-69-88

VI, B, Expulsion Bladder Development (cont.)

(U) The remaining four bladders of the six previously delivered to Aerojet-General were flame-sprayed in a manner similar to that used on S/N 65 to provide the additional actuation pressure margin.

c. S/N 83 Bladder Evaluation of Larger Wires

(U) Bladder S/N 83 was fabricated with 0.250-in. wire as shown on Figure No. 85. It was tested to evaluate collapse mode with an acrylic tank half which permitted observation of the shell reversal. Prior to its assembly into the acrylic tank, the bladder was pre-set with a 50 psi differential in a flanged metal tank assembly to simulate the expected oxidizer vapor pressure during long-term storage. The bladder gutter roll at the girth was partially pulled out as a result of the shell axial movement during the 50 psi exposure. The shell had the expected catenary yielding between the 1/4-in. wires in the thin area of the shell.

(U) The reversal test of S/N 83 bladder was terminated when the bladder was approximately one-third through reversal. The initial collapse of the shell occurred in the thin hemispherical area at a differential pressure of approximately 5 psi. The desired girth reversal was never achieved because the bladder continued to apex roll after initial collapse. The test was terminated when control wire interference occurred and actuation pressure increased. The condition of the bladder after termination of the test is shown on Figures No. 93 and No. 94. This test demonstrated that the increase in wire diameter from 3/16-in. to 1/4-in. in the thin zone of the shell did not adequately eliminate localized buckling of the shell when actuation pressure was increased. The remainder of the bladders under fabrication at Arde, Inc. then were committed to the more uniform 3/16-in. wires and flame-spray coated with nickel-aluminide at Aerojet-General in the thin area of the shell to increase effective thickness as well as shell column strength.

C. BLADDER EXPULSION EVALUATION

1. Rated Pressure Expulsion

(C) Bladder S/N 69 was used to demonstrate a rated pressure level expulsion in the Arde flanged metal tank. This bladder, which is shown on Figure No. 95, had 3/16-in. diameter wires that were the same configuration as used in S/N 65. Prior to the expulsion test, the flanged tank was filled with water to measure total volume without a bladder and was proof tested to 500 psi. The tank held 1130 lb of water. Then, the tank was drained and the S/N 69 bladder installed. The bladder was seated with 50 psi differential pressure and then filled with water. The tank with the bladder held 1110 lb of water. The tank then was pressurized to 400 psi with gaseous nitrogen and the water outlet flow controlled to achieve a limited duty cycle demonstration. Outlet flow was alternately controlled at 3 lb/sec for 115 sec and 0.2 lb/sec for

CONFIDENTIAL

UNCLASSIFIED

Report C AFRPL TR 69-133

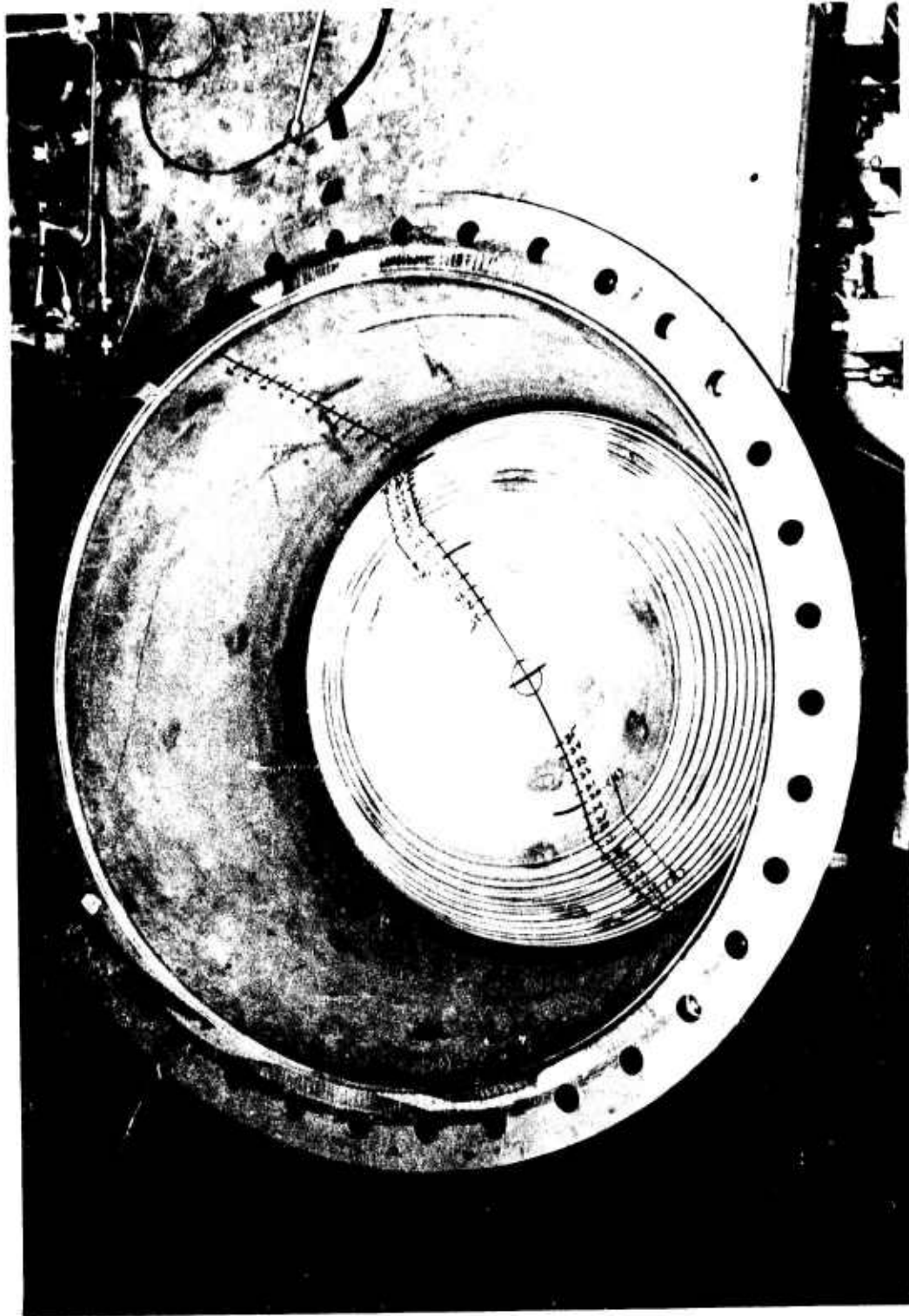


Figure 93. Bladder S/N 83 After Reversal Attempt

Page 207

UNCLASSIFIED

UNCLASSIFIED

Report AERPL TR 69-83

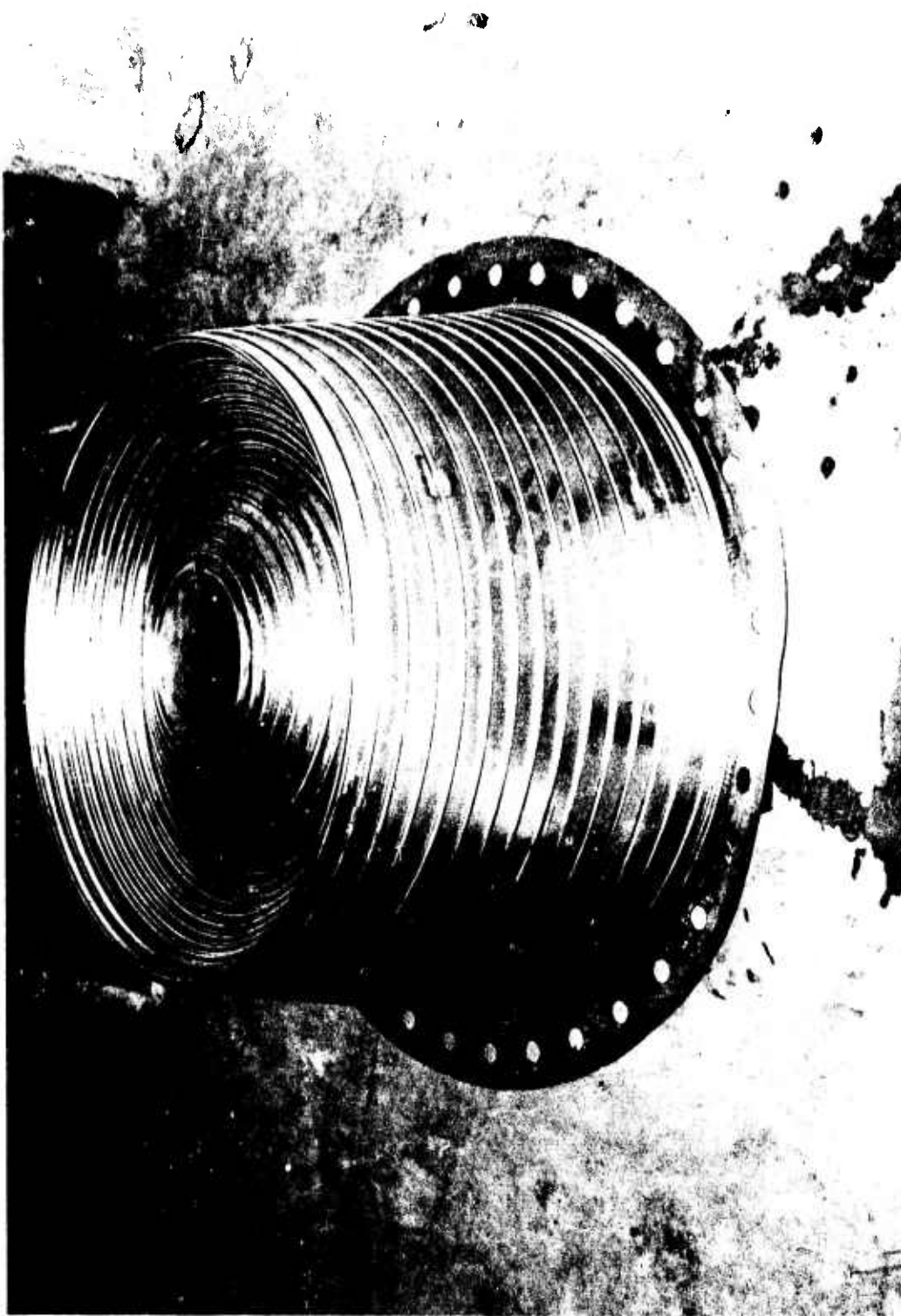


Figure 94. Bladder S/N 83 After Reversal Attempt

UNCLASSIFIED

CONFIDENTIAL

Report AFRPL TR 69 88

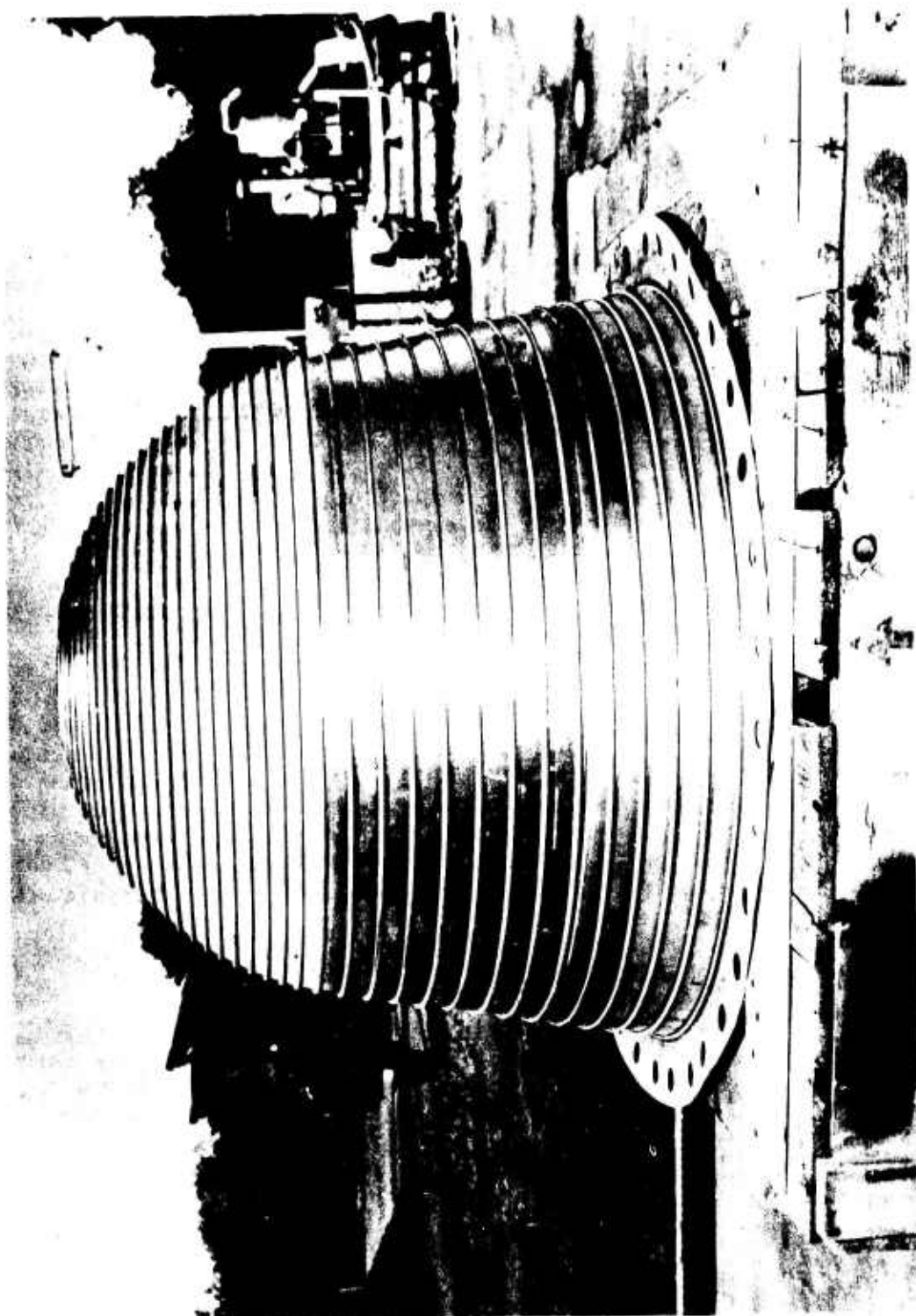


Figure 95. Bladder S/N 69 Prior to Expulsion Demonstration

Page 209

CONFIDENTIAL

(This page is Unclassified)

VI, C, Bladder Expulsion Evaluation (cont.)

250 sec until water expulsion stopped. The residual water was measured to be 7.1 lb for an expulsion efficiency of 99%. The bladder was in excellent condition without leakage after reversal as shown on Figure No. 96.

2. Hot Gas Expulsion

a. Monopropellant N_2H_4 Gas Pressurization Checkout

(U) Preparation for hot gas expulsion of the Arde ring-stabilized bladder propellant tank was initiated with the recalibration of the first-stage gas generator of the monopropellant gas generator subsystem supplied by the Hamilton Standard Division of United Aircraft under previous contract (AF 04(611)-11614). The first-stage of the developed gas generator subsystem was designed to provide an outlet pressure of 700 psia when operated as a two-stage subsystem. The first-stage bootstrap circuit was recalibrated to incorporate the prototype AM355 stainless steel tank and provide an outlet pressure of 400 psi to 420 psi for direct expulsion of a propellant tank. The differential area of the prototype bootstrap tank had a pressure ratio of 1.56 as compared with the 1.4 ratio of the previously tested workhorse aluminum tank (Contract AF 04(611)-11614). The recalibration was achieved by disassembling and resetting the pressure switch controls provided with the gas generator subsystem by Hamilton Standard Division of United Aircraft. The integrated test set-up is shown on Figure No. 97.

(U) Six gas generator subsystem tests had been conducted under Contract AF 04(611)-11614 to demonstrate the satisfactory gas generator operation for tank hot gas expulsion. In the final test, the displacement of water from a flanged Arde tank without a bladder was demonstrated to permit evaluation of the tank wall thermodynamics. Water was displaced over a 425 sec limited duty cycle demonstration with alternate flow rates of 80 sec of 2.42 lb/sec and 10 sec of 0.07 lb/sec. The maximum tank wall temperature achieved was 480°F adjacent to the hot gas inlet flange.

b. Initial Hot Gas Expulsion - S/N 75 Bladder

(U) A major program milestone was achieved with the hot gas expulsion of water from a flanged bladder assembly. Expulsion bladder S/N 75 was used in the test and thermocouple instrumentation was tack-welded to the shell to measure shell temperatures at several points along the surface during the expulsion. The thermocouple leads were brought out through tapped holes in the tank flange. In addition, the tank shell temperatures also were recorded at similar positions to identify structural integrity and propellant compatibility. Figure No. 98 is a schematic of the test set-up and instrumentation.

UNCLASSIFIED

Report AFRTI TR 69-55

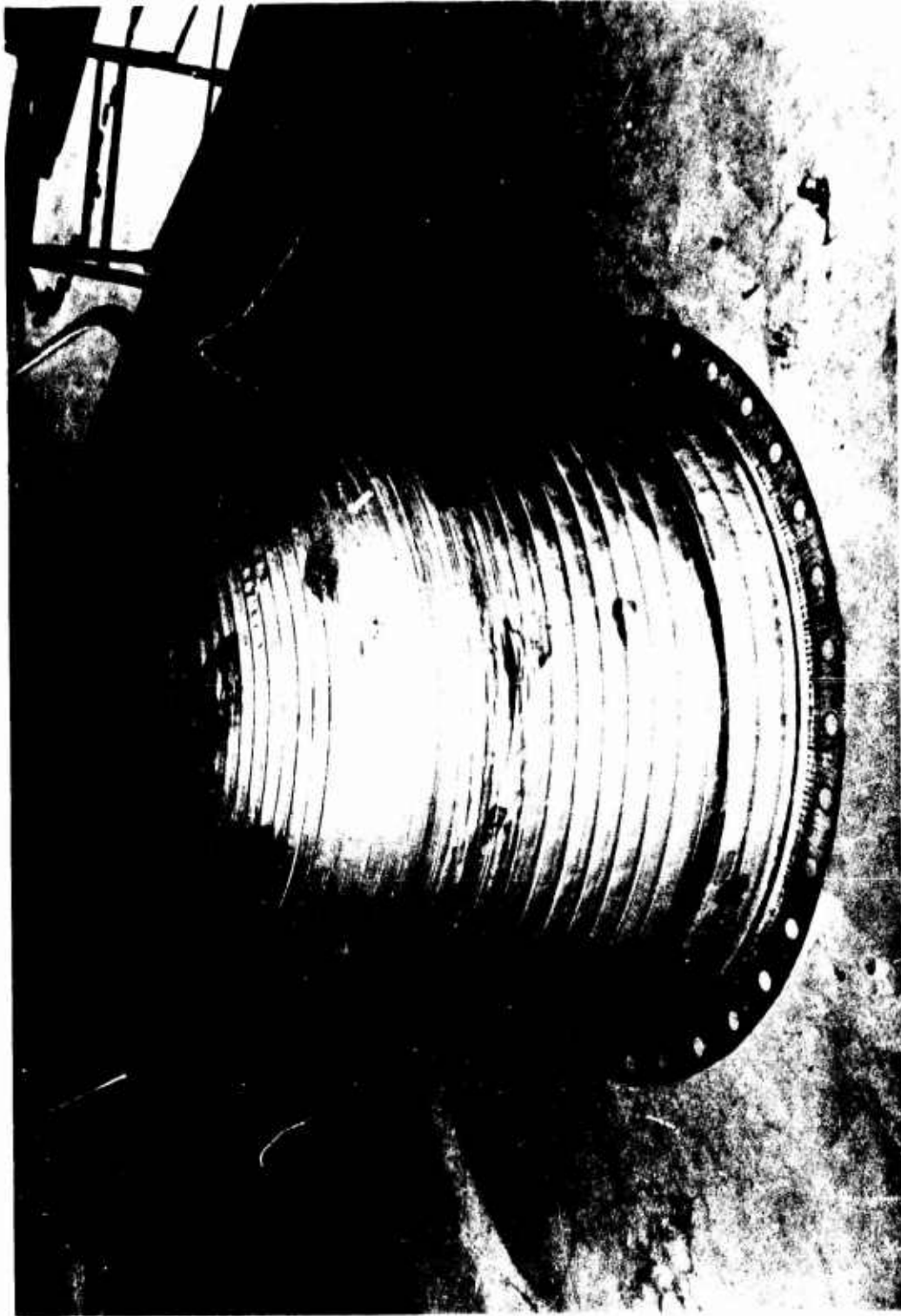


Figure 96. Bladder S/N 69 After Rated Pressure Expulsion

Page 211

UNCLASSIFIED

UNCLASSIFIED

Report AFRPL TR 69-88

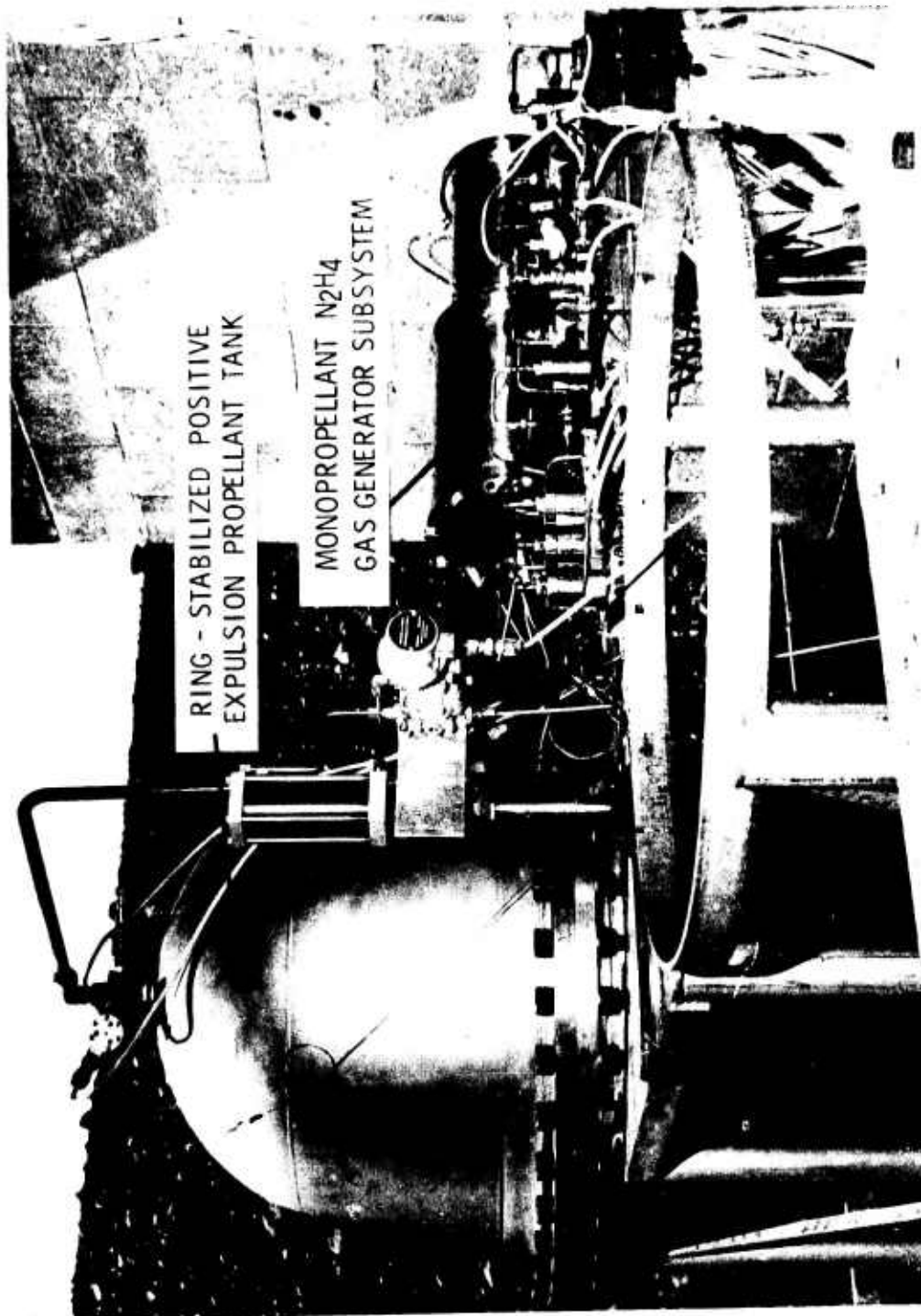















Figure 97. Integrated Test Set-Up

UNCLASSIFIED

CONFIDENTIAL

Report AFPPL-TR-69-88

VC 	CHECK VALVE	PI 	PRESSURE INDICATOR
FM 	FLOWMETER	PRR 	PRESSURE REDUCING REGULATOR
PSV 	PRESSURE SAFETY VALVE	O 	ORIFICE
LF 	FILTER G: GAS	PS 	PRESSURE SWITCH
GF 	L: LIQUID	T 	TEMPERATURE INDICATOR
VG 	GLOBE VALVE	ELCD 	ELECTRIC LOADING CONTROL DEVICE
ROV 	REMOTE OPERATED VALVE		

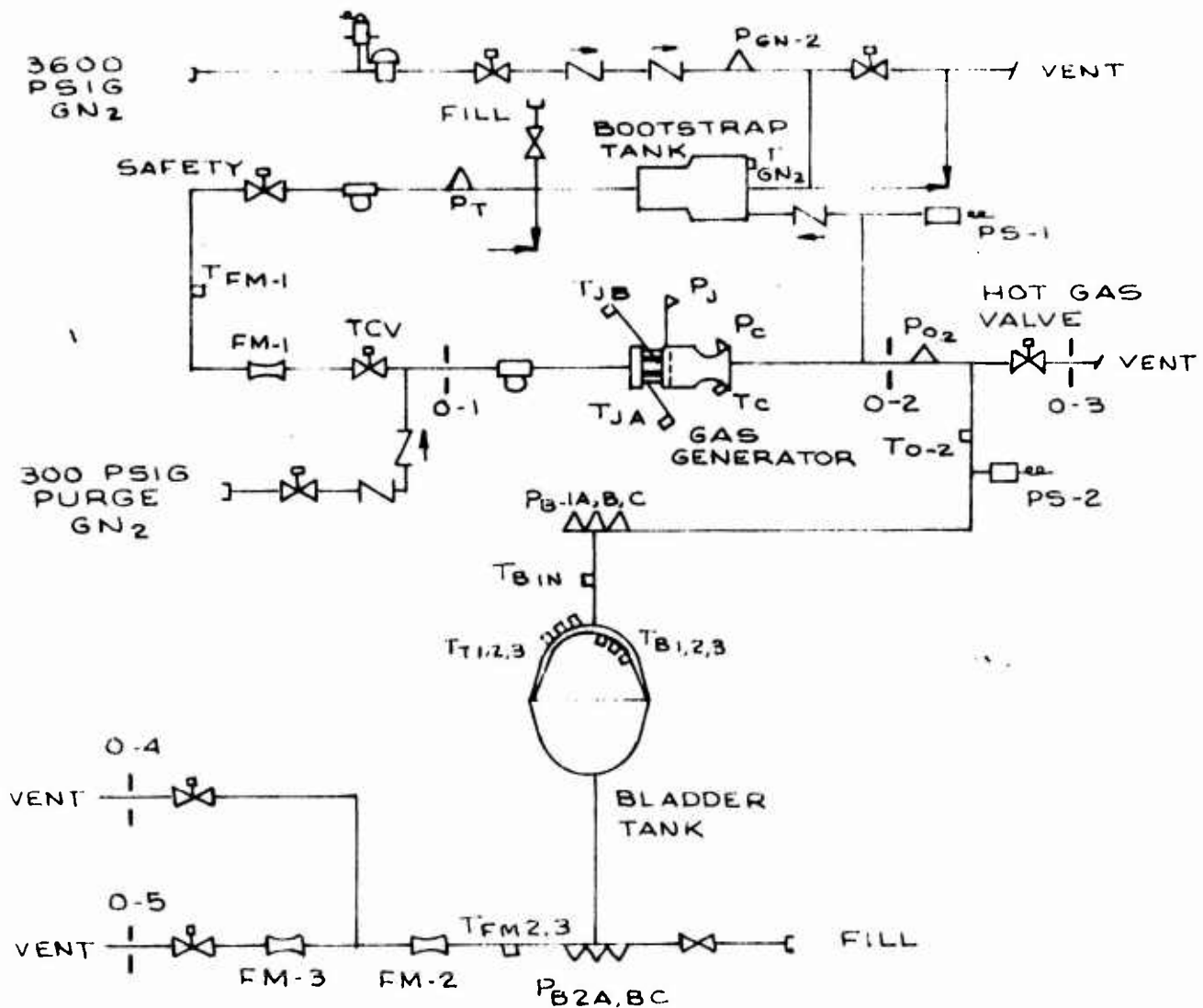


Figure 98. PBPS Integration Test Schematic

CONFIDENTIAL

(This page is Unclassified)

CONFIDENTIAL

Report AFRPL-TR-69-88

VI, C, Bladder Expulsion Evaluation (cont.)

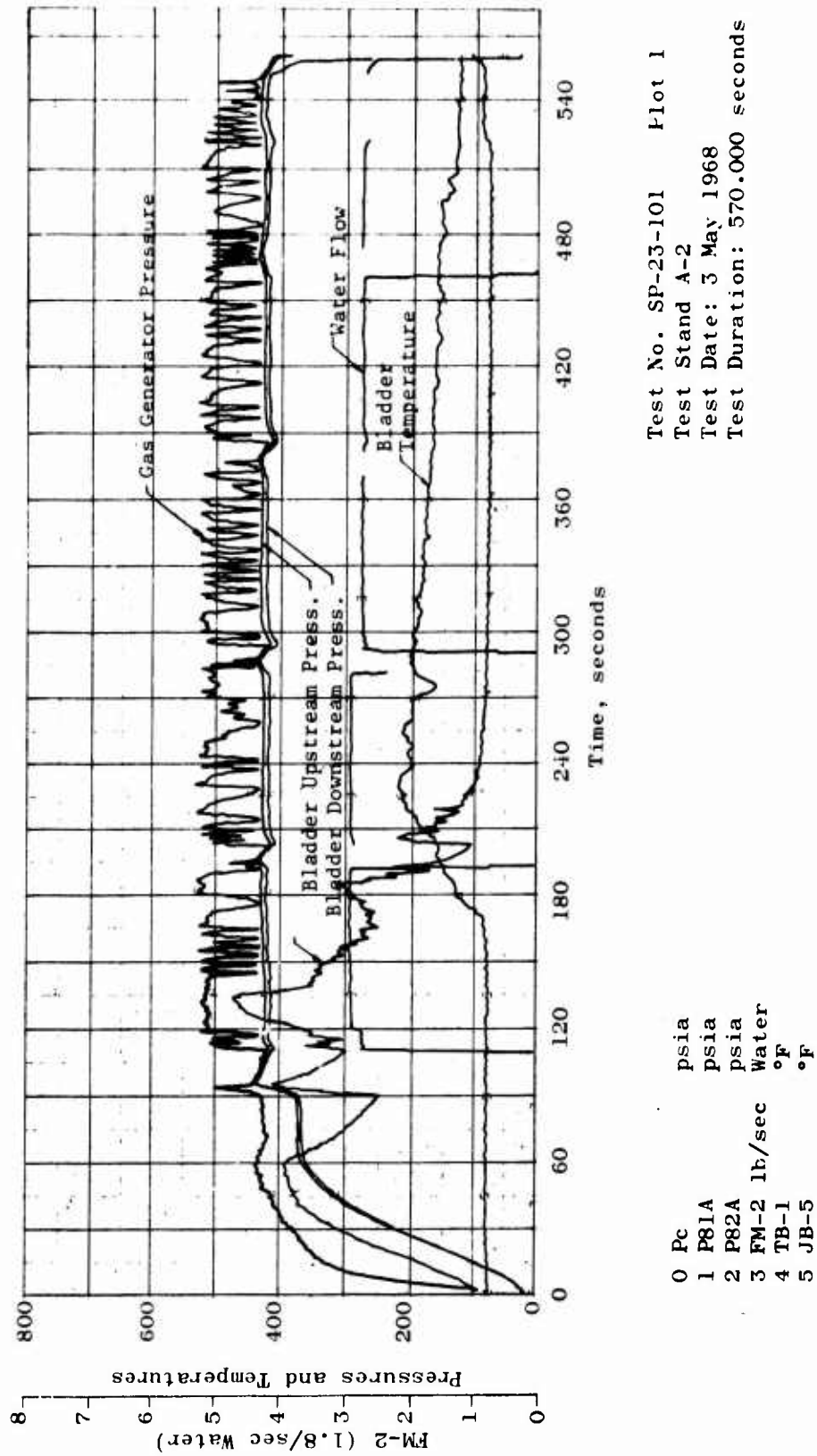
(C) The flanged tank and bladder assembly was vacuum-loaded with 1075 lb of water prior to the expulsion test. Without the bladder, the flanged tank held 1130 lb of water. The bootstrap gas generator was started with nitrogen supply pressure to the bootstrap tank until bootstrap operation was sustained. During the pressure build-up, a hot gas dump valve between the gas generator and the expulsion tank was open to vent hot gas and verify satisfactory gas generator operation. A controlled duty cycle water expulsion was initiated at 110 sec after gas generator start-up by opening downstream water valves. The water was expelled over a duty cycle of 80 sec "on" at 2.7 lb/sec to 2.9 lb/sec and 10 sec "off" for four cycles, followed by 45 sec "on" at 2.7 lb/sec, 30 sec "off", and 5 sec "on" until the water was completely exhausted. There was insufficient residual water for measurement because the bladder yielded to the inside contour of the tank at final exhaustion.

(U) The recorded data from the test are presented via four plots (see Figure No. 99). An analysis of the temperature data measured on the bladder dome during the first 120 sec of the test caused some concern because an indicated bladder temperature of 470°F was recorded. These temperatures resulted from the combination of an accumulated small air bubble entrapped on the water side of the bladder and the vertical test attitude of the expulsion tank. This condition resulted in the direct stagnation of the incoming hot gas on the thin metal dome area during the initial phase of the expulsion test. Apparently, the bubble isolated the thin shell from the water and removed that potential heat transfer capability. This condition would be minimized during an operational hot gas expulsion cycle by the closely-controlled vacuum filling of the propellant. Therefore, the isolated ullage would be a propellant vapor which would condense with the initial pressure rise and displacement of the bladder shell. These recorded temperature levels dropped to the expulsion fluid temperatures (ambient) as the bladder shell reversed during the expulsion cycle.

(U) The gas generator output pressure oscillated between 430 psia and 520 psia as a result of the pressure switch "dead-band", which provides the on-off signal to the N_2H_4 valve upstream of the gas generator. This operation is normal with the workhorse controls used with the mono-propellant gas generator subsystem and did not adversely influence expulsion tank pressure.

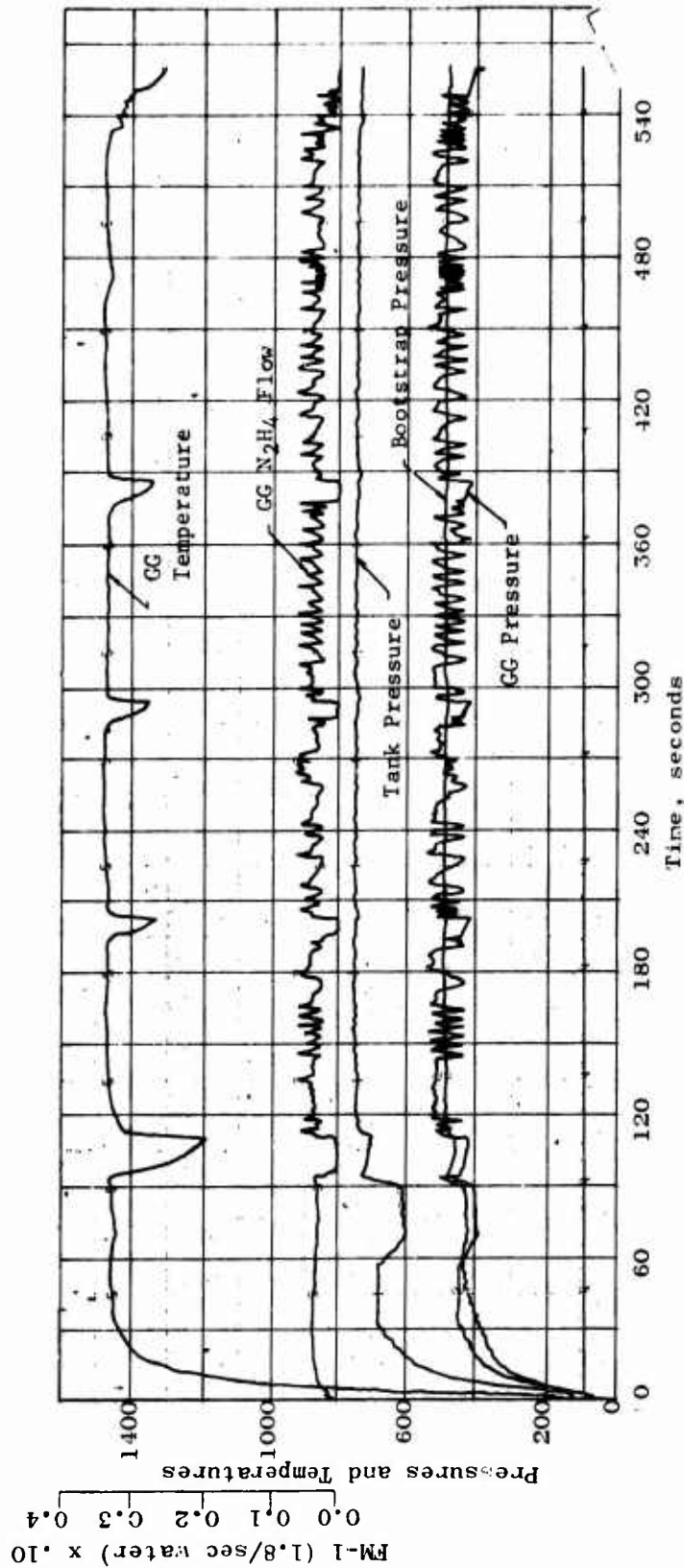
(U) A maximum propellant tank wall temperature of 540°F was recorded adjacent to the hot gas inlet boss. The recorded tank wall temperature levels were well within the structural capability of the cryogenically-stretched steel tank. The ultimate and yield strengths of the tank material dropped only 22% from ambient to 800°F. A factor of safety of 2 remained at a wall temperature of 850°F and an operating pressure of 450 psia.

CONFIDENTIAL



Test No. SP-23-101 Plot 1
Test Stand A-2
Test Date: 3 May 1968
Test Duration: 570.000 seconds

Figure 99. Hot Gas Water Expulsion Test No. SP-23-101
(Sheet 1 of 4)



Test No. SP-23-101 Plot 2
 Test Stand A-2
 Test Date: 8 May 1968
 Test Duration: 571.000 seconds

Figure 99. Hot Gas Water Expulsion Test No. SP-23-101
 (Sheet 2 of 4)

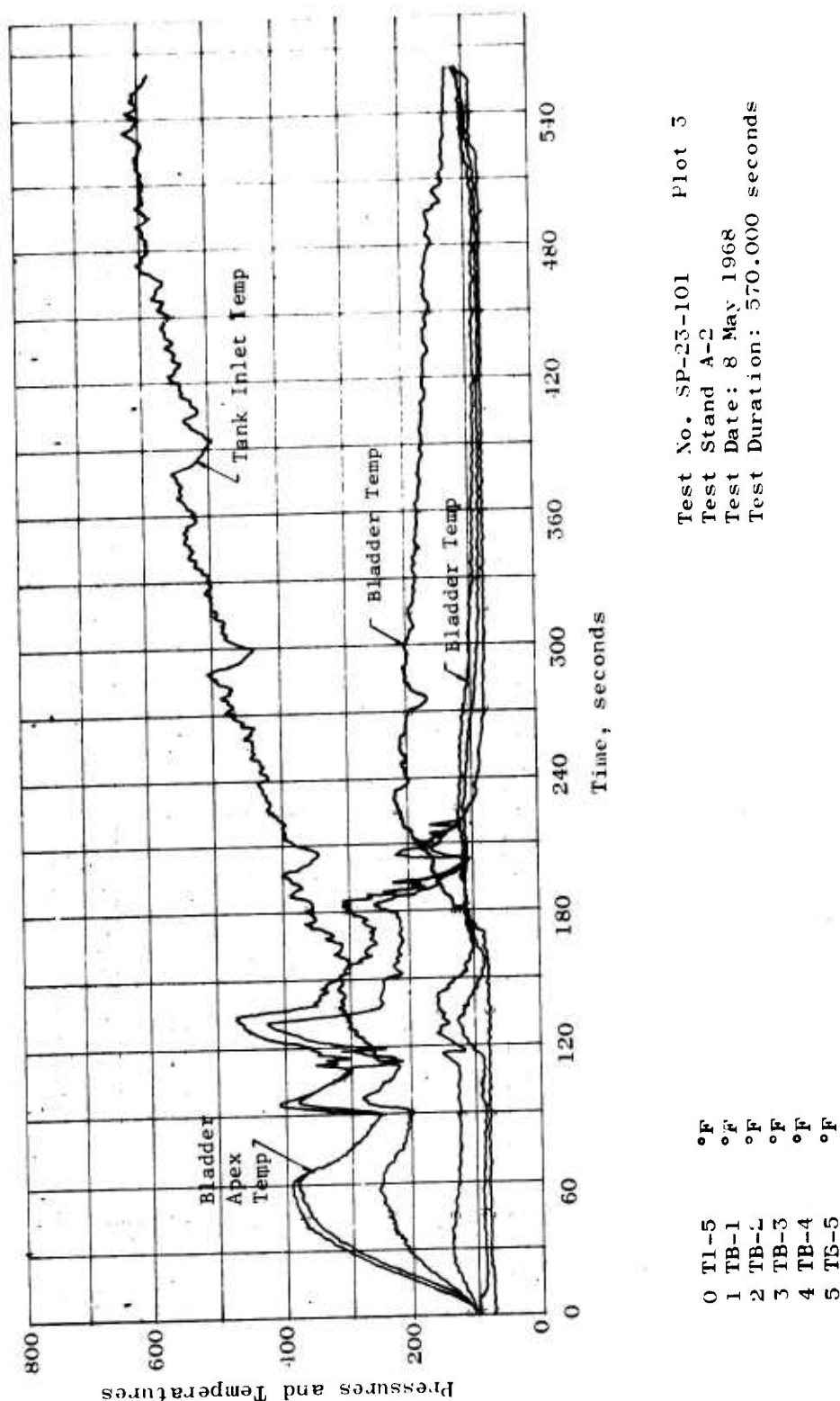


Figure 99. Hot Gas Water Expulsion Test No. SP-23-101
 (Sheet 3 of 4)

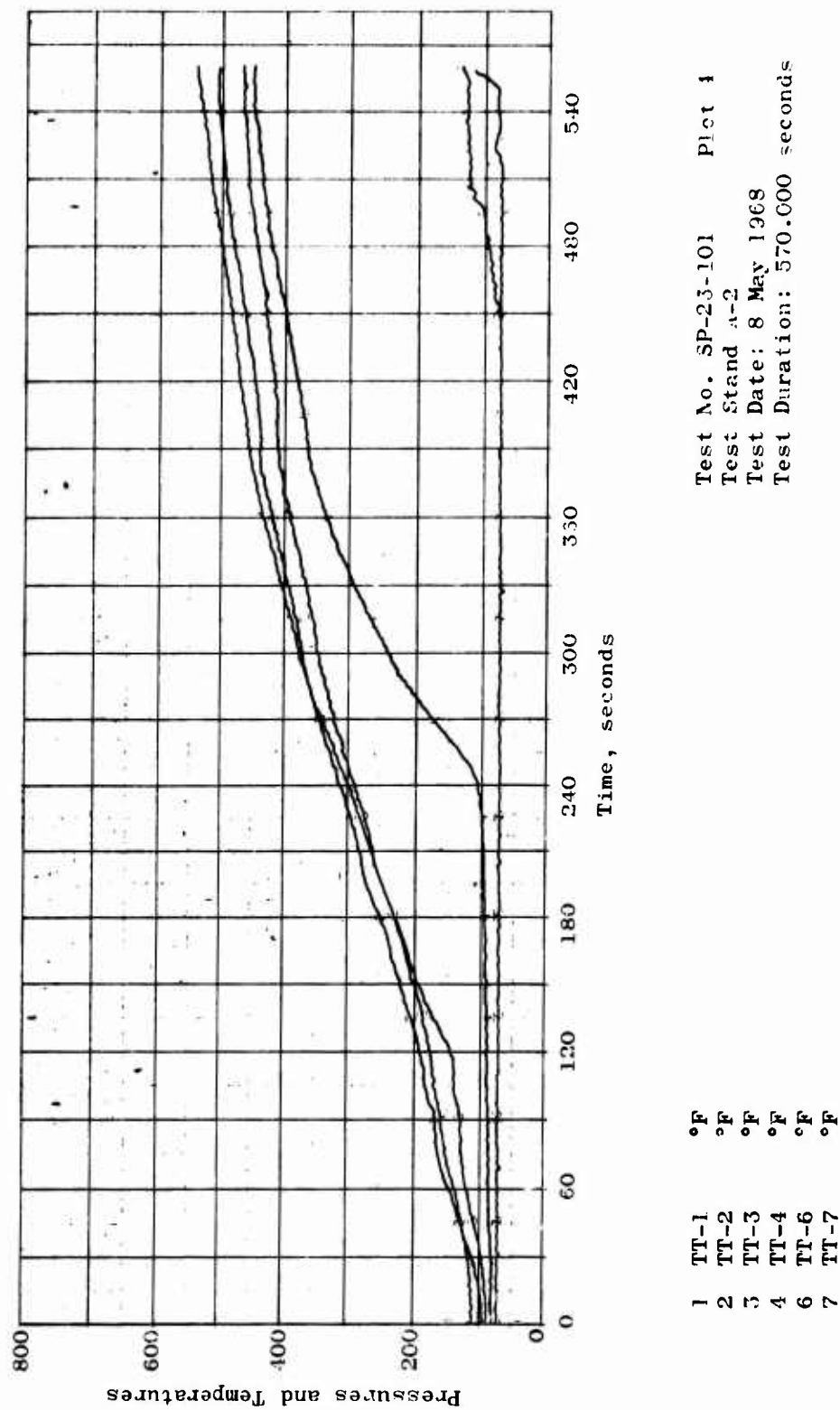


Figure 99. Hot Gas Water Expulsion Test No. SP-23-101
 (Sheet 4 of 4)

UNCLASSIFIED

Report AFRPL-TR-69-88

VI, C, Bladder Expulsion Evaluation (cont.)

The inspection of the bladder after the expulsion test verified the integrity of the bladder with no shell leakage or wrinkling indicated.

c. Bladder Rework Verification Expulsion Tests

The S/N 66 and S/N 62 flanged bladders were utilized in a water expulsion test demonstration wherein hot gas pressurant was utilized. Both bladders had experienced fabrication difficulties similar to the bladder shells used in flightweight tanks S/N's 4 and 5. These difficulties included the previously discussed wire ring brazing problems and the flame-sprayed area deformations.

The hot gas expulsion test of bladder S/N 66 was successfully completed and all measurable water was expelled from the flanged Arde tank. A water control valve was used downstream of the tank to control output flow through 21 cycles of 20 sec of approximately 2.7 lb/sec flow "on" and 10 sec "off". The test was terminated when the bladder completed reversal and flow stopped. Post-test inspection of the bladder verified that the bladder shell had completed the reversal cycle; however, there was evidence that the wire rings had not controlled the reversal. Wires No. 13, 14, and 15 (numbered from the flange) showed evidence of buckling (see Figures No. 100 and No. 101). In addition, a pinhole tear in the bladder shell resulted between wires Nos. 13 and 14 as shown on Figure No. 102. No data for this test was recorded after the 13th flow cycle, but the available recorded data is included as Figure No. 103.

A second, flanged bladder expulsion test was conducted using bladder S/N 62. A differential pressure transducer was installed to measure the pressure drop across the expulsion bladder during the test. This pressure drop was used as an indication of the condition of the reversal because an abrupt increase in pressure drop could be expected if wire ring interference occurred. The transducer was used to shutdown the test of S/N 62 bladder when the pressure drop exceeded 25 psi. The bladder wire rings were overlapped as shown on Figures No. 104 and No. 105. The bladder had completed approximately 85% of the expulsion. The measured data from this test is included as Figure No. 106.

These two tests, following the three successful reversals with the flame-spray coated bladders, verified that the ring-stabilized bladder propellant tanks were marginal because of the bladder structural characteristics. The flame-sprayed metal coating did not provide a sufficient margin of strength for the thin area of the shell. It was agreed to proceed with the planned hot gas expulsion of N_2O_4 and MMH from flightweight tank assemblies using a differential pressure transducer to monitor bladder pressure drop.

UNCLASSIFIED

UNCLASSIFIED

Report AFRL TR 69-38



Figure 100. Bladder S/N 66 After Hot Gas Water Expulsion

page 220

UNCLASSIFIED

UNCLASSIFIED

Report AFRPL-TR 69-38

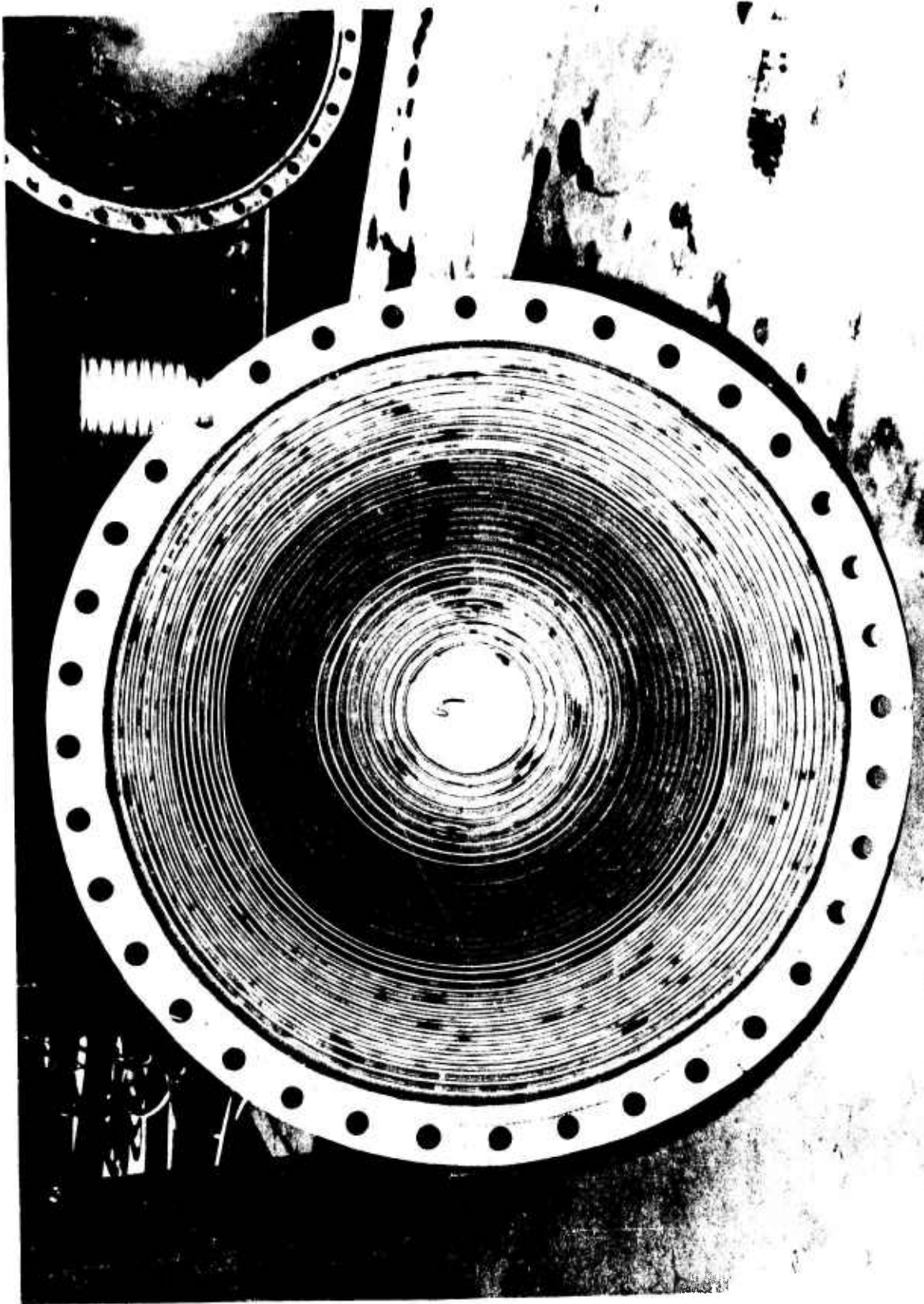


Figure 101. Bladder S/N 66 After Hot Gas Water Expulsion

Page 221

UNCLASSIFIED

UNCLASSIFIED

Report AERPL-TR-69-38



Figure 102. Bladder S/N 66 After Hot Gas Water Expulsion

Page 222

UNCLASSIFIED

UNCLASSIFIED

Report AFRPL TR-69-88

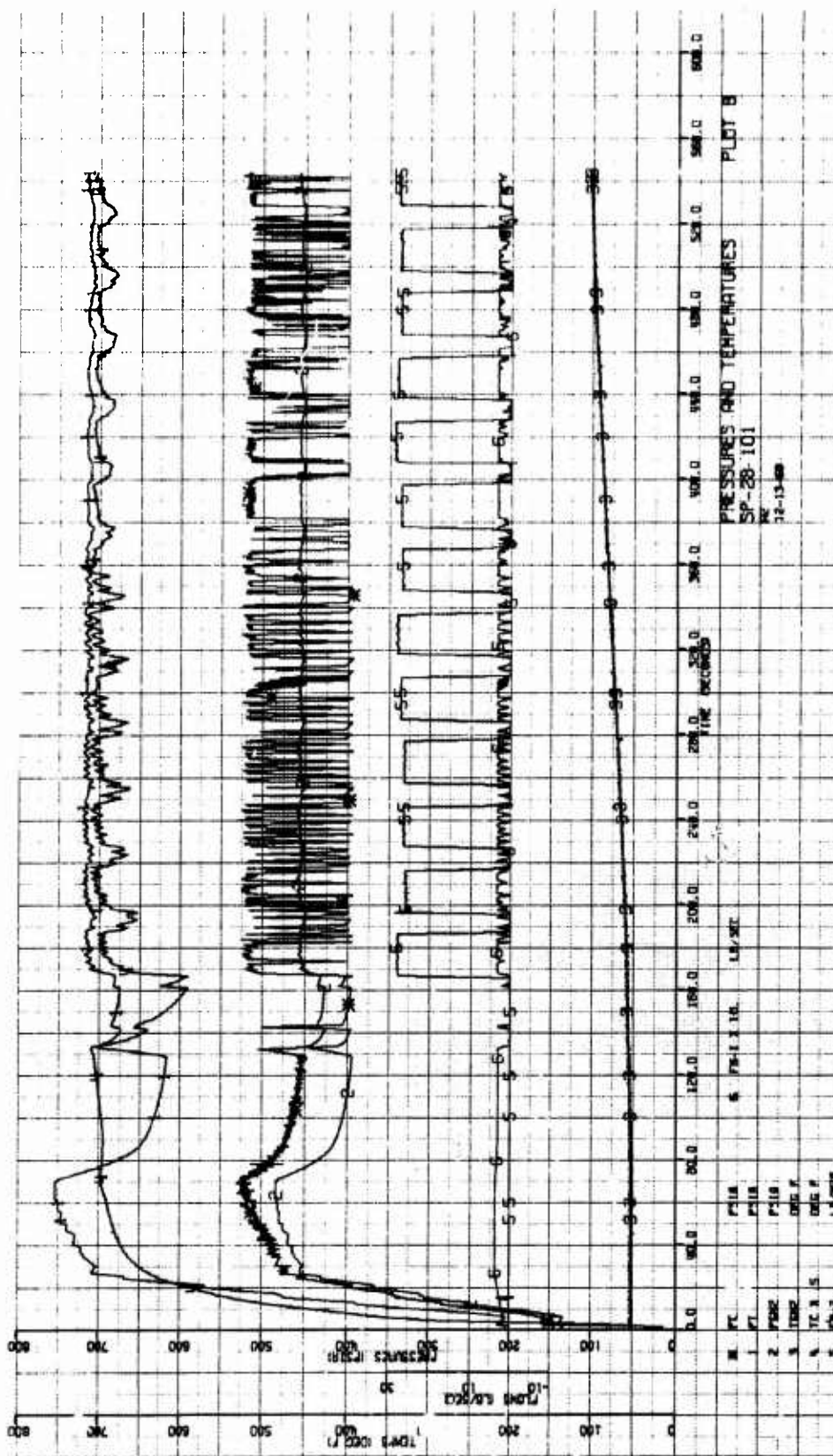


Figure 103. Bladder S/N 66 Hot Gas Water Expulsion Data
(Sheet 2 of 3)

UNCLASSIFIED

UNCLASSIFIED

Report AFRPL-TR-69-88

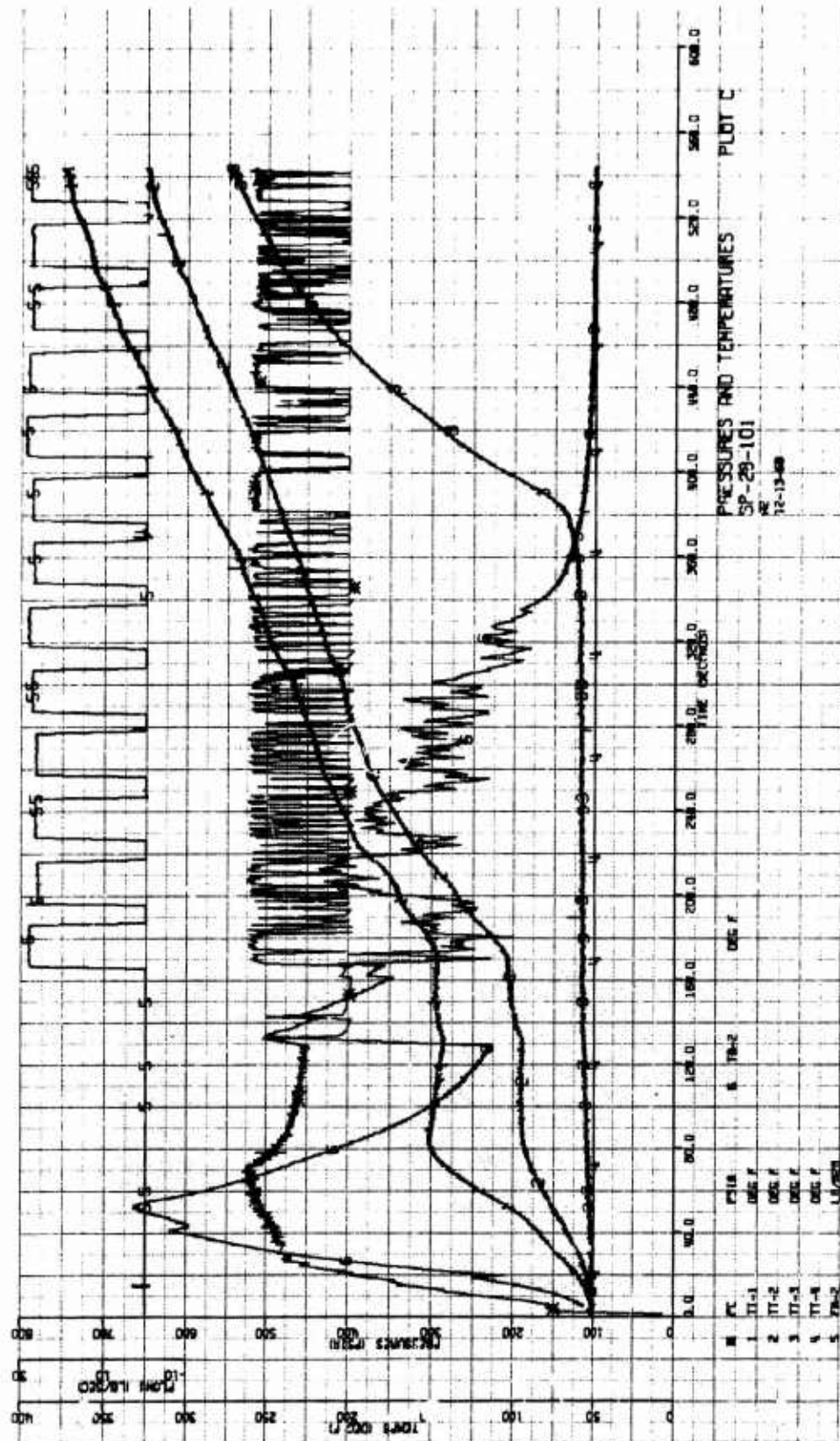


Figure 103. Bladder S/N 66 Hot Gas Water Expulsion Data
(Sheet 3 of 3)

UNCLASSIFIED

UNCLASSIFIED

Report AFRPL TR 69-38

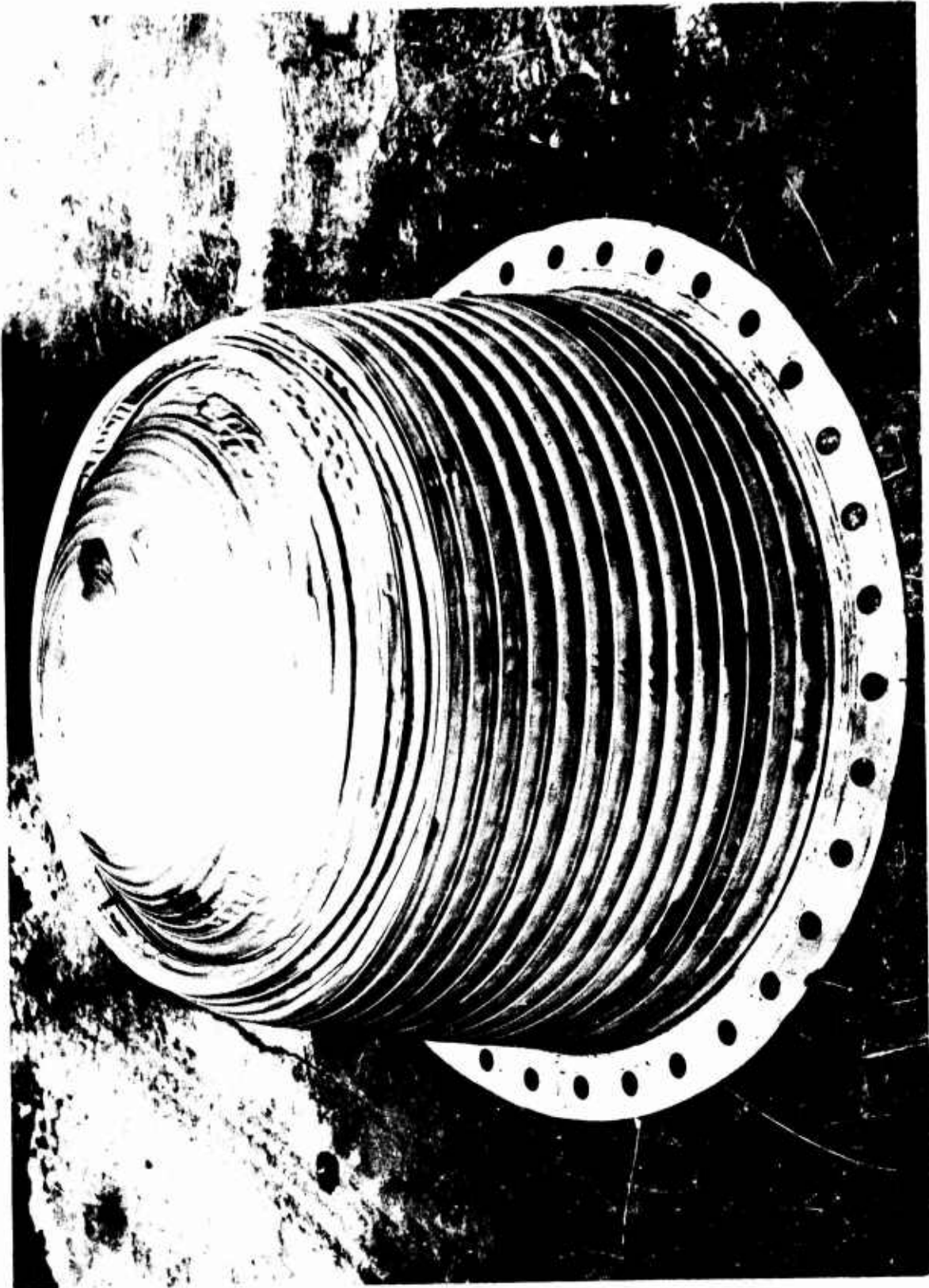


Figure 104. Bladder S/N 62 After Hot Gas water Expulsion

Page 226

UNCLASSIFIED

UNCLASSIFIED

Report AFRPL-TR-69-88

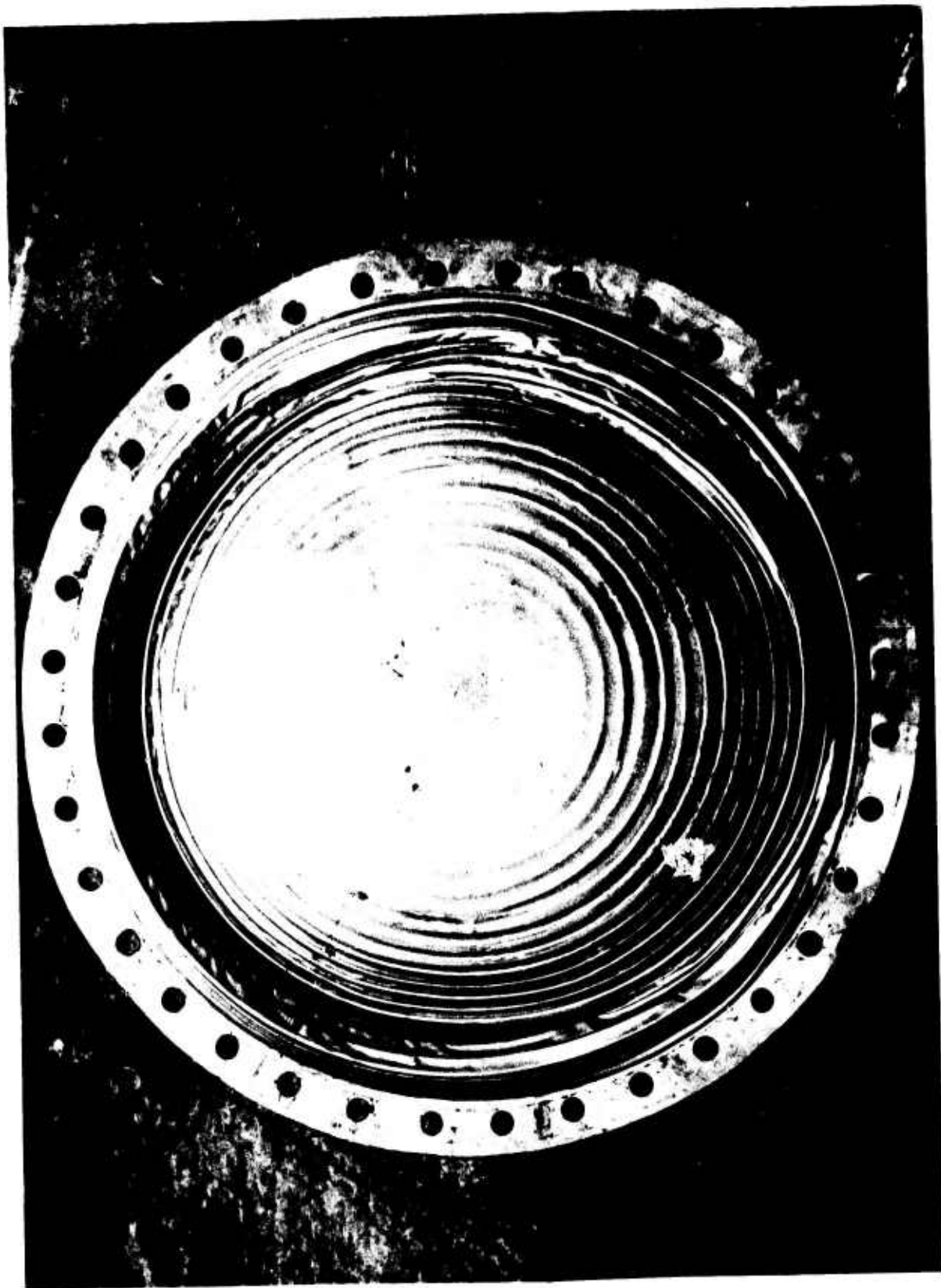


Figure 105. Bladder S/N 62 After Hot Gas Water Expulsion

Page 227

UNCLASSIFIED

UNCLASSIFIED

Report AFRPL TR-69-88

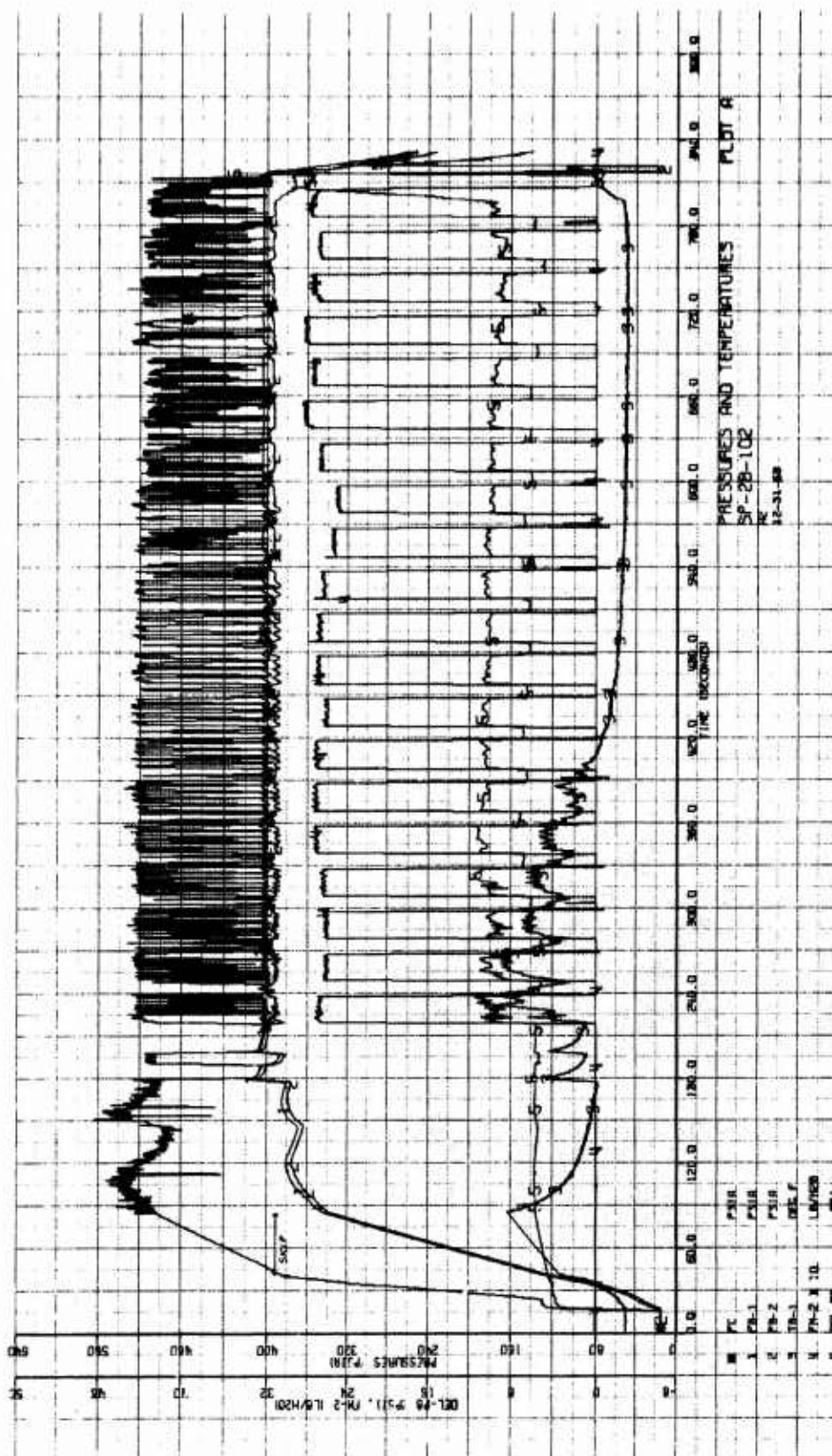


Figure 106. Bladder S/N 62 Hot Gas Water Expulsion Data
(Sheet 1 of 3)

UNCLASSIFIED

UNCLASSIFIED

Report AFRPL-TR-69-88

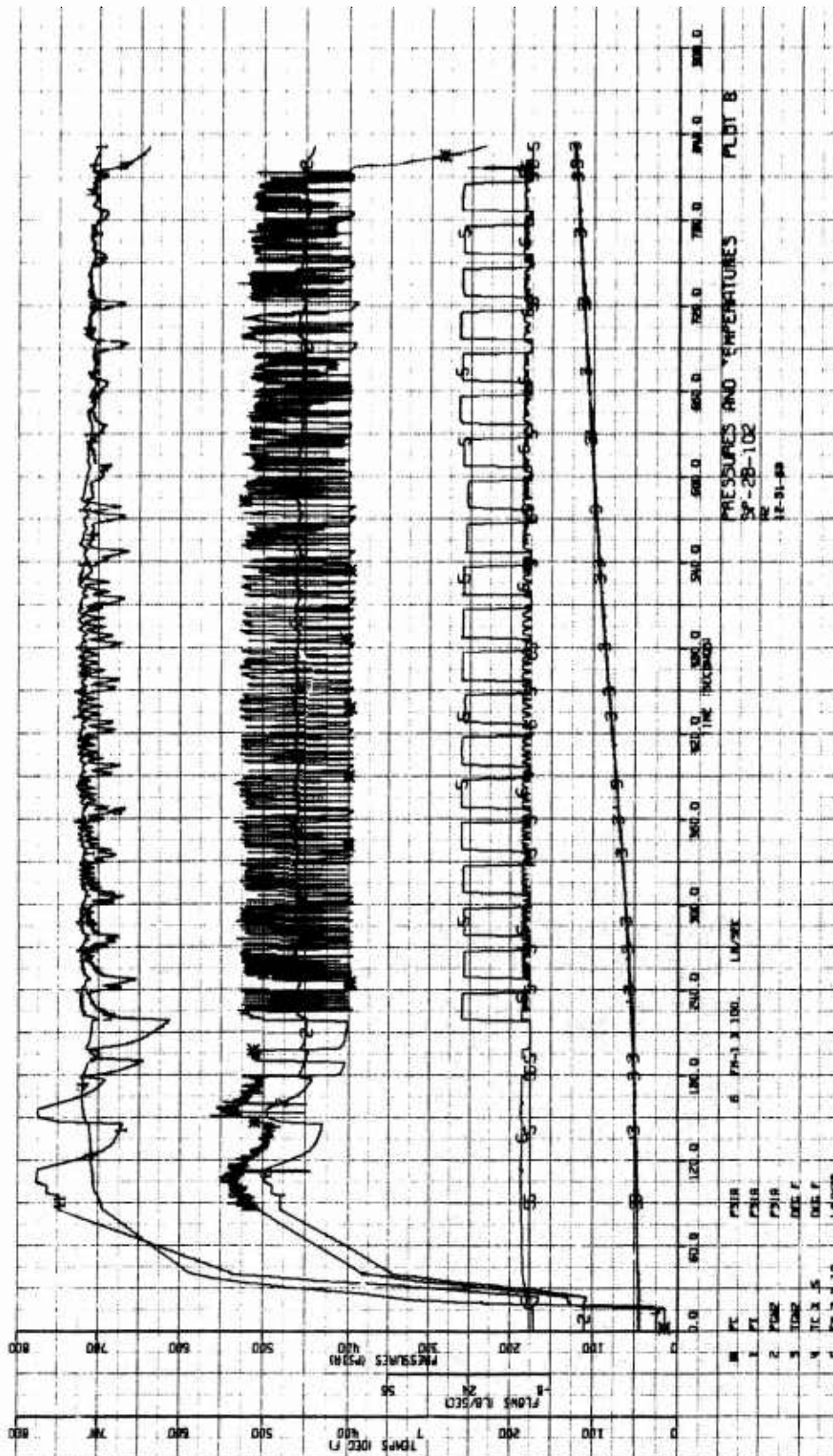


Figure 106. Bladder S/N 62 Hot Gas Water Expulsion Data
(Sheet 2 of 3)

UNCLASSIFIED

CONFIDENTIAL

Report AFRPL-TR-69-88

VI, Positive Expulsion Propellant Tank Demonstration (cont.)

D. FLIGHTWEIGHT TANK EVALUATION

1. Flightweight Tank Fabrication

a. Verification Tank Assembly - S/N 1

The initial fabrication of a flightweight tank assembly was conducted under the AFRPL contract (AF 04(611)-11614). Figure No. 82 shows this unit during fabrication, flow testing, and burst testing. Fabrication, as illustrated on the referenced figure, consisted of trimming the bladder, precisely locating and tack-welding the trimmed bladder to the tank half, and the final encapsulation of the bladder between the two tank halves via the final girth closure weld. The two tank valves were stretched individually at cryogenic temperatures to achieve the necessary structural properties prior to complete assembly of the tank. Stretching of the girth area was limited to assure that the closure weld could be made in "soft" material.

The verification tank assembly demonstrated a pressure capability to 1320 psig at ambient temperatures during the burst test. This pressure level was indicative that stress levels in excess of the 23,000 psi design stress value were reached and the initial design of the pressure vessel was verified.

b. Demonstration Tank Assemblies

The four, flightweight tank assemblies were fabricated using the procedures previously demonstrated with the S/N verification tank assembly. The tank halves were welded into preforms and then stretched to their final shape within a female die using 1800 psig liquid nitrogen. Following this, each tank half was hydrostatically-pressurized to 440 psi at room temperature. The tank halves were matched to the available bladders so as to provide the best fit possible and the girth weld joint was prepared for the final assembly weld.

Each of the completed tank assemblies was inspected by the supplier utilizing the following procedures:

- Dye penetrant check of the tank girth joint
- Gaseous helium leak check across bladder shell and through tank
- X-ray inspection of girth joint weld for penetration and voids
- Proof test of tank assembly to 440 psig

CONFIDENTIAL

Report AFRPL-TR-69-88

VI, D, Flightweight Tank Evaluation (cont.)

(U) The leakage checks across the bladders were conducted at a pressure gradient of 50 psi. This 50 psi differential pressure also seats the bladder into the tank inlet half to simulate the maximum propellant vapor pressure (N_2O_4) expected during operational storage.

(U) Subsequent X-ray inspections of the four tanks were conducted at Aerojet-General to evaluate the condition of the expulsion bladders within the weld tanks. This inspection was possible through the use of its high-intensity X-ray facility. The inspection was conducted to evaluate the degree of expulsion bladder deformation resulting from the 50 psi maximum storage pressure simulation. The pressure test provided the seating of the bladder during the supplier leakage check and the X-ray provided an excellent view of the tank cross-section as well as the bladder contained within the steel tank as shown on Figure No. 107. The inspection verified that the bladder had yielded as expected and partially-opened the gutter area formed into the bladder adjacent to the girth weld.

(C) The physical characteristics and disposition of the four delivered flightweight tank assemblies are as follows:

<u>Tank S/N</u>	<u>Disposition</u>	<u>Liquid Volume (cubic inches)</u>	<u>Tank Weight (pounds)</u>
2	MMH expulsion	30,348.2	154
3	RPL storage	30,321.0	153
4	RPL storage	30,363.9	153.8
5	N_2O_4 expulsion	30,382.2	153.5

2. Flightweight Tank Propellant Expulsion

a. Propellant Expulsion Test Set-Up

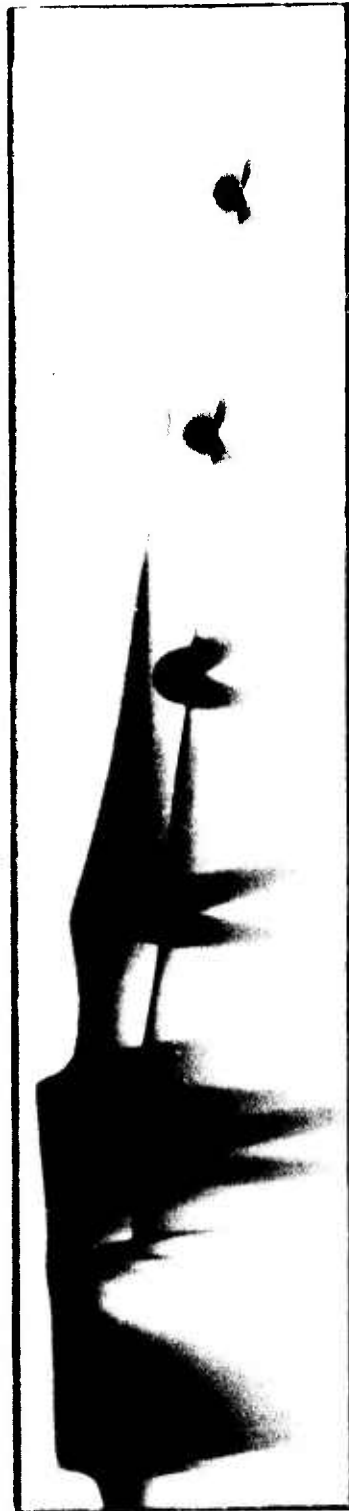
(U) Minor changes were made to the facility set-up prior to the hot gas expulsion of propellant from the flightweight tank assemblies. These flightweight tanks were mounted horizontally in a stand which supports the propellant tank by rings clamped to each end cap and a pad support under the girth ring. This support structure more closely simulates the expected installation in a flight vehicle than does the vertical attitude used in previous hot gas expulsions of water from the workhorse flanged bladder and tank assemblies. The installed propellant tank is shown installed for testing on Figure No. 108.

(U) The monopropellant gas generator subsystem used to provide the hot gas to the propellant tank was the same unit used for the earlier workhorse tank tests. Propellant flow out of the flightweight tank was controlled by a valve sequenced to satisfy a flow demand that was similar

CONFIDENTIAL

UNCLASSIFIED

Report AFRPL-TR-69-88



Girth Area



Cone to Dome Area

Figure 107. Flightweight Tank X-Ray Inspection

UNCLASSIFIED

UNCLASSIFIED

Report AFRPL-TR-69-88



Figure 108. Flight-Type Tank During Propellant Expulsion

Page 234

UNCLASSIFIED

CONFIDENTIAL

Report AFRPL-TR-69-88

VI, D, Flightweight Tank Evaluation (cont.)

to the axial engine flow requirements of a PBPS mission duty cycle. The flanged workhorse tank from the earlier flanged bladder expulsion testing was used as a propellant catch vessel. The propellant entered the bottom of the flanged tank and a vent line with a check valve at the top of the catch tank maintained a constant low pressure in that vessel. Figure No. 109 shows this facility.

b. Hot Gas Expulsion of MMH

(C) Propellant tank assembly S/N 2 was vacuum-loaded with 934 lb of monomethylhydrazine, which represented a 96.3% volume load at the propellant temperature of 48°F during loading based upon the volumetric measurements of the propellant tank by Arde, Inc.

(U) The hot gas expulsion of the MMH was conducted with the MMH flow controlled through a complete expulsion; 21 cycles of 20 sec of "on" at 2.5 lb/sec and 10 sec of "off" (simulating axial engine coast periods). This test was terminated halfway through the 22nd cycle when the pressure drop across the bladder reached 25 psi. The pressure gradient across the bladder was irregular throughout the last 30% of the expulsion cycle with the bladder actuating pressure fluctuating between 7 psi and 12 psi during the first 15 flow cycles as shown on Figure No. 110. The pressure drop increased to ~20 psi for two flow cycles and then returned to between 12 psi and 14 psi until the final cycle when the pressure drop suddenly increased above 25 psi when the bladder completed its reversal cycle.

(U) The leakage check of the bladder after completing the test revealed a substantial leak through the bladder shell. The tank was parted by grinding through the inlet side of the girth flange. The bladder had wire ring distortion and shell buckling substantiating that the wire rings did not effectively control the reversal. The condition of the bladder is shown on Figure No. 111. The possibility of this occurring was recognized before the test because of the known deficiencies in the bladder shell fabrication. The horizontal attitude of the tank added another variable as it represented the first test of a bladder with 1 g of acceleration perpendicular to the bladder reversal.

c. Hot Gas Expulsion of N₂O₄

(C) The expulsion of N₂O₄ from flightweight tank S/N 5 was accomplished by loading the tank with 1578 lb of nitrogen tetroxide. A vacuum was created on both sides of the tank bladder and then the N₂O₄ was introduced into the evacuated liquid side at a pressure in excess of the propellant vapor pressure. The tank had a calculated capacity of 1633 lb based upon the measured liquid volume during final acceptance of the unit at Arde, Inc.

CONFIDENTIAL

CONFIDENTIAL

Report APRM-TP-60-30

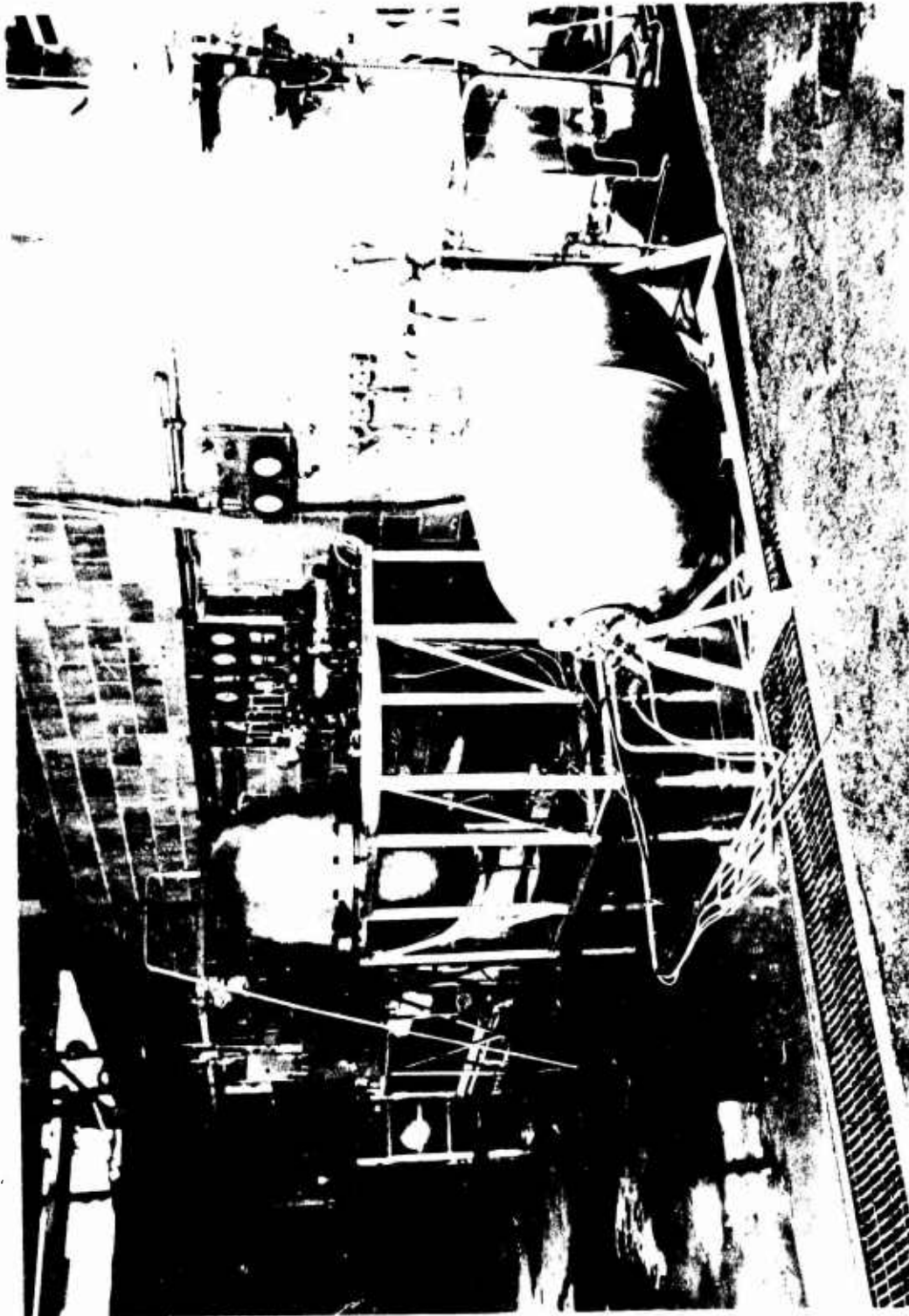


Figure 109. Propellant Tank Hot Gas Expulsion Test Setup

Page 236

CONFIDENTIAL

(This page is Unclassified)

UNCLASSIFIED

Report AFRPL-TR-69-88

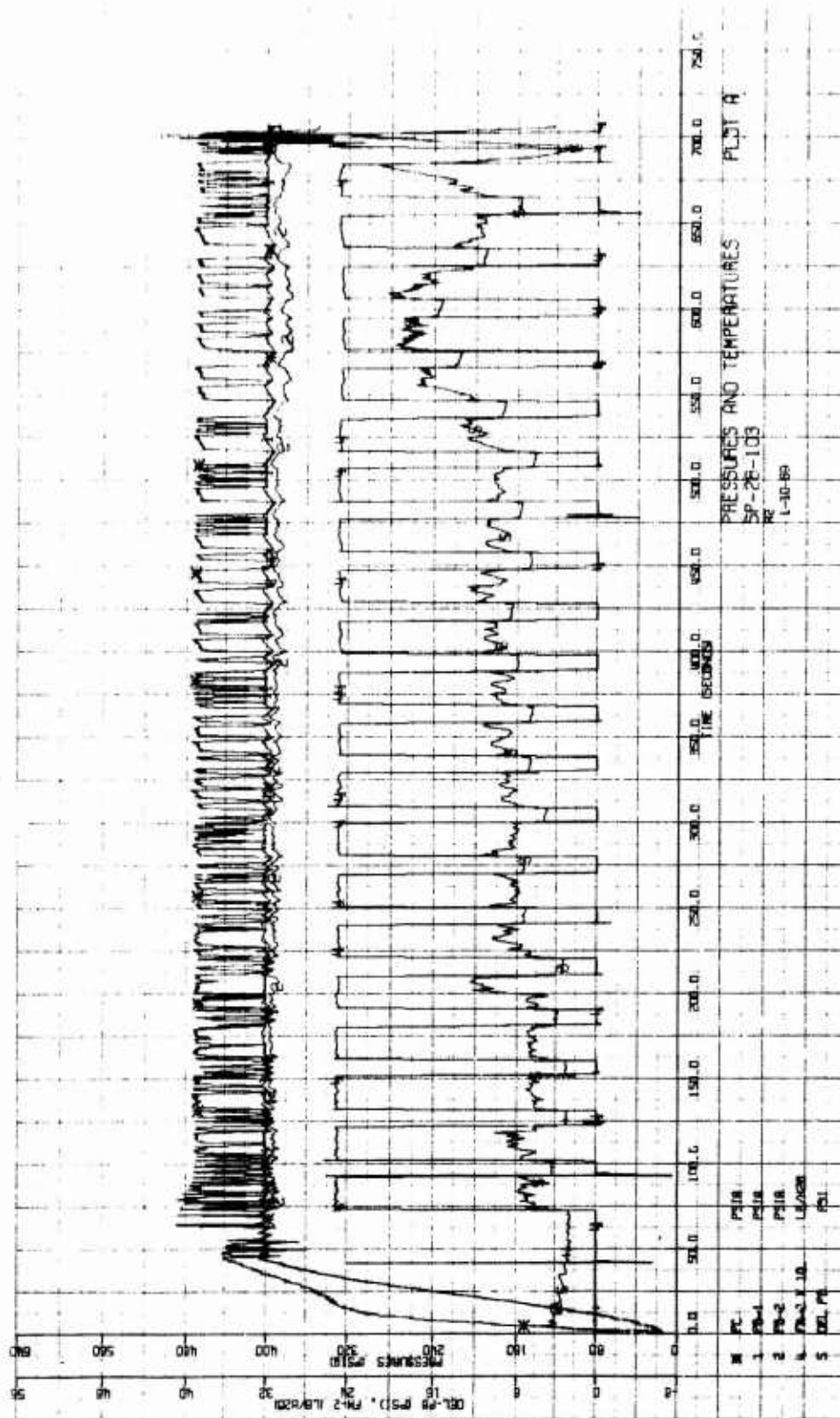


Figure 110. Tank S/N 2 Hot Gas Expulsion of NMH - Recorded Data
(Sheet 1 of 3)

UNCLASSIFIED

UNCLASSIFIED

Report AFRPL-TR-69-88

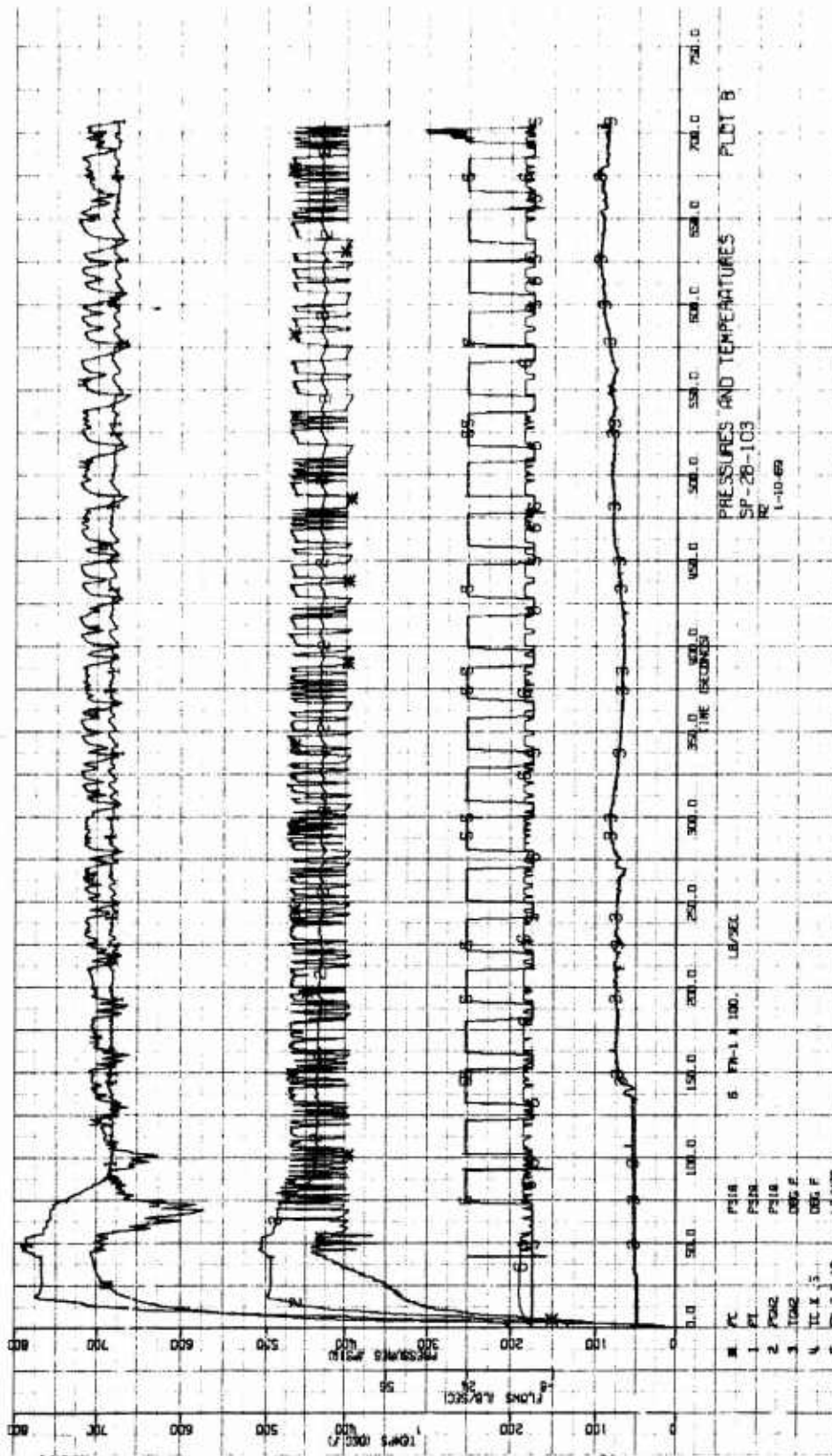


Figure 110. Tank S/N 2 Hot Gas Expulsion of NMH - Recorded Data
(Sheet 2 of 3)

UNCLASSIFIED

UNCLASSIFIED

Report AFRPL-TR-69-88

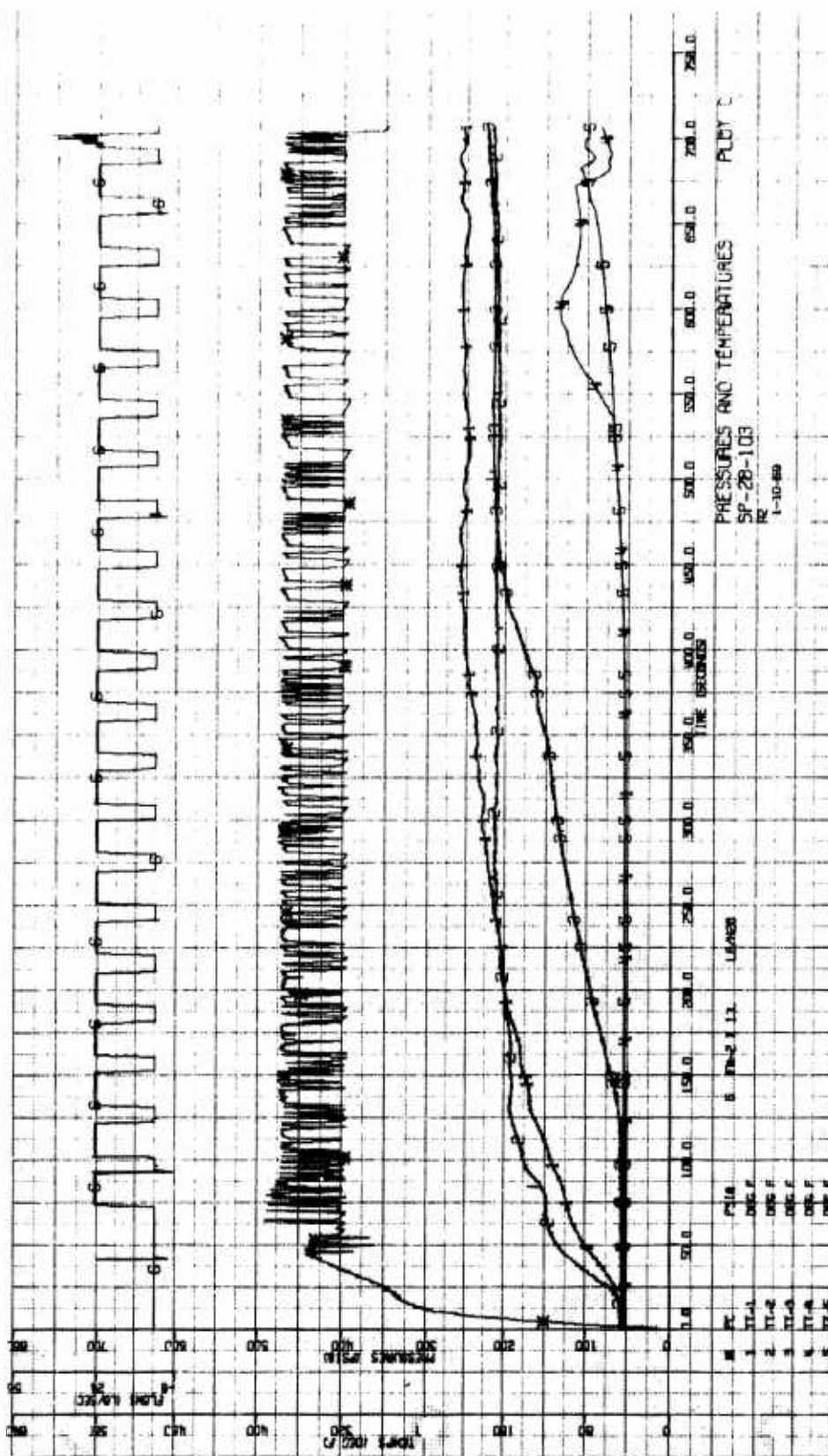


Figure 110. Tank S/N 2 Hot Gas Expulsion of NMH - Recorded Data
(Sheet 3 of 3)

UNCLASSIFIED

UNCLASSIFIED

Report AFRL-TP-69-88



Figure 111. Propellant Tank S/N 2 After Hot Gas Expulsion of VMd

Page 240

UNCLASSIFIED

UNCLASSIFIED

Report AFRPL-TR-69-88

VI, D, Flightweight Tank Evaluation (cont.)

The hot gas expulsion of N_2O_4 was completely successful. The test ran much longer than expected because of an electrical reversal in the programmed duty cycle. It was intended that the duty cycle be the same as the MMH expulsion; however, the reversed cycle provided 10 sec of oxidizer flow at 3.4 lb/sec followed by 20 sec of coast for each flow cycle. This resulted in 44 complete cycles during a 1430 sec time period. The test was terminated in the 45th cycle when the bladder reached the end of the reversal and pressure drop increased above 25 psi. The pressure drop across the bladder remained uniform at 6 psi to 8 psi, except for a brief period in the 13th and 14th cycles when a level of 10 psi to 12 psi was reached.

The measured data from the N_2O_4 expulsion (see Figure No. 112) supported the recorded tank temperatures of the MMH expulsion test. The data from both of these tests indicated that the tank wall temperatures were substantially lower than in the previous workhorse flanged tank expulsions. The measured temperatures on the workhorse tank adjacent to the hot gas inlet approached 480°F in comparison to the measured 220°F at the end of the N_2O_4 expulsion test. The apparent heat transfer into the propellant indicated the inlet gas temperatures were not substantially different between tests. All of the hot gas expulsions produced a 31°F to 40°F temperature rise in the final propellant forced out of the tank. The more-prototype aluminum tank mount used with the horizontal propellant expulsions could have provided a source of heat transfer for the thin metal end cap at the tank inlet.

Examination of the bladder after the test was accomplished by cutting a window through the wall of the inlet tank half. The satisfactory reversed bladder is shown on Figure No. 113.

E. CONCLUSIONS AND RECOMMENDATIONS

1. Ring-Stabilized Expulsion Propellant Tank

The ring-stabilized expulsion propellant tank concept was successfully demonstrated with the fabrication and testing of flanged bladders and the flightweight propellant tank assemblies. The operational implementation of a developed propellant containment and positive expulsion vessel with the characteristics demonstrated under this AFRPL program provide the following key benefits to a large-size Post-Boost Vehicle.

- Mass Fraction

The vehicle mass fraction would be minimized by the low weight of the tank assembly. No other demonstrated large-scale metallic expulsion concept can compete with the demonstrated mass fraction of this tank concept.

UNCLASSIFIED

UNCLASSIFIED

Report AFRPL-TR-69-88

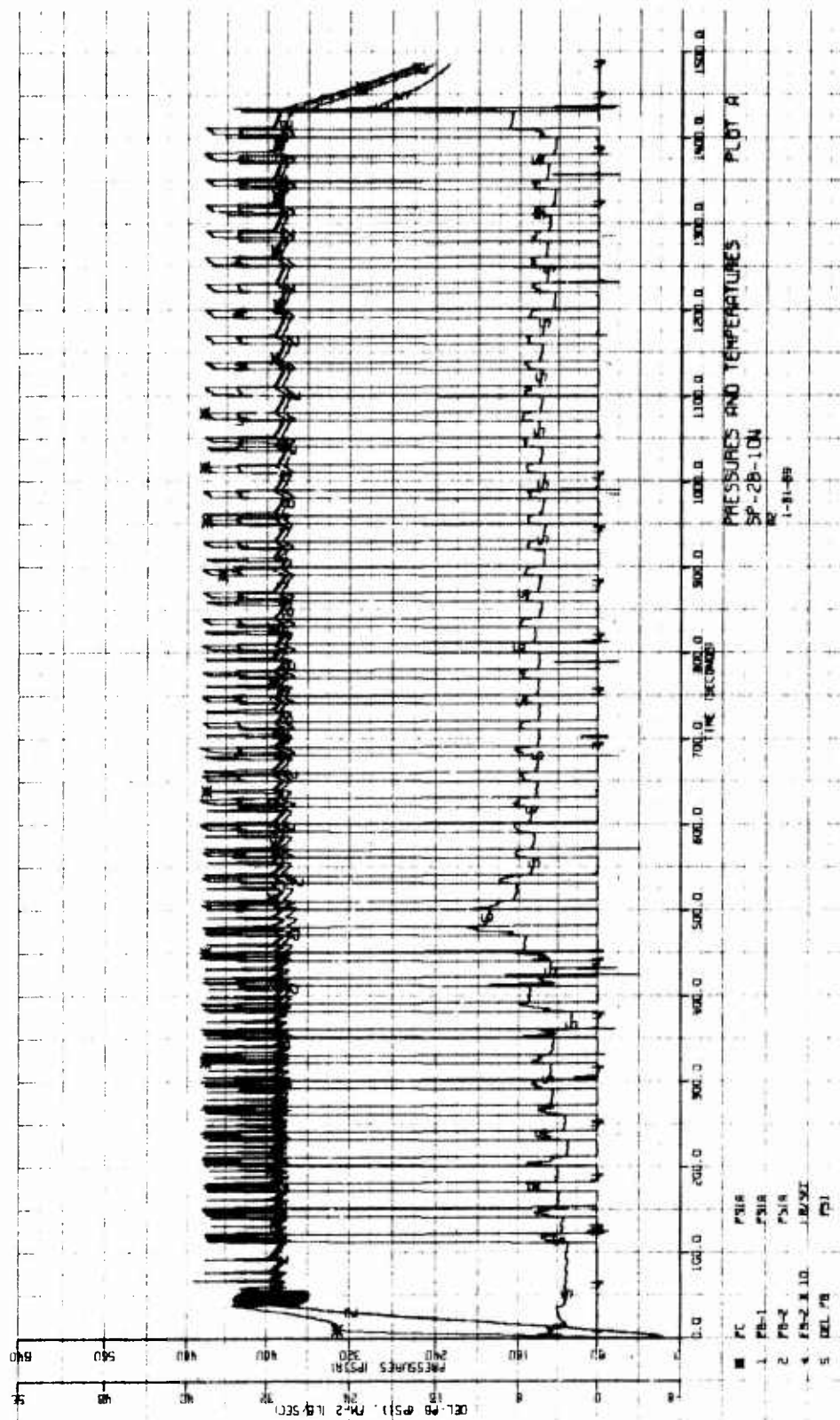


Figure 112. Tank S/N 5 Hot Gas Expulsion of N_2O_4 - Recorded Data
(Sheet 1 of 3)

UNCLASSIFIED

UNCLASSIFIED

Report AFRPL-TR-69-88

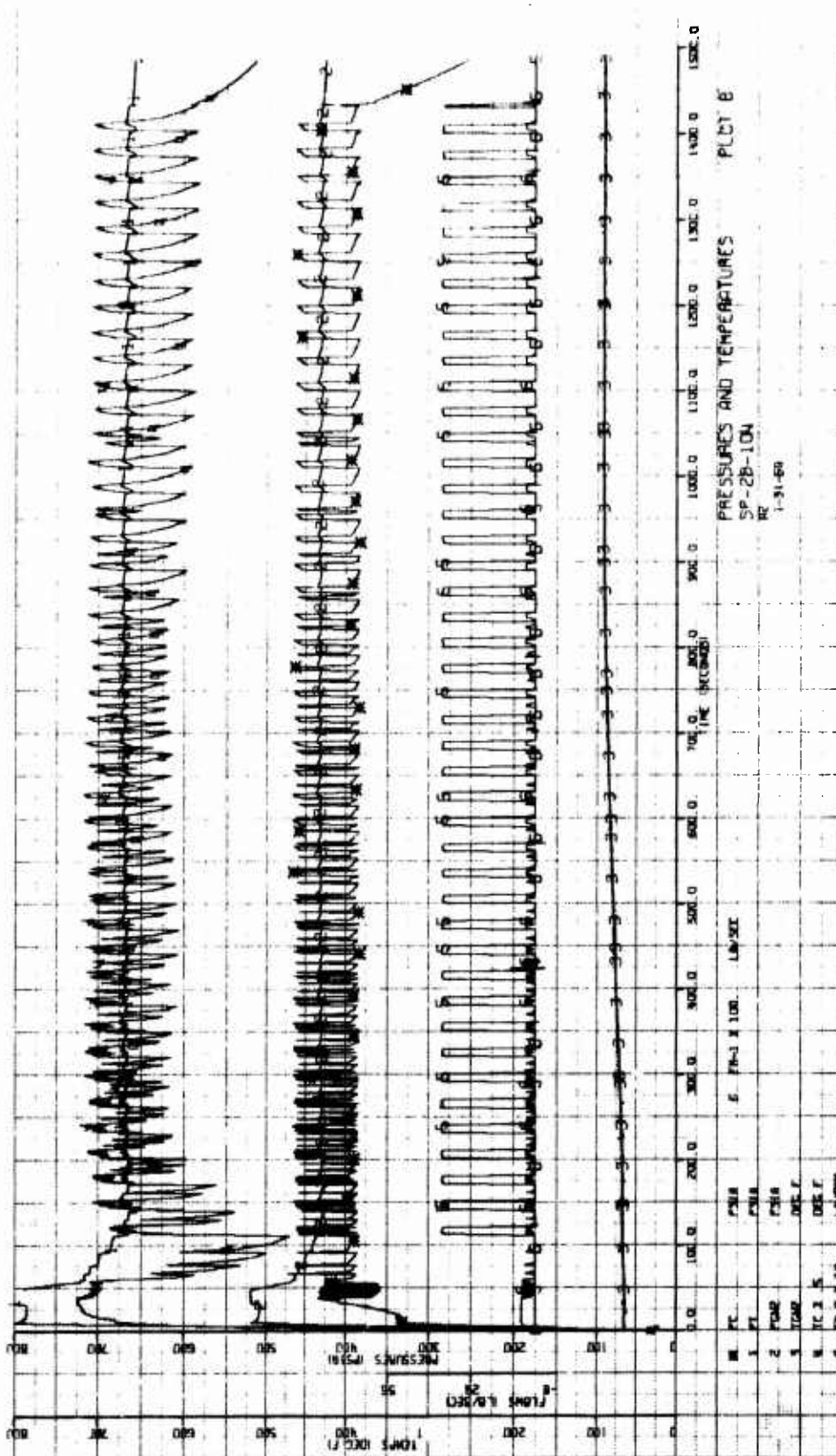


Figure 112. Tank S/N 5 Hot Gas Expulsion of N_2O_4 - Recorded Data
(Sheet 2 of 3)

UNCLASSIFIED

UNCLASSIFIED

Report AFRPL-TR-69-88

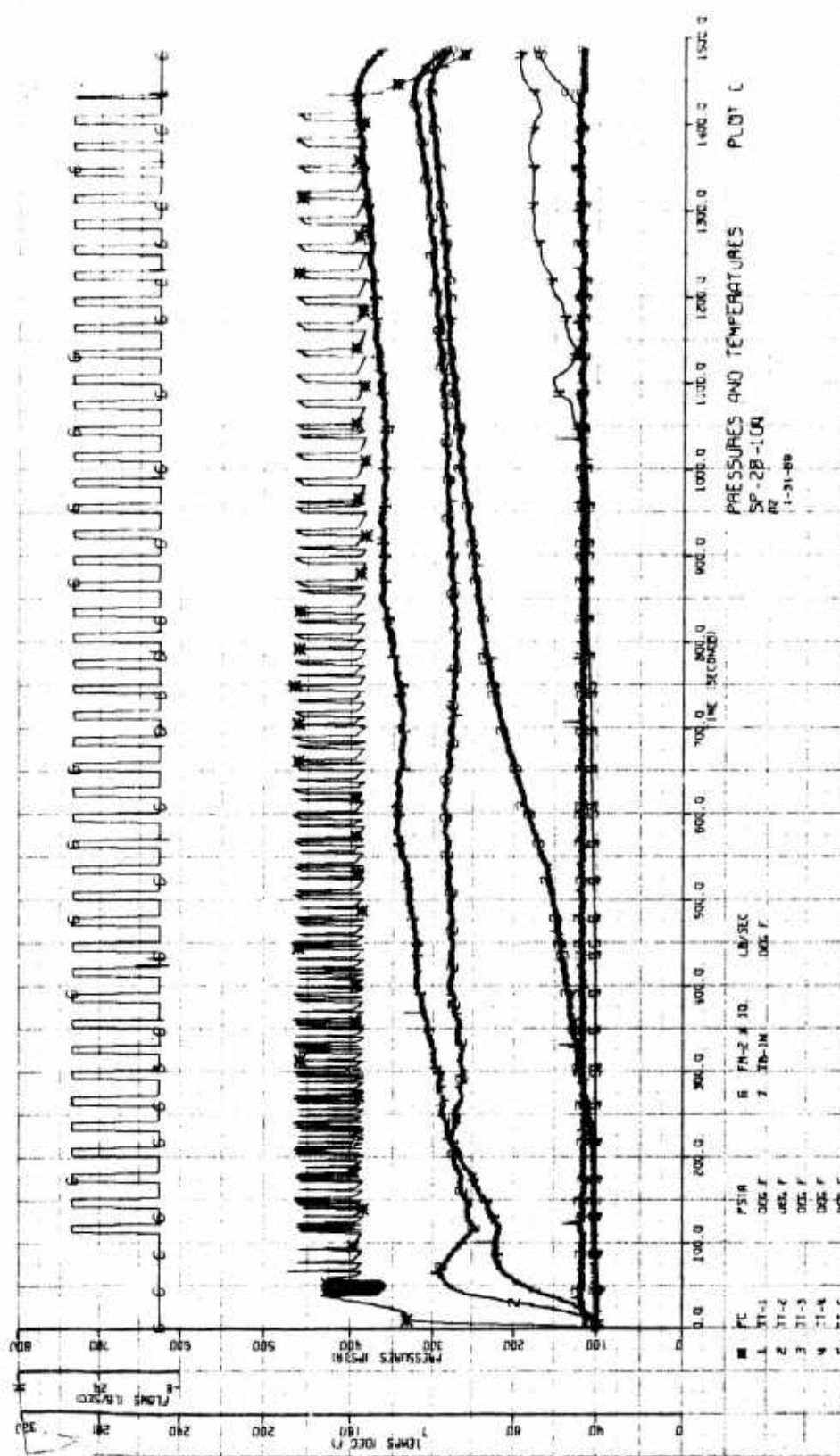


Figure 112. Tank S/N 5 Hot Gas Expulsion of N_2O_4 - Recorded Data
(Sheet 3 of 3)

UNCLASSIFIED

UNCLASSIFIED

Report AFRPL-TR-69-88

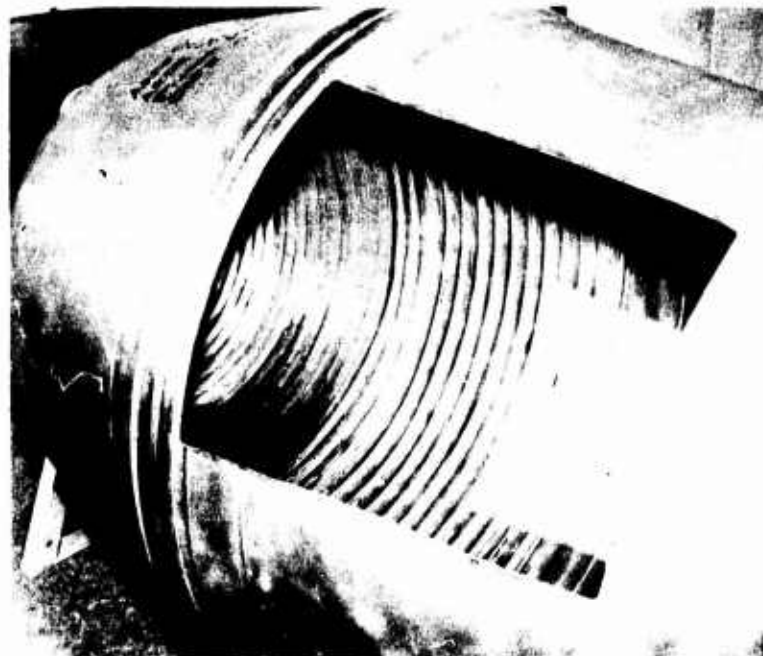
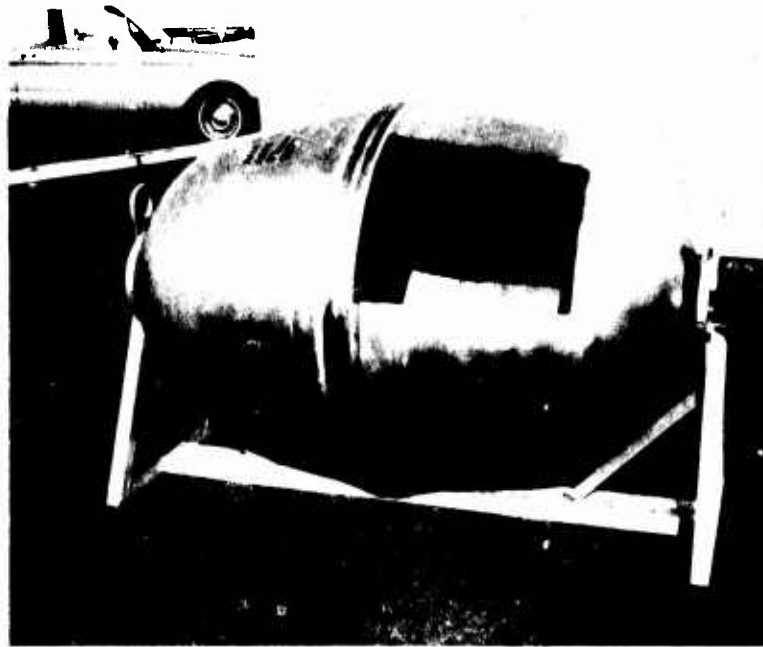


Figure 113. Propellant Tank S/N 5 After Hot Gas Expulsion of N_2O_4

Page 245

UNCLASSIFIED

UNCLASSIFIED

Report AFRPL-TR-69-88

VI, E, Conclusions and Recommendations (cont.)

- Expulsion Efficiency

The basic mode of operation of the expulsion bladder must consistently provide expulsion efficiencies >99% because the bladder yields to fit the outlet tank half contour at the completion of an expulsion.

- Structural Integrity

The tank has demonstrated that the high ultimate strength imparted to it by the cryogenic stretch process, provides sufficient structural margin without the use of exotic materials or composites.

- Inherent Storability

The all-welded, stainless steel structure should provide the required propellant storability needed for a strategic weapon system. This will be demonstrated with the two remaining propellant tank assemblies in a propellant storage program to be conducted by AFRPL.

- Unit Fabrication Cost

The concept provides a capability for the quantity production of the large size expulsion tank at a low relative cost which results from the unique fabrication procedure. After the final configuration is defined and the reusable stretch tooling is purchased, the fabrication costs will be low because of the limited need for precision fabrication.

However, further expulsion bladder fabrication development is required prior to the final application of this tank. The initial bladder shell fabrication was a major problem during the AFRPL programs as a result of the deep sheet metal forming requirements for the selected shape of the tank. The resulting non-uniform shell thickness caused control problems regarding the achievement of the desired rim-roll reversal mode. Fabrication tooling and procedural changes would be required to correct this shell deficiency for future applications.

The deep forming requirements of the tank bladder shell could be reduced if the final vehicle application of the tank concept would allow for a more spherical tank shape. Minimizing the tank L/D (length over diameter) also provides greater assurance the reversal mode of the bladder will be predictable and uniform.

UNCLASSIFIED

VI, E, Conclusions and Recommendations (cont.)

2. Monopropellant Gas Pressurization

The demonstration of a monopropellant N_2H_4 gas generator subsystem as a pressurization source for thin-wall propellant expulsion devices has been successful. The intermittent use of the bootstrap subsystem as a pressurization source for these tests over a one-year period demonstrated the functionability and relative storability of the subsystem concept. The gas generator operated satisfactorily in excess of 7000 sec of testing within that period. The AM355 bootstrap tank demonstrated propellant storability as a result of the hydrazine never being completely removed within that period.

The incorporation of better pressure regulations controls and a propellant (N_2H_4) isolation device in the bootstrap tank for long-term storage would provide an available pressurization subsystem for vehicle application.

UNCLASSIFIED

Report AFRPL-TR-69-88

REFERENCES

1. Demonstration of Advanced Post-Boost Propulsion Subsystems, Aerojet-General Final Report, AFRPL-TR-68-126, August 1968
2. Priem, R. J. and Heidmann, M. F., Propellant Vaporization as a Design Criterion for Rocket Engine Combustion Chambers, NASA TR R-67, 1960
3. High Energy Propellant Beryllium Thrust Chamber Program, Rocketdyne Phase I Report R-7057, AFRPL-TR-67-150, May 1967
4. Bartz, D. R., "A Simple Equation for Rapid Estimation of Rocket Nozzle Convective Heat Transfer Coefficients," Jet Propulsion, 27, 1957
5. Schoenman, L. and Block, P., Application of Laminar Boundary Layer Heat Transfer Theory to Low Thrust Rocket Nozzles, AIAA Paper No. 67-447, July 1967

BIBLIOGRAPHY

Anon. (Same as 1 Above)
Anon. (Same as 3 Above)
Priem (Same as 2 Above)
Schoenman (Same as 5 Above)
Bartz (Same as 4 Above)

UNCLASSIFIED

DOCUMENT CONTROL DATA - R&D		
(Security classification of title, body of abstract and indexing annotation must be entered when the overall report is classified)		
1 ORIGINATING ACTIVITY (Corporate author)		2a REPORT SECURITY CLASSIFICATION
Aerojet-General Corporation		Confidential
		2b GROUP 4
3 REPORT TITLE		
PBPS Engine Development Program and System Design (U)		
4 DESCRIPTIVE NOTES (Type of report and inclusive dates)		
Final Report 1 April 1967 through 31 January 1969		
5 AUTHOR(S) (Last name, first name, initial)		
Jones, Roy E.		
6 REPORT DATE	7a. TOTAL NO. OF PAGES	7b. NO. OF REFS
April 1969	248	5
8a. CONTRACT OR GRANT NO.	9a. ORIGINATOR'S REPORT NUMBER(S)	
F04611-67-C-0095	None	
b. PROJECT NO.		
c.	9b. OTHER REPORT NO(S) (Any other numbers that may be assigned this report)	
d.	None	
10. AVAILABILITY/LIMITATION NOTICES		
"In addition to security requirements, which must be met, this document is subject to special export controls and each transmittal to foreign governments or foreign nationals may be made only with prior approval of AERPL (RPOB/STINCO), Edwards CA 93523."		
11. SUPPLEMENTARY NOTES		12. SPONSORING MILITARY ACTIVITY
None		Air Force Rocket Propulsion Laboratory Air Force Systems Command Edwards, California
13 ABSTRACT		
<p>The increased size and extended mission duty cycles of planned Post-Boost Propulsion Systems (PBPS) for Advanced ICBM applications identified the need for improvements in liquid propellant propulsion technology. Although liquid propellant propulsion systems have demonstrated an operational flexibility and performance capability, improvements in the inherent storability, maintainability, and reliability were desired for an optimum strategic weapon system.</p> <p>The PBPS Engine Development Program was initiated to develop a bipropellant N_2O_4 and MMH attitude control system (ACS) wherein integral fluidic controls are used to perform ACS propellant flow control, thereby controlling vehicle attitude with a minimum of moving parts. Developmental problems with the fluidic control elements resulted in the termination of the integral fluidic ACS development and the associated minimum ACS engine studies.</p> <p>The program was redirected to provide the development of a conventionally-controlled 75 lb thrust attitude control engine as well as the demonstration testing of PBPS pressurization and positive expulsion propellant tank subsystems. An Aerojet-General proprietary injector concept in conjunction with a bimetallic, conductively-cooled combustion chamber was used in the ACS engine developed. This engine was demonstrated in altitude performance and pulse testing. The monopropellant hot gas pressurization subsystem was used to demonstrate propellant expulsion (both monomethylhydrazine and N_2O_4) from the full-size ring-stabilized expulsion propellant tanks.</p>		

14 KEY WORDS	LINK A		LINK B		LINK C
	ROLE	WT	ROLE	WT	ROLE
ACS with Integrated Fluidic Controls ACS Engine Fluidic Controls Evaluation Minimum ACS Engine Study Bipropellant ACS Engine Development Positive Expulsion Propellant Tank Demonstration					

INSTRUCTIONS

1. **ORIGINATING ACTIVITY:** Enter the name and address of the contractor, subcontractor, grantee, Department of Defense activity or other organization (*corporate author*) issuing the report.

2a. **REPORT SECURITY CLASSIFICATION:** Enter the overall security classification of the report. Indicate whether "Restricted Data" is included. Marking is to be in accordance with appropriate security regulations.

2b. **GROUP:** Automatic downgrading is specified in DoD Directive 5200.10 and Armed Forces Industrial Manual. Enter the group number. Also, when applicable, show that optional markings have been used for Group 3 and Group 4 as authorized.

3. **REPORT TITLE:** Enter the complete report title in all capital letters. Titles in all cases should be unclassified. If a meaningful title cannot be selected without classification, show title classification in all capitals in parenthesis immediately following the title.

4. **DESCRIPTIVE NOTES:** If appropriate, enter the type of report, e.g., interim, progress, summary, annual, or final. Give the inclusive dates when a specific reporting period is covered.

5. **AUTHOR(S):** Enter the name(s) of author(s) as shown on or in the report. Enter last name, first name, middle initial. If military, show rank and branch of service. The name of the principal author is an absolute minimum requirement.

6. **REPORT DATE:** Enter the date of the report as day, month, year, or month, year. If more than one date appears on the report, use date of publication.

7a. **TOTAL NUMBER OF PAGES:** The total page count should follow normal pagination procedures, i.e., enter the number of pages containing information.

7b. **NUMBER OF REFERENCES:** Enter the total number of references cited in the report.

8a. **CONTRACT OR GRANT NUMBER:** If appropriate, enter the applicable number of the contract or grant under which the report was written.

8b, 8c, & 8d. **PROJECT NUMBER:** Enter the appropriate military department identification, such as project number, subproject number, system numbers, task number, etc.

9a. **ORIGINATOR'S REPORT NUMBER(S):** Enter the official report number by which the document will be identified and controlled by the originating activity. This number must be unique to this report.

9b. **OTHER REPORT NUMBER(S):** If the report has been assigned any other report numbers (*either by the originator or by the sponsor*), also enter this number(s).

10. **AVAILABILITY/LIMITATION NOTICES:** Enter any limitations on further dissemination of the report, other than those

imposed by security classification, using standard statements such as:

- (1) "Qualified requesters may obtain copies of this report from DDC."
- (2) "Foreign announcement and dissemination of this report by DDC is not authorized."
- (3) "U. S. Government agencies may obtain copies of this report directly from DDC. Other qualified DDC users shall request through _____."
- (4) "U. S. military agencies may obtain copies of this report directly from DDC. Other qualified users shall request through _____."
- (5) "All distribution of this report is controlled. Qualified DDC users shall request through _____."

If the report has been furnished to the Office of Technical Services, Department of Commerce, for sale to the public, indicate this fact and enter the price, if known.

11. **SUPPLEMENTARY NOTES:** Use for additional explanatory notes.

12. **SPONSORING MILITARY ACTIVITY:** Enter the name of the departmental project office or laboratory sponsoring (*paying for*) the research and development. Include address.

13. **ABSTRACT:** Enter an abstract giving a brief and factual summary of the document indicative of the report, even though it may also appear elsewhere in the body of the technical report. If additional space is required, a continuation sheet shall be attached.

It is highly desirable that the abstract of classified reports be unclassified. Each paragraph of the abstract shall end with an indication of the military security classification of the information in the paragraph, represented as (TS), (S), (C), or (U).

There is no limitation on the length of the abstract. However, the suggested length is from 150 to 225 words.

14. **KEY WORDS:** Key words are technically meaningful terms or short phrases that characterize a report and may be used as index entries for cataloging the report. Key words must be selected so that no security classification is required. Identifiers, such as equipment model designation, trade name, military project code name, geographic location, may be used as key words but will be followed by an indication of technical context. The assignment of links, rules, and weights is optional.